A Study of the Role of Spermidine/Spermine N^1-Acetyltransferase (SSAT) in Polyamine Homeostasis in Human Prostate Cancer Cells

By

JUN LI

B.Sc. (Hons) Biomedical Sciences (Physiology)

University of Aberdeen, July 2009

Submitted in partial fulfilment of the requirements for the degree of Doctor of Philosophy, University of Aberdeen

School of Medicine & Dentistry

Jan 2014

Abstract

Prostate cancer is the second leading cancer in men. A large amount of polyamines are synthesised in the human prostate and are involved in prostate cell growth and its physiological functions. The content of intracellular polyamines is closely related to cell growth. An increase in cell growth is accompanied by a rise of intracellular polyamine content, and a depletion of intracellular polyamine pools can cause growth arrest or cell death. Therefore, maintaining polyamine concentrations is critical to the cell. Spermidine/spermine N^1-acetyltransferase (SSAT) is the first and rate-limiting enzyme in the polyamine catabolic pathway. SSAT gene is highly inducible, with many stimuli including polyamine analogues and some anticancer drugs producing dramatic increases in activity. Many studies have focussed on polyamine analogues as inducers of SSAT activity as increases in SSAT are associated with a growth inhibition in many tumour cells. However, the mechanisms of this inhibition are not fully understood with respect to polyamine content. Additionally, *in vivo* results in SSAT transgenic mice studies are contradictory. For example, prostate carcinogenesis is reduced in TRAMP mice but $Apc^{min/+}$ mice show a promoted intestinal tumorigenesis. It is thus necessary to characterise the regulation of polyamine content and metabolism by SSAT in prostate cancer cells.

The aim of the present study was to characterise the role of SSAT in both the growth of LNCaP prostate carcinoma cells and the response of these cells to anticancer drugs. Our hypothesis is that increased SSAT activity will inhibit cell growth and that this is associated with a decrease of intracellular polyamine pools. Furthermore, if SSAT induction is an essential part of the response of cancer cells to anticancer drugs, then altered SSAT activity should affect sensitivity of the cells to the drugs.

The present study used a cell culture model of human prostate cancer: LNCaP wild type (WT) and SSAT cDNA transfected prostate carcinoma cell lines. The expression of SSAT in the transfected cell line ($SSAT^-$ & $SSAT^+$) was controlled through the "Tet-off" system. This model system provided a background for comparison of effects under basal (WT), low ($SSAT^-$), and high ($SSAT^+$) SSAT activity.

Due to our interest in acetylpolyamine derivatives and their low concentrations in cells, a new method for quantifying polyamine concentrations was developed using liquid chromatography-mass spectrometry (LC-MS). This method was highly sensitive and can detect polyamines about 250 fold lower than HPLC, as well as N-acetylpolyamines and N^1,N^{12}-diacetylspermine. In addition, a variety of methods were utilised to measure cell growth, enzyme activity, protein expression, polyamine efflux and apoptosis, which includes enzyme assays, western blot, radiochemical labelled assays, flow cytometry, spectrophotometry and fluorescent microscopy.

A stable increase in SSAT activity was inhibitory to the cell growth. This inhibition was associated with significant changes in the activity of the polyamine pathway. The alterations included an increase in ODC, APAO, and SMO activity; an accumulation of intracellular N^1-acetylspermidine and putrescine; a decrease in intracellular spermidine and spermine; an increased polyamine flux and efflux; and an increase in apoptosis. Combination treatment to the cells with DFMO and MDL72527 partially restored the growth of $SSAT^+$ cells.

The original contribution of this study to the field is that the cells with a higher SSAT activity are less sensitive to aspirin and 5-FU, and the sensitivity increased while the overexpressed SSAT activity decreased. The growth inhibition was associated with a depletion of total intracellular polyamine pools by the drug treatments. Moreover, to our knowledge, it is first time that the extracellular polyamine concentrations were quantified by LC-MS in human tumour cells.

Overall, an increase in SSAT activity led to an inhibition of prostate cancer cell growth, and *vice versa*. Thereby, this study suggests that SSAT is a potential target for novel drug discovery for cancer chemotherapy or chemoprevention. For example, a combination treatment could be designed that acts as an inducer of SSAT activity in tumour cells, leading to an inhibition of the cell growth in the first place and increased sensitivity to cytotoxic agents. This would then be followed by an agent to decrease SSAT activity when the sensitivity of cancer cells to the cytotoxic treatment was optimal.

Declaration

I hereby declare that this thesis has been composed by myself, and has not been accepted in any previous application for a degree. This work of which it is a record, except where specifically acknowledged, has been completed by myself. All sources of information have been specifically acknowledged by means of references.

Jun Li

Acknowledgements

I am sincerely grateful to the following people for their valuable help during this work over the previous 4 years. It would not have been possible to complete this work without them:

Professor Heather Wallace, my supervisor, for her strict supervision, advice, and guidance throughout the project and those tough times;

Mr Gary Cameron who has the most optimistic outlook on life and provided huge support on LC-MS and guidance on beers;

Dr. Keith Thompson who gave generous support on flow cytometry and advice on western blot;

Dr. Julie C. Crockett and ***Miss Lucy Wight*** who helped me with DAPI assay and fluorescent microscopy;

Dr. Alun Hughes who supported me with q-PCR;

Ms Jacqui Morrison, ***Mrs Fiona Ashby***, ***Ms Denise Tosh***, ***Mr Bob Glennie***, and ***Mrs Fiona Insch*** who provided numerously support during my study;

I would also like to thank my uncle ***Mr Fenghui Xia***, my girlfriend ***Miss Xu Han*** for their care; my dear friends ***Mr Junyou Song***, ***Dr. Gordon Black***, ***Dr. Tommy Riley***, ***Dr. William Thorne***, ***Miss Lingbo Zhou***, ***Miss Hanhong Zheng*** and ***Miss Yao Ding*** for their friendships.

Abbreviations

AdoMetDC	S-adenosyl-methionine decarboxylase
AG	Aminoguanidine
APAO	N^1-acetylpolyamine oxidase
BSA	Bovine serum albumin
COX	Cyclo-oxygenase
dcAdoMet	Decarboxylated S-adenosyl methionine
DCFDA	2',7'-Dichlorofluorescin diacetate
DFMO	α-Difluoromethylornithine
DMSO	Dimethylsulfoxide
DTT	Dithiothreitol
EDTA	Ethylenediamine tetra-acetic acid
5-FU	5-Fluorouracil
FBS	Foetal bovine serum
HPLC	High-performance liquid chromatography
LC-MS	Liquid chromatography mass spectrometry
MDL72527	N^1,N^4-bis(2,3-butadienyl)-1,4 butanediamine
MTT	3-(4,5-dimethylthiazol-2-yl)-2,5-diphenyl tetrazolium bromide
NSAID	None-steroidal anti-inflammatory drugs
ODC	Ornithine decarboxylase
OPA	o-phthaldialdehyde
PBS	Phosphate buffered saline
ROS	Reactive oxygen species
SAM	S-adenosylmethionine
SAMDC	S-adenosylmethionine decarboxylase
SMO	Spermine oxidase
SSAT	Spermidine/spermine N^1-acetyltransferase
TBS	Tris buffered saline
Tet	Tetracycline

Contents

1 Introduction

1.1 Cancer

1.1.1 Epidemiology of cancer

Current cancer-control strategies do not seem work effectively according to *the Lancet* (Cavalli, 2013). In 2010 an estimation of 8 million people died from cancer, a 38% rise on the annual cancer death toll compared to 1990 (Lozano *et al.*, 2013). A dramatic increase in cancer incidence has occurred in low- and middle-income countries undergoing rapid socioeconomic transition (Soerjomataram *et al.*, 2012), such as China. By 2030, it is predicted that almost two-thirds of cancer cases will occur in these countries (Bray *et al.*, 2012) and more than 13 million deaths from cancer are estimated by WHO (Globocan 2008, IARC, 2010).

Cancer is a leading cause of death and a major health concern worldwide. The main types of cancer are lung, stomach, liver, colorectal, breast, prostate and cervical cancer (Cancer fact sheet 2013, World Health Organisation). Cancer is not a single disease but many diseases. Transformation of a normal cell into a cancer cell is a multistage process including changes such as oncogene activation, loss of telomerase and aneuploidy induction (Bergers & Benjamin, 2003). Tumorigenesis is a long term process that cells may generate mutations as a result of exposure to external carcinogens, which include physical carcinogens, such as ultraviolet and ionizing radiation; chemical carcinogens, such as asbestos and tobacco; and biological carcinogens, such as viruses and bacteria. In addition, the incidence of cancer rises with age in that overall risk factors accumulate with age whereas cellular repair systems attenuate (Cancer fact sheet N°297, WHO, 2013).

A group of key risk factors attributable to more than 30% of cancer death exist that can be modified or avoided. These include: tobacco use, being overweight or obese, unhealthy diet with low fruit and vegetable intake, lack of physical activity, alcohol use, sexually transmitted human papilloma virus (HPV)-infection, urban air pollution, and

indoor smoke from household use of solid fuels. Effective strategies to reduce cancer incidence and mortality are: avoidance of these risk factors; early detection, diagnosis and treatment; and screening of asymptomatic population at risk (WHO, 2013).

1.1.2 Biology of cancer

A comprehensive review by Hanahan & Weinberg (2011) highlights the six hallmarks of cancer for understanding the complex biology of cancer (Fig. 1.1).

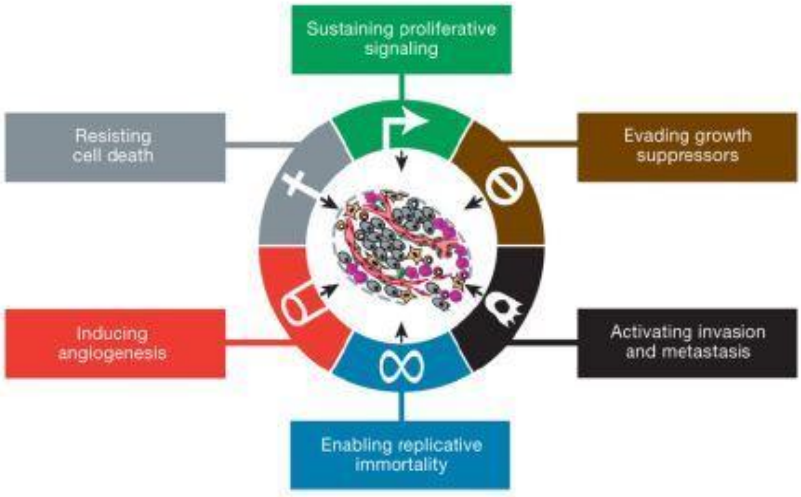

Fig. 1.1 The six hallmarks of cancer (Hanahan & Weinberg, 2011)

In addition to the six hallmarks, there are two emerging hallmarks i.e. reprogramming energy metabolism and evading immune destruction, which have not been fully validated yet. Cancer cells have developed two enabling characteristics to facilitate acquisition of these hallmarks: the development of genome instability and mutation and tumour-promoting inflammation (Hanahan & Weinberg, 2011).

In terms of cellular metabolism, there are three fundamental requirements of proliferating cells: rapid ATP generation to maintain energy status; enhanced macromolecular biosynthesis; and tightened maintenance of the appropriate cellular redox status. The metabolism of four major classes of macromolecules (carbohydrates, proteins, lipids, and nucleic acids) is altered by cancer cells to meet these requirements

(Cairns *et al.*, 2011). As a result, many cellular signalling pathways are affected in cancer cell metabolism, such as an activation of the PI3K pathway by mutations in tumour suppressor genes (Wong *et al.*, 2010), a loss of AMP-activated protein kinase (AMPK) signalling (Kuhajda, 2008), and an altered NADPH function providing reducing power for glutathione scavenging ROS (Nathan & Ding, 2010).

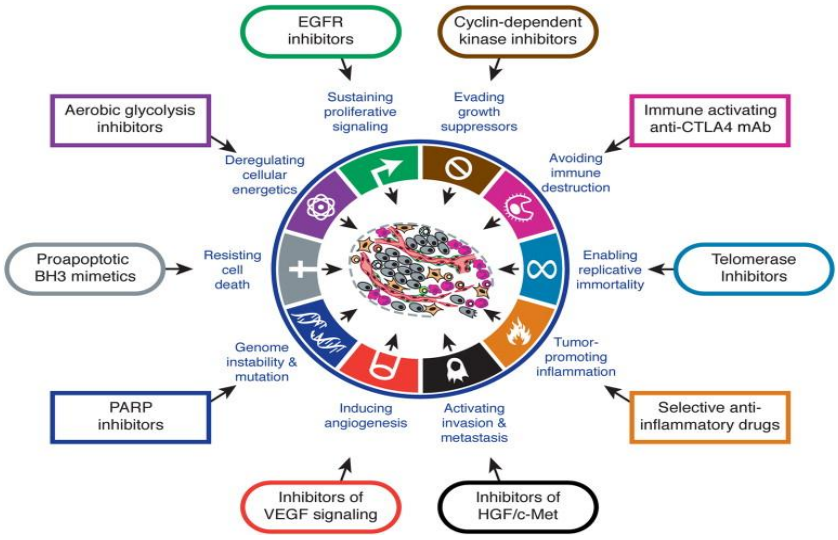

Fig. 1.2 Therapeutic targeting of the hallmarks of cancer (Hanahan & Weinberg, 2011)

Therapeutic targeting of cancer is specifically based on the hallmarks of cancer as stated above. Inhibitors targeting each of the pathways in cancer cells are summarised by Hanahan & Weinberg (2011) (Fig. 1.2). It is noteworthy, however, that inhibition of one hallmark pathway by a therapeutic agent may allow some cancer cells to survive and eventually adapt to the stress imposed by the treatment. In order to accomplish such adaptation, these cells or their progeny will undergo mutation, epigenetic reprogramming, or remodelling of the stromal microenvironment, leading to re-establishment of the functional hallmark capability. Ultimately, tumour cell growth renews and the disease relapses. In addition to the adaptation in survived cancer cells, tumour cells can develop resistance to anticancer drugs which may be largely due to a switch from one particular dominant hallmark capability to another (Hanahan & Weinberg, 2011). Thus, therapeutic targeting of multiple hallmark pathways is urgently needed.

1.2 Polyamines

1.2.1 History of polyamines

Spermine was the first polyamine discovered in human semen by Van Leeuwenhoek in 1678. In the late 1800s, putrescine was identified in microbes and spermidine was eventually found in early twentieth century (Gerner & Meyskens Jr, 2004). The first research article “polyamines and cancer cells” was published by the Proceedings of the National Academy of Japan in 1958 (Criss, 2003). Since then, over 85,000 papers have been published on polyamines in the past 55 years. Polyamines have undoubtedly contributed to the knowledge of biological sciences and are still doing so as the mystery of their molecular functions has not been fully elucidated yet, despite the huge progress has been achieved thus far.

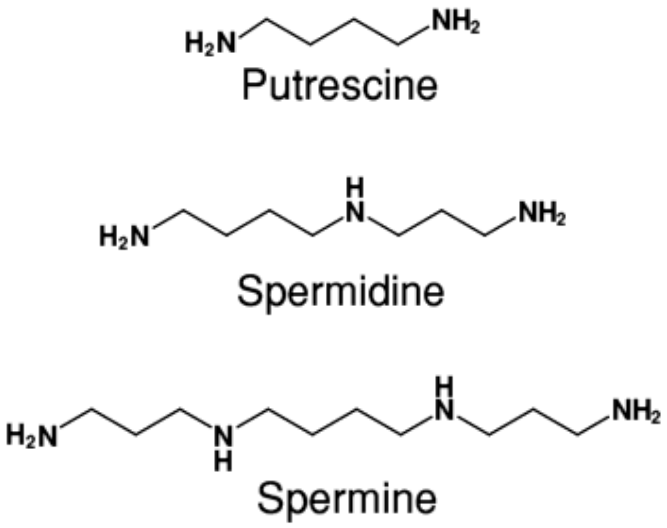

Fig. 1.3 Structure of putrescine, spermidine and spermine (Seiler, 2004)

1.2.2 Polyamines and their functions

The major source of polyamines (putrescine, spermidine and spermine) in the cell is from *de novo* biosynthesis. They also exist naturally in our daily diet and some are obtained from the metabolism from intestinal microorganisms (Thomas & Thomas, 2001). Foods with high polyamine content include cheese, citrus fruit, red meat and broccoli and they are also abundant in human milk (Larqué *et al.*, 2007; Ali *et al.*, 2011). Polyamines are therefore critical molecules required by human body for its physiological functions.

Polyamines are small aliphatic polycationic alkylamines (Fig. 1.3) present in all living cells as they are essential substances required for many cellular functions. In mammalian cells, putrescine, spermidine and spermine, are found in micromolar to millimolar concentrations, depending on the status of cell growth (quiescent cells have relatively low polyamine content, but proliferating cells require more polyamines). At physiological pH the primary and secondary amino groups of polyamines are protonated, forming divalent putrescine, trivalent spermidine and tetravalent spermine (Heby *et al.*, 1975; Khuhawar & Qureshi, 2001; Thomas & Thomas, 2001).

These biologically indispensable molecules perform significant roles in cell growth and development in eukaryotes. Stimulation of cell proliferation is the major function of polyamines in most cell types (Thomas & Thomas, 2001). They bind to acidic sites of various anionic macromolecules including DNA, RNA, ATP, proteins and acidic phospholipids, resulting in conformational changes (Wallace, 2000; Wallace *et al.*, 2003; Criss, 2003). The polyamine-DNA interaction is believed to be electrostatic in origin and this binding appears to stabilise DNA structure and is associated with compacted mitotic chromosomes, conformational transitions in certain DNA sequences, and promoting DNA bending involved in transcriptional regulation of gene expression (Thomas & Thomas, 2001). Studies using polyamine depletion illustrate, for example, that spermidine and spermine are associated with DNA condensation into chromatin and modification in nucleosomal structure (Marton & Pegg, 1995). It is thought that most polyamines exist as a polyamine-RNA complex (Battaglia *et al.*, 2013). This binding has a stimulating effect on the efficiency of protein synthesis due to the structural changes caused by the polyamine-

RNA complex (Igarashi & Kashiwagi, 2010). Taken together, polyamines appear to play a fundamental role in the cell, therefore, regulating cell functions.

In addition to stabilising the macromolecular structures, polyamine broader functions are further indicated in modulating rectification of inwardly potassium (Kir) channels, affecting the activities of NMDA glutamate receptors in the mammalian brain, specific gene expression regulation, conservation of membrane stability and eliminating free radicals (Casero & Marton, 2007; Pegg & Casero, 2011; Battaglia *et al.*, 2013). It is generally believed, for instance, that the eukaryotic translation initiation factor eIF5A requires a posttranslational modification to form hypusine in which spermidine is required as a precursor, indicating that polyamines are involved in the synthesis of some proteins regulating eukaryotic translation (Park, 2006). The complexity of polyamine involved interactions is probably due to the fact that most of them are readily reversible ionic interactions (Nowotarski *et al.*, 2013).

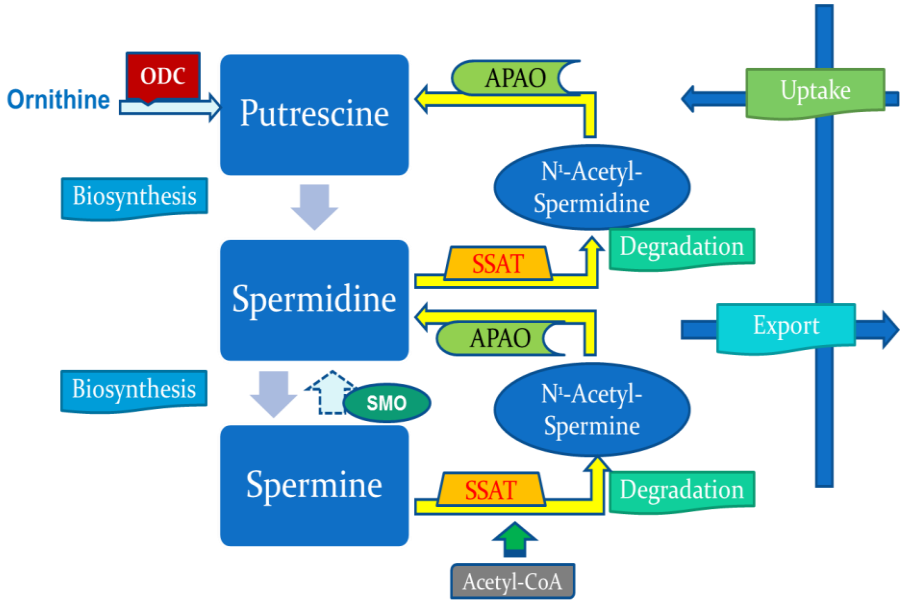

Fig. 1.4 Scheme of polyamine homeostasis

1.2.3 Polyamine biosynthesis

Increased intracellular polyamine pools are associated with proliferating cells including cancer cells (Babbar & Gerner, 2011). L-Ornithine decarboxylase (ODC) is located in both the cytoplasm and the nuclei of mammalian cells and is the first, rate-limiting enzyme in the polyamine biosynthetic pathway. Putrescine is generated by the pyridoxal, phosphate-dependent ODC reaction via decarboxylation of L-ornithine, which is the end product of the urea cycle (Criss, 2003; Wallace & Fraser, 2003). As putrescine is the precursor of spermidine, inhibition of ODC activity leads to a reduction of both putrescine and spermidine, but not spermine (Fig. 1.4). Cell growth declines when spermidine becomes depleted (Marton & Pegg, 1995). The hypothesis that has been accepted generally is that *de novo* synthesis of putrescine is required for neoplastic growth in mammals (Pegg & Feith, 2007). Therefore, the production of putrescine by ODC is an indispensable factor in tumour development (Pegg & Feith, 2007). On the other hand, accumulation of putrescine seems to be associated with the cells undergoing apoptosis (Tome *et al.*, 1997; Yanagawa *et al.*, 1998). Resultant accumulation of putrescine by overexpression of ODC in murine myeloma cells induced apoptosis was inhibited by α-difluoromethylornithine (DFMO), which is a suicide inhibitor of ODC (Mamont *et al.*, 1978). This indicates that high level of putrescine could be toxic to the cell.

ODC is regulated at multiple levels including transcription, translation and protein degradation. ODC is active as a dimer but with a very short half-life of 10-30 min. Its degradation is accelerated by excess concentrations of intracellular polyamines and independent of ubiquitination (Pegg, 2009). Inactivation of ODC activity is achieved by noncovalent binding with the antizyme 1 (AZ1) and the subsequent targeting to the 26S proteasome. Synthesis of AZ1 is proportional to the increase in polyamine content. The mechanism is via a +1 frameshifting that allows read through a stop codon during the translation of AZ1 mRNA, which is stimulated by polyamines (Casero & Marton, 2007; Pegg & Feith, 2007; Pegg, 2009). An increase in AZ1 induced by high levels of polyamines inactivates ODC and therefore decreasing their own biosynthesis (Pegg *et al.*, 2003). Polyamine uptake is also negatively regulated by AZ1 (Murakami *et al.*, 1993) and polyamine efflux may be positively associated with AZ1 (Sakata *et al.*, 2000). In addition,

overexpression of AZ1 in keratin 5 (K5)/AZ transgenic mice decreased spermidine content, stimulated apoptosis and decreased N-nitrosomethylbenzylamine (NMBA) induced forestomach carcinogenesis, suggesting AZ may work as a tumour suppressor gene (Fong *et al.*, 2003).

The other important protein involved in ODC activation is antizyme inhibitor (AZIn). AZIn is structurally similar to ODC but more stably bound to AZ and thus prevents ODC degradation by replacing it in the heterodimer (Pegg, 2009; Pegg & Casero, 2011). The physiological function of AZIn is not yet known, although some studies show expression of AZIn enhanced proliferation and anchorage-independent growth in 3T3 cells (Keren-Paz *et al.*, 2006; Kim *et al.*, 2006). Thus, ODC degradation is inhibited when intracellular polyamine concentrations are low. These regulatory mechanisms are designed for one purpose only that is to maintain intracellular polyamine homeostasis.

ODC activity can be enhanced by a variety of tumour promoters (Marton & Pegg, 1995). ODC is a direct transcriptional target of *c-Myc* oncogene and a target of the *Ras* oncogene as well (Pegg, 2009). Overexpression of *Ras* leads to an increase in ODC activity that plays a central role in tumour development (Pegg *et al.*, 2003). ODC is upregulated in the intestinal mucosa of patients with adenomatous polyposis, a heritable form of colon cancer. The tumour suppressor adenomatous polyposis coli gene (*Apc*) is mutated in these patients. Loss of *Apc* can lead to an increased expression of the *Myc* oncogene (Gerner & Meyskens, 2004).

Evidence indicates that cell transformation can be caused by ODC overexpression. *In vitro* overexpression of ODC led to transformation of NIH 3T3 cells into a malignant phenotype, implying ODC is an oncogene (Moshier *et al.*, 1993; Auvinen *et al.*, 1997). However, *in vivo* ODC overexpression in transgenic mice did not promote tumorigenesis and the polyamine homeostasis was maintained in the physiological levels (Heljasvaara *et al.*, 1997; Alhonen *et al.*, 1995). On the contrary, O'Brien *et al.* (1997) showed ODC overexpression was sufficient for epidermal tumour formation using a keratin 6-driven ODC transgenic mouse model.

ODC is irreversibly inactivated by DFMO. *In vitro,* DFMO caused decreases in putrescine and spermidine, but no change or even an increase in spermine content (Seiler, 2003). This may explain the low toxicity of DMFO to the cell due to its inability to eliminate spermine and consequently total polyamine pools are not depleted completely (Thomas & Thomas, 2001). In addition, daily oral dose of DFMO plus sulindac decreased the recurrence of colorectal adenoma in clinical trials, indicating a chemopreventive effect of DFMO via inhibition of ODC activity (Meyskens *et al.*, 2008). DFMO is successful in inhibiting tumour cell growth *in vitro* studies but failed in clinical trials due to a compensatory uptake of polyamines from extracellular sources such as intestinal microbes or diet. This outcome further emphasises the essence of polyamines and why polyamine homeostasis is highly controlled within the cell (Seiler, 2003).

The other rate-limiting biosynthetic enzyme in polyamine pathway is the pyruvoyl-dependent S-adenosylmethionine decarboxylase (AdoMetDC), which is activated by putrescine and negatively regulated by spermidine/spermine ratio. S-adenosylmethionine, converted from methionine by methionine adenosyltransferase, is decarboxylated by the AdoMetDC to create decarboxylated S-adenosylmethionine (dcAdoMet) (Tolbert *et al.*, 2001). The aminopropyl moiety is donated by dcAdoMet to two constitutive aminopropyltransferases, i.e. spermidine synthase and spermine synthase. Putrescine together with the addition of aminopropyl group provided by dcAdoMet is catalysed by the spermidine synthase to form spermidine. Spermine is formed by spermine synthase via the addition of the aminopropyl group to the N^8-position of spermidine. Polyubiquitination is required for AdoMetDC breakdown (Pegg *et al.*, 2003; Pegg & Casero, 2011). Drug treatment causing reduction of polyamines can increase the half-life of AdoMetDC protein (Pegg, 2009; Nowotarski *et al.*, 2013). In mammalian cells, there are much higher amounts of spermidine and spermine than putrescine. Therefore, the conversion rate of putrescine to spermidine and spermine is not only determined by ODC but also by AdoMetDC (Pegg, 2009).

Polyamines are absolutely essential in mammalian development and critical for normal physiology. ODC (Pendeville *et al.*, 2001) and AdoMetDC (Nishimura *et al.*, 2002) gene knockouts are lethal in embryonic development in mice since spermidine cannot be

synthesised. Snyder-Robinson syndrome (SRS) is an inherited disease caused by a defect in the *SpmS* gene that encodes spermine synthase located on the X chromosome at Xp22.1 (Pegg, 2009). Accordingly, polyamine biosynthetic pathway provides targets for therapeutic intervention.

1.2.4 Polyamine catabolism

Polyamine catabolism refers to the degradation of polyamines in excess. The rate-limiting catabolic enzyme spermidine/spermine N^1-acetyltransferase (SSAT) acetylates by transferring the acetyl group from acetyl-CoA to the N^1 position of spermine (K_m 5-60 μM) and spermidine (K_m 55-140 μM) to form N^1-acetylspermine and N^1-acetylspermidine respectively (Fig 1.4) (Pegg, 2009; Mandal *et al.*, 2013). The physiological level of SSAT is low. SSAT is predominately located in the cytosol. But a large portion of the SSAT was discovered in the mitochondria when induced by BE-3-3-3 in a breast cancer cell line (Holst, *et al.*, 2008; Pegg, 2008). Specific inhibitors of SSAT are so far not available (Pegg & Feith, 2007).

The two catabolic enzymes (SSAT and APAO) are shared by the polyamine retroconversion pathway that converts finally to putrescine from acetylation of spermine and spermidine and subsequent oxidation (Wallace *et al.*, 2003), which forms a loop together with the biosynthetic pathway.

An increase in SSAT activity occurs in response to an increase in intracellular polyamine content and a variety of stimuli including toxins (interferons), hormones (corticosteroids), cytokines (insulin-like growth factor-1), polyamine analogues (BENSpm), cell stress and ischemia-reperfusion injury (Pegg, 2009; Mandal *et al.*, 2013; Casero & Pegg, 2009). The acetylated polyamines can be exported out of the cell or alternatively oxidised by acetylpolyamine oxidase or spermine oxidase. The presence of acetylpolyamines in urine, cell extracts or culture medium is marker of increased SSAT activity (Pegg, 2008).

The second step in polyamine catabolism is catalysed by a constitutively expressed, FAD-dependent, peroxisomal N^1-acetylpolyamine oxidase (APAO) that oxidises N^1-

acetylspermine to produce spermidine and N^1-acetylspermidine to form putrescine. APAO activity may depend upon the availability of its substrates provided by SSAT rather than alterations in enzyme activity or expression (Casero & Marton, 2007; Pegg, 2009). The preference for high affinity substrates by APAO is N^1-acetylspermine > N^1-acetylspermidine > N^1,N^{12}-diacetylspermine >>> spermine (Wu *et al.*, 2003; Wang *et al.*, 2005). APAO produces spermidine and putrescine with the reaction by-products of 3-aceto-aminopropanal (3-AAP) and hydrogen peroxide (H_2O_2), which can be toxic to the cell and cause oxidative stress and consequently cell death (Wang & Casero, 2006; Pegg, 2009; Battaglia *et al.*, 2013). Thus, as a result of the SSAT induction, cellular spermidine and spermine decrease with an increase mainly in putrescine and N^1-acetylspermidine (Mandal *et al.*, 2013).

SMO, the most recent discovered FAD-dependent oxidase by Vujcic *et al.* in 2002, directly converts spermine to spermidine (Fig 1.2). The by-products of the reaction by SMO are the aldehyde, 3-aminopropanal (3-AP), and H_2O_2, which can be toxic to the cell (Casero & Marton, 2007; Battaglia *et al.*, 2013). SMO activity is generally low but it is highly inducible by several polyamine analogues such as N^1,N^{11}-bis(ethyl)norspermine (BENSpm) (Wang *et al.*, 2001; Vujcic *et al.*, 2002). The recombinant SMO has a high affinity for spermine (Km ~ 8 µM) but not polyamine analogues as substrates including BENSpm and N^1-ethyl-N^{11}-((cyclopropyl)methyl)-4,8-diazaunde-cane (CPENSpm) (Wang *et al.*, 2003). Pledgie *et al.* (2005) demonstrated in breast cancer cell lines both SSAT and SMO were induced by BENSpm, leading to antiproliferative effects. Furthermore from this study, the reaction catalysed by SMO was found to be the source of H_2O_2 production, and not the SSAT/APAO pathway. This is because APAO did not seem to play a role in the analogue-induced polyamine catabolism and homeostasis in the MDA MB 231 breast cancer cell line. It was also found that efflux was thought to be the fate of acetylpolyamines rather than oxidation by APAO in the same cell model (Wang & Casero, 2006).

In summary, it is strongly suggested by many studies that the inhibition of cell growth by SSAT induction was directly or indirectly related to H_2O_2 and aldehyde production by both the SSAT/APAO and SMO pathways, which are toxic to the cell. It is thus difficult to distinguish the contribution from either of the pathways to the toxic effects when they

are activated by common molecules such as polyamine analogues (Pegg & Feith, 2007). However, oxidative stress can be a double-edged sword. The growth inhibition may be dependent on the amount of ROS produced as chronic exposure to moderate to high levels of ROS may stimulate tumour cell growth but acute exposure to high levels of ROS can cause DNA damage and cell death (Acharya *et al.*, 2010; Khandrika *et al.*, 2009).
An effective inhibitor of both APAO and SMO is N,N'-(butadienyl)-1,4-buanediamine (MDL72527) (Wang & Casero, 2006), which has been widely recognised and applied in research. MDL72527 is a more potent competitive inhibitor to APAO than SMO (Wu *et al.*, 2005; Bellelli *et al.*, 2004).

It is important to remember that the net outcome of polyamine retroconversion pathway is to recycle higher polyamines back to putrescine which can then be exported out of the cell, degraded by diamine oxidase, or re-enter the cell for polyamine biosynthesis. In addition, acetylated polyamines produced by SSAT are also excreted from the cell including N^1,N^{12}-diacetylspermine (Pegg, 2009). Thus, SSAT is a key regulator in maintaining polyamine homeostasis.

1.2.5 Polyamine transport

Intracellular polyamine homeostasis is systematically regulated by biosynthesis, catabolism, uptake and export. Polyamine transport system (PTS) consists of uptake and export of polyamines. In mammalian cells, the PTS has not yet been isolated successfully. What is known is that the PTS is a time-, temperature- and energy-dependent, carrier mediated, saturable, selective but non-specific system (Seiler, 2003; Casero & Marton, 2007; Palmer & Wallace, 2010). It not only transports polyamines but also delivers polyamine structurally-related compounds such as polyamine analogues and conjugates (Pegg, 2009). Studies by Felschow *et al.* (1997) and Cullis *et al.* (1999) illustrated that polyamine uptake was mediated by transport proteins or putative receptors, which had specific affinities for natural polyamines. Soulet *et al.* (2004) described that an unknown membrane carrier-mediated polyamine uptake system with the polyamine-sequestering vesicles harboured the uptaken polyamines before releasing them into the cytosol in Chinese hamster ovary cells. Another transport model was illustrated by Belting *et al.*

(2003) that glypican 1 played a role in the transport of spermine in mammalian cells. Roy *et al.* (2008) indicated that there is a dynamin-dependent and clathrin-independent endocytic polyamine uptake pathway. SLC3A2 was recently discovered as a transporter involved in putrescine and acetylpolyamine efflux by Uemura *et al.* (2008). This efflux system was closely connected to polyamine acetylation due to that SSAT was co-immunoprecipitated by an anti-SLC3A2 antibody.

Two transport systems have been recognised in most mammalian cell types: a sodium dependent transport system with a preference for putrescine and a sodium independent system capable of transporting spermidine and spermine but not putrescine (Seiler & Dezeure, 1990; Seiler *et al.*, 1996). It is believed that there is an export system for putrescine and N^1-acetylspermidine, but it remains unidentified. The putrescine and N^1-acetylspermidine exported by this mechanism from one cell can be taken up by other cells using the same system (Wallace *et al.*, 2003; Gerner & Meyskens, 2004; Pegg & Feith, 2007).

Using the PTS as a means of delivering cytotoxic drugs such as polyamine conjugates into tumour cells is an attractive strategy of selectively targeting cancer cells being investigated in our laboratory (Palmer *et al.*, 2009; Palmer & Wallace, 2010).

1.3 SSAT, polyamines and cancer

1.3.1 Regulation of SSAT gene

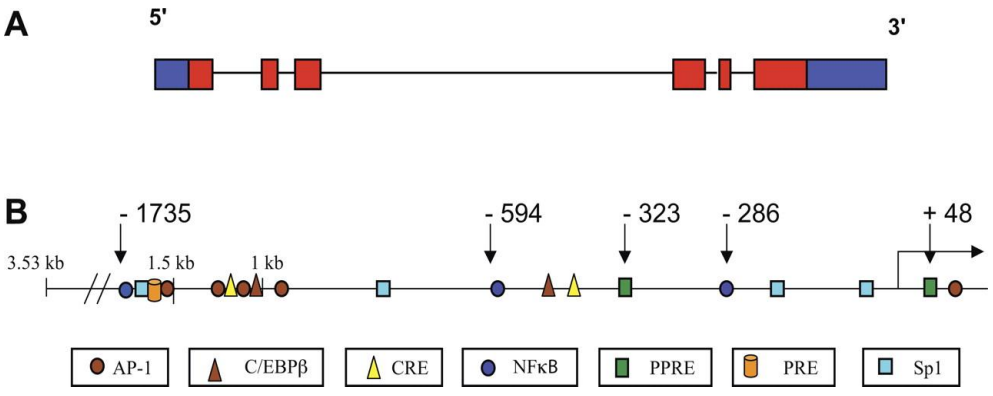

Fig. 1.5 Structure of human SSAT gene. Activation protein-1 (AP-1); CCAT/enhancer binding protein-β (C/EBPβ); cAMP response element (CRE); Nuclear factor-κB (NF-κB); peroxisome proliferator-activated protein response element (PPRE); specificity protein-1 (SP-1) and the polyamine response element (PRE) (Pegg, 2008).

The human SSAT gene (*Sat1*) is located at the Xp22.1 locus on the chromosome X and consists of 6 coding exons. There is a lack of TATA box in the promoter region (Xiao *et al.*, 1992). However, a group of binding sites have been discovered for multiple transcription factors including specificity protein-1 (Sp-1), activator protein-1 (AP-1), cAMP response element binding protein (CREB), NF-κB, and peroxisome proliferator-activated proteins (PPARs) (Fig. 1.5) (Babbar *et al.*, 2006; Choi *et al.*, 2006; Fogel-Petrovic *et al.*, 1993; Xiao *et al.*, 1992). SSAT2 is another protein encoded by *Sat2* gene. However, SSAT2 does not increase acetyl-polyamines or reduce free polyamine content (Chen *et al.*, 2003). The *Sat1* gene codes for a 20 kDa cytosolic enzyme (Wang & Casero, 2006). Regulation of human SSAT occurs at the levels of transcription, post-transcription, translation, and post-translation (Pegg, 2008). A polyamine-response element (PRE), which is located in the *Sat1* gene, allows an increase in SSAT transcription when polyamine content is beyond the requirement of the cell. Nrf-2 interacts constitutively with the PRE, together with polyamine-modulated factor-1 (PMF-1) initiate the SSAT transcription responsive to polyamines (Wang & Casero, 2006; Wang *et al.*, 1999) (Fig. 1.6).

Superinduction of SSAT by polyamine analogues in certain tumour cell types is initiated from an increase in transcription regulated by PRE (Pegg, 2008). In addition, the stability of SSAT mRNA is augmented by polyamines and their analogues. The half-life of SSAT protein is prolonged from ~15 min to >> 12 h by binding of polyamines or polyamine analogues, which prevents SSAT polyubiquitination (Coleman & Pegg, 1997; Fogel-Petrovic *et al.*, 1996; Fogel-Petrovic *et al.*, 1997). A dramatic increase in SSAT protein results to a lesser extent in the increase in SSAT mRNA in response to polyamine analogues. Although the upregulation of SSAT transcription is indispensable for the cell type-specific SSAT induction by polyamine or polyamine analogues, the SSAT protein stabilisation plays a major role (Fogel-Petrovic *et al.*, 1997; McCloskey *et al.*, 1999; Wang & Casero, 2006; Xiao & Casero, 1996). It is noteworthy that the superinduction of SSAT protein has only been seen in cells treated with polyamine analogues, regardless of whether SSAT expression is endogenous or transfected (Wang & Casero, 2006).

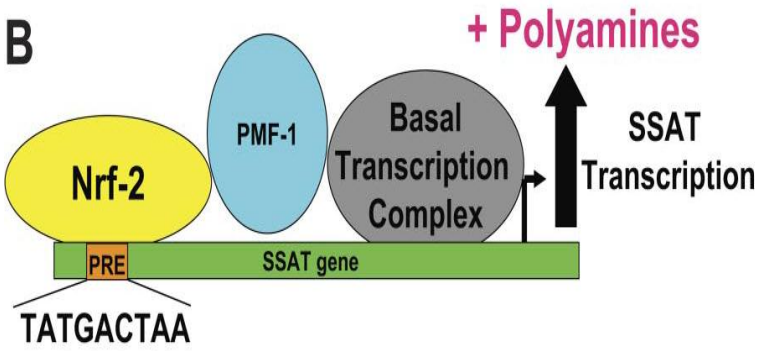

Fig. 1.6 Transcriptional regulation of SSAT gene (Pegg, 2008)

$H_2N(CH_2)_3NHR$ is the general structure of SSAT substrates. The high affinity substrates include spermidine, N^1-acetylspermine, sym-norspermine, and sym-norspermidine. Spermine can be acetylated at either end because of its symmetrical structure. Polyamines with terminal aminobutyl groups are not substrates for SSAT, including putrescine, N^1-acetylspermidine, and sym-homospermidine. Additionally, N^1,N^{12}-diacetylspermine is formed from N^1-acetylspermine by SSAT (Della Ragione & Pegg, 1983).

1.3.2 SSAT in carcinogenesis

Alteration in polyamine homeostasis is associated with carcinogenesis. SSAT has been elucidated as having an important role in either promoting or suppressing carcinogenesis in both *in vitro* and *in vivo* model systems. For example, ODC and SSAT activity were both increased in the epithelial cells of the rat bladder treated with N-butyl-N-(4-hydroxybutyl)nitrosamine (BBN) and in the hyperplastic epithelial cells in the bladder of rats by melamine, implying the role of SSAT in bladder carcinogenesis (Matsui-Yuasa *et al.*, 1992). Likewise, an induction of SSAT activity by CB3717, a quinazoline analogue of folic acid, was seen as a proliferative response in mouse kidney undergoing hyperplasia and hypertrophy (Dudkowska *et al.*, 2002). Furthermore, it was believed that a high spermidine/spermine ratio observed in many cancers suggested an accelerated

conversion of spermine to spermidine by increased SSAT activity. SMO contributes to this reaction as well, however, it was not identified until 2002 by Vujcic *et al.*

1.3.2.1 SSAT transgenic mice models

It may have been supposed that an elevated SSAT activity leads to a decline of polyamine content, therefore, impairing the development of neoplasia. However, the role of SSAT in carcinogenesis is paradoxical.

The SSAT transgenic mice present a unique phenotype including hair loss, female infertility, weight loss, CNS effects and altered lipid metabolism and a tendency to develop pancreatitis (Pegg & Feith, 2007). In the study of transgenic adenocarcinoma of mouse prostate (TRAMP)/SSAT biogenic mice, SSAT overexpression effectively suppressed tumour outgrowth and interfered the disease progression. The perturbation of polyamine homeostasis in the mice was substantial accumulation of putrescine and N^1-acetylspermidine. The spermidine pools were relatively unaffected while spermine was slightly decreased by ~33%. This inhibition of tumour growth was found to be associated with an inhibition of fatty acid synthesis because of the depletion of the polyamine acetylation co-factor acetyl-CoA content in the SSAT transgenic mice (Kee *et al.*, 2004a). This result is consistent with the *in vitro* findings in LNCaP/SSAT transgenic prostate cancer cells (Kee *et al.*, 2004b). The effect of acetyl-CoA consumption by polyamine acetylation was further investigated on fat and glucose homeostasis. Studies on white adipose tissue by Liu *et al.* (2013) found increased glucose metabolism, deficient ATP by enhanced polyamine metabolic flux in SSAT-overexpressed mice. SSAT-knockout mice showed accumulation of acetyl-CoA and ATP, decreased β-oxidation, increased lipogenesis and body weight. The results suggest an important role of SSAT induction in prevention of the development of obesity. Overall, induction of SSAT inhibits tumorigenesis in the TRAMP mice.

In contrast, the SSAT transgenic mice models can be system dependent (Pegg & Feith, 2007). *Apc*$^{Min/+}$ multiple intestinal neoplasia (Min) mice bear a truncation mutation in the adenomatous polyposis coli (*Apc*) tumour suppressor gene so that the mice are

predisposed to the development of intestinal adenomas. The *Apc*$^{Min/+}$ mice were then crossed bred with *Sat1* overexpressed mice. As a result, overexpression of SSAT was demonstrated to stimulate formation of polyps in both the intestine and the colon in the Min mice. On the other hand, 75% tumour reduction was seen in the crosses of the *Apc*$^{min/+}$ mice with SSAT knockout mice (Tucker *et al.*, 2005). The mechanism by which increased SSAT promoted tumorigenesis in mice is thought due to a metabolic ratchet or flux driven by spermidine and spermine homeostasis. The consequences of this increased polyamine metabolic flux are consumption of substrates in polyamine biosynthetic pathway, such as putrescine, methionine, and S-adenosylmethionine, and substantial release of reactive products of polyamine catabolism pathway, such as putrescine, N^1-acetylspermidine, H_2O_2, and 3-acetamidopropanal (Fig 1.7). Tucker *et al.* (2005) proposed that a phenotype is changed at some turning point when either a substrate becomes rate-limiting or a product becomes toxic.

Similar results were illustrated by Coleman *et al.* (2002) using the keratin (K6) promoter to express SSAT cDNA only in the skin of the K6/SSAT transgenic mice. Both the tumour incidence and development in the skin were increased in response to the two-stage tumorigenesis protocol with 7,12-dimethyl-benz[a]anthracene (DMBA) and phorbol ester 12-O-tetradecanoylphorbol-13 acetate (TPA). This finding is intriguing because at the resting state there was only a very small extent of SSAT overexpression. But SSAT activity and protein were further elevated in the tumours compared with that in the non-transgenic littermates. Moreover, most of the tumours progressed rapidly to carcinomas in the K6/SSAT mice. Total polyamines were not affected by induced SSAT but increased polyamine acetylation was found in the skin tumours supported by increased content of putrescine and N^1-acetylspermidine. Thus, the increased tumour incidence in the K6/SSAT mice indicates a key role of altered polyamine homeostasis in tumorigenesis and a responsible possibility of the heightened oxidative stress by SSAT/APAO pathway (Pegg *et al.*, 2003).

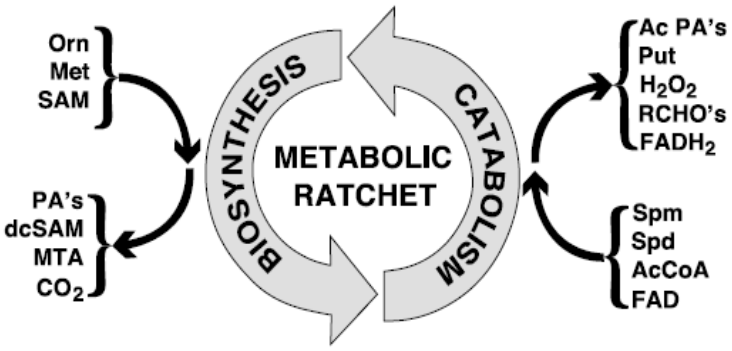

Fig. 1.7 Metabolic ratchet model of polyamine homeostasis (Tucker *et al.*, 2005)

Both the skin and intestine of transgenic mice with SSAT overexpression had a dramatic increase in intracellular putrescine and N^1-acetylspermidine but a small fall in spermidine and spermine. Unfortunately, extracellular polyamines and their export were not measured in these studies.

Nevertheless, the products of acetylation, i.e. acetylpolyamines, are unlikely to stimulate this tumour formation. MDL72527, the APAO inhibitor, was shown to reduce the tumour incidence in K6/SSAT mice. This is because that MDL72527 caused a further increase of N^1-acetylspermidine (Wang *et al.*, 2007), suggesting N^1-acetylpolyamines may be growth-inhibitory rather than growth-stimulating to the tumour cells. This, on the other hand, implies that the other products of polyamine oxidation could contribute to the tumour formation, i.e. putrescine, ROS, aldehydes, and N-acetylaminopropanal (Pegg & Feith, 2007). Without doubt, oxidative stress by ROS can lead to DNA damage and further contribute to tumour development. A study by Basu *et al.* (2009) demonstrated that ROS production by an androgen analogue R1881 was due to SSAT induction followed by oxidation of acetylpolyamines by APAO rather than a direct oxidation of spermine by SMO in LNCaP cells. In their TRAMP/FVB mouse model of prostate carcinogenesis MDL72527 slowed the prostate tumour growth, indicating the potential of MDL72527 as a new therapeutic agent for prostate cancer.

In addition to the toxic effect caused by oxidative stress, the net outcome to polyamine content in these transgenic mice was markedly increased putrescine, but with a small

decline in spermidine and spermine. The increase in putrescine was achieved not only from the upregulation of polyamine biosynthesis but also from the retroversion pathway via SSAT/APAO. Therefore, the focus of attention is conversion to putrescine rather than spermidine as a critical factor in promoting neoplasia (Pegg, 2008). Evidence showed the treatment of the K6/SSAT tumour-bearing mice with DFMO caused regression of established tumours strongly supporting the hypothesis that *de novo* synthesis of putrescine by ODC is needed in carcinogenesis (Pegg & Feith, 2007).

Transgenic mice models, however, might not be suitable for studies on carcinogenesis and tumour development due to the fact that the maintenance of these mice is based on a mixed genetic background, the nature in polyamine metabolism is altered, and the presence of multiple secondary phenomena in the mice (Pegg *et al.*, 2003).

1.3.2.2 *In vitro* SSAT transgenic models

In vitro transgenic models are easier to manipulate under controlled conditions with less mixed environment than *in vivo* models. Mandal *et al.* found (2013) that the overexpression of SSAT in Hela cells led to polyamine depletion, total inhibition of protein synthesis and growth arrest. The results by Vujcic *et al.* (2000) using human SSAT cDNA transfected MCF-7 breast cancer cell line showed a growth inhibition by SSAT overexpression because of a progressive reduction of polyamine pools, with an absence of increased ODC activity in the cells. However, in human SSAT cDNA transfected prostate carcinoma LNCaP cells, the growth inhibition by overexpression of SSAT is not due to the depletion of polyamines, but the loss of acetyl-CoA pools caused by an increase in metabolic flux through the polyamine pathway (Kramer *et al.*, 2008). In addition, embryonic stem cells with the SSAT gene knocked out grow normally and contain normal polyamine content (Niiranen *et al.*, 2002). Taken all together, this might suggest that the outcome of SSAT induction depends on cell types.

1.3.3 Induction of SSAT by polyamine analogues and anticancer drugs

There are a great many studies focusing on induction of SSAT using polyamine analogues, such as BENSpm. Polyamine analogues can cause inhibition of ODC and AdoMetDC activity and subsequent polyamine biosynthesis, induction of SSAT and subsequent depletion of intracellular polyamines.

Under physiological conditions SSAT expression is repressed at the translational level (Perez-Leal & Merali, 2012). However, the SSAT gene is identified as one of the most highly inducible genes (Allen *et al.*, 2007). Polyamine analogues are structural derivatives of natural polyamines, such as N^1,N^{11}-diethylnorspermine (DENSpm or BENSpm). The polyamine analogues with a structure of the bis(ethyl)polyamine are the most potent inducers of SSAT activity to date (McCloskey *et al.*, 1999). The mechanism is not clear how the analogues are able to cause "superinduction" in SSAT activity and whether SSAT induction is integral to the cytotoxicity of the analogues (McCloskey *et al.*, 1999). It is generally known that the "superinduction" by the analogues is a result of an increase in SSAT transcription, translation, and stabilisation of the protein (Coleman & Pegg, 2001). However, the binding of polyamine analogues to SSAT can also inhibit the enzyme activity. This could result in an overestimation of *in vivo* SSAT activity, depending upon the values obtained in *in vitro* assays (Pegg & Feith, 2007). It is intriguing that in an *in vitro* model of transgenic tumour cells, an increase in SSAT protein is initiated from an increase in the mRNA. However, in the transgenic mice study, only after exposures to polyamine analogues do they express a high level of SSAT protein and activity (Pietila *et al.*, 1997).

SSAT induction contributes significantly to the polyamine analogue mediated growth inhibition and/or apoptosis (Kramer *et al.*, 2008). An *in vitro* study shows that SSAT overexpression led to a growth arrest in MCF-7 SSAT gene transfected breast cancer cells due to the depletion of intracellular polyamines by BENSpm. These cells were found to be more sensitive to BENSpm than the WT MCF-7 (Vujcic *et al.*, 2000). It is generally considered that one of the mechanisms by which cell growth inhibition by polyamine analogues occurs is at least partially due to the superinduction of SSAT. This

superinduction is a result of SSAT protein stabilisation (Murray-Stewart *et al.*, 2003; Wang & Casero, 2006).

SSAT mRNA expression was induced by 5-FU in HCT116, H360, HT-29, LoVo, HCT175, and HCT248 colorectal cancer cell lines (Allen *et al.*, 2007). Exposure of MCF-7 cells to 5-FU alone also led to an increase in expression of SSAT mRNA (Maxwell *et al.*, 2003). The combination of 5-FU with BENSpm not only resulted in a synergistic increase in SSAT mRNA expression but also an increased apoptosis in contrast to either treatment alone. However, these studies did not present data on SSAT protein or activity. In addition, results from Hector *et al.* (2004) demonstrated that the combination of oxaliplatin and DENSpm produced a synergistic effect increasing SSAT mRNA and protein and growth inhibition in melanoma and ovarian cancer cells. Without DENSpm, there was a lack of increase in SSAT protein, indicating a regulation at translational, post-translational and protein stabilisation in SSAT induction by polyamine analogues. Moreover, compared to DENSpm treatment alone, a lower dose of DENSpm is able to achieve the same SSAT induction while combined with the classic cytotoxic agents. Thus, it provides promising indications that such combinations may surpass the limitations of using polyamine analogues alone (Wang & Casero, 2006). A combined treatment of DENSpm with 5-FU or oxaliplatin led to a dramatic increase in SSAT mRNA and protein than treatment alone and synergistic effect of cell death in HCT116 colorectal cancer cells. Additionally, the combination of chemotherapeutic agent and DENSpm sensitises the drug-resistant cell lines to cell death induced by cytotoxic drugs (Allen *et al.*, 2007).

1.3.4 Induction of SSAT by NSAIDs

It is known that NSAIDs are inducers of SSAT. Aspirin is one of the classic NSAIDs. There are two mechanisms involved in the induction of SSAT by aspirin according to Babbar *et al.* (2006 & 2003). The binding of NF-κB on *Sat1* gene was increased by aspirin, which led to a rise in SSAT transcription. TNF-α induced SSAT is also via NF-κB signalling. The other mechanism of aspirin induced SSAT transcription was via the peroxisome proliferator-activated receptor (PPAR) element and PPAR-γ as there are two PPAR response elements in the SSAT gene.

An increase in SSAT by aspirin and sulindac sulfone led to a fall in intracellular polyamines and cell growth inhibition in a cyclooxygenase-independent manner (Turchanowa *et al.*, 2001; Hughes *et al.*, 2003; Babbar *et al.*, 2003). Aspirin is now an accepted chemopreventative agent in colon cancer. Therefore, it is likely that SSAT induction by aspirin plays a role in reducing carcinogenesis caused by inflammatory stress.

1.3.5 Association of SSAT with other diseases

Acute pancreatitis can be induced by increased polyamine catabolism and resultant polyamine loss in transgenic rats overexpressing SSAT treated with zinc. This is supported by the evidence that supplementation with methylated polyamine analogues prevented the pancreatitis as they are not SSAT substrates (Hyvonen *et al.*, 2007; Merentie *et al.*, 2007).

Increased SSAT activity was seen in the kidney epithelial cells after ischemia-reperfusion. This led to DNA damage and G2 arrest (Zahedi *et al.*, 2007). However, SSAT seemed to be protective in the cell death of ischemic myocardium (Ryu *et al.*, 2008).

Spermidine is critically required for liver regeneration after partial hepatectomy as it is essential for DNA synthesis and hepatocyte proliferation (Pegg, 2008; Alhonen *et al.*, 2002). The liver regeneration was prevented by overexpression of SSAT in transgenic mice unless 1-methylspermidine was provided, which is not a SSAT substrate (Hyvonen *et al.*, 2007; Rasanen *et al.*, 2003).

Hair loss and wrinkling skin are the typical phenotype in transgenic mice of SSAT overexpression, resulting from the loss of hair follicles to dermal cysts (Wang & Casero, 2006). It is interesting because ODC overexpressing mice presents similar hairless phenotype (Soler *et al.*, 1996). This is believed to be due to a very high level of putrescine on hair follicle development from both ODC and SSAT overexpression (Wang & Casero, 2006; Pegg, 2008; Pietilä *et al.*, 2001).

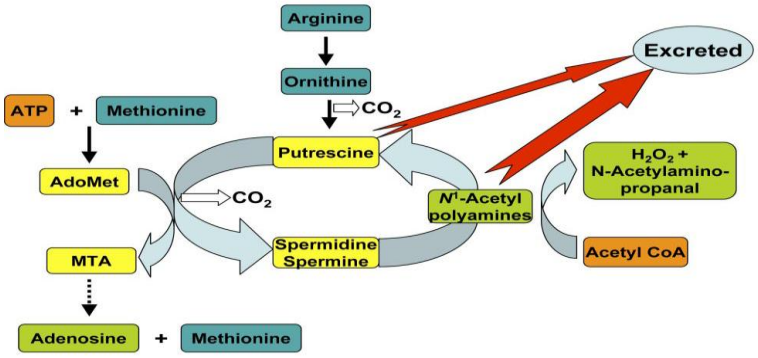

Fig. 1.8 Consumption of ATP and acetyl-CoA and increased oxidative stress as a result of enhanced SSAT activity (Pegg, 2008)

SSAT overexpression has been indicated in association with carbohydrate and lipid metabolism. SSAT transgenic mice are leaner with a low body fat and high basal metabolic rate than the WT mice. The fall in acetyl-CoA is thought to be the trigger because SSAT uses acetyl-CoA as a cofactor for its acetylation (Fig. 1.8). Fatty acid oxidation is increased due to the fall in acetyl-CoA and related to a decline in malonyl-CoA. This leads to an augmentation in oxidation of glucose and palmitate and eventually a loss of fat (Jell *et al.*, 2007; Kramer *et al.*, 2008). Evidence by Pirinen *et al.* (2007) reveals that DFMO reversed the loss of body fat and decrease in white adipose tissue in SSAT overexpressing mice. This therefore indicates that SSAT could be a useful target in treatment of obesity and type 2 diabetes (Pegg, 2008).

On the other hand, an increase in polyamine catabolism by SSAT overexpression leads to a significant loss of ATP. Overexpression of SSAT causes an increase in ODC and AdoMetDC activity. Polyamine biosynthesis is an energy dependent process that three ATP molecules are needed when methionine is converted to AdoMet and two molecules of AdoMet are required for spermine synthesis. Thus, it is possible that ATP is used up in a futile cycle created by SSAT overexpression (Pirinen *et al.*, 2007; Pegg, 2008) (Fig 1.8).

The only discovered genetic disease linked to SSAT overexpression is keratosis follicularis spinulosa decalvans (KFSD). The disease is found to have a gene duplication including *Sat1* region on the X chromosome. Increased SSAT, reduced spermidine and increased putrescine were observed in cultured fibroblasts from the patient. Except for follicular

hyperkeratosis and vision defect, similar skin changes were seen in KFSD patient to those observed in SSAT-overexpressing mice. It is thought this is derived from gain-of-function mutants in *Sat1* gene (Gimelli *et al.*, 2002; Pegg, 2008).

1.4 Polyamines and cancer

The interest in polyamine metabolism in cancer cell biology and anticancer therapy is based on two main findings: increased polyamine biosynthesis is associated with cell proliferation, decreased apoptosis and increased expression of genes affecting tumour invasion and metastasis. The other is that depletion of intracellular polyamines are associated with inhibition of cell growth, increased apoptosis and decreased expression of genes affecting tumour invasion and metastasis (Gerner & Meyskens, 2004). The polyamines have a fundamental role in the cell growth and differentiation in both normal and tumour cells. A survival advantage in tumour cells versus normal cells is due to their higher capacity of polyamine synthesis since ODC and SAMDC are upregulated in tumour cells. One of the main characteristics of cancer cells is uncontrolled proliferation and polyamine biosynthesis is upregulated in most solid tumours. On the other hand, polyamine induced apoptosis occurs when intracellular polyamines are extremely high with the resultant loss of polyamine homeostasis regulation (Gerner & Meyskens, 2004).

Nilsson *et al.* (2005) illustrated that lymphoma development induced by activation of *c-Myc* was delayed in $Odc^{(+/-)}$ transgenic mice. In addition, ODC reduction by transgenic AZ expression blocked skin carcinogenesis and reduced tumour incidence in mice models (Fong, *et al.*, 2003; Feith *et al.*, 2007). Clinical evidence shows that ODC activity was significantly higher in cancer tissue than pair-matched benign tissue of patients with prostate cancer. So was it higher in the prostatic fluid (Mohan *et al.*, 1999).

Taken all together, these observations make polyamine metabolic pathway a reasonable target for cancer chemotherapy and chemoprevention.

Although the link between polyamines and cancer has been well known for more than 50 years, direct evidence indicating that polyamines have a causative rather than associative

role in the mechanism of carcinogenesis is lacking. In other words, specific underlying mechanisms of polyamine regulated cellular response have not been defined. Thus, this has become a key criticism in polyamine research field (Gerner & Meyskens, 2004).

1.5 Prostate cancer

1.5.1 Physiology of prostate gland

The human prostate gland is located in front of the rectum and just below the bladder surrounding the urethra (Fig. 1.9). The size of the prostate gland is slightly larger than a walnut with an average weight of 11 grams (Leissner & Tisell, 1979). It can be detected by a digital rectal examination. The prostate gland functions to secrete a slight alkaline milky fluid that constitutes 50-75% of the seminal fluid so as to facilitate transporting sperm during male orgasm (Myers, 2000; Omabe & Ezeani, 2011).

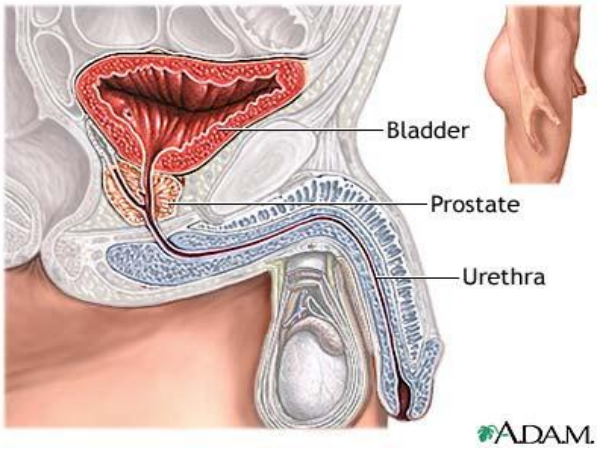

Fig. 1.9 Anatomical illustration of human prostate gland
(http://www.umm.edu/patiented/articles/what_benign_prostatic_hyperplasia_000071_1.htm)

1.5.2 Epidemiology and aetiology of prostate cancer

Prostate cancer is the second most frequently diagnosed cancer in men after lung cancer and the fifth most common cancer overall worldwide (Globocan, 2008). The geographic variation in the incidence of prostate cancer is the first enigma (De Marzo *et al.*, 2007). The prevalence of prostate cancer in Asia is lower than western countries. The highest incidence rates are found in Australia/New Zealand, western and northern Europe, such as Scandinavian countries, and northern America and it is particularly high in African Americans. The lowest rates are in Asia, for instance in Chinese and Japanese, suggesting a geographical association of incidence. However, the risk of developing this disease is increased in Asian men who migrate to the US, indicating that environmental factors participate in carcinogenesis of the prostate gland (Sandhu & Schlegel, 2004; Benedettini *et al.*, 2008; Omabe & Ezeani, 2011; Thapa & Chosh, 2012) (Fig. 1.10).

The second enigma is the organ selectivity of prostate cancer within the genitourinary system due to the fact that approximately 280,000 new cases occur in US each year compared with less than 50 cases of primary seminal vesicle carcinoma reported (De Marzo *et al.*, 2007).

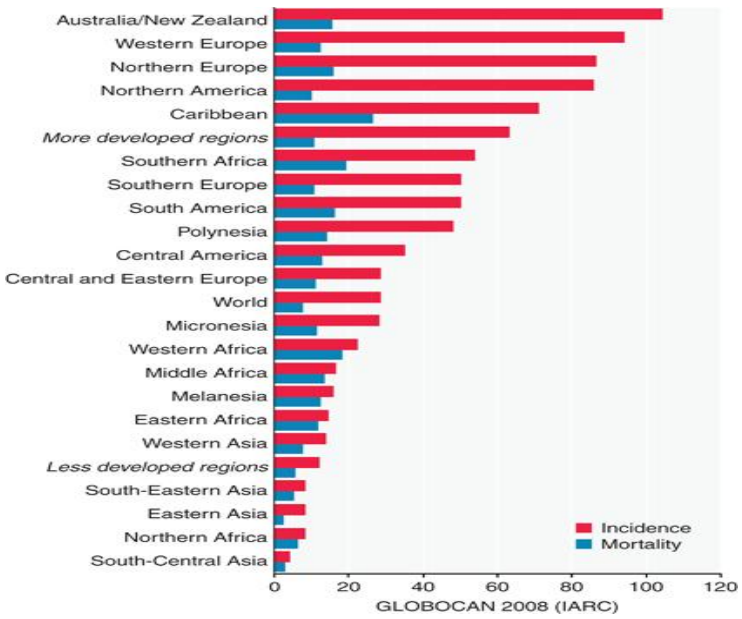

Fig. 1.10 Estimated age-standardised rates of prostate cancer incidence (World) per 100,000 (http://globocan.iarc.fr/factsheet.asp)

Important risk factors contributing to the incidence of prostate cancer are advancing age, race, geographical distribution, diet and family history (Isaacs *et al.*, 2002). Prostate cancer is mainly a disease of aging. It is rare in men who are younger than 45 years as most cases are discovered above age 50. This indicates that slow cellular metabolic alterations are occurring over the years having an influence on the development of this disease (Khandrika *et al.*, 2009). A high saturated fat enriched diet (such as from red meat) and obesity are also thought to be critical risk factors in prostate tumour development. Lycopenes from tomatoes, soy protein and cruciferous vegetables have been shown to have anti-tumour effects with a reduced prostate cancer risk due to their high antioxidant activity (Cohen *et al.*, 2000), implying a loss of redox balance is important in prostate cancer cells. Hormones such as testosterone are necessary for the development of prostate cancer since it is an androgen dependent disease in the early stages (Isaacs *et al.*, 2002; Sandhu & Schlegel, 2004).

1.5.3 Carcinogenesis of prostate cancer

The prostate gland is classified pathologically into four zones: peripheral (~70% by volume), central, transition (~25%), and anterior fibromuscular zone or stroma. However, it is difficult to histologically determine the three zones in a normal prostate (Lalani *et al.*, 1997; Benedettini *et al.*, 2008) (Fig. 1.11).

Prostate cancer refers to a malignant non-cutaneous neoplasm of the glandular cells of the prostate gland. Adenocarcinoma is the most common form (> 90%) derived from the peripheral zone of the prostate. Around 80% of prostate cancer lesions are developed from the periphery region of prostate gland, most of the remaining lesions stem from the periurethral region (Sandhu & Schlegel, 2004; Benedettini *et al.*, 2008). This becomes the third unsolved enigma that the carcinogenesis of prostate cancer has a zonal predilection (De Marzo *et al.*, 2007).

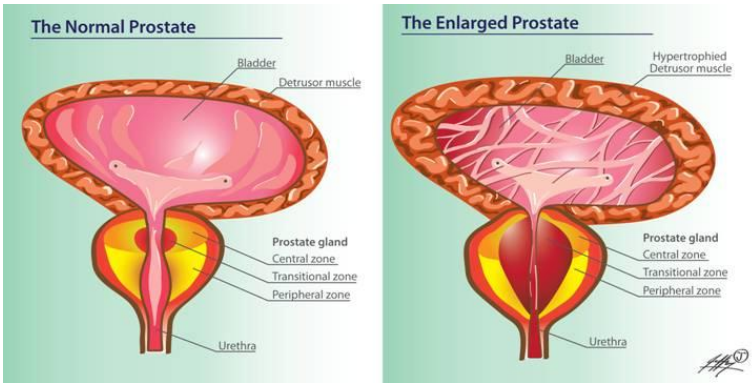

Fig. 1.11 Zones of the normal and enlarged human prostate
(http://www.endotext.org/male/male9/male9_clip_image004_0010.jpg)

Androgens are fundamental elements in the growth, differentiation and development of the prostate. They play a critical role in prostate carcinogenesis as the androgen deprivation therapy is initially effective in inhibiting prostate tumour growth. However, advanced prostate cancer becomes incurable when the disease has spread beyond the prostate and the cancer cells are able to sustain proliferation even in the absence of androgens (Khandrika *et al.*, 2009).

The Gleason score system is used clinically to evaluate the glandular pattern in prostate tumour cells. It is a critical index of the progression of prostate cancer. A grade of 1-5 is assigned to identify predominant and secondary patterns of glands within the tumour, i.e. how resemblance of the cells in cancerous tissues compared with normal prostate tissue.

Grade 1 represents the least aggressive or most differentiated. Grade 5 represents the most aggressive or least differentiated. Grade 2-4 represents the pathological features between grade 1 and 5. As prostate cancers usually have areas with different grades in a biopsy sample, a grade is assigned to the two areas that consist of most common pattern and pattern with the highest grade. These two grades are added together to provide a "Gleason score" that is evaluated between 2 to 10 (Sandhu & Schlegel, 2004). In general, prognosis of cancer by Gleason score indicates:

2-4: cancers rarely progress early or cause death within 10 years;
5-6: localised tumours;

7: prognosis is significantly worse than 5 or 6;

8-10: at least microscopically metastasised prior to detection.

In the UK the description of Gleason score for prostate cancer is shown in Table 1.1 (prostate cancer UK, 2012).

Gleason score	Description
3 + 3	All of the cancer cells found in the biopsy look likely to grow slowly.
3 + 4	Most of the cancer cells found in the biopsy look likely to grow slowly. There were some cancer cells that look more likely to grow at a more moderate rate.
4 + 3	Most of the cancer cells found in the biopsy look likely to grow at a moderate rate. There were some cancer cells that look likely to grow slowly.
4 + 4	All of the cancer cells found in the biopsy look likely to grow at a moderately quick rate.
4 + 5	Most of the cancer cells found in the biopsy look likely to grow at a moderately quick rate. There were some cancer cells that are likely to grow more quickly.
5 + 4	Most of the cancer cells found in the biopsy look likely to grow quickly.
5 + 5	All of the cancer cells found in the biopsy look likely to grow quickly.

Table 1.1 Description of Gleason scores in prostate cancer
(http://prostatecanceruk.org/toolkits/how-prostate-cancer-is-diagnosed)

The higher the Gleason score, the more aggressive the cancer and the more likely it is to spread. Thus, the extent of cellular differentiation or grade is generally defined in accordance to their Gleason score:

Well differentiated or *low-grade*: a Gleason score of 6 or less

Moderately differentiated or *intermediate-grade*: a Gleason score of 7

Poorly differentiated or *high-grade*: a Gleason score of 8-10

High-grade prostatic intraepithelial neoplasia (PIN) associated with invasive carcinoma and proliferative inflammatory atrophy (PIA) of prostate cells are thought to be the precursor lesions of prostate cancer. PIA formation is associated with oxidative stress

mediated by inflammatory cells, which plays a key role in the mechanism of prostate carcinogenesis (Isaacs *et al.*, 2002).

Prostate adenocarcinoma presents grade heterogeneity. In the same gland multiple, spatially separate and clonally distinct foci exist (Andreoiu & Cheng, 2010). A "field effect" theory addresses the formation of multifocal cancerous precursor lesion with the hypothesis that prostate cells that possess genetic predisposition and are exposed to chemical and biological carcinogens develop to form multiple precursor lesions and finally evolve into spatially separated and distinct cancers. Additionally, distinct foci seem to arise independently (Andreoiu & Cheng, 2010).

It has been demonstrated that a number of oncogenes such as *RNAse1* and *MSR1* appear to be associated with progression and severity of hereditary prostate cancer. Moreover, the androgen receptor (AR), *p53*, *Bcl2*, *ETV1* and *ERG1* genes are also involved in prostate cancer progression and metastases (Benedettini *et al.*, 2008).

Benedettini *et al.* (2008) speculated that prostate tumorigenesis is promoted by an increase in fatty acid synthesis. Acetyl-CoA that is necessary for fatty acid synthesis is supplied via the aerobic glycolysis associated with a high intake of glucose. Fatty acid synthase (FASN) and acetyl-CoA carboxylase are overexpressed in many tumour types including prostate cancer. The role of FASN is to maintain energy homeostasis through conversion of spare carbon intake into fatty acids for storage. In the transgenic adenocarcinoma of the mouse prostate (TRAMP) model inhibition of FASN activity by its inhibitors, cerulenin and C75, resulted in apoptosis and reduction in tumour size (Benedettini *et al.*, 2008).

1.5.4 Inflammation in prostate cancer

It is already known that chronic infection and inflammation can cause cancers in the stomach, liver and large intestine. In the prostate, PIA has been termed by De Marzo *et al.* (2007) that describes the histological lesions in the prostate epithelium exposed to infectious agents and dietary carcinogens. Histological transitions between the PIA and

high-grade PIN or adenocarcinoma have been reported (De Marzo *et al.*, 1999; Montironi *et al.*, 2002; Putzi & De Marzo, 2000). The somatic epigenetic alterations in PIA lesions, such as hypermethylation of cytosine bases in the gene encoding the π-class glutathione S-transferase (*GSTP1*), is believed to the mechanistic link between inflammation and prostate cancer (Bardia *et al.*, 2009). The infectious agents inducing inflammation in the prostate include sexually and non-sexually transmitted bacteria such as *Chlamydia trachomatis* (Poletti *et al.*, 1985) and *Escherchia coli* (De Marzo *et al.*, 2007), viruses such as human papillomavirus (HPV) (Strickler & Goedert, 2001). In addition to the infectious organisms, chemical compounds in the urine reflux might be toxic to the prostate epithelial cells (De Marzo *et al.*, 2007), such as crystalline uric acid released from dying cells can cause the production of inflammatory cytokines (Martinon *et al.*, 2006). Men with a history of prostatitis also present an increased risk of developing prostate cancer (Bardia *et al.*, 2009).

Heterocyclic amines (HCAs) have been implicated in the mechanisms of prostate cancer development in relation to the consumption of red meat and animal fats (Sugimura *et al.*, 2004). High temperature cooking especially charbroiling fatty meats can generate HCAs (Bardia *et al.*, 2009). Evidence supporting this hypothesis shows dietary 2-amino-1-methyl-6-phenylimidazo[4,5-b]pyridine (PhIP) led to carcinoma in the prostate in rats through induction of inflammation and atrophy (Sugimura *et al.*, 2004; Knize & Felton, 2005; Borowsky *et al.*, 2006).

In relation to polyamine pathway, SMO expression is an early event in the development of the prostate cancer (Goodwin *et al.*, 2008). A strong link has been established between the inflammation and DNA damage via the production of H_2O_2 by SMO pathway, indicating a role of SMO in ROS-induced DNA damage and carcinogenesis (Cervelli *et al.*, 2012).

A study by Mahmud *et al.* (2006) demonstrated use of aspirin, a classical nonsteroidal anti-inflammatory drug (NSAID), was inversely associated with a 42% reduction in the odds of prostate cancer detection. This result indicates a role of inflammation in tumorigenesis of the prostate.

The association between chronic inflammation associated with oxidative stress and free radical production has already been addressed. Reactive oxygen species (ROS) are released from activated phagocytic inflammatory cells of the innate immune system and then cause oxidative damage to genomic DNA and facilitate the carcinogenesis in the prostate (Bardia *et al.*, 2009; Ames & Wakimoto, 2002; De Marzo *et al.*, 2007). It seems that inflammation and oxidative stress are reciprocal cause and effect.

1.5.5 Oxidative stress in prostate cancer

ROS includes hydroxyl radicals, peroxides and superoxides that are normal metabolites generated by the cell during aerobic metabolism. These highly reactive molecules play a central role in redox signalling. Factors that can increase cellular ROS production include aging, radiation, carcinogens, inflammation and activated oncogenes (Thapa & Ghosh, 2012). Increased ROS levels inside cells are associated with tissue injury, DNA damage, neoplastic transformation and aberrant growth and proliferation, which could eventually contribute to the initiation and progression of cancer. Oxidative stress to cells can be caused by excess ROS production and/or inefficiency of antioxidant defence systems (Khandrika *et al.*, 2009). Enzymes that consist of the backbone of the antioxidant defence system include superoxide dismutase, catalase, glutathione peroxidase, glutathione reductase and (nicotinamide adenine dinucleotide phosphate) NADPH. For example, superoxide dismutase converts superoxide ($2O_2^-$) and $2H^+$ into H_2O_2 and O_2, while catalase and glutathione peroxidase eliminate H_2O_2 (Thapa & Ghosh, 2012). Glutathione (GSH) is a well-known antioxidant molecule. It is synthesised in the cytosol and imported into the mitochondria. It protects the mitochondria from the damage by ROS as a result of electron transport (Armstrong *et al.*, 2002).

It is generally agreed that chronic exposure to moderate to high levels of ROS stimulates tumour cell growth, whereas acute exposure to high levels of ROS leads to cell death and irreversible damage. Therefore, development of prostate tumours would be promoted when chronically exposed to an environment of moderately elevated ROS (Khandrika *et al.*, 2009). Impairment of cellular redox balance is an important contributor to carcinogenesis. Formation of prostate cancer is associated with a shift from the status of

antioxidant-prooxidant towards increased oxidative stress (Ripple *et al.*, 1997). Mitochondria are known as a major source of ROS generation. The increase in ROS by mitochondria results from the accelerated mtDNA mutations (Khandrika *et al.*, 2009).

High intracellular ROS has been shown to be a manifestation of aggressive growth, proliferation and metastatic ability of prostate cancer cells (Kumar *et al.*, 2008; Szatrowski & Nathan, 1991). Large amounts of ROS generated by prostate cancer cells could be necessary to stimulate tumorigenesis and maintain their invasive phenotype (Lim *et al.*, 2005; Kumar *et al.*, 2008).

A series of biochemical events mediate cell signalling in response to oxidative stress. PI3K-Akt, MAPK and protein kinase C have been deregulated in prostate cancer. Malfunction of these molecules is associated with uncontrolled cell growth and malignant transformation of prostate cells (Cai *et al.*, 2009; Chen *et al.*, 2011). Furthermore, redox sensitive transcription factors such as Nrf-2, NF-κB, HIF-1, AP-1, p53, PPAR-γ and their antioxidant response elements (AREs) can be activated by these upstream kinases responsive to ROS accumulation and resultant oxidative injuries (Thapa & Ghosh, 2012).

1.5.6 Metabolic alterations in prostate cancer

Aerobic glycolysis, one of the distinctive features in cancer metabolism, is adopted by tumour cells due to its faster ATP production than mitochondrial oxidation, providing sustained energy for tumorigenesis, which is termed “the Warburg effect”. The Warburg effect is a shift of ATP generation pathway from oxidative phosphorylation to glycolysis (Warburg, 1956). However, this has only been seen in advanced prostate cancers (Bauer *et al.*, 2005; Flavin *et al.*, 2011). The second feature in cancer metabolism is the high requirements of energy consumption for increased protein synthesis and DNA synthesis (Voeller *et al.*, 2004). The third characteristic of cancer cells is an increase in *de novo* fatty acid synthesis that is dependent on the availability of acetyl-CoA content produced by ATP citrate lyase from pyruvate, which is the end product of glycolysis (Kuhajda, 2000; Flavin *et al.*, 2011). In order to provide lipids, phospholipids in particular, for membrane production, fatty acid *de novo* synthesis is continuously required in proliferating cancer

cells via an upregulation of the enzyme fatty acid synthase (FASN), indicating the importance of lipogenesis in prostate tumorigenesis (Flavin *et al.*, 2011). Studies have proved that an enhanced *de novo* synthesis of fatty acids and sterol and increased protein synthesis are common features of prostate cancer (Ettinger *et al.*, 2004; Rossi *et al.*, 2003; Swinnen *et al.*, 2000). FASN is highly expressed in prostate cancer and inhibition of FASN leads to cell death of prostate cancer cells. The FASN inhibitors, for example, cerulenin and C75 demonstrate antitumor effect (Pizer *et al.*, 1996; Rendina *et al.*, 2005).

1.5.7 Diagnostics of prostate cancer

Prostate specific antigen (PSA) is an androgen-regulated serine protease cleaving semenogelin I and II in the seminal coagulum and a member of the tissue kallikrein family. PSA is produced by the ductal and acinar epithelium of the prostate (Yousef & Diamandis, 2001; Lilja *et al.*, 1987). Most PSA exists in semen with a small amount is in the blood. PSA blood levels below are generally considered in a normal range (Cancer Research UK): 3 ng/ml or less: for men under 60 years old; 4 ng/ml or less: for men aged 60-69; 5 ng/ml or less: for men over 70 years old.

A PSA reading higher than the above values but less than 10 ng/ml usually suggests a benign enlarged prostate. The higher the reading the more likely it is to be a prostate cancer. However, PSA cannot discriminate between prostate cancers that will progress and those that are already fully disseminated disease (Isaacs *et al.*, 2002). In order to improve the specificity, the percentage of free PSA has been applied, which is a measurement of the proportion of PSA protein in the blood against that bound to other proteins. When blood PSA levels are between 3-10 ng/ml, the percentage of free PSA is useful to determine whether there is a need for a biopsy (Sandhu & Schlegel, 2004). On the other hand, according the clinical guidelines (2008) by National Institute for Health and Care Excellence (NICE), the aim of prostate biopsy is to detect whether the disease can cause potential harm rather than detecting the cancer.

Diagnosis of prostate cancer depends upon two clinic evaluations according to Isaacs *et al.* (2002): one is histological evaluation by needle biopsy and the other is elevated

plasma PSA levels. On the other hand, potential morbidity of prostate cancer declines dramatically via the diagnostic detection using digital rectal examination (DRE) plus the PSA blood test.

Clinical stages of the prostate tumour are classified via a TNM (Tumour-Nodes-Metastases) category. T stage shows how far the cancer has spread in and around the prostate gland (Fig 1.12). This is measured by a DRE. The N stage shows whether or not the cancer has spread from the prostate to the nearby lymph nodes. This is accessed by an MRI or CT scan. (**NX**: The lymph nodes are not measured; **N0**: The lymph nodes are not seen to contain cancer cells; **N1**: The lymph nodes contain cancer cells). The M stage shows whether the cancer has metastasised to other parts of the body, such as the bone. This is measured by a bone scan. (**MX**: The spread of the cancer was not measured. **M0**: The cancer has not spread to other parts of the body. **M1**: The cancer has spread to other parts of the body) (Prostate Cancer UK, 2012).

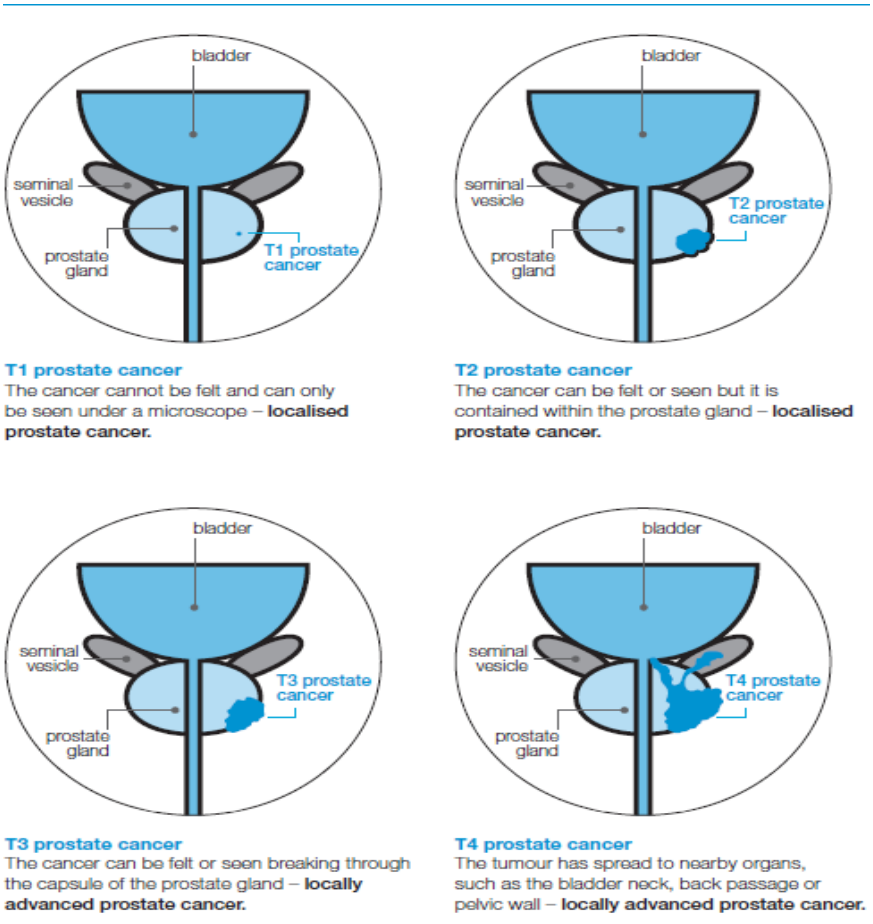

Fig. 1.12 Illustration of the tumour stages of the prostate (Prostate Cancer UK)

For men with localised prostate cancer, their risks of recurrence are stratified (Table 1.2).

	PSA		Gleason score		Clinical stage
Low risk	< 10 ng/ml	**and**	≤ 6	**and**	T1-T2a
Intermediate risk	10–20 ng/ml	**or**	7	**or**	T2b-T2c
High risk	> 20 ng/ml	**or**	8-10	**or**	T3-T4[5]

Table 1.2 Risk stratification for men with localised prostate cancer (NICE clinical guideline 58, 2008)

1.5.8 Signs and symptoms of prostate cancer

Patients with early stage prostate cancers usually do not have symptoms. However, some patients present symptoms of urinary dysfunction, which is often similar to the diseases such as benign prostatic hyperplasia (BPH). These symptoms include frequent urination, nocturia, hematuria, and dysuria (Miller *et al.*, 2003). Hormone refractory patients with bone metastases can have bone pain, vertebral collapse, deformity pathological fractures and spinal cord compression (Heidenreich *et al.*, 2008; van der CRUIJSEN-KOETER *et al.*, 2005).

1.5.9 Treatment of prostate cancer

Surgical removal or localised radiotherapy is the primary procedure to treat localised prostate cancer (Isaacs *et al.*, 2002). With eradication of all a localised tumour it is a potentially curable disease. For most men with a life expectancy more than 10 years, radical prostatectomy is the first choice to remove localised prostate tumour (Sandhu & Schlegel, 2004). However, it may be more appropriate to do an active surveillance (watchful waiting) for patients with PSA < 10 ng/ml, biopsy Gleason score ≤ 6, a life expectancy < 10 years and well-differentiated localised tumours (Heidenreich *et al.*, 2008). It is recommended that radical treatment is not offered to men in active surveillance until there is evidence of the disease progression that is defined by changes in PSA or Gleason score on repeat biopsy (Graham *et al.*, 2008). Radiation therapy can be

limited by insensitivity of the tumour cells and damage to the normal surrounding tissues (Sandhu & Schlegel, 2004). Patients with low risk prostate tumours may not need immediate treatment although this is often not the case in reality (Benedettini *et al.*, 2008).

The prostate gland is an androgen-dependent organ (Sandhu & Schlegel, 2004; Benedettini *et al.*, 2008). With regard to recurring and metastasising prostate cancers, androgen ablation therapy is a standard and effective systemic treatment regimen. Gonadotropin-releasing hormone (GnRH) agonists are usually used to block the secretion of luteininzing hormone (LH) resulting in an inhibition of testosterone production from the testes (Sandhu & Schlegel, 2004). As an alternative to this therapy, bilateral orchidectomy is offered to patients with metastatic prostate cancer (Graham *et al.*, 2008). However, when the disease develops into an advanced stage or relapses, it becomes eventually an androgen independent disease i.e. hormone refractory state. The tumour cells develop the ability to sustain growth in the absence of androgens, leading to a failure of androgen ablation therapy. Unfortunately, molecular mechanism of this phenomenon is still poorly elucidated.

Prostate cancer chemotherapy refers to the treatment using therapeutic chemical compounds after the disease has recurred with a failure of the addressed treatment strategies above (Perez-Stable, 2011). Docetaxel in combination with prednisone (synthetic glucocorticoid steroid) represents the cytotoxic regime for men with hormone-refractory or castration-resistant prostate cancer, which has been approved by the Food and Drug Administration (FDA) (Perez-Stable, 2011; Heidenreich *et al.*, 2008). Unfortunately, a median duration of survival is 18 months even with this treatment of the late hormone refractory stage (Isaacs *et al.*, 2002; Benedettini *et al.*, 2008; Khandrika *et al.*, 2009; Flavin *et al.*, 2011).

In general, chemotherapy shows limited success in the treatment of prostate tumours. Only a 10-20% response is seen in patients treated with a single agent. 40-60% response is seen with combined treatment, for example, estramustine based regimens plus docetaxol. Thus, there is an urgent need of effective systemic therapy (Sandhu & Schlegel,

2004). There is also an urgent need to discover new biomarkers to help with risk stratification in the relevant pathways and to develop novel agents prolonging survival (Benedettini *et al.*, 2008).

1.5.10 Prostate cancer and polyamines

The prostate gland has the highest polyamine biosynthesis of any human organ and is the only one in which massive amounts of synthesised polyamines are purposely exported into semen. In human prostate tissue spermine is the dominant polyamine (Schipper *et al.*, 2003; Kee *et al.*, 2004; Palavan-Unsal *et al.*, 2006). Seminal spermine is associated with the modulation of sperm fertilisation competence (Rubinstein & Breitbart, 1994). Thus, polyamine associated biochemistry in the prostate may be different from other organs.
Polyamines are crucial for the regulation of proliferation and differentiation of prostatic glandular epithelial cells. It is believed that putrescine and spermidine are required for prostate cancer cell proliferation whereas spermine seems to play more roles in functional and secretory state of the prostatic epithelium. Thus, a decrease in spermidine and/or an increased in spermine might suggest a transition state of cells from proliferation into differentiation (Schipper *et al.*, 2003).

Polyamine biosynthesis is associated with the development of prostate cancer. Polyamine biosynthetic enzyme, ODC, protein (Mohan *et al.*, 1999) and mRNA expression (Saverio *et al.*, 2000) were found higher in prostate tumour than benign tissues. An increased ODC activity and polyamine concentrations were correlated with the pathogenesis of benign prostate hyperplasia (BPH) according to Liu *et al.* (2000). This is further confirmed by Gupta *et al.* (2000) who showed that DFMO, an ODC inhibitor, depleted polyamine pools and prevented the development of prostate cancer in the TRAMP model. Studies also showed that in BPH, putrescine (2.2 fold), spermidine (3.4 fold) and spermine (6.0 fold) contents were all elevated in contrast to normal tissues, indicating a critical role of polyamine biosynthesis in prostate neoplasia. In addition, Kim *et al.* (2006) reported that overexpression of antizyme inhibitor led to an increased cell proliferation in AT2.1 Dunning rat prostate carcinoma cells and HIH-3T3 mouse fibroblast cells. This was accompanied by an increase in putrescine content but little change in spermidine and

spermine. The mechanism is believed to involve antizyme inhibitor inhibiting antizyme activity and preventing the degradation of ODC by antizyme. This leads to increased ODC activity and therefore putrescine synthesis. Overall, polyamine biosynthesis may play an important role in the development of prostate neoplasia.

On the other hand, the study by van der Graaf *et al.* (2000) showed higher spermine content in normal and benign hyperplastic prostate tissues and reduced level of spermine in tumour tissue, especially in metastasised prostate carcinoma, and in xenografts of human prostatic carcinoma cells. A decrease of the prostatic spermine content is therefore thought to be a sign of the conversion of prostate tissue from benign to malignant (Schipper *et al.*, 2003). Earlier study by Smith *et al.* (1995) demonstrated that spermine inhibited the growth of both *in vitro* and *in vivo* prostatic carcinoma. Likewise, Cheng *et al.* (2001) found depleted levels of spermine and citrate in the intact prostate cancerous specimen analysed by the high resolution proton nuclear magnetic resonance (NMR) spectroscopy, indicating spermine may have an inhibitory role in prostate cancer growth. Similar results by Giskeødegård *et al.* (2013) revealed a higher concentration of spermine (1.92 mmol/kg) and putrescine (0.38 mmol/kg) in normal samples adjacent to the prostate compared to the spermine (1.22 mmol/kg) and putrescine (0.02 mmol/kg) in the cancer samples of the prostate. It was therefore proposed by Giskeødegård *et al.* (2013) that the concentration of spermine can be used as discriminative magnetic resonance biomarker for prostate cancer aggressiveness. However, spermidine content was not measured in this study. Regarding the role of spermidine in prostate, it was noted that the addition of exogenous spermidine restored the growth inhibition, suggesting spermidine might be the key polyamine in the growth of prostate cancer cells (Schipper *et al.*, 2003). Taken together, spermine appears to have a special role in the prostate carcinogenesis, indicating an alteration in intracellular polyamine homeostasis has a fundamental influence on cellular malignant transformation.

1.6 Hypothesis and aims of this study

With literatures of polyamine metabolic pathways particularly their catabolism by SSAT in cancers, it is generally acknowledged that SSAT is a very important regulator of polyamine content in the cell. On the other hand, prostate carcinogenesis is a complex process with a participation of multiple factors. Polyamines, as one of the factors, have direct effect on the growth of prostate cancer of both *in vivo* and *in vitro* models. Therefore, the association of SSAT activity with prostate tumour growth may be related, although the effect of SSAT seems paradoxical (either suppresses or promotes carcinogenesis).

The hypothesis of this study was that SSAT plays a critical role in the regulation of growth of prostate cancer cells. Overexpression of SSAT activity is linked to decreased cell growth in response to cytotoxic therapy and so cells with increased SSAT activity may respond better to such agents.

The aims of this study were to characterise the effect of altered SSAT expression on:

1. The growth of prostate cancer cells.
2. ODC, APAO, and SMO activity of the polyamine pathway.
3. Intracellular and extracellular polyamine concentrations.
4. Polyamine efflux.

The aims included were also to determine SSAT alteration on these parameters in the presence of inhibitors and anticancer drug treatment.

2 Materials & Methods

2.1 Materials

2.1.1 General chemicals

Acetyl-coenzyme A	Sigma Aldrich, Co., Poole, UK
Ambion® RNaseZap®	Life Technologies Ltd., Paisley, UK
Acetylsalicylic acid (Aspirin)	Sigma Aldrich Co., Poole, UK
Aminoguanidine hemi-sulphate	Sigma Aldrich Co., Poole, UK
Benzethonium	Sigma Aldrich Co., USA
Blotto nonfat dry milk	Santa Cruz Biotechnology, Inc. USA
Bovine serum albumin	Sigma-Aldrich Co., Poole, UK
Brain Heart Infusion	Oxoid Ltd., Basingstoke, UK
cDNA reverse transcription kit	Applied Biosystems, USA
Chloroform	Acro organics. Geel, Belgium
Copper sulphate	Sigma-Aldrich, Co., Gillingham, UK
Copper tartrate	BDH Chemical Co., Poole, UK
Cycloheximide	Sigma-Aldrich, Co., China
DCFDA	Sigma-Aldrich, Co., Poole, UK
1,7-Diaminoheptane	Sigma-Aldrich, Co., Poole, UK
α-Difluromethylornithine	a kind gift from Wayne State University, USA
Dimethyl Sulphoxide	Sigma-Aldrich, Co., Poole, UK
Dithiothreitol	Sigma Chemical Co., St. Louis, USA
5-Fluorouracil	Sigma Aldrich Co., Poole, UK
Folin's-Ciocalteau Reagent	BDH Chemical Co., Poole, UK
Etoposide	Sigma-Aldrich, Co., Poole, UK
Firefly luciferase assay kit	Biotium, Inc. Hayward, USA
Geneticin (G418)	PAA Laboratories Ltd., Yeovil, UK
Homovanillic acid	Sigma-Aldrich Co., Austria
Horse radish peroxidase (Type II)	Sigma-Aldrich Co., USA

Hydrochloric acid	Sigma-Aldrich Co., Gillingham, UK
Hydroxylamine	Sigma-Aldrich Co., Poole, UK
Hygromycin B	PAA Laboratories Ltd., Yeovil, UK
Light Cycler 480 probe master	Roche Diagnostics, Germany
Methanol	BDH, Leicester, UK
MDL72527	Sigma-Aldrich Co., Poole, UK
MTT	Sigma-Aldrich, Co., Poole, UK
Pargyline	Cayman Chemical Co., MI, USA
Penicillin/Streptomycin	PAA Laboratories Ltd., Yeovil, UK
Perchloric acid	VWR International Ltd., Lutterworth, UK
Pierce RIPA buffer	Thermo Scientific Ltd., USA
Poly-D-lysine hydrobromide	Sigma-Aldrich Co., Poole, UK
Potassium sodium tartrate	Sigma-Aldrich Co., Spain
Putrescine dihydrochloride	Sigma-Aldrich Co., Poole, UK
Scintillation cocktail	GE Healthcare, Buckinghamshire, UK
Sodium carbonate	BDH Chemical Co., Poole, UK
Sodium chloride	BDH Chemical Co., Poole, UK
Sodium hydroxide	BDH Chemical Co., Poole, UK
Sodium potassium tartrate	Sigma-Aldrich Co., Gillingham, UK
Sodium pyruvate	BDH Chemical Co., Poole, UK
Sodium tetraborate decahydrate	Sigma-Aldrich Co., Japan
Spermidine trihydrochloride	Sigma-Aldrich, Co., Poole, UK
Spermine tetrachloride	Sigma-Aldrich, Co., Poole, UK
Superscript II Reverse transcriptase	Life Technologies Ltd., Paisley, UK
Tetracycline hydrochloride	Sigma-Aldrich, Co., Poole, UK
Tris base	Melford Laboratories Ltd., Ipswich
TRIZOL reagent	Ambion, USA
Trypan blue	Sigma-Aldrich Co., Poole, UK
Trypsin	PAA Laboratories Ltd., Yeovil, UK
Trypsin-EDTA	PAA Laboratories Ltd., Yeovil, UK

Universal probe library #82	Roche Diagnostics, Denmark
Fluorimeter cuvettes	Fisher Scientific Ltd., Loughborough, UK

2.1.2 LC-MS Materials

Acetone	Fisher Scientific Ltd., Loughborough, UK
Dansyl chloride	Sigma-Aldrich Co., Poole, UK
L-proline	Sigma-Aldrich Co., China
Methanol	VWR International Ltd., Lutterworth, UK
N^1-acetylspermidine hydrochloride	Fluka, Switzerland
N^1-Acetylspermine trihydrochloride	Fluka, Switzerland
Sodium carbonate decahydrate	Sigma-Aldrich, Co., Germany
Toluene	Sigma-Aldrich, Co., Gillingham, UK

2.1.3 Cell culture materials

T75 cm^2 cell culture flasks	PAA Laboratories Ltd., Yeovil, UK
5 cm and 10 cm cell culture dishes	PAA Laboratories Ltd., Yeovil, UK
Foetal bovine serum	Invitrogen, Paisley, UK
LNCaP cell line wild type	ECACC, Salisbury, UK
LNG53 (SSAT transfected LNCaP) cell line	Roswell Park Memorial Institute, Buffalo, USA
96-well microtitre tissue culture plates	Fisher Scientific Ltd., Loughborough, UK
RPMI1640 medium	PAA Laboratories Ltd., Yeovil, UK
2ml cryovials	Fisher Scientific Ltd., Loughborough, UK

2.1.4 Radiochemical

[^{3}H] Acetyl-coenzyme A	PerkinElmer, Cambridge, UK
[^{14}C] L-Ornithine	PerkinElmer, Cambridge, UK
[^{3}H] Putrescine	American Radiolabeled Chemicals, Inc. St. Louis, USA
[^{14}C] L-Amino acids mixture	PerkinElmer, Cambridge, UK

2.1.5 Antibodies

Rabbit polyclonal to SAT1	Abcam plc, Cambridge, UK
Polyclonal Goat IgG against Rabbit	R&D systems, Inc. UK
Rabbit polyclonal to AZ1	Abcam plc, Cambridge, UK

2.1.6 Western blot materials

Novex Bis-Tris SDS 4-12% polyacrylamide gel	Life Technologies Ltd., Paisley, UK
NuPAGE LDS Sample Buffer (4X)	Life Technologies Ltd., Paisley, UK
NuPAGE Reducing Agent (10X)	Life Technologies Ltd., Paisley, UK
XCell Mini Cell blot module	Life Technologies Ltd., Paisley, UK
NuPAGE MOPS SDS running buffer (20X)	Life Technologies Ltd., Paisley, UK
polyvinylidene difluoride (PVDF) membrane	Fisher scientific Ltd., Loughborough, UK
NuPAGE transfer buffer (20X)	Life Technologies Ltd., Paisley, UK
Filter papers	Fisher scientific Ltd., Loughborough, UK
ECL kit	GE Healthcare Life Sciences, Buckinghamshire, UK
Autoradiography X-ray films	Santa Cruz Biotechnology, Inc., Heidelberg, Germany

2.1.7 Cell Lines

Fig. 2.1 Morphology of WT, SSAT$^-$, and SSAT$^+$ LNCaP prostate cancer cells in culture under an EVOS light microscope (scale bar 100 µm)

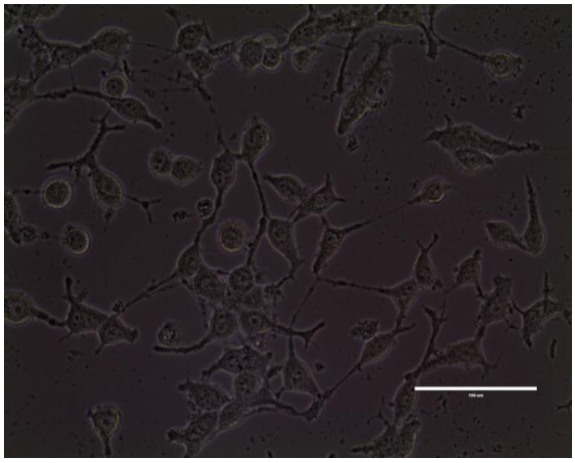

WT 48 h (X40)

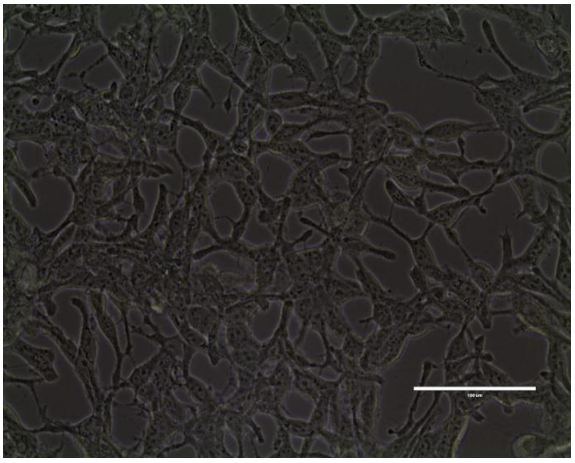

WT 96 h (X40)

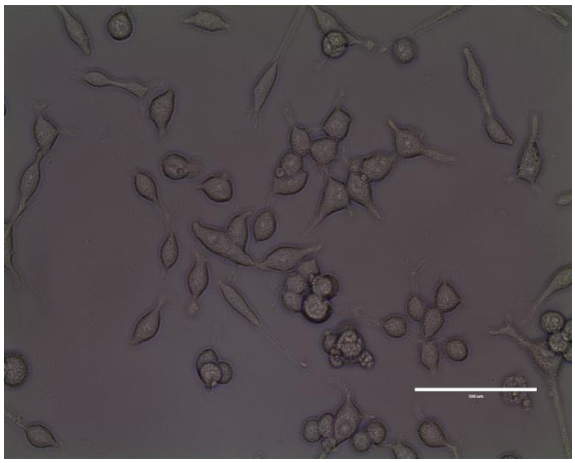

SSAT$^-$ 48 h (X40)

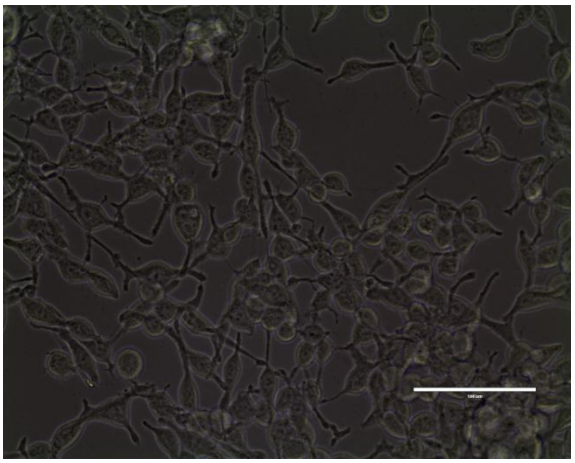

SSAT$^-$ 96 h (X40)

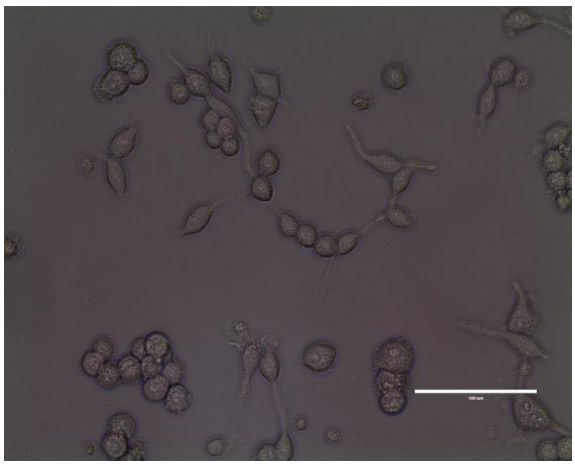

SSAT$^+$ 48 h (X40)

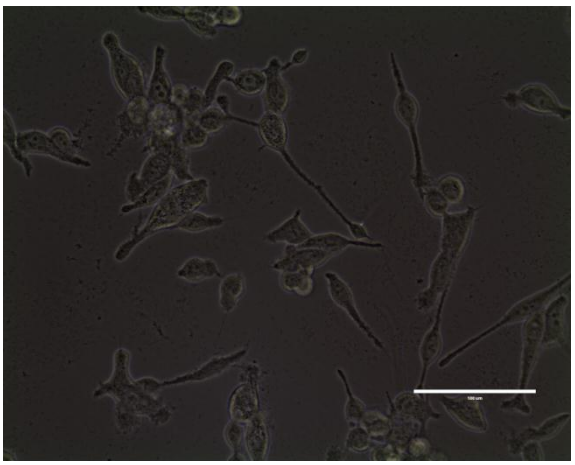

SSAT$^+$ 96 h (X40)

LNCaP Fast Growing Clones (FGC) wild type (WT) cell line was purchased from the European Collection of Cell Cultures (ECACC). This human metastatic prostate adenocarcinoma cell line was derived from a metastasis at the left supraclavicular lymph node of a 50 year old patient who was diagnosed of metastatic prostate carcinoma. LNCaP cell line is an androgen dependent cell line (Horoszewicz *et al.*, 1980; Horoszewicz *et al.*, 1983) (Fig. 2.1).

LNCaP WT cells were able to reach 70 – 80% confluence and were prone to aggregate. The cells detached from the culture flasks as clumps if they were over confluent as they did not firmly attach to the culture flasks. Medium of LNCaP WT was rapidly acidified and usually changed every two days. These cells grew slowly if plated sparsely. LNCaP cell seeding density was 2.4 x $10^4/cm^2$.

LNCaP culture medium: RPMI1640 with L-glutamine + 1.0 mM sodium pyruvate + 10 % (v/v) FBS + penicillin (100 units/ml) and streptomycin (100 µg/ml). This medium was also always supplemented with 1 mM aminoguanidine to prevent serum amino oxidase from converting polyamines to toxic products (Coffino & Poznanski, 1991; Schipper *et al.*, 2000).

SSAT human cDNA transfected LNCaP (LNG53) cell line was a kind gift from Dr Carl Porter and Dr Debora Kramer (Roswell Park Memorial Institute, Buffalo, USA) (Fig. 2.1). This cell line was genetically modified by the tetracycline-off (Tet-off) Advanced Inducible Gene Expression System. Cells were cultured routinely in the presence of tetracycline (Tet) that inhibited the *SAT1* gene transcription, only producing basal SSAT enzymatic activity (represented as **SSAT**$^-$ cells). In the absence of Tet, the *SAT1* gene transcription was overexpressed leading to a significant increase in SSAT enzymatic activity (represented as **SSAT**$^+$ cells). Medium of LNG53 was replaced every two days due to a short half-life of Tet in culture (< 48 h). LNG53 cell seeding density was 2.4 x $10^4/cm^2$ (Kee *et al.*, 2004b; Kramer *et al.*, 2008).

LNG53 culture medium: RPMI1640 with L-glutamine + 50 mg/ml G418 + 150 µg/ml hygromycin B + 1 mM aminoguanidine + 10% (v/v) Tet free FBS + 0.4 µg/ml Tet (Tet-free culture medium was the same but without Tet supplementation) (Table 2.1).

2.1.8 Removal of Tet from culture to induce SSAT expression

Tet was very difficult to wash off. In order to remove completely, Tet concentration in medium was decreased to 100 ng/ml 24 h prior to passage. On the day of passage, cell culture was washed twice in PBS before trypsinisation. After the cells detached, Tet-free culture medium was added to neutralise trypsin. The cell pellet was resuspended in Tet-free culture medium after centrifugation at 200 g for 3 min. $SSAT^+$ (Tet-off) cells were plated first and then $SSAT^-$ (Tet-on) cells. After 24 h growth, medium was replaced with fresh medium to ensure complete wash-off of Tet.

Cell line	WT	$SSAT^-$	$SSAT^+$
Culture medium supplements	10% (v/v) FBS, 100 units/ml penicillin, 100 µg/ml streptomycin, 1 mM AG, and 1 mM sodium pyruvate	10% (v/v)Tet-free FBS, 50 mg/ml G418, 150 µg/ml hygromycin B, 1 mM AG and 1 µg/ml Tet	10% (v/v)Tet-free FBS, 50 mg/ml G418, 150 µg/ml hygromycin B and 1 mM AG
Seeding density	$2.4 \times 10^4/cm^2$	$2.4 \times 10^4/cm^2$	$2.4 \times 10^4/cm^2$
Saturation density	$9.3 \times 10^4/cm^2$	$18 \times 10^4/cm^2$	-
Generation time (96 h)	54	36	59
Subculture split ratio	1:4	1:5	-

Table 2.1 Growth characteristics in WT, $SSAT^-$ and $SSAT^+$ cells

2.2 METHODS

2.2.1 Aseptic techniques

Standard good laboratory practice is always essential. Cell culture procedures were carried out aseptically in a Class II air-flow biohazard hood (microbiological safety cabinet). Gloves were worn all the time. The work area of cabinet was wiped with 70% (v/v) ethanol before and after use. Items for cell culture use in the cabinet must be either sprayed with 70% ethanol or autoclaved prior to use. Solutions were usually sterile filtered using a 0.22 µm syringe filter prior to use on cells. Cell culture waste was autoclaved at 121°C for 20 min before disposal.

2.2.2 Maintenance and subculture of anchorage dependent cells (Passage)

LNCaP and LNG53 (human SSAT cDNA transfected LNCaP) cell lines were cultured routinely in a T75 cm^2 cell culture flask containing 15 ml culture medium at 37°C in a humid incubator supplemented with 5% CO_2. Cells were passaged when they became 80% confluent in the culture flask. Confluence was defined as maximal cell growth without spare space for cell spreading. Reagents were warmed to 37°C in a water-bath before use. Used medium was discarded from the flask to a waste bottle. Cells were washed with 10 ml PBS and then 2-3 ml trypsin-EDTA for LNCaP or 0.25% (v/v) trypsin for LNG53 was added. Cells were further incubated for 3-5 min until detached (gently tapping the flask can help the cells detach). 7-8 ml culture medium was added to neutralise trypsin; the cell solution was transferred to a 15 ml sterile universal tube and centrifuged at 200 g for 3 min. The supernatant was removed and the cell pellet was loosened from the tube bottom by tapping; cells were resuspended in culture medium and flasks were reseeded at a split ratio of 1:3 - 1:5. Around 2 million cells were seeded routinely into a new T75 cm^2 flask for regrowth.

2.2.3 Cell cryopreservation and storage

It is essential to freeze down a validated and uncontaminated stock of cells early in the growth process for a variety of reasons such as the potential for contamination by microorganisms or equipment failure. More importantly, continuous cell lines are genetically and phenotypically less stable. Their growth characteristics may change after certain numbers of passages (Freshney, 2005). In our laboratory cells are not used beyond 20 passages from recovery.

In order to achieve optimal cell freezing for maximal cell recovery, a hydrophilic cryoprotectant (DMSO) is applied to sequester water inside the cell in order to minimise intracellular ice crystal formation. DMSO is usually selected as a cryoprotectant because it penetrates the cell more effective than others.

DMSO concentration in the freezing medium is 10% (v/v). To make 10 ml freezing medium = 7 ml cold medium (e.g. RPMI1640) + 2 ml FBS + 1 ml DMSO

For cryopreservation, cells were used within five passages after recovery and had not reached confluence when preserved. Procedure of passage is described in Section 2.2.2. After centrifugation, the cell pellet was resuspended in the freezing medium above. Cells survive freezing best when frozen at a high cell concentration (Freshney, 2005). The cell pellet obtained from one T75 cm^2 flask was usually resuspended in 3-4 ml of the freezing medium. 1-2 ml of the cell suspension was transferred into a cryovial and kept in a Nunc Mr. Frosty freezing container, which allows temperature cooling at 1°C/min in a −80°C freezer. Cells were later stored in −135°C freezer or liquid nitrogen (−196°C) dry store to minimise protein denaturation (Freshney, 2005).

2.2.4 Cell recovery

Cell recovery refers to bringing cells back to growth from freezing by rapid thawing at 37°C in a water-bath. Rapid thawing will minimise ice crystal formation within the cell and the resultant solute gradients when the ice melts (Freshney, 2005). After thawing, the cell suspension was added into a T25 cm^2 flask containing culture medium and then kept in an incubator. Sudden dilution of cell suspension after thawing can cause osmotic damage and reduce cell viability particularly with DMSO (Freshney, 2005). After cells attach (within 24 h) medium was replaced with fresh medium. Some cell types are highly sensitive to DMSO and an alternative method was used, thawed cells can be diluted slowly in a 15 ml universal tube with medium first and centrifuged at a low speed of 100 g_{av} for 5 min before incubation.

2.2.5 Trypan Blue cell exclusive assay

Prior to plating the correct number of cells for an experiment, viable cell numbers must be counted and calculated. This method was applied for cell counting to distinguish viable cells from non-viable cells by using a Hawksley Improved Neubauer Haemocytometer (Fig.2.2). 100 µl of cell suspension was mixed thoroughly with 900 µl of 0.4% (w/v) trypan blue solution (1:10 dilution) in an Eppendorf tube (less dilution may be necessary if cell numbers were low). A glass cover slip was moisturised and laid onto the centre of the haemocytometer. Each side of the haemocytometer chamber was filled up with 10 µl of the cell suspension.

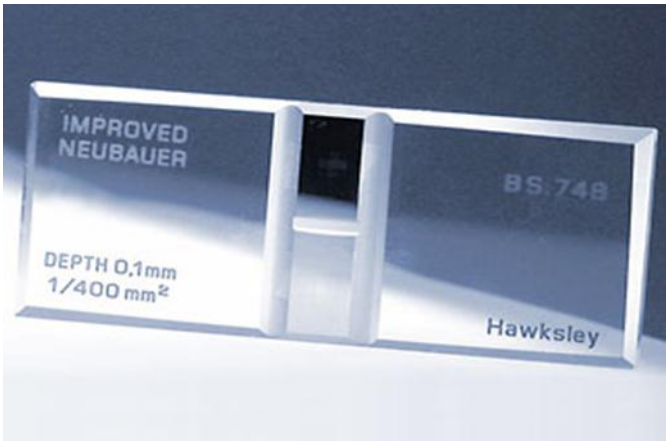

Fig. 2.2 Hawksley Improved Neubauer Haemocytometer

Cell counting was performed using a light microscope with 10x magnification. Viable cells appeared round, clear and bright while non-viable cells were stained blue. Cells in squares A, B, C, and D were counted and the average value was calculated from the total cell number in the 4 squares divided by 4 (Fig. 2.3). The correction factor of counting is x 10^4/ml. For example, if an average counted value was 10, cell number was equal to 10 x 10^4/ml. However, cells were diluted 10x by trypan blue so that the actual cell number = 10 x 10^4 x 10/ml. Cell number was finally expressed as 1 x 10^6/ml.

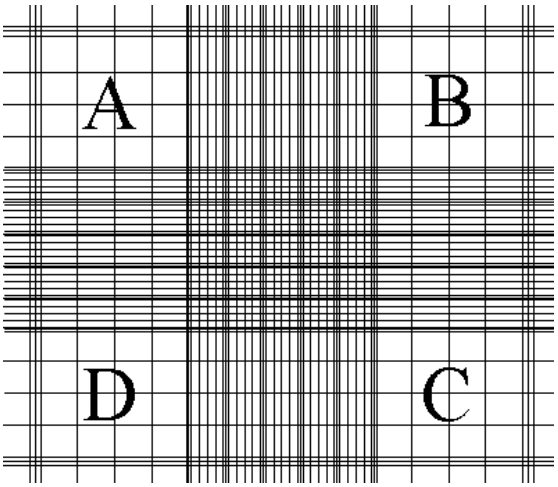

Fig. 2.3 Illustration of the counting chamber of the haemocytometer

Total cell number = viable cell number + dead cell number (x 10^6); Cell viability (%) = viable cell number / total cell number x 100 %. Ideally, cell viability should be more than 90 % for experimental use.

2.2.6 Generation time

Generation time (G_t), or population doubling time, was the period of time required for a culture to double in cell number. This was calculated as follows:

$G_t = \log 2 * \Delta t / \log (N/N_0)$

N = Final cell number, N_0 = Initial cell number, Δt = duration between N and N_0 (h)

2.2.7 Cell harvesting

This method was used to collect cells required to determine cell growth and the effect of antiproliferative agents on cell growth. Samples harvested by this method were used to determine cell number, total cellular protein content (Lowry assay, Section 2.2.8), and polyamine concentration analysis (LC-MS or HPLC, Section 2.2.13).

The cells were harvested in the following order: discarding medium, rinsing with cold PBS, adding 1 ml trypsin-EDTA and incubating 3-5 min until the cells detached. 4 ml of culture medium was added to the plate to neutralise trypsin; the cell solution was transferred to a 15 ml conical tube and centrifuged at 200 g_{av} for 3 min using a Centaur 2 centrifuge machine. The supernatant was removed and cell pellet was resuspended in 1 ml PBS and transferred to a 1.5 ml Eppendorf tube. 100 µl was taken out and used for cell counting (see Section 2.2.5). The rest of the cell suspension was spun down at 1,600 g_{av} for 3 min using a bench top Thermo scientific Pico 17 centrifuge machine. After the supernatant was removed, the cell pellet was resuspended in 0.5 ml of 0.2 M perchloric acid (PCA) and kept on ice for 30 min to precipitate protein and extract acid soluble fraction that contains polyamines. After 30 min, the Eppendorf tube was centrifuged again at 16,000 g_{av} for 2 min. The supernatant containing polyamines was transferred to a new 1.5 ml Eppendorf tube and stored at -20°C for polyamine concentration analysis. The acid

insoluble pellet was dissolved in 0.5 ml of 0.3 M sodium hydroxide (NaOH) overnight in an incubator at 37°C for protein content determination by Lowry assay.

2.2.8 Total cellular protein determination (Lowry assay)

Total cellular protein content was determined by a modified method from Lowry *et al.* (1951) using a 96-well plate without a lid.

A standard curve for protein was prepared in the range of 0 – 250 µg/ml using 0.5 mg/ml bovine serum albumin (BSA) and 0.3 M NaOH as follows:

Final BSA concentration (µg/ml)	0.5mg/ml BSA (ml)	0.3 M NaOH (ml)
0	0	1
25	0.05	0.95
50	0.1	0.9
100	0.2	0.8
150	0.3	0.7
200	0.4	0.6
225	0.45	0.55
250	0.5	0.5

Table 2.2 BSA standards for Lowry assay

It was necessary to dilute samples to ensure they were all within the range of the standards (0-250 µg/ml). The standard curve was ideally a linear line within this range. If the protein content of the sample is higher than the maximal standard, the correlation may not be linear so that the actual protein content may be underestimated.

Samples were usually diluted with 0.3 M NaOH in a ratio of 1:10. 50 µl of the standard and diluted samples were added in triplicate into a 96-well plate. 100 µl of Lowry A solution was added to each well and the plate was left on bench for 10 min before adding Lowry B solution. After addition of Lowry B solution (made fresh), the 96-well plate was stored in the dark for 20 min and then analysed using a Tecan Sunrise colorimetric/spectrophotometric plate reader. Absorbance was measured at a

wavelength of 690 nm. Total cellular protein content was calculated using an equation generated from the slope of the standard curve (Appendix, Fig. 6.9) and results were expressed as total mg/culture.

Lowry A solution: 14.7 ml 2% (w/v) Na_2CO_3 + 0.15 ml 1% (w/v) $CuSO_4 \cdot 5H_2O$ + 0.15 ml 2% (w/v) NaK tartrate;
Lowry B solution: 14 ml dH_2O + 1 ml Folin–Ciocalteu reagent

NB: If 100 µl of cells was used for cell counting (see Section 2.2.5) the protein content was then obtained from only 900 µl cell suspension. Multiplying the correction factor 1.1 needs to be included in the calculation. If samples were diluted 10x, multiplying dilution factor 10 was also included in the calculation.

2.2.9 MTT cytotoxicity assay

MTT assay is a non-radioactive, colorimetric assay first described by Mosmann (1983) and modified by Denizot & Lang (1986). This assay is based on the reaction catalysed by the enzyme, succinate dehydrogenase, that cleaves the yellow MTT salt (3-(4,5-dimethylthiazol-2-yl)-2,5-diphenyl tetrazolium bromide) to form formazan crystals in active mitochondria of living cells. The formazan crystals formed are solubilised by DMSO into a purple coloured solution the absorbance of which can be quantified by measuring at wavelength 570 nm and the reference wavelength 690 nm using the Sunrise Tecan scanning multiwell spectrophotometer. The potency of an agent (the half maximal inhibitory concentration, IC_{50}) can be calculated via the amount of purple formazan produced by cells treated with the agent in comparison with the amount of formazan produced by untreated control cells through the generation of a dose response curve.

The MTT assay was carried out on a 96 well flat-bottomed (for anchorage dependent cells) micro-titre plate (round-bottomed plate for anchorage independent cells). 200 µl of sterile water was placed in the outside wells of the plate to reduce evaporation (Fig 3). 100 µl of culture medium was in wells B2-G2, performing as a blank. In the remaining wells B3-G11, 100 µl of cells in medium was plated (seeding density depends on cell line). The cells were incubated for 48 h for growth. Following 48 h incubation, medium was

removed from wells B2-G11. Fresh medium was added to B2-G2. To B3-G3, 100 µl of medium containing the vehicle control (the solvent to dissolve the compound) was used. The vehicle control concentration was the same as it is in the highest final concentration of the drug in column 11. Increasing concentrations of the drug starting from control of absence of the drug were added to wells B4-G11 (six replicates per column). The drug working solution (e.g. 1 mM 5-FU) was diluted from the drug stock (10 mM 5-FU) which was usually made 10x more concentrated than the highest final drug concentration (0.1 mM 5-FU). According to the range of final drug concentrations (e.g. 0-0.1 mM), eight mixtures (for column 4-11) of drug working solution and medium were prepared separately. The percentage of medium was no less than 90% in the mixture to ensure optimal cell growth. 100 µl of each mixture was added to the corresponding column (Fig. 2.4).

On completion of the drug exposure, 10 µl of 5 mg/ml MTT was added per well (B2-G11). MTT is light sensitive which should be wrapped in aluminium foil. The plate was further incubated for 3-4 h for formazan development. After the formazan crystals formed, the medium was removed from each well using a syringe with a bent tip needle. 100 µl of DMSO per well was used to solubilise formazan crystals using a multi-channel pipette. After 20 min colour generation, the plate was read at 570 nm test wavelength with 690 nm reference wavelength by a Tecan Sunrise colorimetric plate reader.

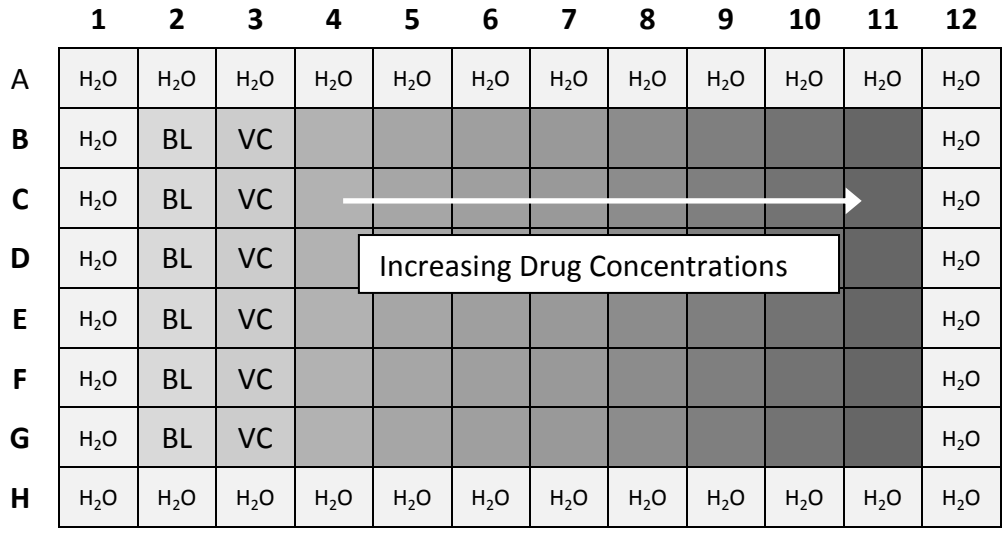

BL - Blank contains medium only; **VC -** Vehicle Control

Fig. 2.4 Layout of 96-well plate used for MTT assay

2.2.10 Measurement of SSAT activity

The method of measuring SSAT activity was described by Wallace & Evans (1998). The principle of the SSAT assay is to measure the incorporation of radioactivity of [^{3}H]-acetylCoA into the end product monoacetylspermidine. It can be retained on cellulose phosphate paper and quantified using a radioactivity scintillation counter.

Cells were seeded at an appropriate density in triplicate in a 60 mm diameter cell culture plate. The cells were allowed to attach and incubated for 48 h. In the experiment involving treatment, the culture medium was changed with fresh medium containing the drug(s) and the cells were exposed to the drug(s) for a certain period of time. The cells were harvested by discarding the medium, washing three times with 1 ml ice-cold PBS and then scraping off in 3 ml PBS. The same replicates were pooled together into a 15 ml universal tube at this point. The tube was centrifuged at 220 g_{av} for 5 min at 4°C using an ALC PK121R multispeed refrigerated centrifuge machine. The supernatant was removed and the cell pellet was resuspended in 0.5 ml hypotonic lysis buffer (10 mM Tris (pH 7.2 at 4°C), 1 mM EDTA and 2.5 mM DTT).

The cell suspension was left on ice for 20 min for the cells to swell and then sonicated for 10 sec to burst the cells (sonication can cause an increase in sample temperature and subsequent protein denaturation so that samples must be kept on ice before and after sonication).

40 µl of the cell homogenate was mixed with 10 µl of 1M ice-cold PCA in a clean Eppendorf tube and stored on ice for 30 min for protein precipitation. The Eppendorf tube was then centrifuged at 1,600 g_{av} for 2 min using a Thermo scientific Pico 17 bench top centrifuge machine. The supernatant was discarded and the cell pellet was dissolved in 0.5 ml of 0.3 M NaOH at 37°C overnight for total cellular protein determination by Lowry method (see section 2.3.4).

The remaining cell homogenate was transferred to a 1 ml polycarbonate ultracentrifuge tube and placed in a specific titanium rotor. Samples were ultra-centrifuged at 100,000 g_{av} (32,500 rpm) for 70 min at 4°C using a Centrikon 1160 ultracentrifuge.

60 µl of the cytosol from each sample was assayed in duplicate in addition of 10 µl of 30 mM spermidine and 10 µl of 1 M Tris HCl (pH 7.8 at 37°C), and the samples were then incubated at 37°C for 2 min using a heater blocker.

A non-enzymatic blank containing the lysis buffer in duplicate was prepared. The reaction was started in ten second cycles on the addition of 10 µl of 250 µM acetyl CoA and 10 µl of 0.33 µCi (1:3 dilution with dH_2O) [^{3}H]-acetyl CoA to the blank and samples. All the samples were incubated for 10 min at 37°C. 20 µl of 1 M hydroxylamine was added on the ten second cycles and then placed on ice to stop the reaction. Samples were boiled for 3 min to precipitate any remaining protein. All the tubes were centrifuged at 1,600 g_{av} for 3 min to pellet the protein using a Thermo scientific Pico 17 bench top centrifuge machine. 30 µl of the sample supernatant was spotted in duplicate onto a Whatman P81 cellulose phosphate-loaded disc. The discs were left to dry in a hot air oven, and then each disc was washed once in tap water, three times in distilled water for 2 min each, and finally once in 100% ethanol to remove unbound [^{3}H]-acetyl CoA. The discs were dried again in the oven.

Each dried paper disc was transferred using forceps to a scintillation vial and 4 ml biodegradable scintillation fluid was added. The radioactivity of the samples was determined via tritium protocol (protocol 4) by using a Packard 1900 CA Tris carb scintillation analyser. Results of SSAT activity were calculated and shown as pmol N^1-acetylspermidine formed /min/mg protein.

2.2.11 Measurement of ODC activity

ODC activity can be determined by measuring the amount of radiolabelled carbon dioxide ([^{14}]CO_2) produced during the decarboxylation of L-[l-^{14}C] ornithine to form putrescine (Tabib, 1998). ODC requires pyridoxal phosphate as a cofactor and thiol groups reducing agents are necessary for enzyme activity (Wallace *et al.*, 2003). The reaction was carried out in a sealed glass tube and CO_2 was trapped in an alkaline (benzethonium hydroxide) solution. All enzyme extracts were prepared at 4°C. Tubes and all solutions were chilled on ice prior to incubation.

Cells were seeded at an appropriate density (2.4 X $10^4/cm^2$) in a 10 cm diameter cell culture dish. In the experiment requiring treatment, the medium was replaced with fresh medium containing drug(s) after 48 h cell growth (e.g. 2 mM aspirin or 50 µM 5-FU). The cells were exposed in the drug(s) for 24-48 h and harvested by discarding the medium, washing twice with ice-cold PBS, scraping in 5 ml cold PBS, and transferred to a 15 ml conical tube for centrifuge at 220 g_{av} for 3 min at 4°C using an ALC PK121R multispeed refrigerated centrifuge machine.

The supernatant was discarded. The cell pellet was resuspended in 0.5 ml homogenising buffer (10 mM Tris-HCl, 2.5 mM dithiothreitol and 0.1 mM EDTA) and kept on ice for 20 min to allow cells to swell. To lyse the cells completely, each sample was sonicated in 10 sec bursts for 30 sec. To prevent excessive heating, ultrasonic treatment was applied in multiple short bursts (localised heating within a sample can lead to protein denaturation and aggregation). Samples were immersed in an ice bath during the sonication.

40 µl of the homogenate was taken to a new Eppendorf tube for protein content determination (Lowry assay). 10 µl of 1.0 M perchloric acid was added and stored on ice for 30 min to allow protein precipitation. The Eppendorf tube was centrifuged at 1,600 g_{av} for 3 min using a Thermo scientific Pico 17 bench top centrifuge. The supernatant was removed. 0.5 ml of 0.3 M sodium hydroxide was added to dissolve the pellet and incubated overnight at 37°C. Samples were then assayed as according to Lowry protocol (see section 2.3.4).

The remaining homogenate was transferred to a thin wall 0.7 ml polycarbonate ultracentrifuge tube using a glass Pasteur pipette. The tube was placed into an adapter and then a specific rotor for ultracentrifuge at a speed of 35,000 g_{av} (20,000 rpm), temperature at 4°C, run time 30 min, and rotor code 1 in a Centrikon T-1160 ultracentrifuge.

A stock assay mix was prepared in which 50 µl aliquot was dispensed into each reaction tube. The mixture was composed of 12.5 µl of 1 M Tris-HCl (pH 7.5 at 37°C), 5 µl of 2 mM pyridoxal 5'-phosphate, 2.5 µl of 250 mM dithiothreitol, 5 µl of 20 mM L-ornithine, and

2.5 µl of L-[l-^{14}C] ornithine, and 22.5 µl of deionised water (total volume prepared was overestimated by one or two depending on the number of reactions).

ODC assay tubes, wells and rubber stoppers were assembled including the blank in duplicate. To each pre-chilled tube, 100 µl of deionised water or the homogenising buffer and 50 µl aliquot of the assay mixture stock were added. 100 µl benzethonium hydroxide was placed in each well which had been inserted into the rubber stopper for absorbing released [^{14}]CO_2. Finally, 100 µl of the enzyme extract (from the ultracentrifuge tube) was added to the reaction tube, making a final volume of 250 µl. 100 µl of water or the homogenising buffer was added instead of the enzyme extract into the blanks. All tubes were sealed tightly with the rubber stoppers (with the inserted well containing benzethonium hydroxide) and placed in a shaking water bath for 1 h at 37°C.

After 1 h, 0.3 ml of 2 M perchloric acid was added into each tube to stop the reaction. This was carried out by using a 1 ml syringe and a long needle, piercing the needle through the rubber stopper, along the side of the tube avoiding the well. The tubes were incubated in the water bath for further 45 min.

All the wells from the tubes were transferred into scintillation vials, and then the vials were filled with 4 ml scintillation fluid (avoiding light at this step). The vials were left in dark overnight. Each sample was counted as dpm for 10 min using [^{14}C] protocol by a Canberra Packard 1900A liquid scintillation analyser. Results were calculated as pmol $^{14}CO_2$ generated/h/mg protein.

2.2.12 Measurement of APAO and SMO activity

In polyamine catabolic pathway, the acetylpolyamines provided by SSAT are substrates for APAO. Acetylpolyamines are oxidised by APAO to form spermidine and spermine with the by-products of hydrogen peroxide (H_2O_2) and 3-acetaminopropanal. The APAO enzyme activity was determined by measuring the production of H_2O_2 via oxidation of N^1-acetylspermine by converting homovanillic acid to the highly fluorescent biphenyl structure in the presence of horseradish peroxidase (*Suzuki et al.*, 1984; Wang *et al.*, 2001).

Cells were plated at an appropriate density in a 60 mm diameter cell culture dish in duplicate. In the experiment requiring treatment, cells were grown for 48 h prior to treatment with drug(s) for a certain period of time. The cells were harvested by discarding the medium, washing twice with ice-cold PBS, scraping in 3 ml cold PBS, and transferred to a 15 ml conical tube (identical duplicate dishes were pooled together into one tube for sufficient enzyme activity to be measured) for centrifugation at 220 g_{av} for 3 min at 4°C using an ALC PK121R multispeed refrigerated centrifuge.

The supernatant was discarded. The cell pellet was resuspended in 0.5 ml 10 mM Tris homogenising buffer (pH 7.4 at 4°C), left on ice for 20 min to let cell swell and then sonicated in short bursts for 10 seconds without frothing the sample. 40 µl of the cell homogenate was transferred to a new Eppendorf tube in addition of 10 µl of 1 M perchloric acid on ice for 30 min for protein precipitation and then centrifuged at 1,600 g_{av} for 3 min using a Thermo scientific Pico 17 bench top centrifuge. The supernatant was disposed and the cell pellet was dissolved in 0.5 ml of 0.3 M sodium hydroxide and incubated overnight at 37°C prior to protein quantification by Lowry assay (see Section 2.3.4).

Glass tubes were wrapped in foil and prepared on ice in duplicate including standards and blanks. 300 µl in a total volume of assay mixture was added to each tube as follows:

100 µl of 0.5 M sodium tetraborate buffer (pH 9.0 at 37°C);
50 µl of 1.3 mg/ml semicarbazide-HCl solution (diamine oxidase inhibitor);
50 µl of 0.23 mg/ml pargyline-HCl solution (monoamine oxidase inhibitor);
100 µl of the cell homogenate was added into the tubes (100 µl water instead was added to the standard and blank tubes);
100 µl of 0.4 mg/ml horseradish peroxidise (dissolved in deionised water; prepared fresh only after all the other components have been added to the assay mixture. Working quickly, add appropriate amount to the assay mix on ice, and proceed with assay).

Prior to the addition of homovanillic acid and N^1-monoacetylspermine, tubes containing reaction mix were pre-incubated in a shaking water bath at 37°C for 20 min in order to remove endogenous substrates of H_2O_2 producing enzymes.

The standards were prepared during this 20 min slot. 10 µl of H_2O_2 (30% w/v solution, 8.82 M) was diluted to 100 ml with deionised water in a clean volumetric flask, producing a 0.882 mM H_2O_2. 100 µl of this solution was mixed with 1.6 ml of deionised water, giving a 0.05 mM (5 nmol/100µl) H_2O_2 stock (working quickly to minimize H_2O_2 exposed to air). Standards were prepared as follows (Appendix, Fig. 6.10):

Final concentration Std. (nmol/100µl)	0.05 mM H_2O_2 (µl)	dH_2O (µl)
0	0	500
1	100	400
2	200	300
3	300	200
4	400	100
5	500	0

Table 2.3 Preparation of H_2O_2 standards

After 20 min pre-incubation, in addition of 100 µl of 1 mg/ml homovanillic acid to all the tubes, 100 µl of each standard was added to its corresponding standard tubes, and 100 µl of 0.42 mg/ml N^1-monoacetylspermine-3HCl (the substrate) was added to the sample tubes. All the tubes were incubated at 37°C for 30 min in the shaking water-bath. 2 ml of 0.1 M NaOH was added to stop the enzyme reaction. The background fluorescence was determined by the addition of the substrate N^1-monoacetylspermine into the two blank tubes only after the enzyme inactivation by NaOH.

A Perkin-Elmer LS50 luminescence spectrophotometer was used with the following setting: The fluorescence intensity was measured with excitation at 323 nm with excitation slit width at 10 and emission at 426 nm with emission slit width at 9. The sample was transferred to a fluorescence (4 sided) cuvette and measured once at a time.

APAO activity was calculated as nmol N^1-acetylspermine/min/mg protein. To measure SMO activity, 100 µl of 0.42 mg/ml of spermine tetrachloride was used as reaction substrate.

2.2.13 Measurement of polyamines by Liquid Chromatography Mass Spectrometry (LC-MS)

Intracellular polyamines were conventionally quantified by HPLC method (Seiler, 1983). Based on the same experimental principle, a more sensitive and efficient method was developed using LC-MS to measure both intracellular and extracellular polyamines especially acetylpolyamines in cell culture, which are present in low concentrations and undetectable by HPLC method. The difficulty in this method development was to determine the standard concentration ranges in order to cover each of the seven polyamines (put, spd, spm, N^1-ac-spd, N^8-ac-spd, N^1-ac-spm, and N^1,N^{12}-diac-spm) in the three cell types. On the other hand, there is a higher concentration limit above which the LC-MS detector is not able to handle, i.e. any concentration beyond the detector's limit results in a non-linear calibration standard curve. This was observed particularly in the intracellular spm calibration standard curve and the extracellular N^1-ac-spd calibration standard curve. Two sets of polyamine standards were established (std. 1-6) for WT and $SSAT^{\pm}$ cells, each standard contained five or seven (plus N^8-ac-spd and N^1,N^{12}-diac-spm when detecting extracellular polyamines) polyamines in an order of concentrations from low to high.

Prior to preparation of polyamine standards, two sets working stocks were prepared by a series of dilutions of 5 mM polyamine stocks using 0.2 M PCA (Table 2.4).

	Working stock 1 (mM)	*Working stock 2 (mM)*
Put	0.0025	0.0125
Spd	0.005	0.025 (WT) or 0.05 (SSAT)
Spm	0.02	0.1(WT) or 0.2 (SSAT)
N^1-ac-spd	0.01	0.05
N^8-ac-spd	0.001	0.005 (WT) or 0.01 (SSAT)
N^1-ac-spm	0.001	0.005 (WT) or 0.01 (SSAT)
N^1,N^{12}-diac-spm	0.005	0.025(WT) or 0.05 (SSAT)

Table 2.4 Preparation of working stocks for making polyamine standards

Two sets of standards were needed and prepared because higher concentrations of acetylpolyamines and putrescine in SSAT^{+} cells than in WT were identified. A range of polyamine concentrations were chosen as the standards as follows (Tables 2.5 & 2.6):

	LNCaP WT cell polyamine standards (µM)						
	Put	Spd	Spm	N^1-ac-spd	N^8-ac-spd	N^1-ac-spm	N^1,N^{12}-diac-spm
Std.1	0	0	0	0	0	0	0
Std.2	0.05	0.1	0.25	0.05	0.01	0.01	0.1
Std.3	0.125	0.25	1.25	0.125	0.05	0.05	0.25
Std.4	0.25	0.5	5	0.25	0.125	0.125	0.5
Std.5	0.375	2.5	10	0.5	0.25	0.25	2.5
Std.6	0.5	5	15	1.25	0.5	0.5	5

Table 2.5 Polyamine standard concentrations of WT cells for LC-MS

	LNCaP SSAT transfected cell polyamine standards (µM)						
	Put	Spd	Spm	N^1-ac-spd	N^8-ac-spd	N^1-ac-spm	N^1,N^{12}-diac-spm
Std.1	0	0	0	0	0	0	0
Std.2	0.05	0.1	0.25	0.05	0.01	0.01	0.1
Std.3	0.125	0.25	1.25	0.25	0.05	0.05	0.25
Std.4	0.25	0.5	5	1.25	0.25	0.25	0.5
Std.5	1.25	2.5	10	5	0.5	0.5	2.5
Std.6	2.5	5	15	10	1	1	5

Table 2.6 Polyamine standard concentrations of SSAT$^{\pm}$ cells for LC-MS

Two sets of the standard concentrations (Table 2.5 & 2.6) were made via series of dilutions from the working stocks (Table 2.4) according to the cell lines. Total volume of 2000 µl of the each standard (Std. 1-6) was made as follows (Table 2.7 & 2.8). See appendix (Fig. 6.3 & 6.4) for standard curves and dansylated polyamine ion spectra by LC-MS.

Volume (µl)	Std. 1	Std. 2	Std. 3	Std. 4	Std. 5	Std. 6
Put (0.0025 mM)	0	40	100	200	300	400
Spd (0.005 mM)	0	40	100	200	-	-
Spm (0.02 mM)	0	25	125	500	-	-
N^1-ac-spd (0.01 mM)	0	10	25	50	-	-
N^8-ac-spd (0.001 mM)	0	20	100	250	500	-
N^1-ac-spm (0.001 mM)	0	20	100	250	500	-
N^1,N^{12}-diac-spm (0.005 mM)	0	40	100	200	-	-
Spd (0.025 mM)	0	-	-	-	200	400
Spm (0.1 mM)	0	-	-	-	200	300
N^1-ac-spd (0.05 mM)	0	-	-	-	20	50
N^8-ac-spd (0.005 mM)	0	-	-	-	-	200
N^1-ac-spm (0.005 mM)	0	-	-	-	-	200
N^1,N^{12}-diac-spm (0.025 mM)	0	-	-	-	200	400
PCA (0.2 M)	2000	1805	1350	350	80	50

Table 2.7 Preparation of polyamine standards in WT cells

Volume (µl)	Std. 1	Std. 2	Std. 3	Std. 4	Std. 5	Std. 6
Put (0.0025 mM)	0	40	100	200	-	-
Spd (0.005 mM)	0	40	100	200	-	-
Spm (0.02 mM)	0	25	125	500	-	-
N^1-ac-spd (0.01 mM)	0	10	50	250	-	-
N^8-ac-spd (0.001 mM)	0	20	100		-	-
N^1-ac-spm (0.001 mM)	0	20	100	500	-	-
N^1,N^{12}-diac-spm (0.005 mM)	0	40	100	200	-	-
Put (0.0125 mM)	0	-	-	-	200	400
Spd (0.05 mM)	0	-	-	-	100	200
Spm (0.2 mM)	0	-	-	-	100	150
N^1-ac-spd (0.05 mM)	0	-	-	-	200	400
N^8-ac-spd (0.01 mM)	0	-	-	50	100	200
N^1-ac-spm (0.01 mM)	0	-	-	-	100	200
N^1,N^{12}-diac-spm (0.05 mM)	0	-	-	-	100	200
PCA (0.2 M)	2000	1805	1325	100	1100	250

Table 2.8 Preparation of polyamine standards in $SSAT^{\pm}$ cells

1 mM 1,7-diaminoheptane stock (acting as the internal standard) was diluted 1:20, giving a working stock of 0.05 mM. Dansyl chloride was chosen as the derivatising reagent and was prepared freshly in acetone prior to use.

200 µl aliquot of the polyamine standard and the sample extract was used per assay. Addition of the reagents to all the samples and the polyamine standards was carried out in the following order: 10 µl of 0.05 mM internal standard, 50 µl of 1 g/ml sodium carbonate decahydrate, and 0.5 ml of 15 mg/ml dansyl chloride. Samples were incubated overnight in a water-bath at 37°C in the dark. 125 µl of 10 mg/ml L-proline was added to remove excess dansyl chloride on the next day and thoroughly mixed. All the samples and standards were incubated in the water-bath at 37°C for further 30 min until solutions turned pale yellow or colourless. 0.5 ml of toluene was finally added to extract dansylated polyamines and completely mixed by vortex. After centrifugation at 1,600 g_{av} for 2-3 min using a Thermo scientific Pico 17 bench top centrifuge, the organic phase (on top) and an aqueous phase (on bottom) separated. The organic phase which contains polyamines was transferred to a plastic round bottom tube for evaporation. Samples were evaporated by nitrogen until dry and reconstituted in 200 µl methanol and ready for LC-MS analysis. All results were calculated as nmol/mg protein.

NB: As the polyamine standards crossed a varied range, 1 µl injection into the LC-MS machine was recommended for the higher concentration polyamines such as spermine due to the upper limit of the LC-MS detector, while 5 µl injection may be more suitable for the lower concentration polyamines such as acetylpolyamines.

2.2.14 Extraction of intracellular and extracellular polyamines

Cells were plated at the appropriate density in a 60 mm diameter cell culture dish in duplicate and incubated for 48 h. After 48 h growth, the medium was replaced with fresh medium containing drug(s). The cells were harvested after a certain period of the drug exposure time.

At the time of harvesting, medium was removed from the culture dish into a 15 ml conical tube. The tube was centrifuged at 800 g_{av} for 10 min using an ALC PK121R multispeed refrigerated centrifuge to sediment suspended cellular material. 1 ml of the medium supernatant was transferred to an Eppendorf tube and mixed with 0.25 ml of 1 M $HClO_4$ and kept on ice for 30 min for polyamine extraction. The Eppendorf tube was then centrifuged at 1,600 g_{av} for 3 min using a Thermo scientific Pico 17 bench top centrifuge.

The acid soluble supernatant containing polyamines was stored at -20°C for polyamine analysis at a later stage.

After the medium was removed, the cell sheet on the plate was rinsed twice with ice-cold PBS after the medium was removed. The cells were gently scraped off using a rubber cell scraper in 3 ml of cold PBS and transferred to a 15 ml conical tube. The tube was centrifuged at 220 g_{av} at 4°C for 3 min. The supernatant was discarded and the cell pellet was resuspended in 1 ml of 0.2 M $HClO_4$, transferred to an Eppendorf tube and stored on ice for 30 min for polyamine extraction and protein precipitation. The Eppendorf tube was centrifuged at 1,600 g_{av} for 3 min to sediment the protein fraction. The acid soluble supernatant was stored at -20°C for further polyamine analysis. The protein pellet was dissolved in 0.5 ml of 0.3 M NaOH and incubated overnight at 37°C for Lowry assay to determine total cellular protein content (see Section 2.3.4).

2.2.15 Measurement of protein expression by Western Blotting

Cells were seeded at the appropriate density in a 10 cm diameter cell culture dish in duplicate or triplicate. After 48 h growth, the medium was replaced with fresh medium containing drug(s) for the appropriate period of time of drug exposure.

The cells were washed twice with 5 ml ice-cold PBS. After addition of 1 ml ice-cold RIPA buffer to lyse the cells and 5 µl protease inhibitor cocktail (1:100) to prevent proteolysis to the plate, the cells were scraped off using a rubber cell scraper and transferred to a 2 ml Eppendorf tube. The tube was maintained for 30 min on ice with constant agitation. The cytosolic fraction was separated by centrifugation at 1,600 g_{av} for 20 min in a 4°C pre-cooled Thermo scientific centrifuge to remove cell debris. The Eppendorf tube was gently remove from the centrifuge and placed on ice. The supernatant was transferred to a new 2 ml tube and stored at -20°C.

40 µl of the cell lysate was taken to a new Eppendorf tube in addition of 10 µl of 1 M $HClO_4$ and kept on ice for 30 min for protein precipitation. The tube was then centrifuged at 1,600 g_{av} for 3 min. After the supernatant was disposed, 0.5 ml of 0.3 M NaOH was

added to dissolve the acid insoluble cell pellet and incubated overnight at 37°C prior to protein content determination by Lowry assay (see section 2.3.4).

A mixture solution of sample protein (30 µg/well), NuPAGE LDS Sample Buffer (4X), NuPAGE Reducing Agent (10X) and Deionized water was prepared (addition of the reducing agent was 1 h prior to loading the gel). To denature the protein, samples were heated at 70°C in a heating block for 10 min.

Novex Bis-Tris SDS 4-12% 12 well (1.0 mm) polyacrylamide gel (SDS-PAGE) was used with a maximum loading volume of 20 µl/well. The gel was removed from the pouch. The gel cassette was rinsed with deionised water (dH_2O) and the tape was peeled off from the bottom of the cassette. The comb was pulled out of the cassette. The wells were rinsed with the running buffer. The gel was inverted and shaken to remove the buffer. This was repeated two more time. The gel was placed into the cassette and seated into the XCell II blot module. Gel tension wedge was locked against the cassette. The running buffer was filled up into the chamber of the instrument, exceeding the level of the wells.

5 µl (for 8 x 10 cm gels) of low-range rainbow molecular weight marker (1 mg/ml) mixed with 5 µl of the NuPAGE LDS sample buffer and 10 µl of dH_2O was loaded into the far left lane of the gel. The mixture containing 30 µg sample protein (equal amount of protein per well) was loaded into the gel well. The gel was submerged in the NuPAGE MOPS SDS running buffer (20X) (prepared by thoroughly mixing 50 ml of the NuPAGE MOPS SDS running buffer with 950 ml dH_2O). The gel was run at 100 V for 2 h. Before the dye of the marker molecule (the migration front) reached the bottom of the gel, the power was turned off (proteins should be slowly eluted from the gel at this point so the gel should not be stored but transferred immediately).

Polyvinylidene difluoride (PVDF) membrane (0.45 µm) and filter papers were cut to the dimension of the gel. The PVDF membrane was soaked in methanol for 30 s, rinsed in dH_2O, and incubated in the ice cold NuPAGE transfer buffer (20x) for 5 min (prepared by thoroughly mixing 50 ml of the NuPAGE transfer buffer (20x) with 100 ml methanol and 850 ml dH_2O).

The blotting pads were soaked until saturated in the transfer buffer. Air bubbles were removed by squeezing the blotting pad submerged in the buffer. After electrophoresis, the gel was removed from the cassette by inserting the gel knife into the gap between the two cassette plates. The gel was equilibrated for 3 min in the ice cold transfer buffer. A pre-soaked filter paper was placed onto the gel and air bubbles were removed by using a glass pipette rolling over the surface. The pre-soaked transfer membrane was placed onto the other side of the gel. The pre-soaked filter paper was then placed onto the transfer membrane. Again, air bubbles were removed. The transfer stack was prepared in the order from -ve (black) to +ve (red): sponge / filter paper / gel / transfer membrane / filter paper / sponge (more sponge may be needed to ensure the gel and the transfer membrane tightly contacted. However, the transfer process may fail if the stack was too tight resulting in the squeeze-out of the transfer buffer). The blot module was filled with the transfer buffer until the gel/membrane sandwich was covered in the buffer. The lid was placed on top of the blot unit. The red and black wires were plugged into the power supply before turning on the power. The transfer was run at 60 V for 1 h (this was used for transferring one NuPAGE Bis-Tris gel).

The membrane was blocked using 5% (w/v) nonfat dry milk in the TBST buffer for 1 h at room temperature or overnight at 4°C to prevent non-specific background binding of the primary and/or secondary antibodies.

The membrane was exposed to the anti-SSAT primary antibody (1:1000 dilution) was carried out in 5% dried milk in the TBST for 2 h at room temperature. The membrane was washed three times with the TBST of 5 min each time. Then, the membrane was incubated with a secondary antibody (goat anti-rabbit IgG peroxidase conjugate diluted 1:2000 in 5% dry milk in the TBST) for 1 h at room temperature. The membrane was washed three times of 5 min each with the TBST and then rinse in the TBS. For signal development, the membrane was soaked in 1:1 ECL peroxidase detection reagents and exposed to an X-ray film for 1-3 min in the dark room. The film was inserted into the Kodak X-OMAT 1000 processor machine for film development.

NB: SSAT protein was shown as a ~28 kDa band. β-actin was used as the internal control (43 kDa). Exposure to anti-β-actin (C4) mouse monoclonal IgG_1 primary antibody (200

µg/ml) (1:1000 dilution) was carried out in 5% dry milk in TBST for 2 h at room temperature. The membrane was then washed 3 times with TBST, 5 min each time and blocked with anti-mouse IgG peroxidase conjugate secondary antibody (1:2000) in 5% dry milk in TBST for 1 h at room temperature. The membrane was washed 3 times with TBST of 5 min each time and then soaked in TBS before using the ECL kit.

2.2.16 RNA isolation in cell culture

Cells were plated at the appropriate density on a 60 mm diameter cell culture dish in duplicate. The medium was replaced with fresh medium as required after 48 h growth. In the experiment requiring treatment, the medium was replaced with fresh medium containing drug(s) and the cells were exposed to the drug(s) for the required period of time.

The working area surface, pipettes, and all equipment was cleaned with RNaseZap® decontamination solution or 70% ethanol to ensure a RNase-free working environment.

The cells were harvested by aspirating the medium and washed with 1 ml ice-cold PBS. The PBS was completely discarded, 0.5 ml of Trizol (1 ml Trizol for 10 cm dish) was added to the dish and the cells were scraped off and transferred into a clean 2 ml Eppendorf tube (duplicate dishes were pooled together at this point). The tube was stored on ice for 5 min (alternatively, a cryo vial was used for snap-freezing in liquid nitrogen and stored at -80°C until all samples were collected).

The genomic DNA was sheared using a 1 ml syringe with a 19G 2” needle. The cell lysate was aspirated through the needle slowly 3-4 times until the solution was no longer viscous. After addition of 200 µl chloroform the tube was hand-shaken for about 15 sec and then left at room temperature for 5 min. The tube was centrifuged at 1,600 g_{av} at 4°C for 5 min using a Thermo scientific Fresco 21 refrigerated bench top centrifuge. At this point, 3 layers appeared in the tube: top layer: clear – aqueous; middle layer/interphase – white precipitated DNA; bottom layer – pink organic phase.

The aqueous phase was carefully pipette off (using a small pipette and leaving behind about 1 mm above the DNA layer to prevent DNA contamination) and placed into a clean 1.5 ml Eppendorf tube. 500 µl isopropanol was added to the aqueous phase and gently mixed by hand. The Eppendorf tube was left at room temperature for 10 min and then centrifuged at 1,600 g_{av} for 20 min at 4°C (if a low yield was expected, centrifuging was for 30 min). The eppendorf was placed on ice (there was a pellet barely visible). The isopropanol was removed and 1 ml of ice-cold 75% ethanol was added and mixed gently. The tube was again centrifuged at 1,200 g_{av} for 5 min at 4°C. The ethanol was removed and the tube was allowed to air dry for 1 min. To remove the rest of the ethanol and quicken the evaporation, the tube was briefly centrifuged to force the remaining fluid on the side of the tube to move to the bottom, then as much of the ethanol as feasible was removed (if the pellets dry out for too long, the RNA crystallised and was very difficult to resolubilise, it needed to be heated to 65°C for resolubilisation). The best time to add RNase free water (distilled & filtered) was when there was only a tiny meniscus left around the pellet itself. 30 µl of the water was added to the RNA pellet (the dissolved RNA pellet could be stored at -20°C temporarily for further analysis).

The Nanodrop machine was cleaned and calibrated with 2 µl of PCR grade water and wiped dry with blue tissue. 2 µl of the RNA sample was placed onto the Nanodrop. The wavelengths were set for RNA measurement. The absorbance was measured at 260 & 280 nm (The 260/280 ratio was meant to be greater than 1.8. If the ratio was less than 1.5-1.6 or so, the RNA was likely at least partially degraded. Lower ratios also suggested DNA or thiocyanate contamination.)

2.2.17 Reverse transcription (RT)

2 µg RNA was added to each two 0.2 ml Eppendorf tubes. One tube was used for the RT reaction and the other was served as the no-RT control. The total volume was brought to 11 µl by adding additional diethylpyrocarbonate (DEPC) treated water (to reduce the risk of RNA being degraded by RNases). 1 µl of the 2 µg/µl random primers was added to each tube. The tube was centrifuged in short pulses. The tube was heated up to 70°C for 10 min (to melt the secondary structure of RNA) and cooled down to 4°C for 2 min (primer annealing) using a thermal cycler.

For each reaction, 8 µl of a reagent mixture was made as follows and added per tube: Reaction buffer 4 µl; 10 mM dNTP 1 µl; 0.1 mM DTT 2 µl; Reverse Transcriptase 1 µl (only to the sample tube); and PCR grade H_2O 1 µl (only to no-RT control tube).

The tube was mixed, centrifuged by short pulses and left at room temperature for 10 min. cDNA synthesis was carried out at 42°C for 50 min, and then at 95°C the reverse transcriptase was denatured for 5 min using the thermal cycler. Finally, the reaction volume was made up to 100 µl by adding 80 µl PCR grade H_2O. The sample was stored at -20°C for qPCR analysis.

2.2.18 Measurement of *Sat1* gene transcription by q-PCR

	SAT1					*GAPDH*				
	Standards		Samples			Standards		Samples		
	1	**2**	**3**	**4**	**5**	**6**	**7**	**8**	**9**	**10**
A	Neat	Neat	WT	WT	WT	Neat	Neat	WT	WT	WT
B	1:10	1:10	SSAT-	SSAT-	SSAT-	1:10	1:10	SSAT-	SSAT-	SSAT-
C	1:100	1:100	SSAT+	SSAT+	SSAT+	1:100	1:100	SSAT+	SSAT+	SSAT+
D	1:1,000	1:1,000	WT NO RT	WT NO RT	WT NO RT	1:1,000	1:1,000	WT NO RT	WT NO RT	WT NO RT
E	1:10,000	1:10,000	SSAT- NO RT	SSAT- NO RT	SSAT- NO RT	1:10,000	1:10,000	SSAT- NO RT	SSAT- NO RT	SSAT- NO RT
F	1:100,000	1:100,000	SSAT+ NO RT	SSAT+ NO RT	SSAT+ NO RT	1:100,000	1:100,000	SSAT+ NO RT	SSAT+ NO RT	SSAT+ NO RT
G	BLANK	BLANK				BLANK	BLANK			

Table 2.9 Example of q-PCR plate lay-out

Standards were made by serial of dilutions of the cDNA of $SSAT^+$ cells.

Neat = the non-diluted cDNA; 1:10 = 10 µl of the cDNA + 90 µl of PCR grade H_2O;

1:100 = 10 µl of the solution (1:10) above + 90 µl of PCR grade H_2O; and same methods for further serial dilutions till 1:100,000.

WT no-RT: WT RNA without reverse transcription;

$SSAT^-$ no-RT: $SSAT^-$ RNA without reverse transcription;

$SSAT^+$ no-RT: $SSAT^+$ RNA without reverse transcription

Preparation of the following mixture was carried out in an air-flow cabinet: 50 µl of the original forward and reverse primers (100 µM) was diluted to 20 µM by addition of 200 µl PCR grade H_2O. The area of the 384-well (or 96-well) PCR plate was labeled before addition of the reagents.

SAT1 reagent mixture (total volume was calculated depending on the number of wells used)**:** Probe master 10 µl/well; SSAT forward primer (20 µM) 0.2 µl/well; SSAT reverse primer (20 µM) 0.2 µl/well; Universal probe (No.82) 0.2 µl/well; PCR grade H_2O 6.4 µl/well.

3 µl/well of the 1:10 diluted sample cDNA and subsequently 17 µl/well of the mixture above was added to the PCR plate as shown in Table 5 (10 µl of sample cDNA was diluted 1:10 with 90 µl H_2O and 3 µl of this was added straight to the bottom of the well against the right side of the well when moving the tip out, so the tip does not need to be changed with the same sample. After addition of the sample cDNA, when adding 17 µl of the mixture the tip was against the left side of the well but not down to the bottom).

GAPDH (the reference gene) reagent mixture (total volume was calculated depending on the number of wells used)**:** VIC labeled GAPDH assay mix 1 µl/well; Probe master: 10 µl/well; PCR grade H_2O 6 µl/well.

Again, 3 µl/well of the 1:10 diluted sample cDNA and subsequently 17 µl/well of the mixture above were added to the PCR plate as shown in Table 2.9. The plate was sealed with film and centrifuged at 750 - 1000 rpm for 1 min and then inserted into the Roche Light Cycler 480 PCR machine for analysis.

2.2.19 Determination of protein synthesis rate using radiolabelled amino acids mixture

Cells were seeded at the appropriate density (2.4 X $10^4/cm^2$) in a 60 mm diameter cell culture dish in duplicate and grown for 48 h. The medium was replaced with fresh medium in addition of 1.85 kBq/ml (0.05 µCi/ml) of [^{14}C]-L-amino acid mixture with or without drug(s). The cells were harvested at the drug exposure time of 6, 12, 24, and 48 h by washing twice with 1 ml ice-cold PBS, scraping in 3 ml PBS, and centrifuged at 350 g_{av}

at 4°C for 5 min using a Jouan MR22 refrigerated centrifuge. The supernatant was discarded and the cell pellet was resuspended in 500 µl of 0.2 M perchloric acid, transferred to an Eppendorf tube and stored on ice for 30 min. After 30 min, the cell suspension was centrifuged at 1,600 g_{av} for 3 min using a bench top Thermo scientific Pico 17 centrifuge. The acid soluble supernatant was discarded and the pellet was dissolved in 500 µl of 0.3 M sodium hydroxide at 37˚C overnight.

50 µl of the alkali-soluble material was removed to a scintillation vial and in addition 450 µl of 2.5% (v/v) hydrochloric acid. 4 ml of the biodegradable scintillation fluid was added to each vial. The [^{14}C] radioactivity was counted using a Canberra Packard 1900A liquid scintillation analyser by [^{14}C] protocol. Total cellular protein content was determined by Lowry assay (see section 2.2.8). Results were shown as dpm/mg protein.

2.2.20 Measurement of polyamine efflux

Efflux is an integral part of the regulation of intracellular polyamine homeostasis. Polyamine efflux can be measured by quantifying the total [^{3}H] labelled polyamines in the extracellular media after prelabelling the cells with [^{3}H] putrescine (Wallace & Mackarel, 1998).

Cells were plated at the appropriate density in a 60 mm diameter cell culture dish in duplicate and incubated for 24 h before addition of 18.5 kBq/ml (0.5 µCi/ml) of [^{3}H]-putrescine. The cells were further incubated for 36 h. After 36 h radioisotope incubation (60 h in total cell growth), the medium was removed and the cells were washed twice with 3 ml warm (37°C) RPMI 1640 medium without FBS to remove non-specific binding of [^{3}H]-putrescine to the cell surface. The cells were further incubated for 12 h with fresh medium to allow radiolabelled and free polyamine pools to equilibrate. After 12 h incubation (72 h in total cell growth), the medium was replaced with fresh medium containing drug(s). This time point was assumed as time 0 (efflux of cellular radioactivity was monitored from here).

Cells were harvested at time point of 0, 6, 12, 24 and 48 h. The plates were removed from the incubator and placed on ice. The medium was removed into a 15 ml conical tube,

volume was precisely recorded. The tube was centrifuged at 800 g_{av} at 4°C for 10 min to sediment suspended cellular material. 1 ml of the medium supernatant was transferred to an Eppendorf tube with addition of 0.25 ml of 1 M $HClO_4$. The tube was then thoroughly mixed and kept on ice for 30 min to extract polyamines and precipitate protein. After 30 min, the Eppendorf tube was centrifuged at 1,600 g_{av} for 3 min using a bench top Thermo scientific Pico 17 centrifuge. The acid soluble supernatant containing polyamines was stored at -20°C until further analysis.

The cell sheet on the plate was rinsed three times with 1 ml ice-cold PBS after the medium was removed. 3 ml of cold PBS was added to the plate and the cells were gently scraped off (avoiding damage cell membrane resulting in intracellular polyamine release) and transferred to a 15 ml conical tube. The tube was centrifuged at 350 g_{av} at 4°C for 5 min using a Jouan MR22 centrifuge. The supernatant was discarded and the cell pellet was resuspended in 1 ml of 0.2 M $HClO_4$, transferred to an Eppendorf tube and kept on ice for 30 min for polyamine extraction and protein precipitation. The protein suspension was centrifuged at 1,600 g_{av} for 3 min to sediment the protein fraction. The acid soluble supernatant was stored at -20°C until further analysis. The protein pellet was dissolved in 0.5 ml of 0.3 M NaOH and incubated at 37°C overnight prior to the Lowry assay (Section 2.3.4) for protein content determination.

The acid soluble samples containing polyamines from both cell extract and medium extract were defrosted and centrifuged at 1,600 g_{av} for 5 min to pellet any suspended protein. 50 µl of the supernatant from the cell extract plus 450 µl of cold RPMI 1640 medium were added into a scintillation vial. 450 µl of the supernatant from the [^{3}H] medium extract and 50 µl of 0.2 M $HClO_4$ were added to a separate scintillation vial. Finally 4 ml biodegradable scintillation cocktail was added into each vial and thoroughly mixed. The determination of radioactivity was performed using a Canberra Packard 1900A liquid scintillation analyser with a tritium protocol (protocol 4).

The total radioactivity (dpm) was the sum of the cell (intracellular) and the medium (extracellular) fraction radioactivity. The extracellular radioactivity was expressed as a percentage of the total radioactivity. The intracellular radioactivity was shown as dpm/mg protein.

2.2.21 Measurement of intracellular reduced glutathione (GSH)

Intracellular GSH content of cells in culture was measured using a method by Hissin & Hilf (1976), which was modified from the original method by Cohn & Lyle (1966).

Cellular GSH was extracted in 0.2 M $HClO_4$ (Section 2.2.7) and stored at -20°C before analysis. The acid-insoluble fraction was dissolved in 0.3 M NaOH and used for total cellular protein quantification by the Lowry assay (Section 2.2.8). Samples can only be used for this assay when they were defrosted for the first time. Samples were centrifuged at 1,600 g_{av} for 3 min to precipitate undissolved materials before use. GSH standards (0-100 µM) were prepared in 0.2 M $HClO_4$ fresh from a 10 mM GSH stock. To make 1 ml of 100 µM GSH working stock, 10 µl of 10 mM GSH was mixed with 990 µl of distilled H_2O (Table 2.10).

Final amount of GSH (nmol)	Final concentration of GSH (µM)	100 µM GSH (µl)	0.2 M $HClO_4$ (µl)
0	0	0	100
0.625	25	25	75
1.25	50	50	50
1.875	75	75	25
2.5	100	100	0

Table 2.10 Preparation of GSH standards

25 µl aliquot of the standards and samples were added to a foil wrapped LP3 test tube and then thoroughly mixed with 2.3 ml of the phosphate-EDTA buffer (0.25 M Na_2PO_4 and 5 mM EDTA, pH 8.0). 100 µl of 1 mg/ml o-phthalaldehyde (OPA) made fresh in methanol was added into each tube to initiate the reaction. The solution was thoroughly mixed and incubated at room temp for 15 min and then transferred into a fluorescence cuvette (4 sided).

Fluorescence intensity was measured at 420 nm with the excitation at 350 nm with slit width 5 using a Perkin Elmer Luminescence spectrometer LS50B linked to a computer. Results were analysed using the GSH standard curve and expressed as nmol GSH/ mg protein.

2.2.22 Measurement of ROS by DCFDA using flow cytometry

Intracellular ROS were measured using oxidised 2',7'-dichlorofluorescin diacetate (DCFDA) by flow cytometry according to a method by Eruslanov & Kusmartsev (2010). DCFDA, a fluorogenic dye, is deacetylated to H_2DCF by intracellular esterases after it diffuses in the cell. H_2DCF can be oxidised by ROS to form the highly fluorescent product DCF, which can be detected by an increase in fluorescence at 530 nm when the sample is excited at 485 nm using flow cytometry.

Cells were plated at a density of 2.4 x 10^4 / cm^2 in a 60 mm cell culture dish in duplicate for 48 h and treated with drugs (2 mM aspirin or 50 µM 5-FU) for 48 h. The cells were harvested by trypsinisation and resuspended in 2 ml PBS in a 15 ml conical tube. To stain the cells, 4 µl of 10 mM DCFDA made fresh in DMSO was added to each tube except unstained controls to produce a final concentration of 20 µM DCFDA and then the cells were incubated at 37°C for 45 min. After the staining, the cells were spun down at 200 g_{av} for 3 min using a Centaur 2 centrifuge machine. The cells were resuspended in 2 ml medium (without serum). A final concentration of 50 µM of tert-butyl hydroperoxide (tBHP) was used as the positive control. The cells were further incubated for 3-4 h to allow fluorescence generation. The medium was removed by centrifuge and the cells were resuspended in 0.5 ml of 1% formaldehyde in PBS and transferred to the FACS tubes for flow cytometry analysis.

2.2.23 DAPI nucleic acid staining

Cells were seeded at a density of 2.4 x 10^4 / cm^2 in a 10 cm cell culture dish in duplicate. After 48 h growth, cells were treated with drugs (2 mM Aspirin or 50 µM 5-FU) for 48 h. After 48 h treatment, media were collected in a 15 tube. Cells were washed with 1 ml ice-cold PBS twice and then detached by adding 1 ml of 0.25% trypsin-EDTA for 3-5 min at 37 °C. After cell detachment, 3 ml of medium containing FBS was added to neutralise trypsin-EDTA. Cell suspension was transferred to the corresponding 15 ml tube containing collected medium and centrifuged at 800 g_{av} for 3 min. The supernatant was discarded. The cell pellet was resuspended in 1 ml PBS and transferred to an Eppendorf tube,

centrifuged and the supernatant was discarded. 100 µl of cell suspension was used for cell counting.

Approximately 0.2 ml of 4% [v/v] formaldehyde per 1.0 x 10^6 cells was added to resuspend the cell pellet and incubated for 10 min at room temperature. Slides and filters were placed into appropriate slots in the cytospin with the cardboard filters facing the centre of the cytospin. 100 µl of the cell suspension in formaldehyde was cytospun onto glass microscope slides using a Shandon cytospin at 500 rpm for 5 min. After centrifuge, cells were left air-dry for 10 min. Cells were stained with the VECTASHIELD Hard Set Mounting Medium with DAPI (1.5 µg/ml) for 10 min to allow its permeation before excess DAPI was tapped off gently from the slides. The slides were left dry in the dark and then covered with a cover-slip and the edges were sealed with nail varnish. Slides were stored in the dark at 4 °C protected from light of photobleaching.

The cell images were captured using fluorescence microscopy (excitation/emission: 358 nm/461 nm). Apoptotic cells were shown with typical morphological features: cell shrinkage, chromatin condensation and formation of apoptotic bodies. 500 nuclei were counted per slide. Percentage of cells with apoptotic morphological features of the nuclei was calculated.

2.2.24 Statistical methods

Result values were shown as the mean of all replicate values $\pm$ standard error of the mean (SEM) in which the number of independent repeats was more than or at least equal to 3. Values were displayed as mean $\pm$ range where the number of independent repeats was less than 3. Independent repeat was defined as an experiment that was established from an independent passage of the cell rather than from the same passage, and the experiment was performed individually under the same procedure. Replicates were the number of individual observations within one experiment. Statistical analysis was performed using GraphPad software Prism 5 (GraphPad Software, Inc., 2236 Avenida de la Playa, La Jolla, CA 92037 USA). Results were analysed by two-way analysis of variance (ANOVA) with Bonferroni post-tests. A p value of less than 0.05 was considered as statistically significant.

3 Results

3.1 Characterisation of the experimental model system

3.1.1 Characterisation of cell growth, *Sat1* gene expression, SSAT protein expression and SSAT activity

Introduction

As the cell lines were new to our laboratory it was necessary to characterise the system before beginning the studies using the antiproliferative drugs. SSAT human cDNA transfected LNCaP cells were routinely cultured in the presence of tetracycline (Tet) which inhibited *Sat1* gene transcription using Tet-off advanced inducible gene expression system, resulting in basal or lower *Sat1* gene expression and SSAT enzymatic activity. In contrast, in the absence of Tet, the *Sat1* gene transcription was overexpressed leading subsequently to a significant increase in *Sat1* gene expression and SSAT enzymatic activity.

For convenience, "$SSAT^{-}$" will be used throughout to represent the transfected cells grown **with** Tet and thus low SSAT enzyme activity; and "$SSAT^{+}$" will be used to represent the transfected cells grown **without** Tet and thus high enzyme activity.

In order to characterise the growth of WT and SSAT human cDNA transfected LNCaP cell lines, experiments were carried out initially over a time course of 144 h. $SSAT^{-}$ cells grew the fastest after 48 h growth. On the other hand, $SSAT^{+}$ cells showed the slowest proliferation rate. The growth rate of WT cells was between that of $SSAT^{-}$ and $SSAT^{+}$ (Fig. 3.1). $SSAT^{-}$ and WT cells were confluent by 120 h growth, clumps were formed and the cells started to detach from the culture dishes. Cell viability of all the cells was around 80% (Fig. 3.2).

Fig. 3.1 Growth of WT, SSAT$^-$ and SSAT$^+$ cells

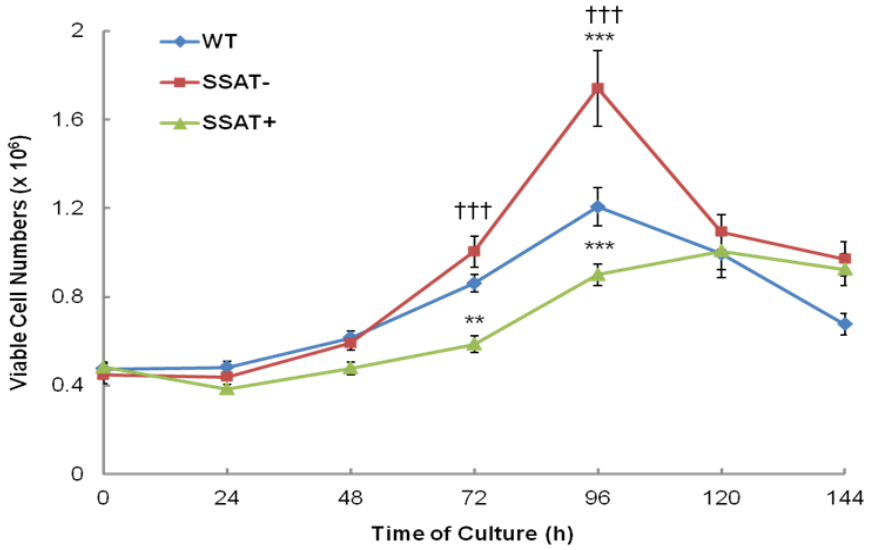

Fig. 3.1 Cells were seeded at a density of 2.4 x 10^4 / cm^2 in 60 mm diam. cell culture dish in duplicate. Cells were harvested at 24 h intervals and viable cell numbers counted using Trypan blue exclusion assay (Section 2.2.1). Results shown are mean ± SEM (n = 4 to 16, with 2 replicate per experiment). Statistical analysis was performed by two-way ANOVA using Prism 5. At 72 h, the differences of WT to SSAT$^+$ and of SSAT$^-$ to SSAT$^+$ are statistically significant. At 96 h, the differences between each cell line are statistically significant. p** < 0.01, p*** < 0.001; p††† < 0.001.

Fig. 3.2 Viability of WT, SSAT$^-$ and SSAT$^+$ cells

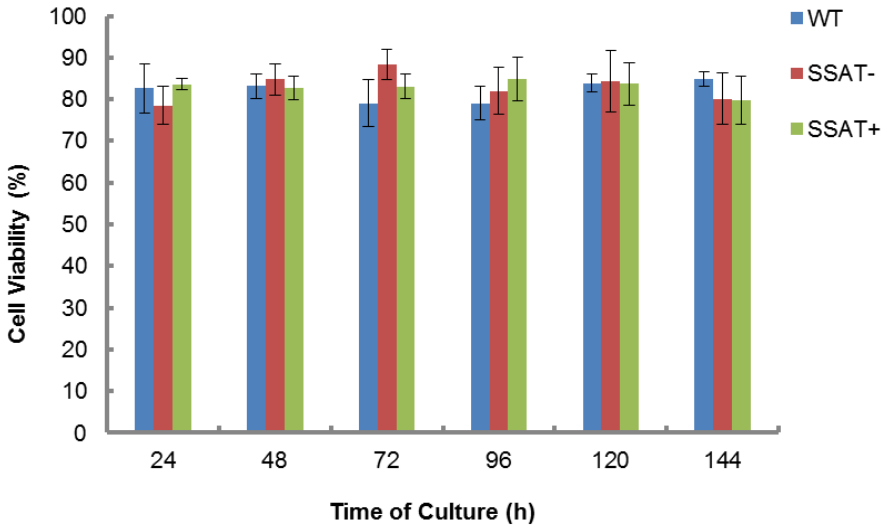

Fig. 3.2 Cell viability of attached cells was calculated by viable cell numbers / (viable cell numbers + dead cell numbers) x 100%. Results shown are mean ± SEM (n=3, with 2 replicates per experiment). Statistical analysis was performed by two-way ANOVA using Prism 5. p > 0.05.

Using the mean of total viable cell numbers at 24 h growth as the initial value, the generation time (Gt; population doubling time) was calculated for each cell type (Table 3.1). The results coincided with the cell counts in Fig. 3.1 with $SSAT^+$ having the longest Gt and $SSAT^-$ the shortest time.

Table 3.1 Generation time in WT, $SSAT^-$ and $SSAT^+$ cells

Cell Type	**Generation Time (h)**		
	48	**72**	**96**
WT	49	50	48
$SSAT^-$	39	34	34
$SSAT^+$	50	62	51

Table 3.1 Mean of the viable cell numbers from Fig. 3.1 were used to calculate generation time (Gt). Results were calculated by the equation $Gt = \log2*\Delta t / \log(N/N_0)$ related to the total viable cell number at 24 h. Gt, generation time; Δt, change in time (h); N, final cell number; N_0, initial cell number.

In addition to characterising cell growth, *Sat1* gene transcription was investigated using qPCR in order to determine whether there was an association of gene regulation with cell growth in a molecular level. *Sat1* mRNA expression in $SSAT^+$ cells was about 6 fold higher than that in WT and $SSAT^-$ cells after 96 h growth. Little difference was seen between WT and $SSAT^-$ cells (Fig. 3.3). This result was consistent with the high level transcription of *Sat1* gene in the absence of Tet under this Tet-off advanced inducible gene expression system.

To determine if the high level of *Sat1* gene transcription in $SSAT^+$ cell gave rise to increased SSAT protein expression, protein blotting (Western) was carried out at 48, 72, and 96 h after growth. Results showed denser bands in $SSAT^+$ cells than WT and $SSAT^-$ cells, particularly at 48 and 96 h (Fig. 3.4). Band density was compared by densitometry showed an increased SSAT protein expression in $SSAT^+$ and a decreased SSAT protein expression in $SSAT^-$ in contrast to that in WT (Fig. 3.5).

Fig. 3.3 SSAT mRNA expression in WT, SSAT$^-$ and SSAT$^+$ cells

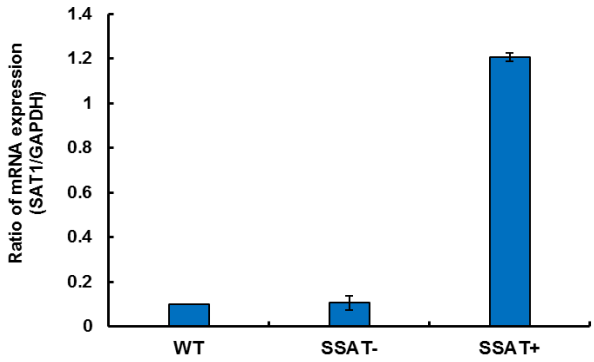

Fig. 3.3 Cells were seeded at a density of 2.4 x 10^4/cm^2 in 60 mm diam. cell culture dish in duplicate. Media was replaced after 24 h incubation and then every 48 h. Cells were harvested after 96 h growth. RNA was isolated by Trizol and quantified by Nanodrop (section 2.2.16). Results shown are mean ± range (n=1, with 3 replicates per experiment).

Fig. 3.4 SSAT Protein expression in WT, SSAT$^-$ and SSAT$^+$ cells

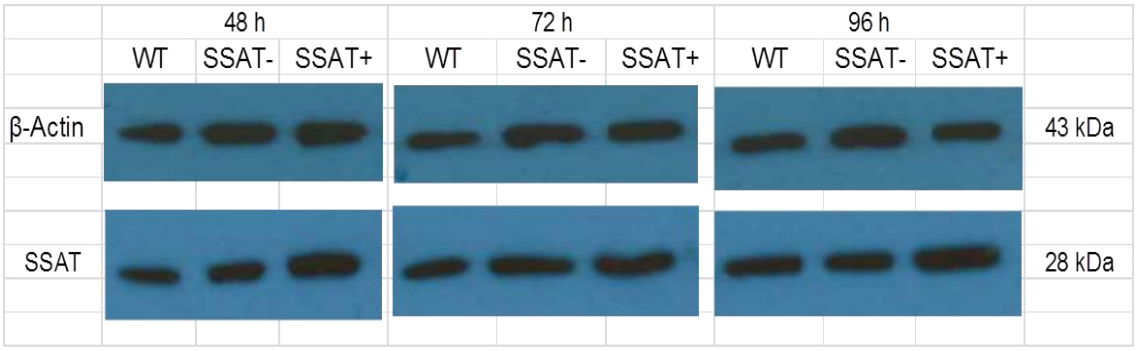

Fig. 3.4 Cells were seeded at a density of 2.4 x 10^4 / cm^2 in 60 mm diam. cell culture dish in duplicate. Cells were harvested after 48, 72, and 96 h growth and lysed (section 2.3.1). Protein content was determined by Lowry assay (section 2.3.4). 14 µg of protein lysates were loaded onto a Novex Bis-Tris SDS 4 – 12 % gel for electrophoresis. The gel was electroblotted onto a PVDF membrane. A rabbit polyclonal SAT1 antibody was used against human SSAT in conjunction with a goat anti-rabbit IgG peroxidase conjugate secondary antibody. β-Actin was used as internal control.

Following the characterisation of SSAT gene and protein expression, SSAT enzymatic activity was measured during a time course (24 – 144 h) in these cell lines. SSAT activity in SSAT$^+$ cells was significantly higher than that of the other two cell lines, with a continuous increase up to 96 h growth (Fig. 3.6).

Fig. 3.5 Densitometry of SSAT protein expression in WT, SSAT$^-$ and SSAT$^+$ cells

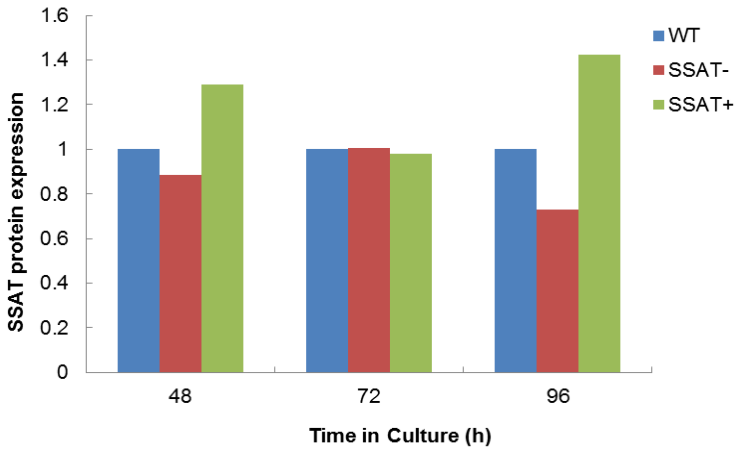

Fig. 3.5 This graph was plotted based on the results from Fig. 3.3 Band density was analysed using ImageJ software (http://rsbweb.nih.gov/ij/) via calculation of the SSAT protein band against its corresponding β-actin band density. The relative value of the SSAT protein expression in WT was calculated as 1, the relative band density values of SSAT$^{\pm}$ cells were compared to that of WT.

Fig. 3.6 SSAT enzymatic activity in WT, SSAT$^-$ and SSAT$^+$ cells

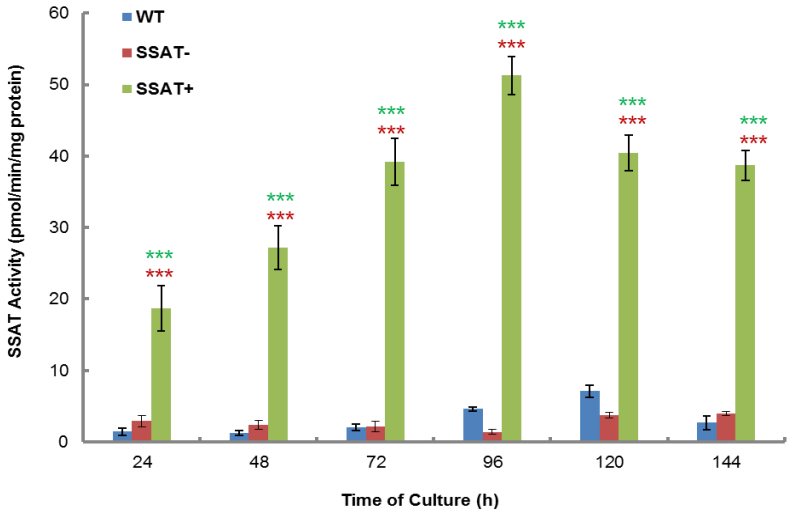

Fig. 3.6 Cells were seeded at a density of 2.4 x 10^4 / cm^2 in 60 mm diam. cell culture dish in duplicate. Cells were harvested at 24 h intervals. Media were replaced with fresh media at 24, 72 and 120 h. Results shown are mean ± SEM (n = 3, with 4 replicate per experiment). Statistical analysis was performed by two-way ANOVA with Bonferroni post-test comparing WT vs. SSAT$^-$, WT vs. SSAT$^+$ (*) and SSAT$^-$ vs. SSAT$^+$ (*) using Prism 5. p*** < 0.001.

In summary, above results (Fig. 3.3 to Fig. 3.6) show SSAT enzymatic activity in the three cell types was regulated at the *Sat1* gene transcription and SSAT protein translation

levels. SSAT activity was overexpressed (10-18 fold) in $SSAT^+$ cells in comparison to that in WT and $SSAT^-$ cells. Thus, this *in vitro* model system using three cell types was found to be able to express basal (WT), suppressed ($SSAT^-$), and overexpressed ($SSAT^+$) SSAT enzyme activity.

3.1.2 Characterisation of enzyme activity in response to SSAT alteration in polyamine pathway

In response to alterations of SSAT activity, WT and $SSAT^{\pm}$ cells showed different proliferative rate. Whether this difference was related to changes of major enzymes' (ODC, APAO and SMO) activity in the polyamine pathway was investigated.

ODC is responsible for putrescine biosynthesis. During a time course (0 - 144 h), ODC activity was significantly enhanced in $SSAT^+$ in contrast to WT and $SSAT^-$ cells (Fig. 3.7), indicating there was an increased requirement for putrescine to compensate the degradation of spermidine and spermine when SSAT was increased.

Fig. 3.7 ODC enzymatic activity in WT, $SSAT^-$, and $SSAT^+$ cells

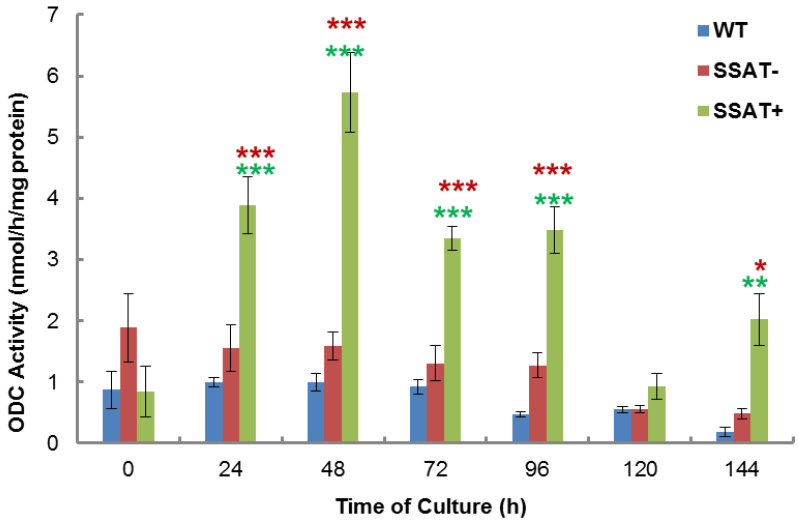

Fig. 3.7 Cells were seeded at a density of 2.4 x 10^4 / cm^2 in 60 mm diam. cell culture dish in duplicate. Cells were harvested at 24 h intervals. Media were replaced with fresh media at 24, 72 and 120 h. Results shown are mean ± SEM (n = 3, with 2 replicate per experiment). Statistical analysis was performed by two-way ANOVA with Bonferroni post-tests comparing WT vs. $SSAT^-$, WT vs. $SSAT^+$ (*) and $SSAT^-$ vs. $SSAT^+$ (*) using Prism 5. p* < 0.05, p** < 0.01, p*** < 0.001.

APAO is the downstream enzyme in the SSAT/APAO retro-conversion pathway, converting the substrates N^1-acetylpolyamines (products of SSAT) to spermidine and eventually putrescine. The enzymatic activity was measured during the same time course (0 - 144 h) as ODC activity in all the three cell types. In general, APAO activity in these cell types illustrated a similar pattern with a raised activity at 24 h after cell seeding followed by a declining trend and staying plateau. APAO activity in $SSAT^+$ cells was generally higher than that in $SSAT^-$ and WT cells (Fig. 3.8). These results suggest that SSAT overexpression can lead to a rise in APAO activity.

Fig. 3.8 APAO enzymatic activity in WT, $SSAT^-$, and $SSAT^+$ cells

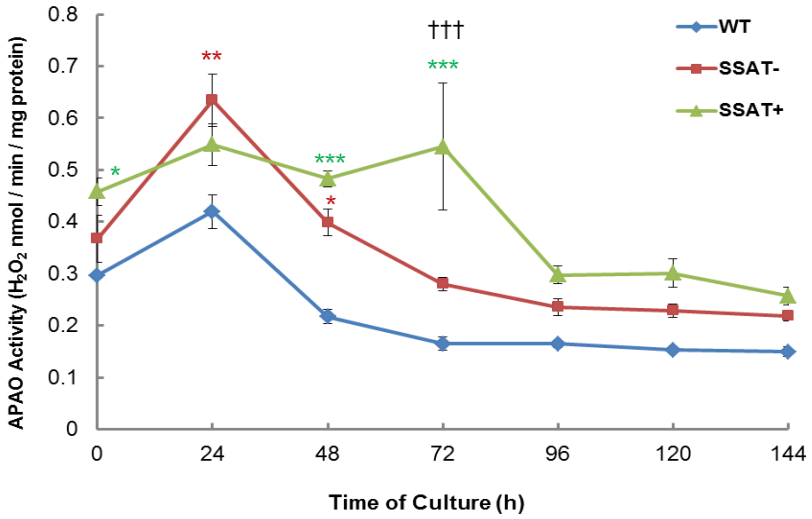

Fig. 3.8 Cells were seeded at a density of 2.4 x 10^4 / cm^2 in 60 mm diam. cell culture dish in duplicate. Cells were harvested at 24 h intervals. Media were replaced with fresh media at 24, 72 and 120 h. Results shown are mean ± SEM (n = 3, with 2 replicate per experiment). Statistical analysis was performed by two-way ANOVA with Bonferroni post-tests comparing WT vs. $SSAT^-$ (*), WT vs. $SSAT^+$ (*) and $SSAT^-$ vs. $SSAT^+$ (†) using Prism 5. $p^* < 0.05$; $p^{**} < 0.01$; $p^{***} < 0.001$; $p^{†††} < 0.001$.

Spermine can be converted directly back to spermidine by SMO generating H_2O_2 as one of the by-products. SMO activity was measured at the same time when measuring APAO activity, using spermine rather than N^1-acetylspermidine as the reaction substrate. The basal SMO activity in $SSAT^+$ was generally higher than that in $SSAT^-$ and WT. A same tendency of SMO activity as APAO activity was observed with an increase at 24 h after cells were plated and a decline afterwards (Fig. 3.9). The overall pattern of SMO activity was higher in $SSAT^+$ cells in comparison with the other two cell types.

Fig. 3.9 SMO enzymatic activity in WT, SSAT-, and SSAT$^+$ cells

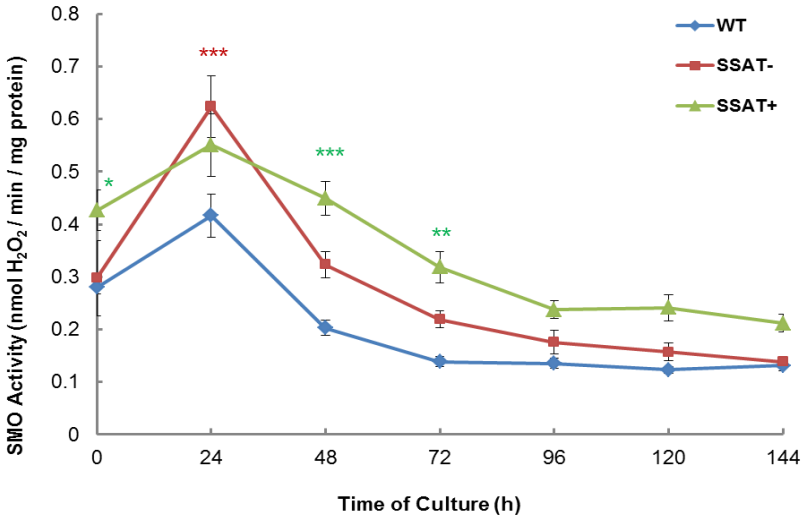

Fig. 3.9 Cells were seeded at a density of 2.4 x 10^4 / cm^2 in 60 mm diam. cell culture dish in duplicate. Cells were harvested at 24 h intervals. Media were replaced with fresh media at 24, 72 and 120 h. Results shown are mean ± SEM (n = 3, with 2 replicate per experiment). Statistical analysis was performed by two-way ANOVA with Bonferroni post-tests comparing WT vs. SSAT$^-$ (*), WT vs. SSAT$^+$ (*) and SSAT$^-$ vs. SSAT$^+$ using Prism 5. p* < 0.05; p** < 0.01; p*** < 0.001.

3.1.3 Rate of protein synthesis in response to SSAT alteration in polyamine pathway

The previous results showed that SSAT$^+$ cells presented the lowest proliferation among the three cell types, protein synthesis was measured to determine the impact of SSAT alteration on total cellular protein synthesis. After an addition of [^{14}C] labelled L-amino acids mixture, protein synthesis declined in SSAT$^+$ compared with that in SSAT$^-$ at 24 and 48 h, suggesting a delayed protein synthesis while SSAT was induced. In contrast to WT at 48 h, total protein synthesis in SSAT$^-$ was slightly increased but decreased in SSAT$^+$ (Fig. 3.10). Thus, this result may reflect the low growth of SSAT$^+$ cells to certain extent.

Fig. 3.10 Protein synthesis in WT, SSAT$^-$, and SSAT$^+$ cells

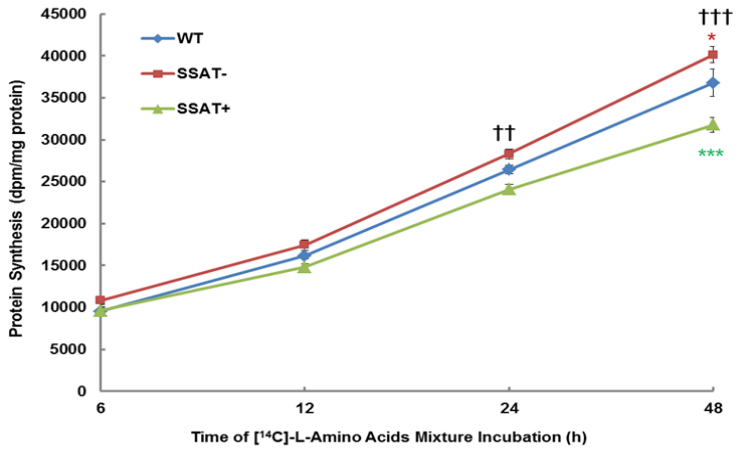

Fig. 3.10 Cells were seeded at a density of 2.4 x 10^4 / cm^2 in 60 mm diam. cell culture dish in duplicate. Cells were grown for 48 h, and then harvested at 6, 12, 24 and 48 h after the addition of [^{14}C]-L-Amino Acids Mixture. Protein fraction was extracted by NaOH. Radioactivity was quantified using liquid scintillation analyser. Results shown are mean ± SEM (n = 3, with 2 replicate per experiment). Statistical analysis was performed by two-way ANOVA with Bonferroni post-tests comparing WT vs. SSAT$^-$ (*), WT vs. SSAT$^+$ (*) and SSAT$^-$ vs. SSAT$^+$ (†) using Prism 5. $p^* < 0.05$; $p^{***} < 0.001$; $p^{†††} < 0.001$.

3.1.4 Polyamine efflux in response to alteration of SSAT activity

It is known that excess polyamines (spermidine and spermine) are degraded by SSAT and converted to N^1-acetylpolyamines. They are then either exported out of the cell or oxidised by APAO. Thus, an increase in SSAT may lead to an enhanced polyamine efflux.

In order to test this in our model system, the cells were labelled with [^{3}H]-putrescine and the amount of [^{3}H] radioactivity (% of total disintegrations per minute (DPM)) in the culture medium was measured during a time course (0 - 48 h). Polyamine efflux was increased significantly in SSAT$^+$ in a time dependent manner on the contrary to WT and SSAT$^-$ cells, indicating that polyamine export or efflux was augmented by SSAT overexpression (Fig. 3.11).

Fig. 3.11 Polyamine efflux in WT, SSAT$^-$, and SSAT$^+$ cells

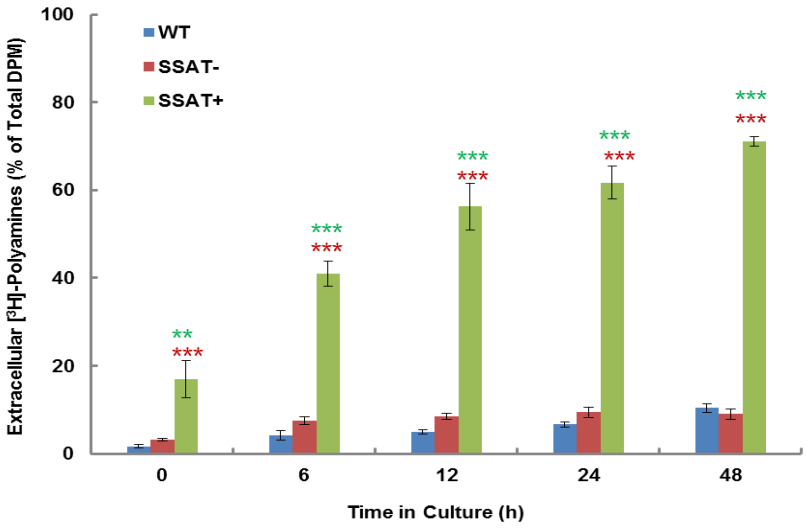

Fig. 3.11 Cells were seeded at a density of 2.4 x 10^4/cm^2 in 60 mm diam. cell culture dish in duplicate. Cells were grown for 24 h, and then cultured with 0.5 µCi/ml [^{3}H]-putrescine for 36 h. After 36 h [^{3}H] exposure time, cells were further incubated without radioisotope for 12 h. The initial cell harvesting was started at a total culture time of 72 h and followed by 6, 12, 24 and 48 h afterwards. Radioactivity was quantified using liquid scintillation analyser. Results shown are mean ± SEM (n = 3, with 2 replicate per experiment). Statistical analysis was performed by two-way ANOVA with Bonferroni post-tests using Prism 5 comparing WT vs. SSAT$^-$, WT vs. SSAT$^+$ (*) and SSAT$^-$ vs. SSAT$^+$ (*). p** < 0.01, p*** < 0.001.

3.1.5 Cellular reduced GSH content in WT, SSAT$^-$ and SSAT$^+$ cells

H_2O_2 is one of the by-products of polyamine oxidation reaction catalysed by APAO and SMO. Accumulation of H_2O_2 would result in oxidative stress. To prevent this from occurring, the cellular antioxidant system such as GSH metabolises excess H_2O_2, leading to a decrease in reduced GSH content.

It would make sense that SSAT$^+$ cells tend to produce more H_2O_2 due to their elevated APAO and SMO activities. Therefore, intracellular reduced GSH content was measured. There seemed to be a slight increase of GSH in SSAT$^-$ cells, which was consistent with its rapid proliferative rate. However, the difference between each cell type was not statistically significant, indicating there might not be a generation of excess H_2O_2 in SSAT$^+$ cells (Fig. 3.12).

Fig. 3.12 Intracellular GSH content in WT, SSAT$^-$ and SSAT$^+$ cells

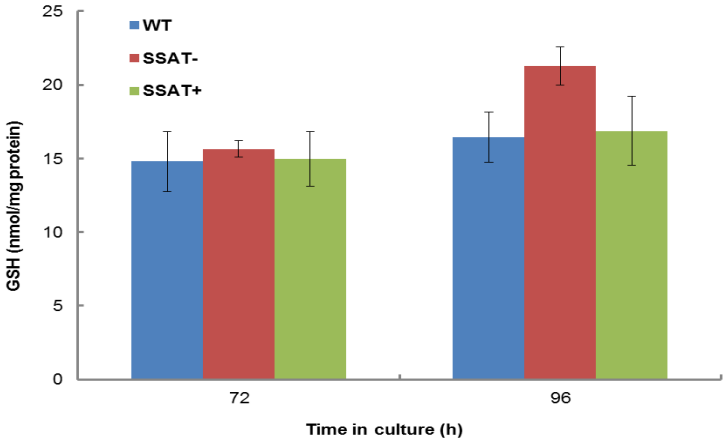

Fig. 3.12 Cells were plated at a density of 2.4 x 10^6 / cm^2 in a 60 mm cell culture dish in duplicate. Medium was replaced after 24 h with fresh medium and then changed every 48 h. The cells were harvested and GSH fraction was extracted by $HClO_4$ (Section 2.3.3). Results shown are mean ± SEM (n = 3, with 2 duplicates per experiment). Statistical analysis was performed by two-way ANOVA with Bonferroni post-tests using Prism 5. $p > 0.05$.

3.1.6 Quantification of intracellular polyamines in WT and SSAT$^-$ and SSAT$^+$ cells

Intracellular polyamine concentrations are finely maintained by the cell within a narrow range via regulation of biosynthesis, degradation, uptake and export. Alteration of intracellular polyamine concentrations, either excess or insufficient, can lead to cellular stress influencing cell growth and/or death. In order to determine the concentration of individual polyamine in these cells with different SSAT activity but without treatment, polyamine concentrations were analysed initially over a time course of growth (0-144 h) by LC-MS. This method was developed to be more sensitive and to allow for the measurement of acetylpolyamines (Section 2.2.13).

It is equally important to characterise the effect of SSAT alteration on total polyamine content since SSAT is responsible for polyamine degradation. In general, total polyamine content of SSAT$^+$ cells appeared higher than that of the other two cell types and it was significantly different at 96 h comparing to WT, although the difference observed was not significant between SSAT$^-$ and SSAT$^+$ (Fig. 3.13). This implies that overexpression of SSAT activity tends to increase total polyamine content and individual polyamine content can also change dramatically.

Fig. 3.13 Total polyamine content in WT, SSAT$^-$, and SSAT$^+$ cells

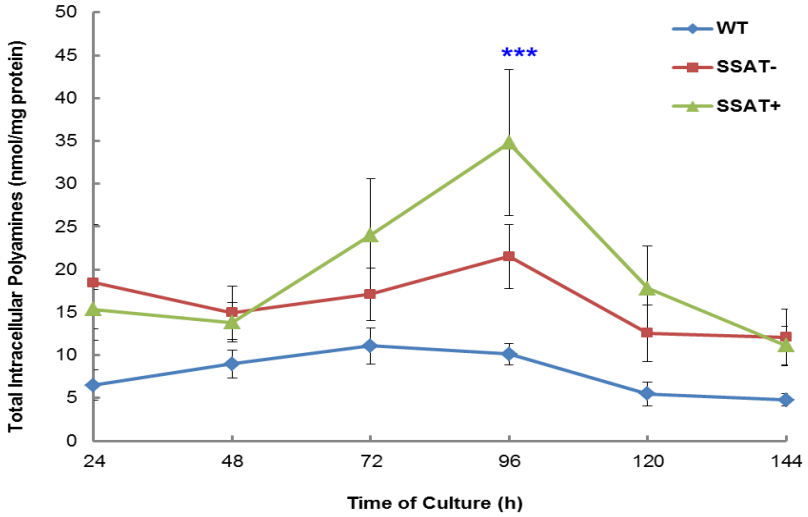

Fig. 3.13 Total polyamine content was obtained by calculating the sum of each individual polyamine in an independent experiment (results are mean ± SEM, n=3 to 6, with 2 duplicates per experiment). Statistical analysis was performed using Two-way ANOVA with Bonferroni post-tests. p*** < 0.001.

WT and SSAT$^-$ had a low content of N^1-acetylspermidine whereas N^1-acetylspermidine in SSAT$^+$ cells was increased significantly (4-7 fold), which confirmed that SSAT activity was induced (Fig. 3.14a). Likewise, N^1-acetylspermine presented the same pattern (Fig. 3.14b), but the concentration was about 10 fold lower than N^1-acetylspermidine in SSAT$^+$ cells. Putrescine content was also significantly higher (4-8 fold) in SSAT$^+$ than the other two cell types (Fig. 3.14c). The increase in putrescine was consistent with the enhanced ODC activity (Fig. 3.7) and putrescine being the final product from the retroconversion pathway. Spermidine tended to decline after 72 h in all the cells (Fig. 3.14d), which was probably because the proliferation rate was gradually slowed down as the cells were reaching high cell density by 72 h growth in a 60 mm culture dish. This may also indicate that spermidine is more likely to be required for cell proliferation rather than differentiation. Furthermore, more spermidine appeared to be present in SSAT$^-$ than the other two cell types, which was likely to be associated with their higher proliferation rate. Spermine was shown to be the dominant polyamine in these cells (Fig. 3.14e), in addition to N^1-acetylspermidine in SSAT$^+$ cells. SSAT$^-$ cells had the highest spermine concentration, which may also reflect their fast growth rate. There was little difference in spermine between WT and SSAT$^+$ cells.

Taken together, spermine is the most dominant polyamine in LNCaP cells. An increase in N^1-acetylspermidine, N^1-acetylspermine, and putrescine is consistent with the increased SSAT activity. Higher concentrations of spermidine and spermine in $SSAT^-$ cells are consistent with inhibited SSAT activity and higher growth rate.

Fig. 3.14 Intracellular polyamine concentration in WT, $SSAT^-$, and $SSAT^+$ cells

a) N^1-acetylspermidine

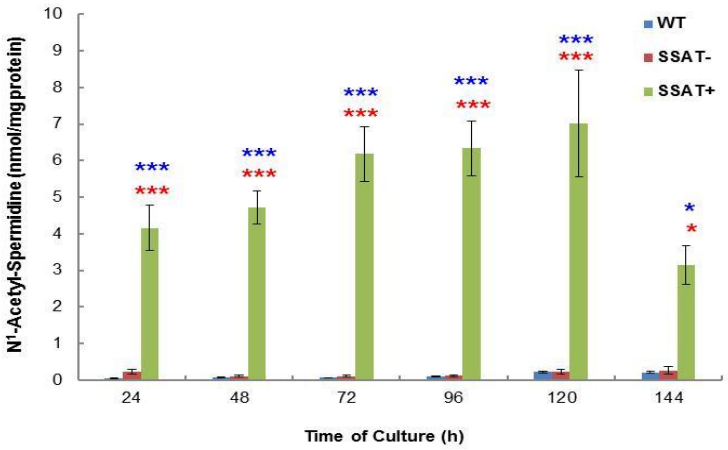

b) N^1-acetylspermine

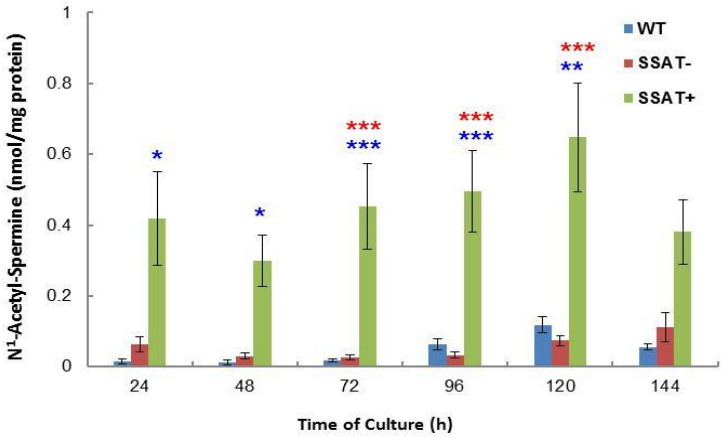

c) Putrescine

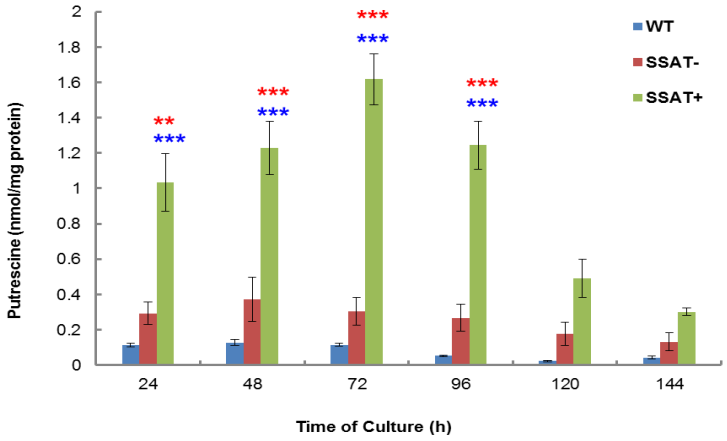

d) Spermidine

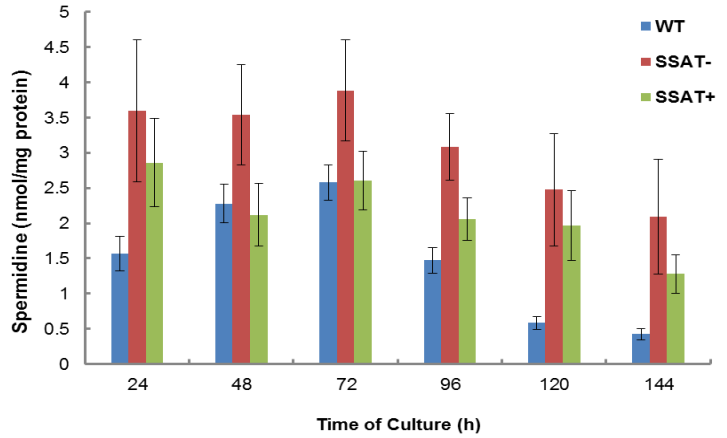

e) Spermine

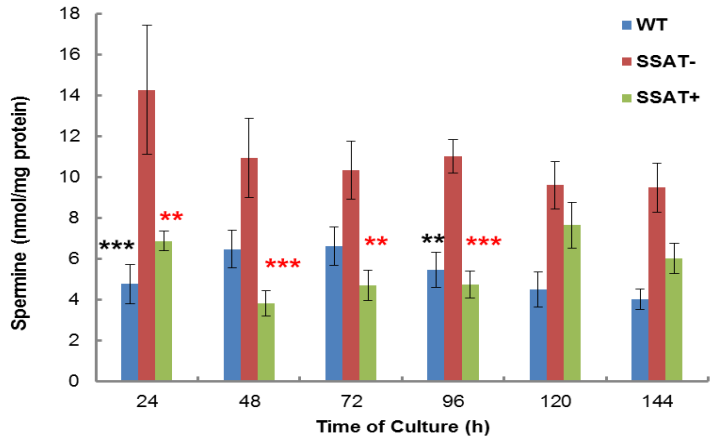

Fig. 3.14 Cells were seeded at a density of 2.4 x 10^4 cells / cm^2 on a 60 x 15 mm cell culture dish in duplicate. Media were replaced after the initial 24 h growth and then at a 48 h interval. Cells were harvested at a 24 h interval; polyamine fraction was extracted by perchloric acid and finally quantified by LC-MS (Section 2.2.13; values are mean ± SEM with n = 3 to 6, two duplicates per experiment). Statistical analysis was performed using Two-way ANOVA with Bonferroni post-tests comparing WT vs. $SSAT^-$ (*), WT vs. $SSAT^+$ and $SSAT^-$ vs. $SSAT^+$ (*). p* < 0.05; p** < 0.01; p*** < 0.001.

3.2 The effect of aspirin and 5-FU in response to SSAT alteration

Introduction

Having characterised WT, $SSAT^-$, and $SSAT^+$ cells without treatment, some insights into the features of these cells possessing altered SSAT enzymatic activity were noted. The features reflect an important role of SSAT in regulating LNCaP prostate cancer cell growth linked to polyamine homeostasis. Our hypothesis was that increased SSAT activity would increase the sensitivity of these cells to drugs and so the next aim was to determine whether these cells responded differently to known antiproliferative or chemopreventative drugs.

The drugs chosen for this study were: aspirin, known as a chemopreventative agent in colorectal cancer and anti-inflammatory drug; 5-FU and etoposide are well recognised classic chemotherapeutic drugs. All of these drugs have been shown to be inducers of SSAT activity in some cancer cell lines (Babbar *et al.*, 2006; Choi *et al.*, 2005).

3.2.1 Cytotoxicity of aspirin, 5-FU, and etoposide on WT, $SSAT^-$ and $SSAT^+$ cells

The MTT assay is a standard method of determining cytotoxicity and the apparent IC_{50} of a drug and was used here to determine the difference in sensitivity of the compounds in the 3 cell types. The range of concentrations of the drugs was selected based on the established IC_{50s} in other cell lines in our lab. Aspirin showed a classic dose response with increasing concentrations of drug causing decreased cell numbers. There was little difference of the cytotoxicity of aspirin in all the cells (Fig. 3.15). The apparent IC_{50} values for aspirin were calculated from the MTT assays as 2.60 ± 0.25 mM (WT, n=3), 2.83 ± 0.09 mM ($SSAT^-$, n=6) and 2.64 ± 0.16 mM ($SSAT^+$, n=6), indicating that cytotoxicity of aspirin does not seem to be affected by the level of SSAT activity in WT and SSAT transfected LNCaP cells.

In response to 5-FU a decrease in cell number was observed in all 3 cell types. There was little difference between WT and $SSAT^-$ with apparent IC_{50} values of 55.3 ± 1.2 μM (n=3) and 54.7 ± 7.1 μM (n=6) respectively. The dose response curve for 5-FU in $SSAT^+$ cells was

shifted to the left and the apparent IC_{50} value was significantly lower (35.2 ± 5.8 µM, n=6) than that of the WT and $SSAT^-$ cells (Fig. 3.16). Thus, enhanced SSAT activity is facilitating the cytotoxicity of 5-FU.

Fig. 3.15 Cytotoxicity of aspirin at 48 h exposure

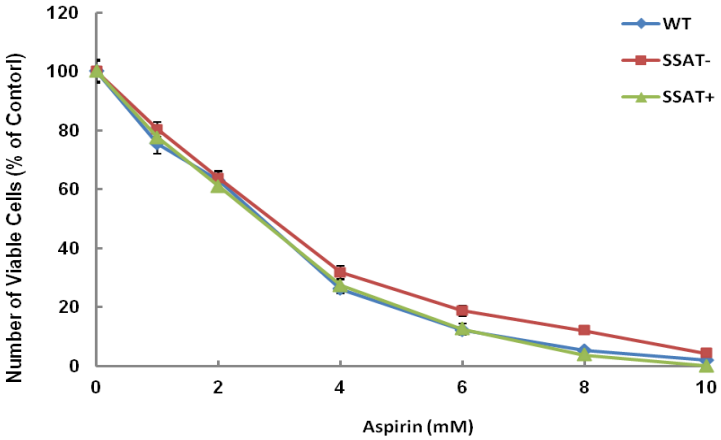

Fig. 3.15 Cells were seeded at a density of 2.4 x 10^4 cells/cm^2 on a 96 well microtitre plate and allowed for 48 h attachment and growth. After 48 h, medium was replaced with medium containing vehicle or the drug. The plate was incubated for further 48 h and assayed by MTT (Section 2.2.9). Results were shown as mean ± SEM (n=3 of WT; n=6 of $SSAT^{\pm}$, with 6 replicates per experiment). Statistical analysis was performed by two-way ANOVA with Bonferroni post-tests comparing WT vs. $SSAT^-$ (*), WT vs. $SSAT^+$ (*), $SSAT^-$ vs. $SSAT^+$ (†). $p > 0.05$.

Fig. 3.16 Cytotoxicity of 5-FU at 48 h exposure

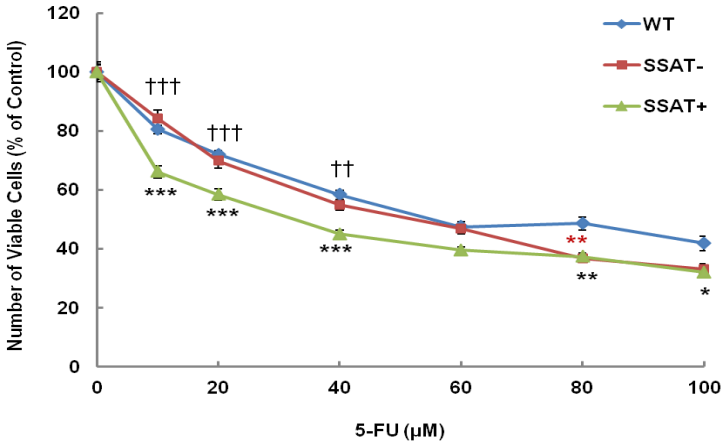

Fig. 3.16 Cells were seeded at a density of 2.4 x 10^4 cells/cm^2 on a 96 well microtitre plate for 48 h growth. Medium was then replaced with medium containing vehicle or the drug. The plate was incubated for further 48 h and assayed by MTT (Section 2.2.9). Results were shown as mean ± SEM (n=3 of WT; n=6 of $SSAT^{\pm}$, with 6 replicates per experiment). Statistical analysis was performed by two-way ANOVA with Bonferroni post-tests comparing WT vs. $SSAT^-$ (*), WT vs. $SSAT^+$ (*), $SSAT^-$ vs. $SSAT^+$ (†). $p^* < 0.05$, $p^{**} < 0.01$, $p^{***} < 0.001$; $p^{\dagger\dagger} < 0.01$, $p^{\dagger\dagger\dagger} < 0.001$.

Interestingly, the LNCaP cells did not respond to etoposide with the drug having limited effect on cell number. An IC_{50} value was not achieved over the concentration range tested up to 100 µM (Fig. 3.17). These results indicate that these prostate cancer cells are not sensitive to etoposide.

Fig. 3.17 Cytotoxicity of etoposide at 48 h exposure

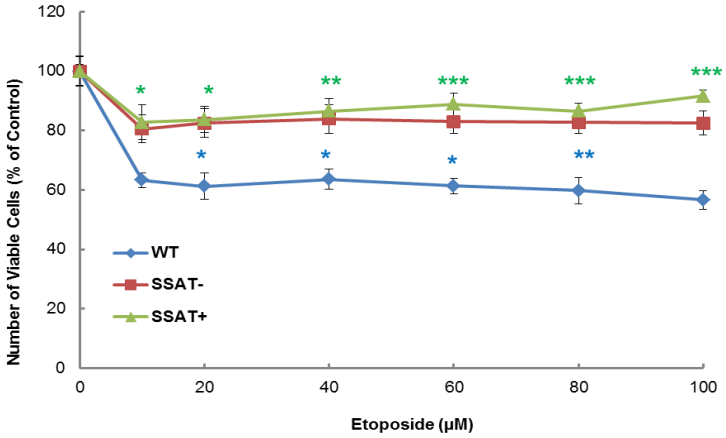

Fig. 3.17 Cells were seeded at a density of 2.4 x 10^4 cells/cm^2 on a 96 well microtitre plate and allowed for 48 h growth. After 48 h, medium was replaced with medium containing vehicle or drug. The plate was incubated for further 48 h and assayed by MTT (Section 2.2.9). Results were shown as mean ± SD or SEM (n=2 of WT; n=3 of $SSAT^{\pm}$, with 6 replicates per experiment). Statistical analysis was performed by two-way ANOVA with Bonferroni post-tests comparing WT vs. $SSAT^-$ (*), WT vs. $SSAT^+$ (*) and $SSAT^-$ vs. $SSAT^+$ (*). p* < 0.05, p** < 0.01, p*** < 0.001.

As a result of these initial experiments only aspirin and 5-FU were chosen for further study.

3.2.2 Effect of aspirin and 5-FU on the growth of WT, SSAT$^-$ and SSAT$^+$ cells

Introduction

Previous results showed SSAT$^+$ cells proliferated slower than the other two cell types in the absence of antiproliferative agents (Fig. 3.1) suggesting increased SSAT activity is inversely associated with cell growth. In order to determine the growth response of these cells with altered SSAT activity to the antiproliferative agents (2 mM aspirin and 50 µM 5-FU), the viable cell numbers were determined at a 24 h interval for a total of 96 h drug exposure.

The viable cell numbers were all significantly decreased by both aspirin and 5-FU in the three types of cells, with the exception of aspirin at 24 h in both SSAT$^-$ and SSAT$^+$ cells (Fig. 3.18a-c) as aspirin is less cytotoxic than 5-FU. In order to easily distinguish the effect of these two drugs on the cell growth, the data were converted into a percentage of growth inhibition against their control values (Fig 3.19a-c). This was also summarised in Table 3.2. In response to aspirin the growth inhibition in WT, SSAT$^-$ and SSAT$^+$ cells was 35%, 25%, and 2% at 24 h, and 65%, 58%, and 28% at 48 h respectively. With respect to 5-FU treatment, the growth inhibition in WT, SSAT$^-$ and SSAT$^+$ cells was 32%, 55% and 29% at 24 h, and 68%, 81% and 72% at 48 h respectively. The difference of growth inhibition at 72 h and 96 h between each cell line was within 10%. These results indicate that although SSAT$^+$ cells proliferated slower than the other two cell types without treatment, their response to aspirin was less sensitive than both WT and SSAT$^-$ and less sensitive to 5-FU than SSAT$^-$ cells at the first 48 h treatments. Thus, an increase in SSAT activity may reduce the sensitivity of the LNCaP cells in response to antiproliferative drugs.

Fig. 3.18 Effect of aspirin and 5-FU on total viable cell numbers

a) WT

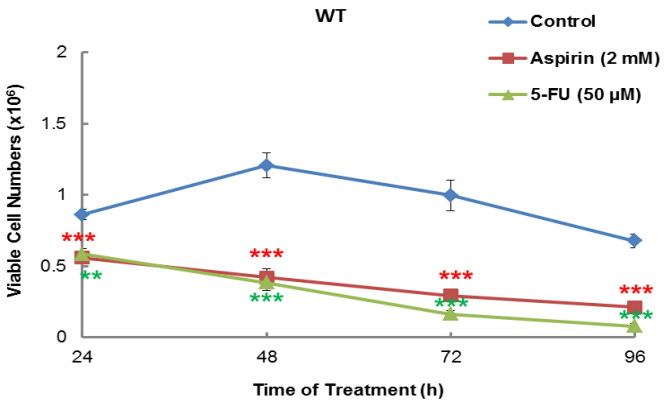

b) SSAT$^-$

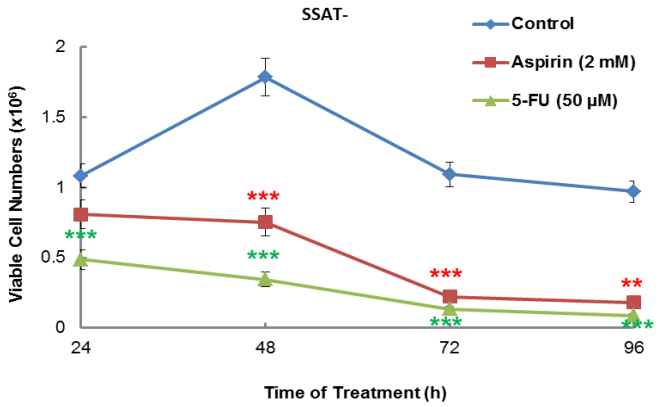

c) SSAT$^+$

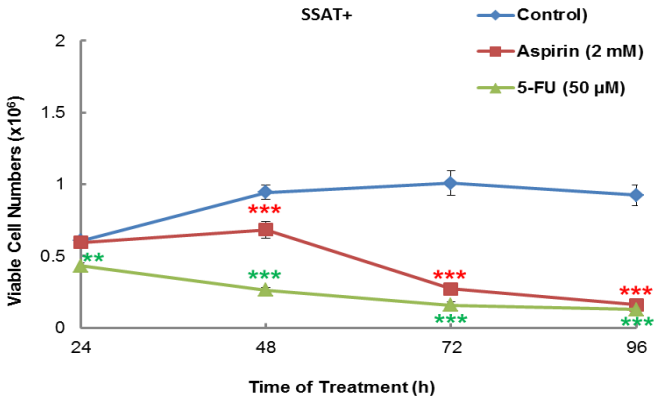

Fig. 3.18 Cells were seeded at a density of 2.4 x 10^4/cm^2 in 60 mm diam. cell culture dish in duplicate. Cells were treated with aspirin and 5-FU after 48 h incubation and then harvested at 24 h intervals and viable cell numbers counted using Trypan blue exclusion assay (Section 2.2.5). Results shown are mean ± SEM (n = 4 to 16, with 2 replicate per experiment). Statistical analysis was performed by two-way ANOVA with Bonferroni post-tests comparing with their own control using Prism 5, WT (*), SSAT$^-$ (*) SSAT$^+$ (*). p** < 0.01, p*** < 0.001.

Fig. 3.19 Effect of aspirin and 5-FU on the growth inhibition

a) WT

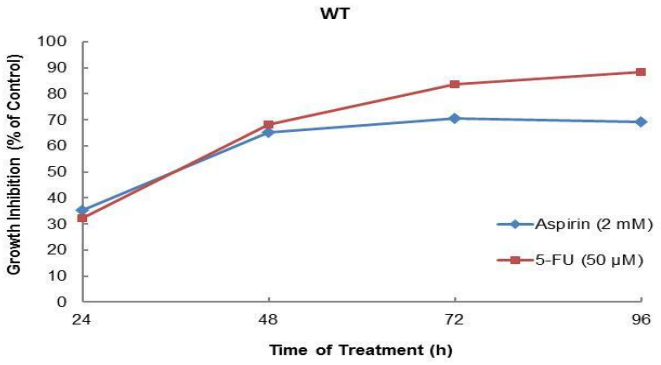

b) SSAT$^-$

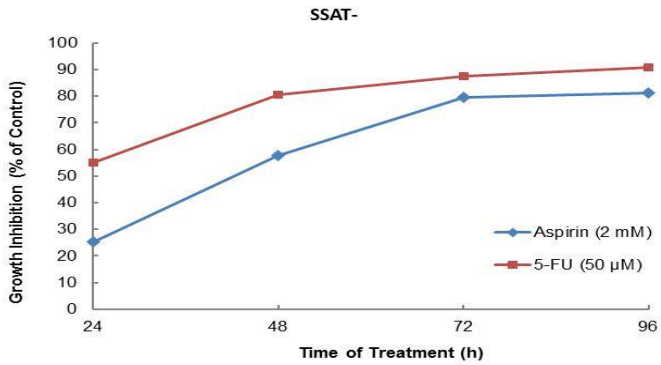

c) SSAT$^+$

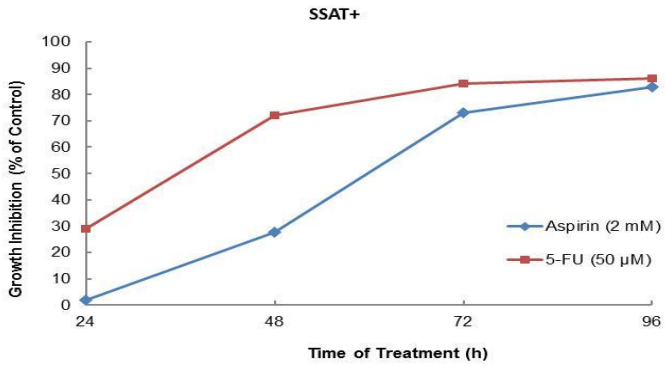

Fig. 3.19 Growth inhibition (%) was calculated by the equation: (viable cell numbers of control / viable cell numbers of control x 100%) – (viable cell numbers of treatment / viable cell numbers of control x 100%) according to the data in Table 3.1a-d. The viable cell numbers of control was defined as 100%.

Table 3.2 Summary of the growth inhibition by aspirin and 5-FU

Growth inhibition (%)	Aspirin (2 mM)				5-FU (50 µM)			
Time of treatment	24 h	48 h	72 h	96 h	24 h	48 h	72 h	96 h
WT	35	65	71	69	32	68	84	88
SSAT$^-$	25	58	80	81	55	81	88	91
SSAT$^+$	2	28	73	83	29	72	84	86

Table 3.2 Summary of the growth inhibition (%) from Fig. 3.19a-c in WT, SSAT$^-$ and SSAT$^+$ cells by aspirin and 5-FU from 24 to 96 h treatment.

3.2.3 Effect of aspirin and 5-FU on SSAT activity in WT, SSAT$^-$, and SSAT$^+$ cells

Introduction

Aspirin (1.5 mM) and 5-FU (10 µM) have been demonstrated as inducers of SSAT activity in several cell lines (Babbar *et al.*, 2006; Choi *et al.*, 2005). However, it is not clear whether these drugs are general inducers of SSAT activity or they act as the inducers only in a cell-type specific manner.

Little difference in SSAT activity was shown after 48 h exposure to aspirin and 5-FU in WT and SSAT$^-$ cells (Fig. 3.20). However, SSAT activity was decreased markedly by the drugs in SSAT$^+$ cells compared with its control. The results indicate that aspirin and 5-FU at these concentrations were inhibitors of SSAT activity but the prerequisite for this inhibition was that SSAT activity needed to be pre-induced. On the other hand, this may also consolidate the theory that the induction of SSAT by antiproliferative drugs is cell-type dependent.

Fig. 3.20 Effect of aspirin and 5-FU on SSAT activity

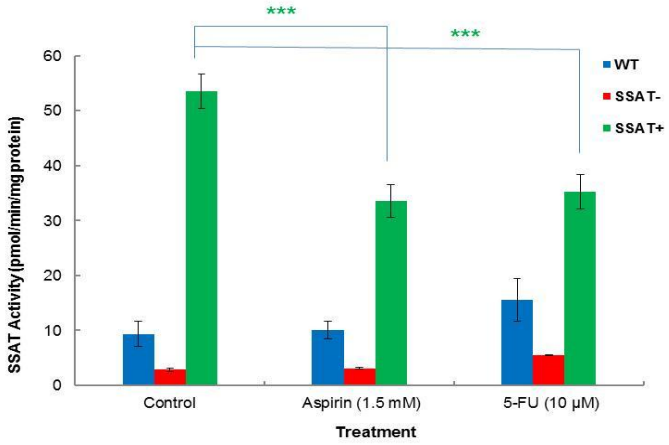

Fig. 3.20 Cells were seeded at a seeding density of 2.4 x 10^4 cells / cm^2 on a 60 x 15 mm cell culture dish in duplicate. After 48 h cell growth, the medium was replaced with fresh medium containing drug. SSAT activity was assayed after 48 h drug exposure (Section 2.3.4). Values were mean ± SEM (n=3 with 4 replicates per experiment). Statistical analysis was performed using two-way ANOVA with Bonferroni post-tests comparing with control. p*** < 0.001.

Exposure to aspirin and 5-FU at 48 h had no effect on the SSAT activity in WT and $SSAT^-$ cells but had an inhibitory effect on SSAT activity in $SSAT^+$ cells. Aspirin at 1.5 mM and 5-FU at 10 µM was lower than the IC_{50} values (~2.5 mM and ~55 µM) in these cells (Fig. 3.15 & 3.16). In addition, the SSAT activity was only measured at one time point (48 h). In order to further characterise the changes in SSAT activity in response to aspirin and 5-FU, the activity was measured over a time course (24-96 h) with higher concentrations of aspirin (2 mM) and 5-FU (50 µM).

SSAT activity in WT cells was low without treatment but did show a greater than 3-fold rise up to 72 h. Both drugs increased SSAT activity at early times (24 and 48 h) but these effects were lost at later points. Aspirin induced a 2-4-fold increase while 5-FU showed a 2-3 fold increase over the time. By 96 h SSAT activity was low in all treatments, which could be due to that the cells were over confluent or dying (Fig. 3.21a).

Comparing with previous results (Fig. 3.20), these results may also indicate that induction of SSAT could be dose dependent in WT cells.

In SSAT$^-$ cells, which the *Sat1* gene expression had been artificially suppressed by Tetracycline, the results showed a statistically significant decrease of SSAT activity by aspirin at 72 and 96 h and by 5-FU at 96 h (Fig. 3.21b). However, since the actual SSAT enzyme activity was extremely low, this might not indicate a biological consequence.

Fig. 3.21 Effect of aspirin and 5-FU on SSAT activity

a) WT

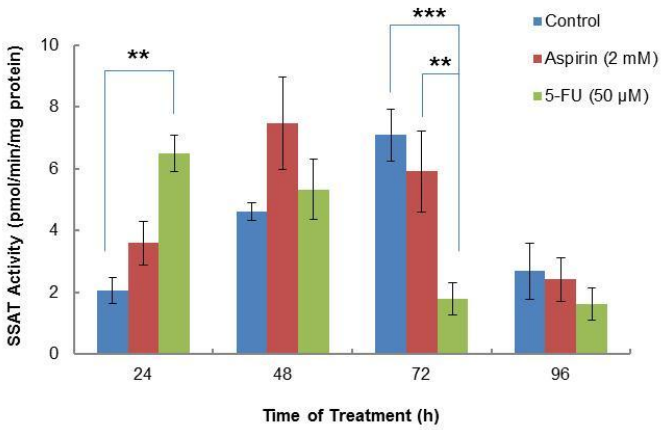

b) SSAT$^-$

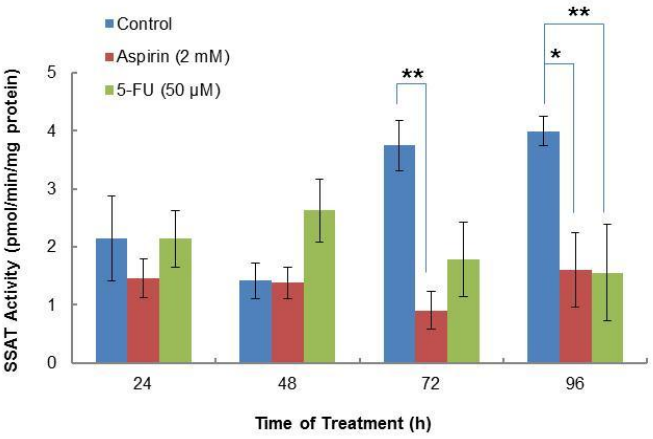

In response to the treatment of aspirin (2 mM) in SSAT$^+$ cells (Fig. 3.21c), there was a 5-fold decline of SSAT activity from 24 to 96 h, indicating a time dependent manner of inhibition. This result was also consistent with the previous result (Fig. 3.20) with a lower concentration of aspirin (1.5 mM) at 48 h, suggesting aspirin is an inhibitor of SSAT activity in SSAT$^+$ cells.

In general, 5-FU (50 µM) had inhibitory effect on SSAT activity and this remained steady (~ 30 pmol/min/mg protein) from 24 to 96 h in $SSAT^+$ cells (Fig 4.5c). This was consistent with the result that SSAT activity was reduced by 5-FU at 10 µM at 48 h (Fig 4.4). The results reveal that inhibition of SSAT activity by 5-FU was neither a dose dependent nor a time dependent response to $SSAT^+$ cells.

Overall, the above results suggest that in response to aspirin and 5-FU there might be different mechanisms involved in the inhibition of enzyme activity in $SSAT^+$ cells.

c) $SSAT^+$

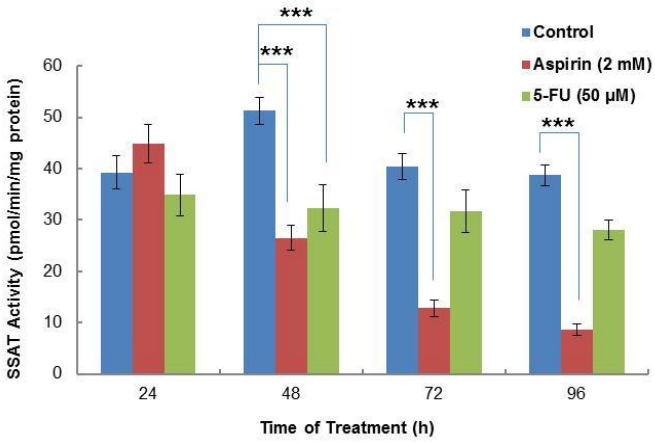

Fig. 3.21 Cells were seeded at a seeding density of 2.4 x 10^4 cells / cm^2 on 60 x 15 mm tissue culture dishes in duplicate. After 48 h cell growth, the medium was replaced with fresh medium containing drug. SSAT activity was assayed after 48 h drug exposures (Section 2.2.10). Values were mean ± SEM (n=3 with 4 replicates per experiment). Statistical analysis was performed using two-way ANOVA with Bonferroni post-tests. p* < 0.05, p** < 0.01, p*** < 0.001.

3.2.4 Inducibility of SSAT

While the antiproliferative drugs aspirin and 5-FU did show some induction of SSAT in WT cells, this was less than predicted from previous data (Babbar *et al.,* 2006; Babbar *et al.,* 2003; Allen *et al.*, 2007). It may be that the enzyme can only be increased so far and no further especially in the transfected cells. To test the inducibility of SSAT the cells were treated with a known potent SSAT inducer, N^1-ethyl-N^{11}-((cyclopropyl)methyl)-4,8-diazaunde-cane (CPENSpm), which is a polyamine analogue. At 48 h exposure to

CPENSpm at different concentrations (1, 5, and 10 µM), SSAT activity in all the cell types was dramatically increased (Fig. 3.22). These results imply that there is a considerable potential of SSAT activity induction in these cells and different mechanisms are likely to be involved in response to polyamine analogue and antiproliferative agents (Table 4.1).

Fig. 3.22 Effect of CPENSpm on SSAT activity

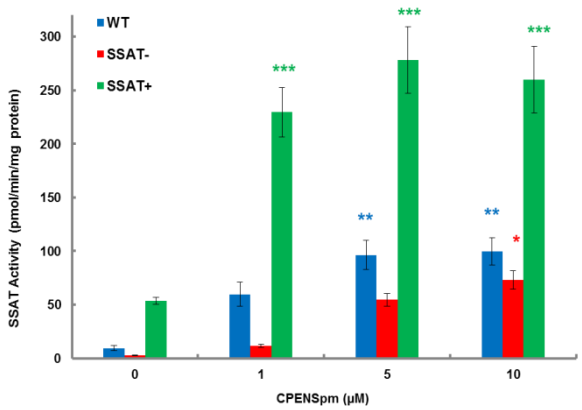

Fig. 3.22 Cells were seeded at a seeding density of 2.4 x 10^4 cells / cm^2 on a 60 x 15 mm cell culture dish in duplicate. After 48 h cell growth, the medium was replaced with fresh medium containing drug. SSAT activity was assayed after 48 h drug exposure (Section 2.3.4). Values were mean ± SEM (n=3 with 4 replicates per experiment). Statistical analysis was performed using two-way ANOVA with Bonferroni post-tests comparing with control: WT (*), $SSAT^-$ (*) and $SSAT^+$ (*). p* < 0.05; p** < 0.01; p*** < 0.001.

Table 3.3 Summary of the percentage of increase of SSAT activity at 48 h treatment

% of increased SSAT activity	Control	Aspirin (2 mM)	5-FU (50 µM)	CPENSpm (1 µM)	CPENSpm (5 µM)	CPENSpm (10 µM)
WT	0	38	13	84	90	91
$SSAT^-$	0	-3#	46	75	95	96
$SSAT^+$	0	-94#	-59#	77	81	79

Table 3.3 Results were obtained by converting the values in Fig. 3.21 & 3.22 at 48 h to a percentage of increase compared with control value. #: negative percentage means control value was smaller than the value of treatment.

3.2.5 Effect of aspirin and 5-FU on ODC activity in WT, SSAT$^-$, and SSAT$^+$ cells

An increase in ODC activity usually correlates with a rapid cell growth. Overexpression of SSAT led to an increase in ODC activity whereas SSAT$^+$ cells grew less than both WT and SSAT$^-$. Less growth inhibition was observed in SSAT$^+$ cells in response to aspirin and 5-FU. What would be the correlation of ODC activity with the growth inhibition in these cells in response to aspirin and 5-FU? In order to investigate this correlation, ODC activity was determined at 24 and 48 h exposure to aspirin (1 and 2 mM) and 5-FU (25 and 50 μM) to see whether it was a dose- or time-dependent response.

Comparing the controls, ODC activity in WT and SSAT$^-$ cells was about 3-fold less than that in SSAT$^+$ cells (Fig. 3.23a-c). ODC activity was inhibited by both aspirin and 5-FU in the cells. The inhibition presented a dose-dependent manner in WT and SSAT$^-$ cells as the effect by higher concentrations of aspirin were more potent. In addition, the inhibition of ODC activity occurred as an early event due to the significance is more profound at 24 h rather than 48 h treatment. Furthermore, the results also suggest that the inhibition of cell growth may be associated with ODC inhibition due to the fact that an increased ODC activity is required in rapid proliferating cells.

Fig. 3.23 Effect of aspirin and 5-FU on ODC activity

a) WT

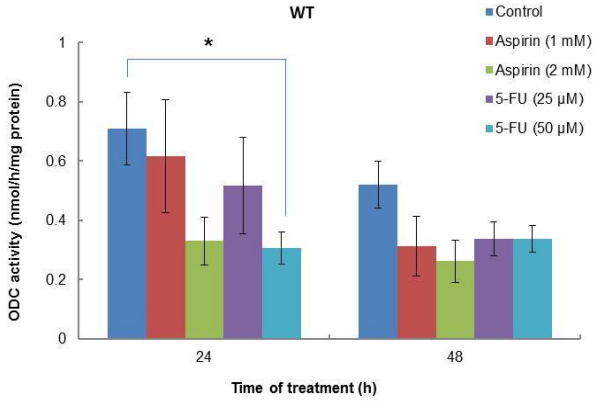

b) SSAT$^-$

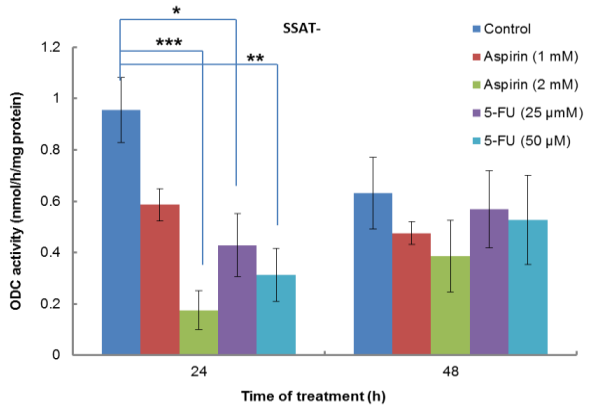

c) SSAT$^+$

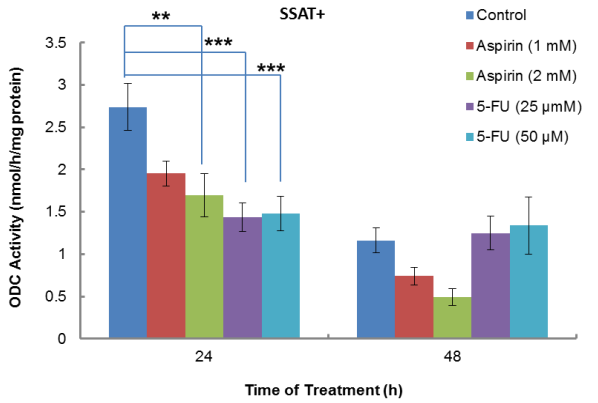

Fig. 3.23 Cells were seeded at a seeding density of 2.4 x 10^4 cells / cm^2 on a 90 mm diameter cell culture dish. After 48 h cell growth, the medium was replaced with fresh medium containing the drug. ODC activity was assayed after 24 and 48 h drug exposure. Values were mean ± SEM (n=3 with 2 replicates per experiment). Statistical analysis was performed using two-way ANOVA with Bonferroni post-tests. p* < 0.05; p** < 0.01, p*** < 0.001.

3.2.6 Effect of aspirin and 5-FU on APAO and SMO activity in WT, SSAT$^-$, and SSAT$^+$ cells

APAO and SMO are constitutionally expressed enzymes with activity depending on the availability of their substrates. Changes in polyamine content by aspirin and 5-FU should therefore affect the activity of APAO and SMO. But there was a lack of evidence that aspirin and 5-FU exert an impact on the enzymes' activity.

Aspirin did not have much effect on APAO and SMO activity in SSAT$^+$ cells. APAO activity was increased by aspirin in WT (5 fold) and SSAT$^-$ (4 fold) cells and by 5-FU in WT (4 fold), SSAT$^-$ (3.5 fold) and SSAT$^+$ (4.5 fold) cells (Fig. 3.24a-c). This was consistent with the results that N^1-acetylpolyamines were increased by 5-FU in WT and SSAT$^-$ cells. SMO activity was also increased by aspirin in WT (6 fold) and SSAT$^-$ (15 fold) cells and by 5-FU in WT (4 fold), SSAT$^-$ (7 fold) and SSAT$^+$ (4.5 fold) cells (Fig. 3.25a-c). This did not correspond to the decreased spermine by 5-FU in SSAT$^-$ and SSAT$^+$ cells. These results suggest that aspirin and 5-FU might be able to work directly on APAO and SMO rather than via altering the concentrations of their substrates.

Fig. 3.24 Effect of aspirin and 5-FU on APAO activity

a) WT

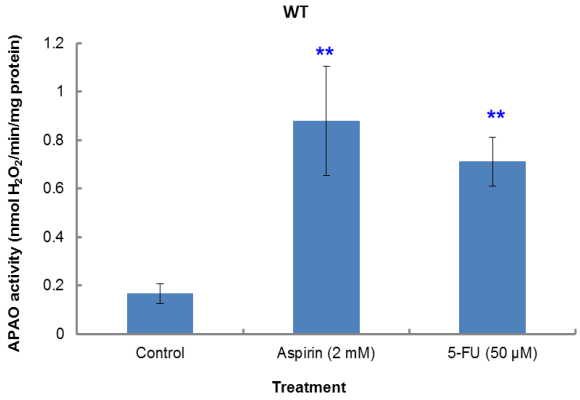

b) SSAT$^-$

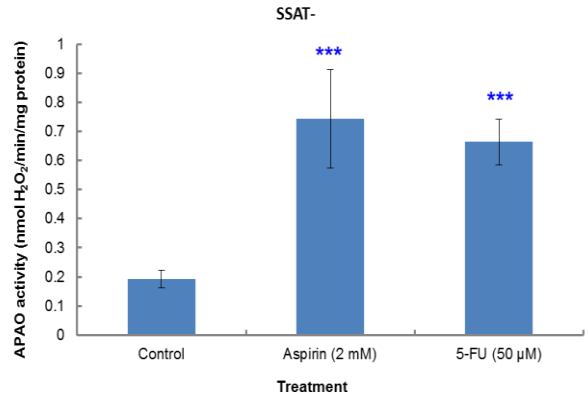

c) SSAT$^+$

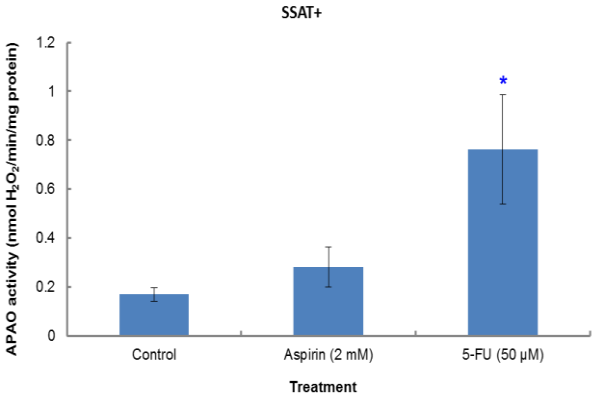

Fig. 3.24 Cells were seeded at a density of 2.4 x 10^6/cm^2 in a 90 mm cell culture dish and incubated for 48 h. Fresh medium was then replaced containing the drugs. The cells were harvested after 48 h treatment and assayed (Section 2.2.12). Results were mean ± SEM (n=3, with 2 replicates per experiment). Statistical analysis was performed by One-way ANOVA with Dunnett's post-test comparing with Control. p* < 0.05; p** < 0.01; p*** < 0.001.

Fig. 3.25 Effect of aspirin and 5-FU on SMO activity

a) WT cells

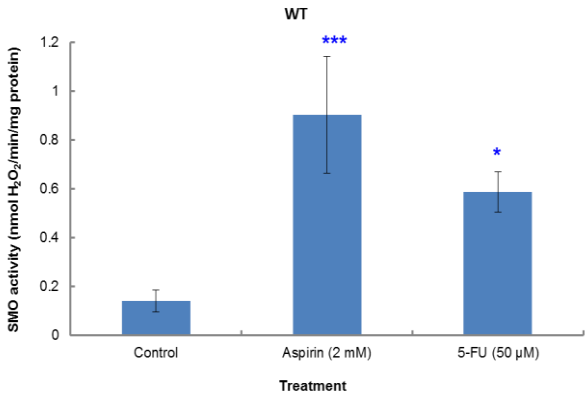

b) SSAT$^-$

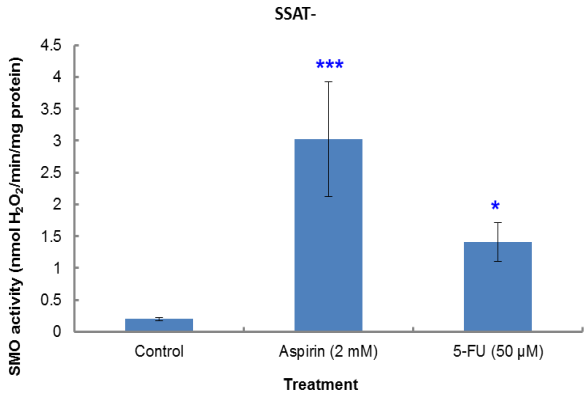

c) SSAT$^+$

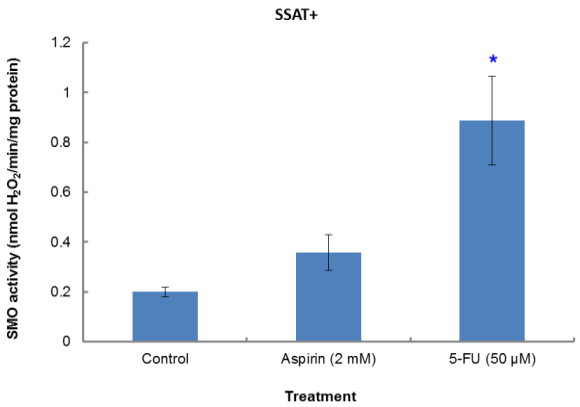

Fig. 3.25 Cells were seeded at a density of 2.4 x 10^6/cm^2 in a 90 mm cell culture dish and incubated for 48 h. Fresh medium was then replaced containing the drugs. The cells were harvested after 48 h treatment and assayed (Section 2.2.12). Results were mean ± SEM (n=3, with 2 replicates per experiment). Statistical analysis was performed by One-way ANOVA with Dunnett's post-test comparing with Control. p* < 0.05; p** < 0.01; p*** < 0.001.

3.2.7 Quantification of intracellular polyamines in the treatment of aspirin and 5-FU in WT, SSAT$^-$, and SSAT$^+$ cells

Inhibition of cell growth by anticancer drugs is often to be associated with a decrease of intracellular polyamine pools. With the increase of SSAT activity, the effect of aspirin and 5-FU on intracellular polyamine content was measured with the aim of investigating the relationship between polyamine concentrations and the cytotoxic effect of the drugs. The cells were exposed to aspirin (2 mM) and 5-FU (50 μM) for a treatment period of 24 to 96 h.

The results showed that N^1-acetylspermidine was increased by 5-FU in both WT (6-9 fold) and SSAT$^-$ (5-6 fold) cells (Fig. 3.26a & b), which is not consistent with the decreased SSAT activity by 5-FU (Fig. 3.21a & b). On the contrary, N^1-acetylspermidine was decreased by aspirin in a time-dependent manner (6 fold at 72 h) and by 5-FU (2 fold) in SSAT$^+$ cells (Fig. 3.26c). This pattern is consistent with the effect of aspirin and 5-FU on SSAT activity in the same cells. This indicates that the effect of these drugs on N^1-acetylspermidine is likely to be dependent on the existing SSAT levels, and the related mechanisms of aspirin and 5-FU could be different.

Fig. 3.26 Effect of aspirin and 5-FU on N^1-acetylspermidine content

a) WT

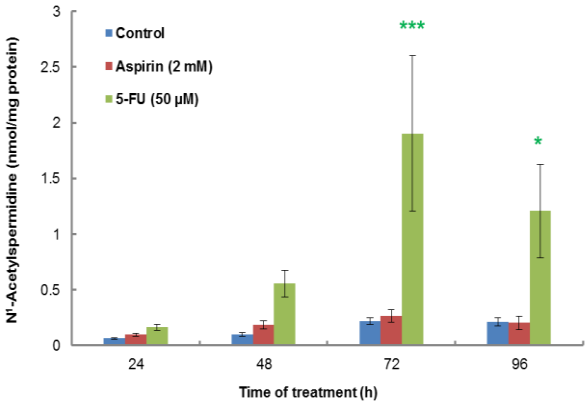

b) $SSAT^-$

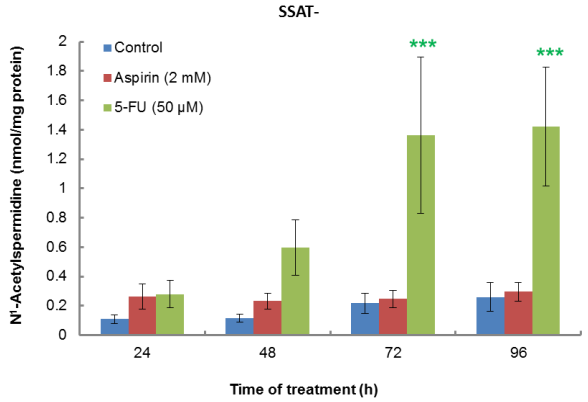

c) $SSAT^+$

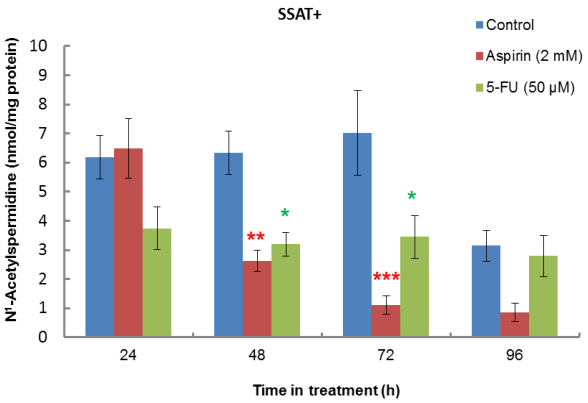

Fig. 3.26 Cells were seeded at a density of 2.4 x 10^4 cells / cm^2 on a 60 x 15 mm cell culture dish in duplicate. Media were replaced after the initial 24 h growth and then at a 48 h interval. Cells were harvested at a 24 h interval; polyamine fraction was extracted by perchloric acid and finally quantified by LC-MS (Section 2.3.7; values are mean ± SEM with n = 3 to 6, two duplicates per experiment). Statistical analysis was performed using Two-way ANOVA with Bonferroni post-tests comparing with Control, i.e. aspirin vs. control (*), 5-FU vs. control (*). p* < 0.05; p** < 0.01; p*** < 0.001.

N^1-acetylspermine content is usually extremely low. Likewise, its content seemed to be increased by 5-FU in both WT and $SSAT^-$ cells (Fig. 3.27a & b). In $SSAT^+$ cells, it appeared to be decreased by aspirin but not significantly different, and 5-FU did not exert any obvious effect (Fig. 3.27c).

Fig. 3.27 Effect of aspirin and 5-FU on N^1-acetylspermine content

a) WT

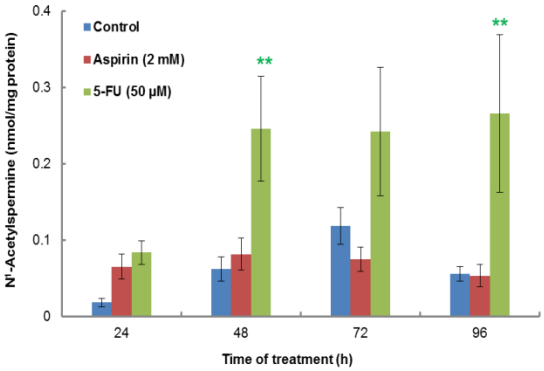

b) $SSAT^-$

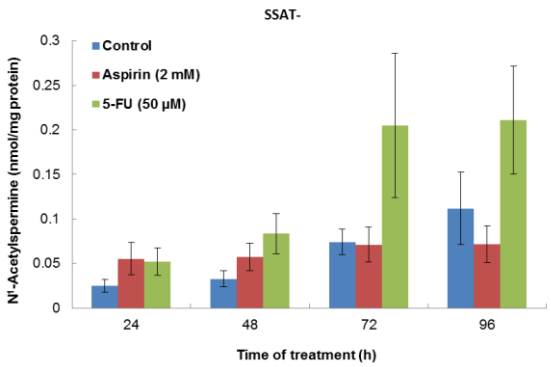

c) $SSAT^+$

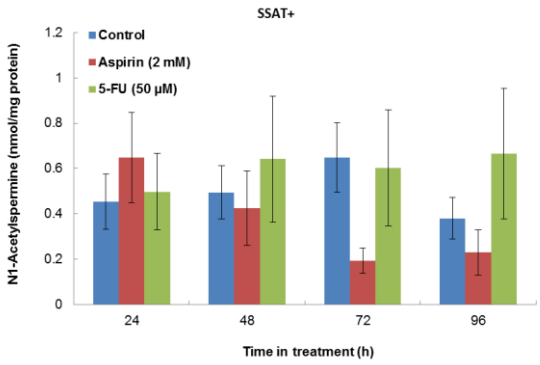

Fig. 3.27 Cells were seeded at a density of 2.4 x 10^4 cells / cm^2 on a 60 x 15 mm cell culture dish in duplicate. Media were replaced after the initial 24 h growth and then at a 48 h interval. Cells were harvested at a 24 h interval; polyamine fraction was extracted by perchloric acid and finally quantified by LC-MS (Section 2.3.7; values are mean ± SEM with n = 3 to 6, two duplicates per experiment). Statistical analysis was performed using Two-way ANOVA with Bonferroni post-tests comparing with Control, i.e. aspirin vs. control (*), 5-FU vs. control (*). p* < 0.05; p** < 0.01; p*** < 0.001.

Putrescine content rose after exposure to 5-FU in both WT and SSAT$^-$ cells (Fig. 3.28a & b), after which the pattern was similar to the above results of N^1-acetylpolyamines. Aspirin did not seem to have any effect on these two cell types. However, in SSAT$^+$ cells putrescine was declined by aspirin (Fig. 3.28c), which was consistent with the decreased ODC activity (Fig. 3.23c).

Fig. 3.28 Effect of aspirin and 5-FU on putrescine content

a) WT

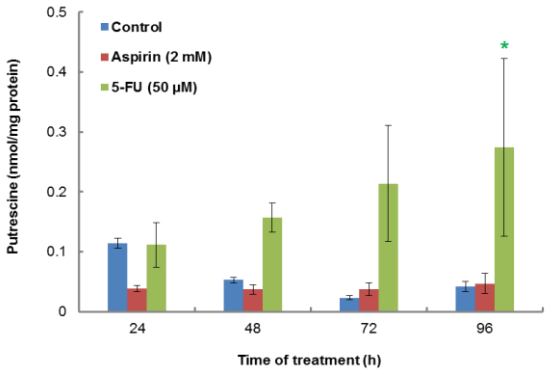

b) SSAT$^-$

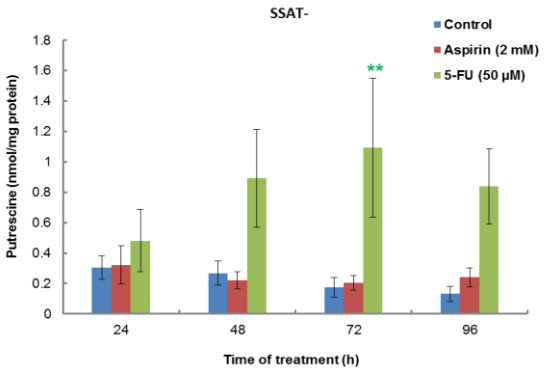

c) SSAT$^+$

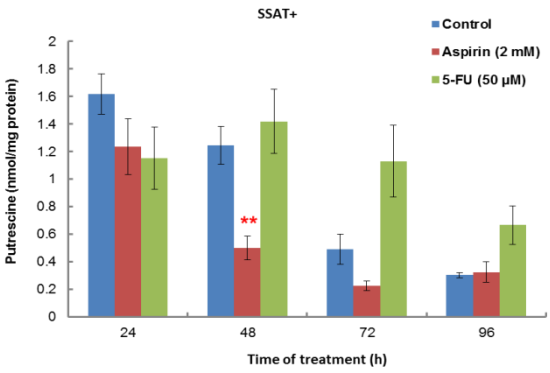

Fig. 3.28 Cells were seeded at a density of 2.4 x 10^4 cells / cm^2 on a 60 x 15 mm cell culture dish in duplicate. Media were replaced after the initial 24 h growth and then at a 48 h interval. Cells were harvested at a 24 h interval; polyamine fraction was extracted by perchloric acid and finally quantified by LC-MS (Section 2.3.7; values are mean ± SEM with n = 3 to 6, two duplicates per experiment). Statistical analysis was performed using Two-way ANOVA with Bonferroni post-tests comparing with Control, i.e. aspirin vs. control (*), 5-FU vs. control (*). p* < 0.05; p** < 0.01; p*** < 0.001.

Spermidine was depleted by both aspirin and 5-FU in WT cells at 24 and 48 h treatment (Fig. 3.29a). The concentration of spermidine fell after aspirin treatment in both $SSAT^-$ and $SSAT^+$ cells but without statistical significance (Fig. 3.29b & c). 5-FU had little effect on spermidine content in the $SSAT^-$ and $SSAT^+$ cells. Accordingly, it might be likely that suppression or overexpression of SSAT could render the cells less sensitive to the drugs.

Fig. 3.29 Effect of aspirin and 5-FU on spermidine content

a) WT

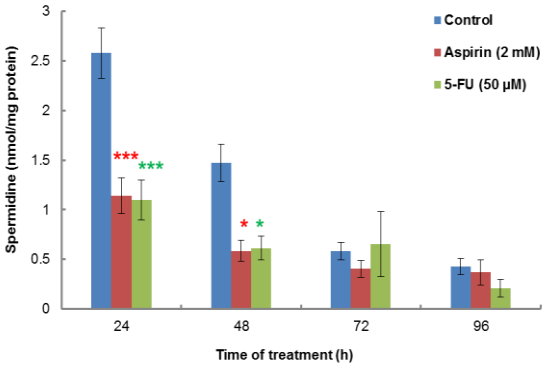

b) $SSAT^-$

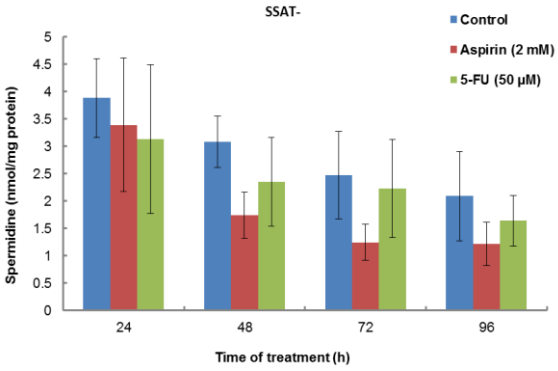

c) $SSAT^+$

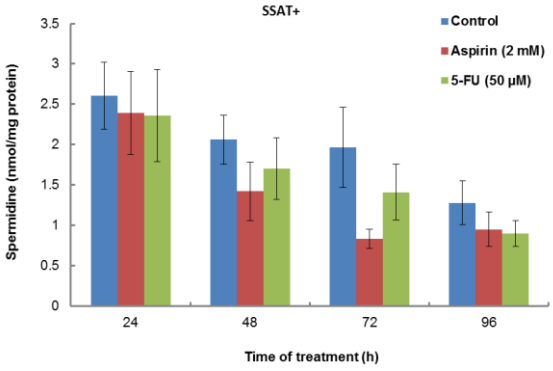

Fig. 3.29 Cells were seeded at a density of 2.4 x 10^4 cells / cm^2 on a 60 x 15 mm cell culture dish in duplicate. Media were replaced after the initial 24 h growth and then at a 48 h interval. Cells were harvested at a 24 h interval; polyamine fraction was extracted by perchloric acid and finally quantified by LC-MS (Section 2.3.7; values are mean ± SEM with n = 3 to 6, two duplicates per experiment). Statistical analysis was performed using Two-way ANOVA with Bonferroni post-tests comparing with Control, i.e. aspirin vs. control (*), 5-FU vs. control (*). p* < 0.05; p** < 0.01; p*** < 0.001.

Spermine was shown to be the most abundant polyamine in all these prostate cancer cell lines. In WT and SSAT$^-$ cells aspirin induced a tendency to decrease spermine but this was not significant. After treatment with 5-FU, spermine content tended to fall in SSAT$^-$ and SSAT$^+$ cells (Fig. 3.30a-c). However, these changes were not significant.

Fig. 3.30 Effect of aspirin and 5-FU on spermine content

a) WT

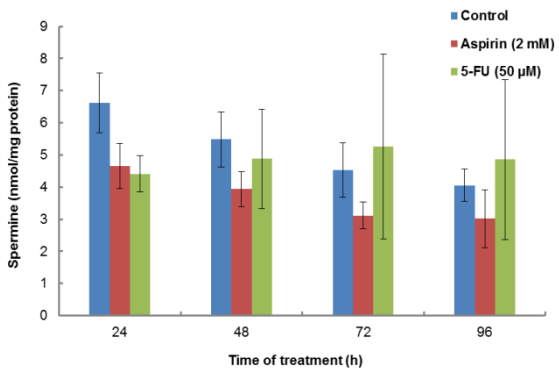

b) SSAT$^-$

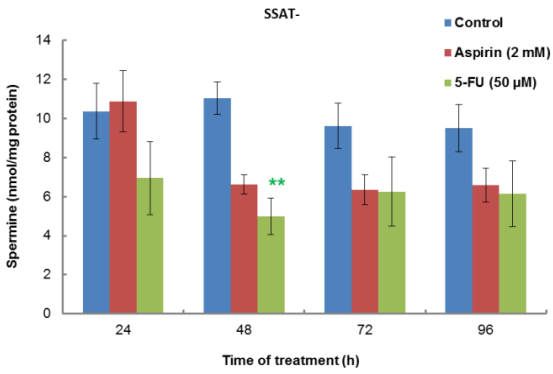

c) SSAT$^+$

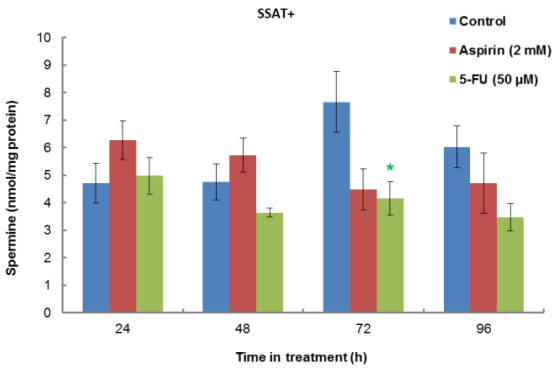

Fig. 3.30 Cells were seeded at a density of 2.4 x 10^4 cells / cm^2 on a 60 x 15 mm cell culture dish in duplicate. Media were replaced after the initial 24 h growth and then at a 48 h interval. Cells were harvested at a 24 h interval; polyamine fraction was extracted by perchloric acid and finally quantified by LC-MS (Section 2.3.7; values are mean ± SEM with n = 3 to 6, two duplicates per experiment). Statistical analysis was performed using Two-way ANOVA with Bonferroni post-tests comparing with Control, i.e. aspirin vs. control (*), 5-FU vs. control (*). p* < 0.05; p** < 0.01; p*** < 0.001.

Maintenance of intracellular polyamine concentrations is extremely important for cell survival. A decrease of total intracellular polyamines by antiproliferative agents is associated with an inhibition of cell growth. Despite the changes in individual polyamine content, it was also critical to understand the effect of the drugs on total polyamine content in these cells.

Both aspirin and 5-FU did not exert much effect on total polyamine content although it did appear to be declined by aspirin. 5-FU seemed less effective than aspirin on depleting polyamines (Fig. 3.31a-c). In return, this indicates intracellular polyamine homeostasis is well maintained in spite of disturbance.

Fig. 3.31 Effect of aspirin and 5-FU on total polyamine content

a) WT

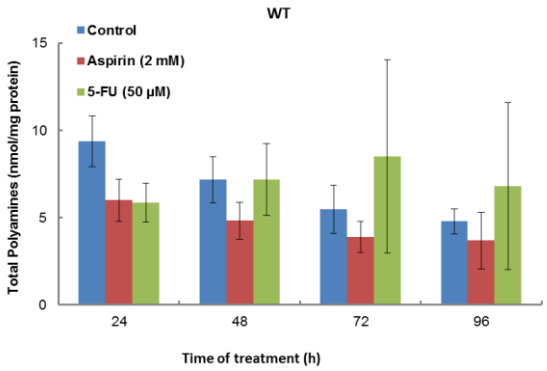

b) SSAT$^-$

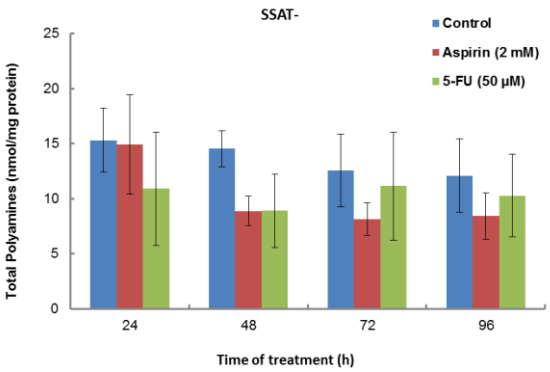

c) SSAT$^+$

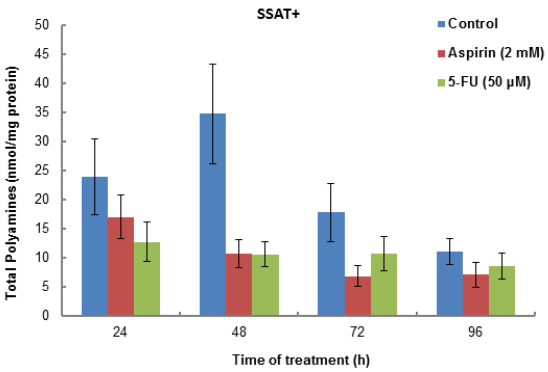

Fig. 3.31 Total polyamine content was obtained by calculating the sum of each individual polyamine concentration in an independent experiment (results are mean ± SEM, n=3 to 6, with 2 duplicates per experiment). Statistical analysis was performed using Two-way ANOVA with Bonferroni post-tests comparing with Control. $p > 0.05$.

3.2.8 Effect of aspirin and 5-FU on polyamine efflux in WT, SSAT$^-$, and SSAT$^+$ cells

Apart from the uptake system, polyamine efflux makes up the other independent part of the polyamine transport system by exporting excess polyamines out of the cell. Depletion of intracellular polyamine pools is proportional to polyamine efflux. It is generally accepted that depletion of intracellular polyamines can result in an arrest of cell growth or cell death. Depletion of intracellular polyamine pools or an increase in polyamine efflux is thought to be associated with the cytotoxic effect of antiproliferative agents.

Therefore, it was believed that as a result of decreased intracellular polyamine pools the inhibition of cell growth by aspirin and 5-FU would correlate with a stimulation of polyamine efflux. To investigate this assumption, the polyamine efflux was measured by quantification of the extracellular radioactivity of [^{3}H]-labelled polyamines after the addition of [^{3}H]-putrescine as a radioactive tracer to the culture medium, which was then taken into the cells by polyamine transport system.

In WT cells, aspirin (from 2% to 85%) was more potent than 5-FU (from 1% to 50%) in increasing polyamine efflux within 48 h. In SSAT$^-$ cells, the difference in polyamine efflux was observed from 9% to 35% by aspirin and from 9% to 52% by 5-FU only at 48 h (Fig. 3.32a & b). However, little difference in polyamine efflux was seen in SSAT$^+$ cells in contrast to the control since it was already enhanced (from 17% at 0 h to 71% at 48 h) in the absence of treatment (Fig. 3.32c). Overall, these results suggest that the antiproliferative effect of aspirin and 5-FU was associated with an increase in polyamine efflux.

Fig. 3.32 Effect of aspirin and 5-FU on the polyamine efflux

a) WT

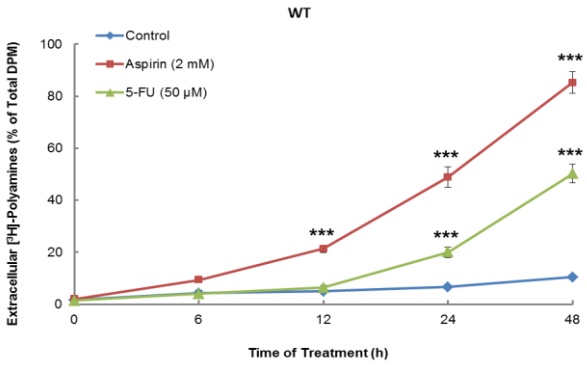

b) SSAT$^-$

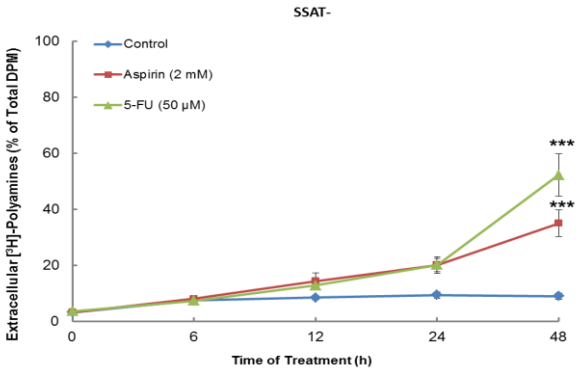

c) SSAT$^+$

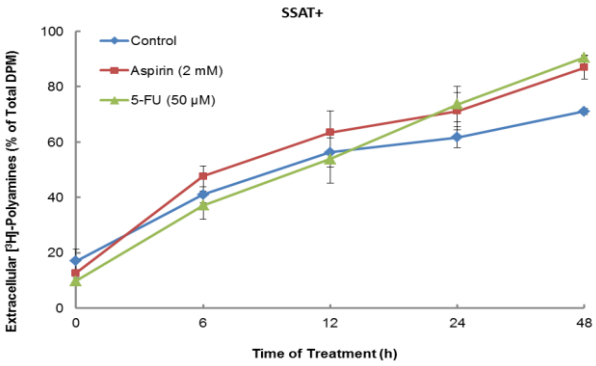

Fig. 3.32 Cells were seeded at a density of 2.4 x 10^4 / cm^2 in a 60 mm diam. cell culture dish in duplicate and incubated for 24 h. The cells was then incubated with [^{3}H]-putrescine for 36 h. After removal of the [^{3}H]-putrescine for 12 h, the cells were dosed with the drug(s) and harvested at 0, 6, 12, 24 and 48 h. Radioactivity was quantified using liquid scintillation analyser (see Section 2.2.20). Results shown are mean ± SEM (n = 3, with 2 replicates per experiment). Statistical analysis was performed by two-way ANOVA with Bonferroni post-tests comparing with Control using Prism5. p*** < 0.001.

3.2.9 Effect of aspirin and 5-FU on intracellular and extracellular polyamine content in WT, SSAT$^-$, and SSAT$^+$ cells

It was demonstrated that polyamine efflux was increased by aspirin and 5-FU in WT and SSAT$^-$ cells using [^{3}H]-labelled putrescine (Fig. 3.32a & b). However, the polyamines transported in response to the treatments have not been identified. Both intracellular and extracellular polyamines were therefore determined after a 48 h treatment of aspirin and 5-FU. Preliminary results showed that the polyamine efflux was more obvious at 48 h than 24 h treatment (results not shown). The reason two different concentrations were used was in order to identify any dose relationship.

N^1,N^{12}-diacetylspermine is synthesised from N^1-acetylspermine by SSAT. There was almost no N^1,N^{12}-diacetylspermine found in SSAT$^-$ cells either intracellularly or extracellularly. Very low amounts were found both inside the WT cells and in the culture medium (Fig. 3.33a & b). SSAT$^+$ cells generated a large amount of N^1,N^{12}-diacetylspermine as a result of the increased SSAT activity (Fig. 3.33c & d). This was decreased intracellularly and extracellularly by treatment with both aspirin and 5-FU. In addition, aspirin showed a dose-dependent change. This result indicates SSAT activity in SSAT$^+$ cells was decreased by aspirin and 5-FU, which is consistent with the previous results (Fig. 3.21c).

Fig. 3.33 Effect of aspirin and 5-FU on N^1,N^{12}-diacetylspermine content

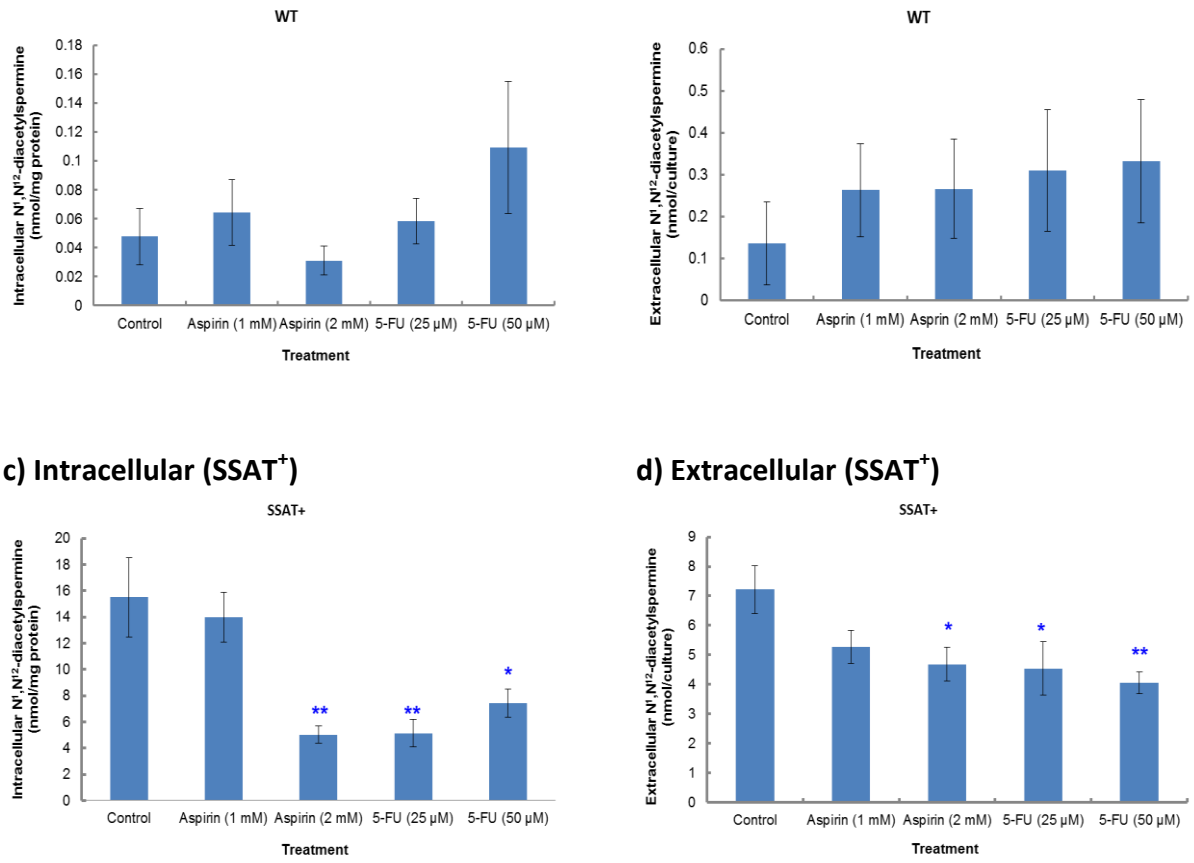

Fig. 3.33 Cells were seeded at a density of 2.4 x 10^4 cells / cm^2 on a 60 x 15 mm cell culture dish in duplicate. The cells were dosed with the drugs after 48 h growth and harvested at 48 h treatment; polyamine fraction was extracted by perchloric acid and finally quantified by LC-MS (Section 2.2.13; values are mean ± SEM with n = 3, two duplicates per experiment). Statistical analysis was performed using One-way ANOVA with Dunnett's post-test comparing with Control. p* < 0.05; p** < 0.01; p*** < 0.001.

N^8-acetylspermidine is thought to be a product of the nuclear SSAT. A small amount was seen only in the extracellular environment of WT and $SSAT^-$ cells (Fig. 3.34a & b). However, it was nearly 10 fold higher in the $SSAT^+$ culture medium. N^8-acetylspermidine production was decreased by both aspirin and 5-FU (Fig. 3.34c & d). Likewise, aspirin illustrated a dose-dependent manner. The decrease of N^8-acetylspermidine by aspirin and 5-FU reflected the decrease in SSAT activity, which was again consistent with the previous results (Fig. 3.21c).

Fig. 3.34 Effect of aspirin and 5-FU on N^8-acetylspermidine content

a) Extracellular (WT)

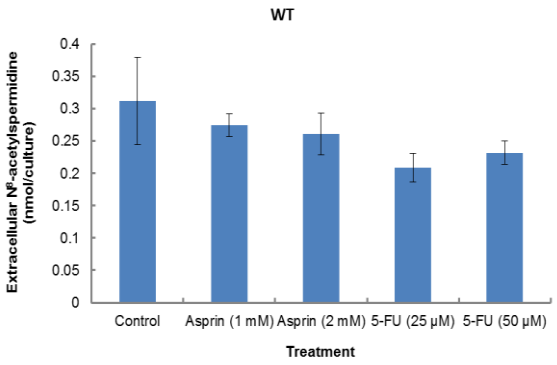

b) Extracellular ($SSAT^-$)

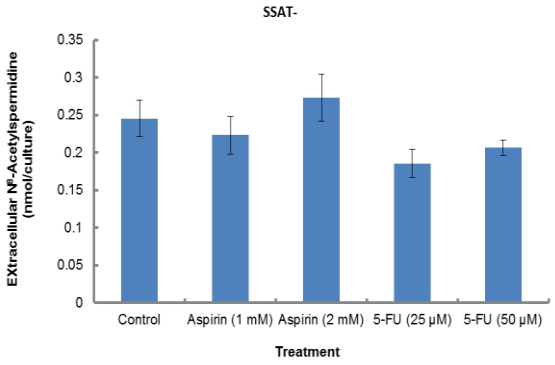

c) Intracellular ($SSAT^+$)

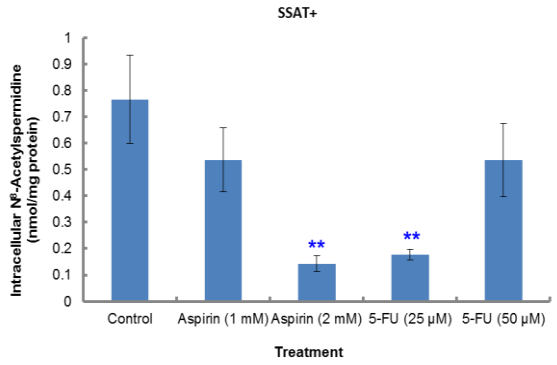

d) Extracellular ($SSAT^+$)

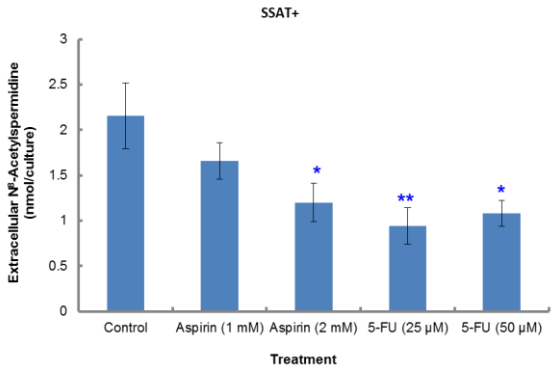

Fig. 3.34 Cells were seeded at a density of 2.4 x 10^4 cells / cm^2 on a 60 x 15 mm cell culture dish in duplicate. The cells were dosed with the drugs after 48 h growth and harvested at 48 h treatment; polyamine fraction was extracted by perchloric acid and finally quantified by LC-MS (Section 2.2.13; values are mean ± SEM with n = 3, two duplicates per experiment). Statistical analysis was performed using One-way ANOVA with Dunnett's post-test comparing with Control. p* < 0.05; p** < 0.01; p*** < 0.001.

The concentration of N^1-acetylspermidine in $SSAT^+$ cells was 200 fold higher in the intracellular compartment and 500 fold higher in the extracellularly environment than that in both WT and $SSAT^-$ cells (Fig. 3.35a-f). Instead of an increase in $SSAT^-$ and WT, there was a decrease of N^1-acetylspermidine in $SSAT^+$ by aspirin and 5-FU. Thus, N^1-acetylspermidine was the most abundant polyamine that was transported out the cells while SSAT was increased.

Fig. 3.35 Effect of aspirin and 5-FU on N^1-acetylspermidine content

a) Intracellular (WT)

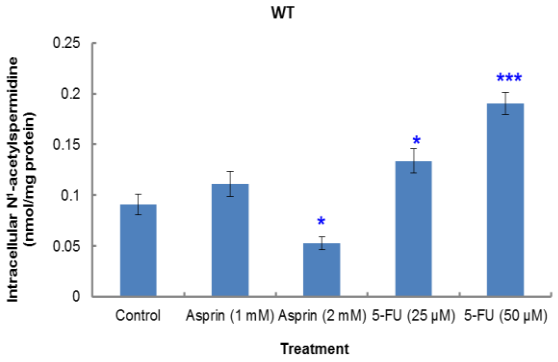

b) Extracellular (WT)

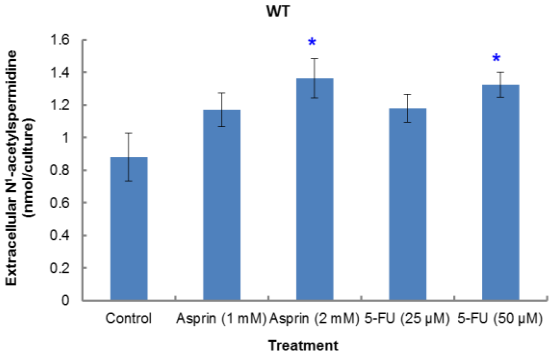

c) Intracellular ($SSAT^-$)

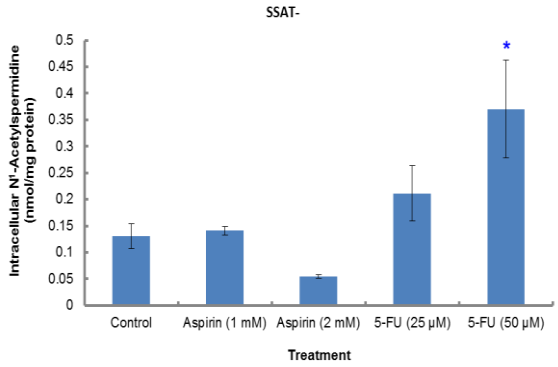

d) Extracellular ($SSAT^-$)

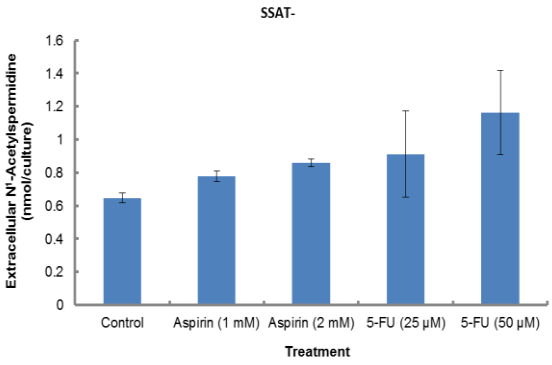

e) Intracellular (SSAT$^+$)

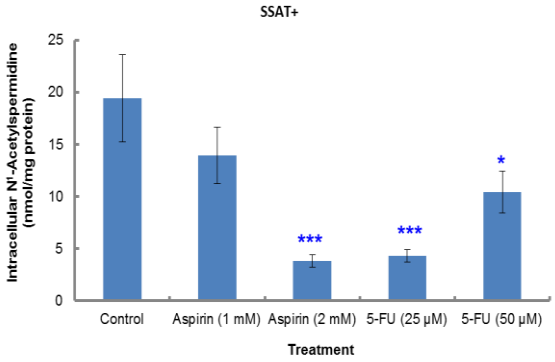

f) Extracellular (SSAT$^+$)

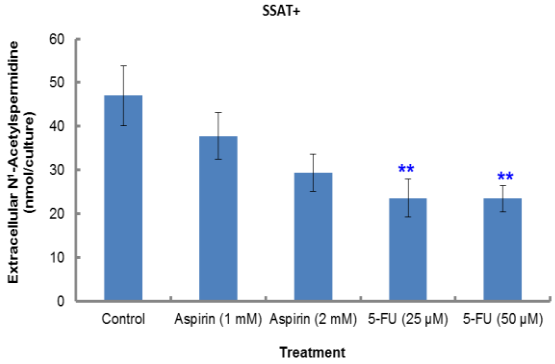

Fig. 3.35 Cells were seeded at a density of 2.4 x 10^4 cells / cm^2 on a 60 x 15 mm cell culture dish in duplicate. The cells were dosed with the drugs after 48 h growth and harvested at 48 h treatment; polyamine fraction was extracted by perchloric acid and finally quantified by LC-MS (Section 2.2.13; values are mean ± SEM with n = 3, two duplicates per experiment). Statistical analysis was performed using One-way ANOVA with Dunnett's post-test comparing with Control. p* < 0.05; p** < 0.01; p*** < 0.001.

Similarly, the concentration of N^1-acetylspermine was very low in both WT and SSAT$^-$ cells due to their low SSAT activity. Aspirin and 5-FU did not have much effect on this (Fig. 3.36a-d). In addition, intracellular N^1-acetylspermine was decreased by the drugs in SSAT$^+$ cells, indicating a decrease of SSAT activity by aspirin and 5-FU (Fig. 3.36e & f).

Fig. 3.36 Effect of aspirin and 5-FU on N^1-acetylspermine content

a) Intracellular (WT)

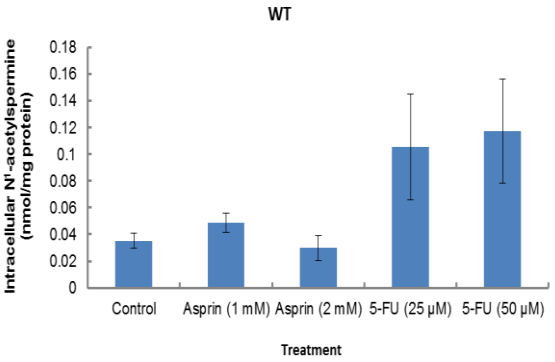

b) Extracellular (WT)

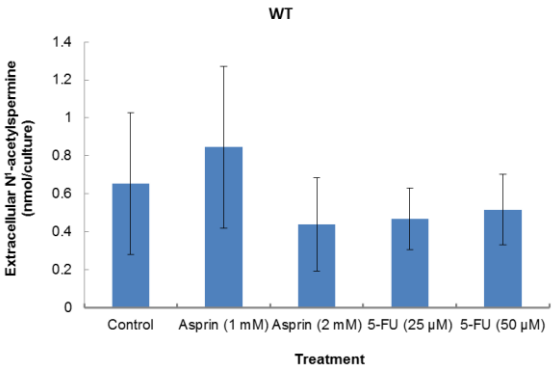

c) Intracellular (SSAT$^-$)

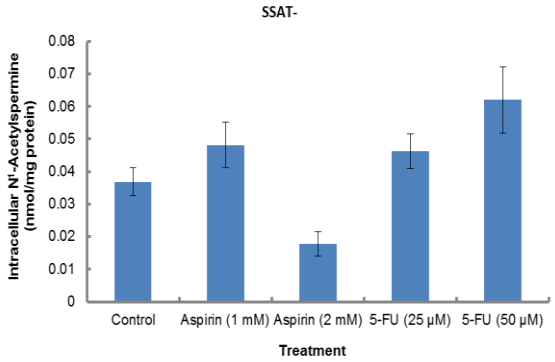

d) Extracellular (SSAT$^-$)

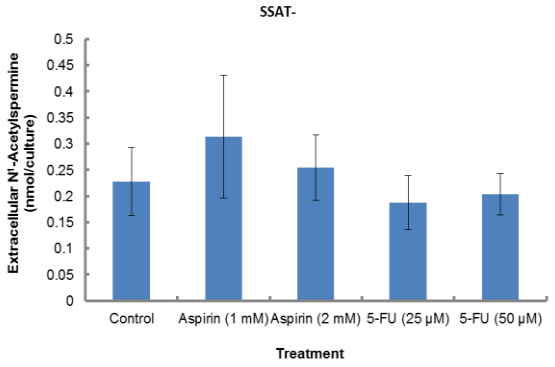

e) Intracellular (SSAT$^+$)

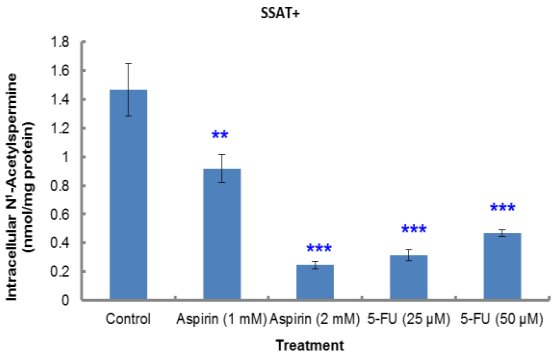

f) Extracellular (SSAT$^+$)

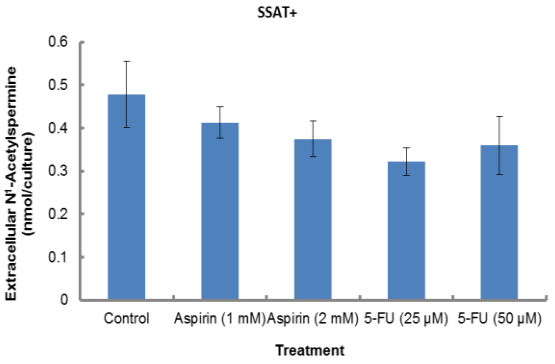

Fig. 3.36 Cells were seeded at a density of 2.4 x 10^4 cells / cm^2 on a 60 x 15 mm cell culture dish in duplicate. The cells were dosed with the drugs after 48 h growth and harvested at 48 h treatment; polyamine fraction was extracted by perchloric acid and finally quantified by LC-MS (Section 2.2.13; values are mean ± SEM with n = 3, two duplicates per experiment). Statistical analysis was performed using One-way ANOVA with Dunnett's post-test comparing with Control. p* < 0.05; p** < 0.01; p*** < 0.001.

A large amount of putrescine was found both intracellularly and extracellularly in SSAT$^+$ cells as a result of increased SSAT activity. Aspirin (2 mM) seemed more potent in inhibiting intracellular putrescine content. However, extracellular polyamines were not affected dramatically by the treatments (Fig. 3.37a-f).

Fig. 3.37 Effect of aspirin and 5-FU on putrescine content

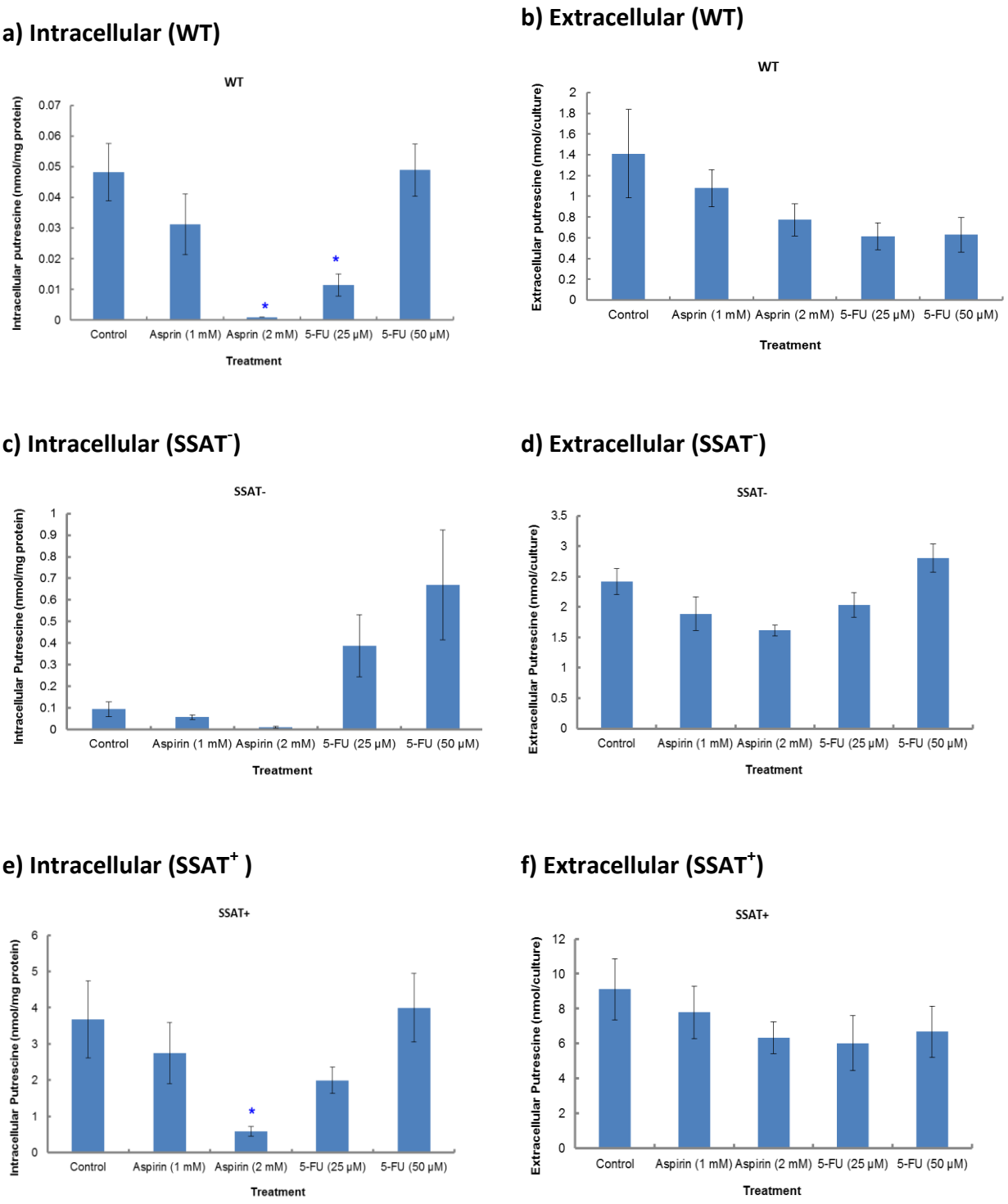

Fig. 3.37 Cells were seeded at a density of 2.4 x 10^4 cells / cm^2 on a 60 x 15 mm cell culture dish in duplicate. The cells were dosed with the drugs after 48 h growth and harvested at 48 h treatment; polyamine fraction was extracted by perchloric acid and finally quantified by LC-MS (Section 2.2.13; values are mean ± SEM with n = 3, two duplicates per experiment). Statistical analysis was performed using One-way ANOVA with Dunnett's post-test comparing with Control. p* < 0.05; p** < 0.01; p*** < 0.001.

Intracellular spermidine was decreased by aspirin (2 mM) and 5-FU in all the cells while extracellular spermidine did not change dramatically (Fig. 3.38a-f).

Fig. 3.38 Effect of aspirin and 5-FU on spermidine content

a) Intracellular (WT)

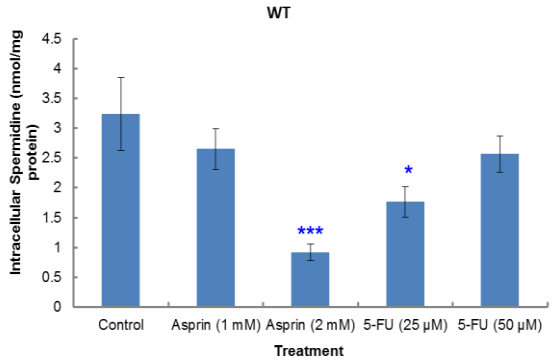

b) Extracellular (WT)

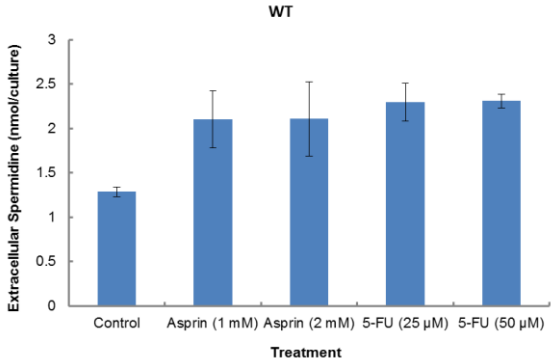

c) Intracellular (SSAT$^-$)

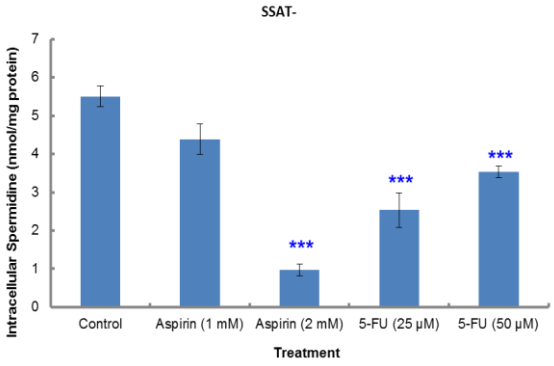

d) Extracellular (SSAT$^-$)

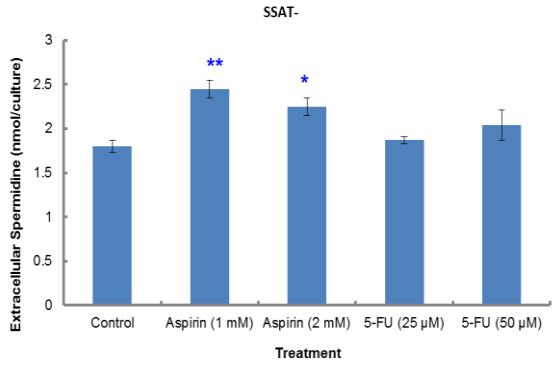

e) Intracellular (SSAT$^+$)

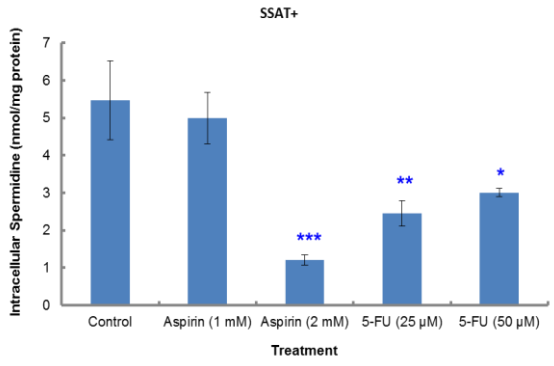

f) Extracellular (SSAT$^+$)

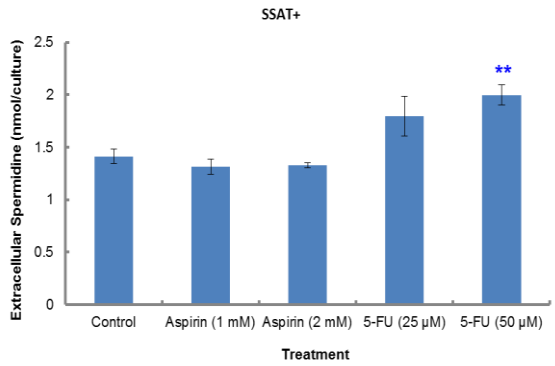

Fig. 3.38 Cells were seeded at a density of 2.4 x 10^4 cells / cm^2 on a 60 x 15 mm cell culture dish in duplicate. The cells were dosed with the drugs after 48 h growth and harvested at 48 h treatment; polyamine fraction was extracted by perchloric acid and finally quantified by LC-MS (Section 2.2.13; values are mean ± SEM with n = 3, two duplicates per experiment). Statistical analysis was performed using One-way ANOVA with Dunnett's post-test comparing with Control. p* < 0.05; p** < 0.01; p*** < 0.001.

There was no spermine found in the culture medium of any of the cells, indicating spermine is the only polyamine that is not exported. Intracellular spermine was decreased by aspirin and 5-FU regardless of the SSAT activity. This might be associated with the inhibition of cell growth (Fig. 3.39a-c).

Fig. 3.39 Effect of aspirin and 5-FU on intracellular spermine content

a) WT

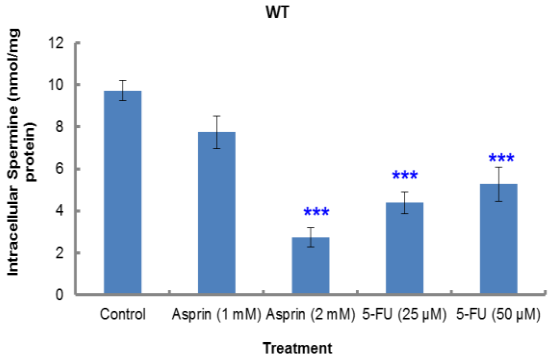

b) SSAT$^-$

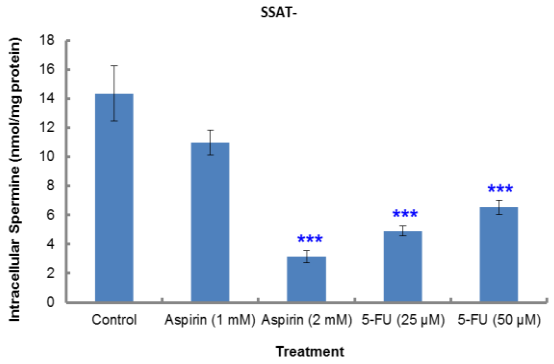

c) SSAT$^+$

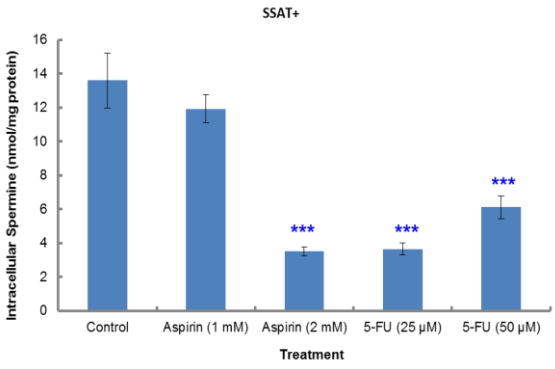

Fig. 3.39 Cells were seeded at a density of 2.4 x 10^4 cells / cm^2 on a 60 x 15 mm cell culture dish in duplicate. The cells were dosed with the drugs after 48 h growth and harvested at 48 h treatment; polyamine fraction was extracted by perchloric acid and finally quantified by LC-MS (Section 2.2.13; values are mean ± SEM with n = 3, two duplicates per experiment). Statistical analysis was performed using One-way ANOVA with Dunnett's post-test comparing with Control. p* < 0.05; p** < 0.01; p*** < 0.001.

Total intracellular polyamine pools were decreased by aspirin and 5-FU in all the cells and aspirin presented a dose response change. However, the drugs did not have much effect on the total extracellular polyamine pools (Fig. 3.40a-f). This indicates that the growth inhibition by the drugs is associated with a depletion of total intracellular polyamine pools.

Fig. 3.40 Effect of aspirin and 5-FU on total polyamine content

a) Intracellular (WT)

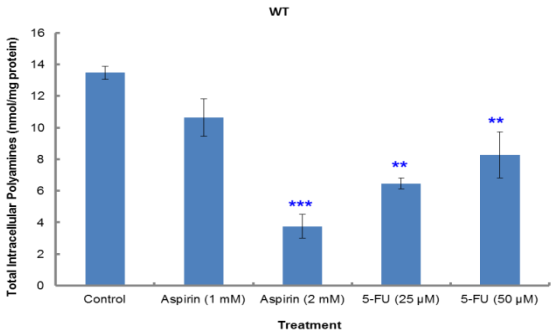

b) Extracellular (WT)

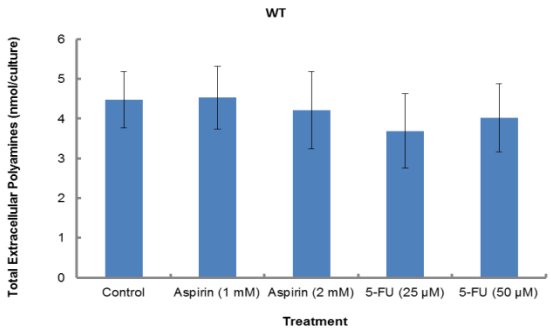

c) Intracellular (SSAT$^-$)

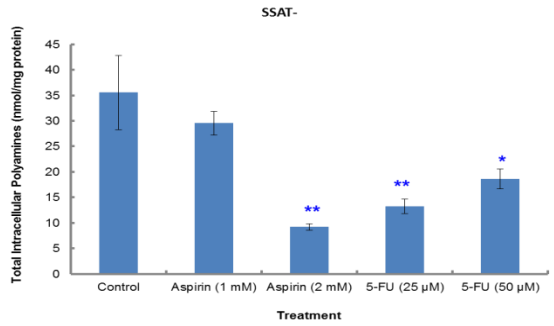

d) Extracellular (SSAT$^-$)

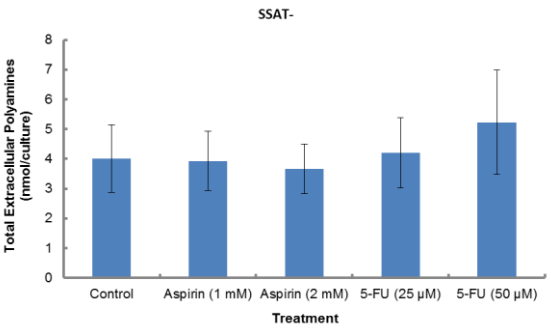

e) Intracellular (SSAT$^+$)

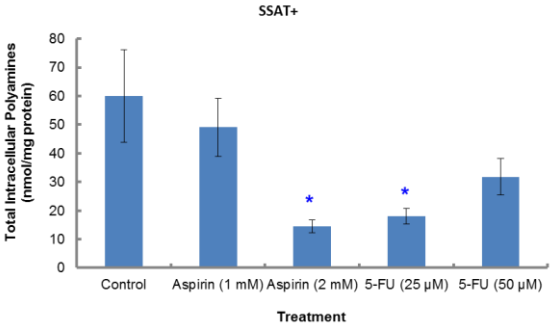

f) Extracellular (SSAT$^+$)

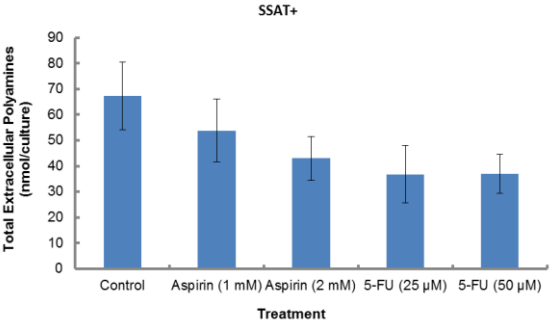

Fig. 3.40 Total polyamine content was obtained by calculating the sum of each individual polyamine content in an independent experiment (results are mean ± SEM, n=3 to 6, with 2 duplicates per experiment). Statistical analysis was performed using One-way ANOVA with Dunnett's post-test comparing with Control. p* < 0.05; p** < 0.01; p*** < 0.001.

Extremely high polyamine export was observed in $SSAT^+$ cells. N^1-acetylspermidine was the predominant polyamine excreted, which was about 73 fold higher than that in $SSAT^-$ and 53 fold higher than that in WT cells. The second predominant polyamine exported was putrescine in $SSAT^+$ cells, which was 4 fold higher than that in $SSAT^-$ cells and 6 fold higher than that in WT cells. N^1,N^{12}-diacetylspermine was the third predominant polyamine exported in $SSAT^+$ cells (Fig. 3.41c). On the contrary, polyamine efflux was very low in WT and $SSAT^-$ cells. Spermidine and N^1-acetylspermidine were the two major polyamines exported in WT cells responsive to aspirin and 5-FU. In $SSAT^-$ cells, spermidine, putrescine and N^1-acetylspermidine were the main polyamines for excretion (Fig. 3.41a & b).

Fig. 3.41 Comparison of the components of extracellular polyamines

a) WT

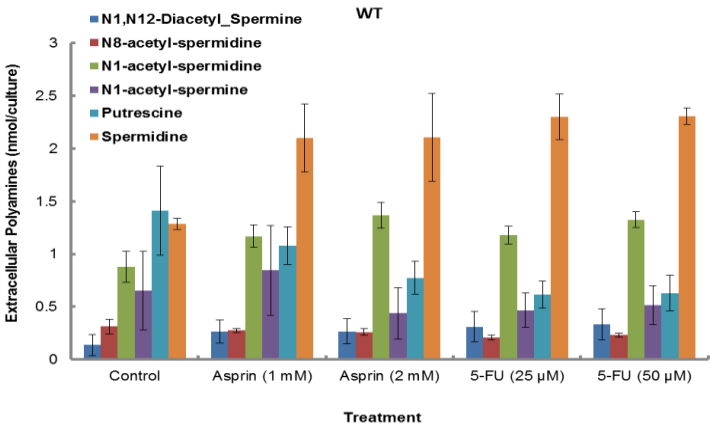

b) SSAT$^-$

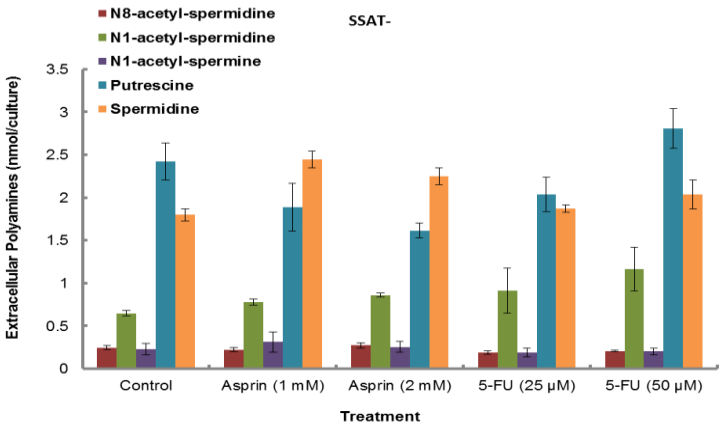

c) SSAT$^+$

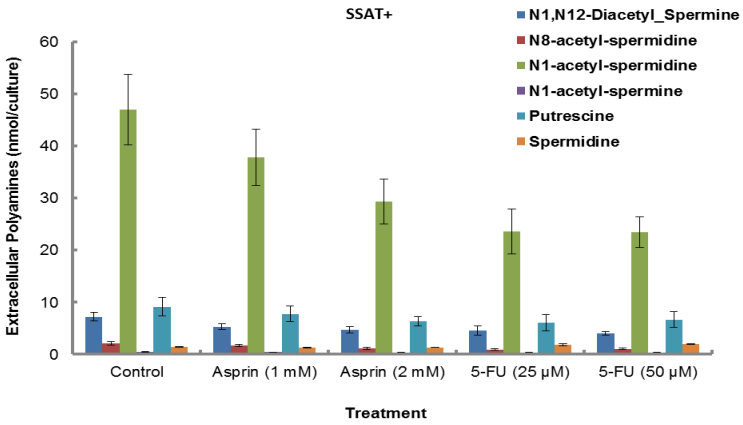

Fig. 3.41 The comparison of extracellular components of polyamines was summarised from the results in Fig. 3.37-3.43. Results shown are mean ± SEM (n=3, with 2 duplicates per experiment).

Total intracellular polyamines were considerably increased in SSAT$^+$ cells compared with WT without treatment. Aspirin at 1 mM had little effect in the reducing total intracellular polyamine content. SSAT$^+$ cells presented the highest polyamine efflux, which was 15 and 17 fold higher than that of WT and SSAT$^-$ cells respectively without treatment. After treatment with aspirin, polyamine efflux in SSAT$^+$ cells was 10-12 fold and 12-14 fold greater than that in WT and SSAT$^-$ respectively. In response to 5-FU, SSAT$^+$ cells had 9-10 fold and 7-9 fold increase of polyamine export than WT and SSAT$^-$ respectively (Fig. 3.42a & b). These results indicate as a result of increased SSAT activity, export is the major mechanism to lower increased intracellular polyamines and is the first destination for N^1-acetylspermidine rather than the retroconversion pathway.

Fig. 3.42 Effect of aspirin and 5-FU on total polyamine content in WT, SSAT$^-$, and SSAT$^+$ cells

a) Intracellular

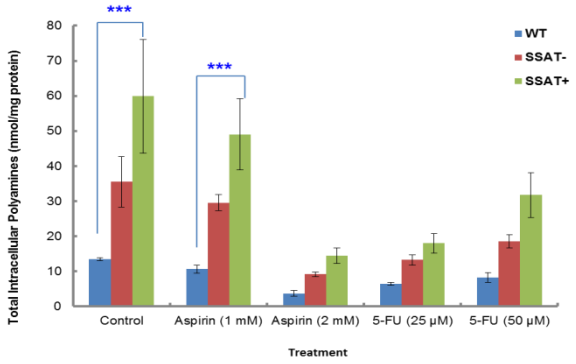

b) Extracellular

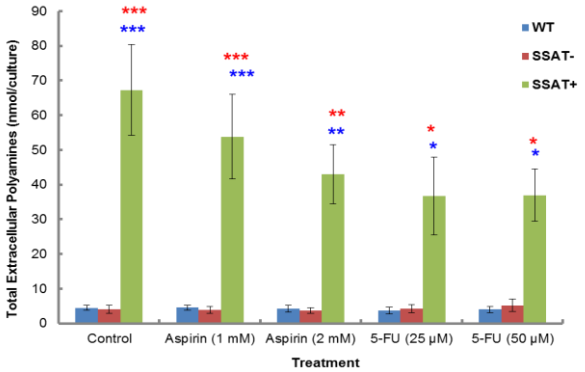

Fig. 3.42 Total polyamine content was analysed by the sum of the each individual polyamine content from each assay. Results shown are mean ± SEM (n=3, with 2 duplicates per experiment). Statistical analysis was performed by Two-way ANOVA with Bonferroni post-tests using Prism 5, comparing WT vs. SSAT$^-$, WT vs. SSAT$^+$ (*), and SSAT$^-$ vs. SSAT$^+$ (*). p* < 0.05; p** < 0.01; p*** < 0.001.

3.3 Effect of inhibition of ODC, APAO and SMO on WT, SSAT$^-$ and SSAT$^+$ cells

3.3.1 Inhibition of ODC, APAO and SMO on the cell growth of WT, SSAT$^-$ and SSAT$^+$ cells

DFMO prevents putrescine synthesis by inactivating ODC, therefore, leading to a decrease in both putrescine and spermidine and subsequently an arrest of cell growth in most cell lines. Application of MDL72527 *in vitro* causes an accumulation of intracellular acetylpolyamines via inhibiting APAO and may also reduce spermidine content by inactivating SMO. Taken together, the consequence of using DFMO and MDL72527 is a disturbance to the intracellular polyamine pools that would cause a subsequent interference to the cell growth. The accumulation of acetylpolyamines and putrescine in SSAT$^+$ cells may lead to the growth inhibition. Inhibition of putrescine synthesis by DFMO and acetylpolyamine synthesis by MDL72527 may therefore restore the cell growth.

1 mM DFMO and 25 μM MDL72527 (Bey *et al.*, 1985) were chosen and they did not exert much effect alone on the growth of WT cells, however the cell numbers appeared to decrease with the combination of these two inhibitors (Fig. 3.43a). This declining trend would be more obvious if the cells were treated up to 72 h. Similarly, DFMO and MDL72527 either alone or combined had no significant effect on the growth of SSAT$^-$ cells (Fig. 3.43b). This indicates that the growth of WT and SSAT$^-$ cells was not dramatically interfered by DFMO and MDL72527 within 48 h treatment.

The viable cell numbers of SSAT$^+$ cells increased slightly by DFMO (1 mM) alone (Fig. 3.43c). The combined treatment of DFMO and MDL72527 markedly stimulated the cell growth compared with the control. This indicates the combined inhibition of ODC, APAO, and even SMO can partially restore the growth inhibition caused by SSAT overexpression in these cells.

Fig. 3.43 Effect of DFMO and MDL72527 on cell growth

a) WT

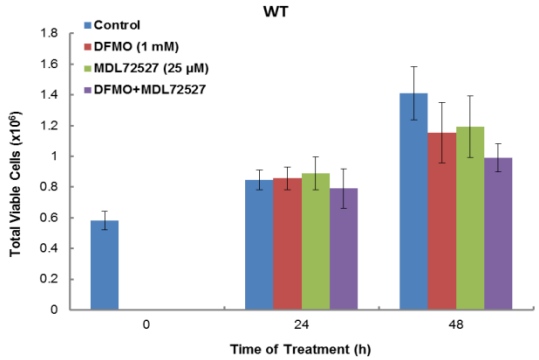

b) SSAT$^-$

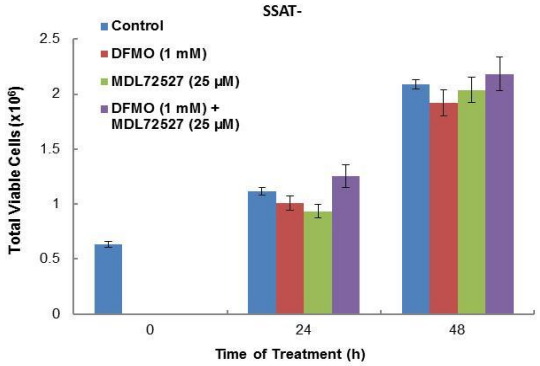

c) SSAT$^+$

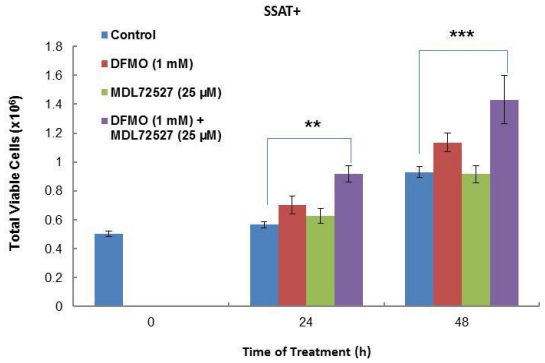

Fig. 3.43 Cells were seeded at a density of 2.4 x 10^4 / cm^2 in 60 mm diam. cell culture dish in duplicate. Cells were treated with DFMO (1 mM) and MDL72527 (25 µM) after 48 h incubation and then harvested at 0, 24 and 48 h. Viable cell numbers were counted using Trypan blue exclusion assay (Section 2.2.1). Results shown are mean ± SEM (n = 3, with 2 duplicate per experiment). Statistical analysis was performed by two-way ANOVA with Bonferroni post-tests using Prism 5, comparing with the control. p** < 0.01; p*** < 0.001.

3.3.2 Inhibition of ODC, APAO and SMO on intracellular polyamine content in WT cells

Inhibition of ODC by its irreversible inactivator DFMO together with the inhibition of APAO by MDL72527 tended to lower the cell growth of WT cells (Fig. 3.43a). However, the combination of DFMO and MDL72527 partially restored the growth of $SSAT^+$ cells (Fig. 3.43c). This was related to an alteration of intracellular polyamine concentrations. Thus, the effect of DFMO and MDL72527 on intracellular polyamine content was measured.

Total intracellular polyamines in WT cells declined with the combination treatments of DFMO and MDL72527. However, treatment with either of the inhibitors alone had little effect (Fig. 3.44a).

Fig. 3.44 Effect of DFMO and MDL72527 on intracellular polyamines in WT cells

a) Total

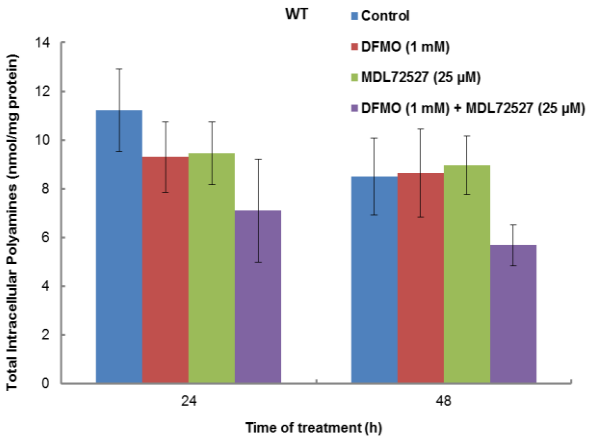

Fig. 3.44a Total polyamine content was obtained by calculating the sum of each individual polyamine concentration in an independent experiment (results are mean ± SEM, n=3, with 2 duplicates per experiment). Statistical analysis was performed using Two-way ANOVA with Bonferroni post-tests comparing with Control. $p > 0.05$.

A very low amount of N^1-acetylspermidine and N^1-acetylspermine was present in the WT cells, which was consistent with a low basal SSAT activity. A slight decrease of N^1-acetylspermidine by DFMO was observed at 48 h treatment (Fig. 3.44b). N^1-acetylspermine was increased (2-6 fold) by MDL72527 (Fig. 3.44c), but N^1-acetylspermidine was not. The lack of accumulation of N^1-acetylspermdine was likely due to the fact that most of it was exported out of the cells.

b) N^1-Acetylspermidine

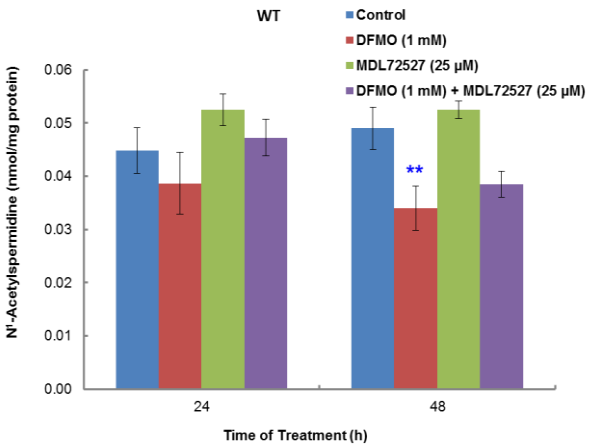

c) N^1-Acetylspermine

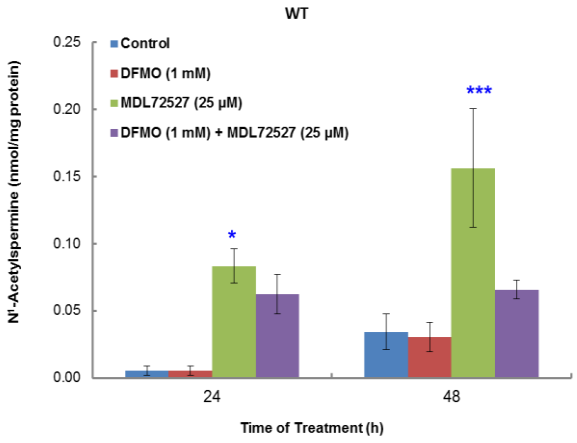

Putrescine was decreased about 2 fold by DFMO alone and DFMO combined with MDL72527 at 24 h (Fig. 3.44d). Likewise, spermidine was decreased 2 fold by the treatments. The fall of spermidine by DFMO resulted in a decline of N^1-acetylspermidine (Fig. 3.44e). MDL72527 alone did not have an effect on putrescine and spermidine content. In addition, very little impact was seen on spermine by these two inhibitors (Fig. 3.44f).

d) Putrescine

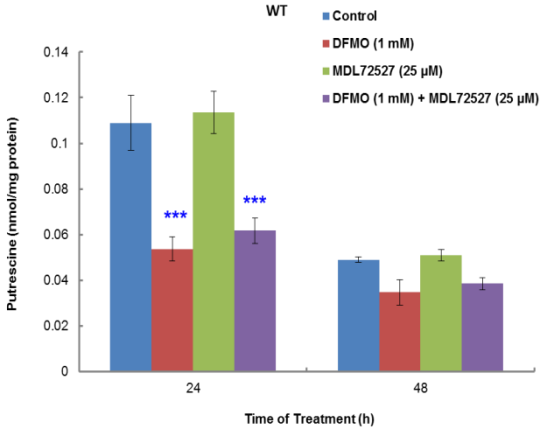

e) Spermidine

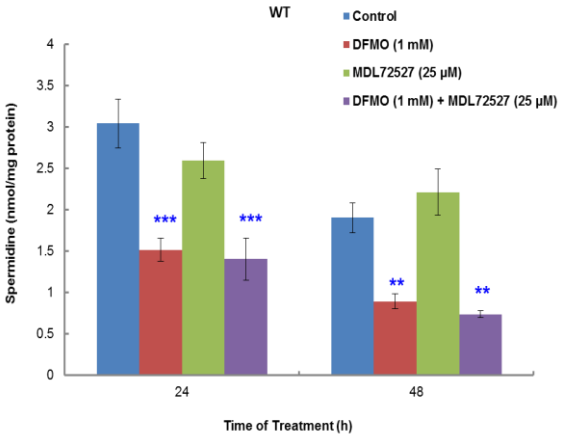

f) Spermine

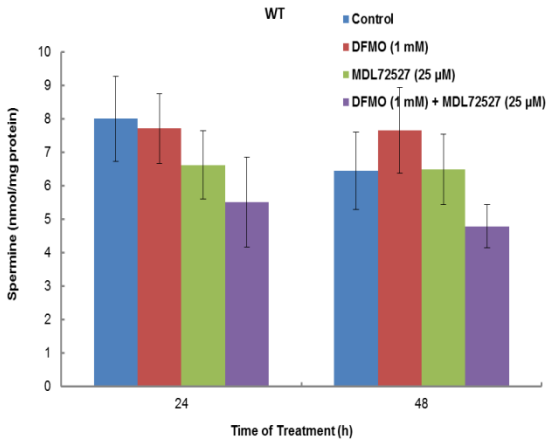

Fig. 3.44 Cells were seeded at a density of 2.4 x 10^4 cells / cm^2 on a 60 x 15 mm cell culture dish in duplicate. The cells were treated with the drugs after 48 h incubation and harvested at 24 and 48 h treatment; polyamine fraction was extracted by perchloric acid and finally quantified by LC-MS (Section 2.3.7; values are mean ± SEM with n = 3, with 2 duplicates per experiment). Statistical analysis was performed using Two-way ANOVA with Bonferroni post-tests comparing with Control. $p^* < 0.05$; $p^{**} < 0.01$; $p^{***} < 0.001$.

3.3.3 Inhibition of ODC, APAO and SMO on intracellular polyamine content in SSAT$^-$ cells

Total intracellular polyamine content in SSAT$^-$ cells decreased with the combined treatment of DFMO and MDL72527, but neither of the inhibitors alone had a marked effect (Fig. 3.45a).

Fig. 3.45 Effect of DFMO and MDL72527 on intracellular polyamines in SSAT$^-$ cells

a) Total

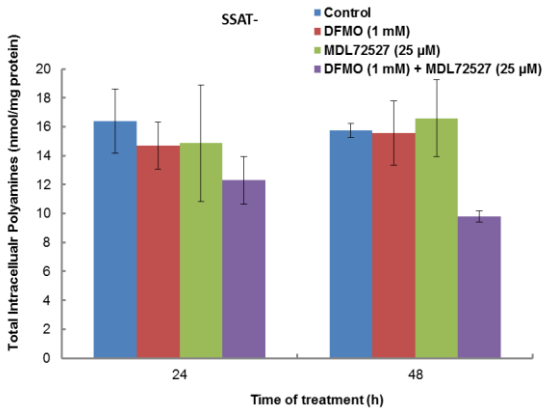

N^1-acetylspermidine and N^1-acetylspermine concentrations were extremely low in SSAT$^-$ cells. N^1-acetylspermidine appeared to increase in response to MDL72527, but was decreased by DFMO (6 fold) and the combined treatments (7-15 fold). N^1-acetylspermine was increased (6-9 fold) by MDL72527 and the combination of the two inhibitors (4-6 fold) (Fig. 3.45b & c).

b) N^1-acetylspermidine

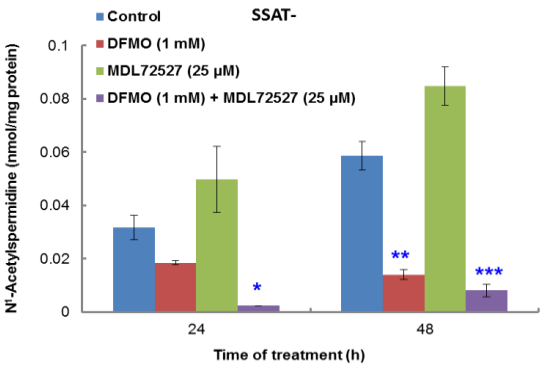

c) N^1-acetylspermine

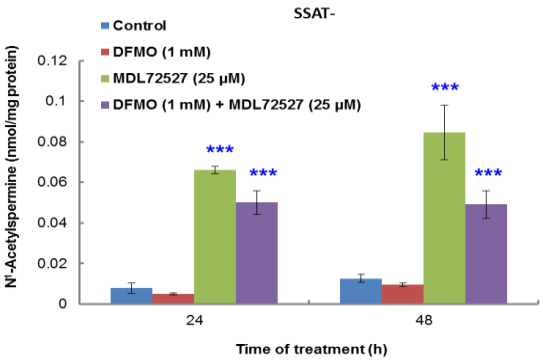

Putrescine was slightly decreased by DFMO, but increased by MDL72527 unexpectly (Fig. 3.45d). Spermidine was decreased by DFMO and the combined treatments (Fig. 3.45e). This could result in the decreased N^1-acetylspermidine by DFMO. Spermine content did not change dramatically with the inhibitors (Fig. 3.45f).

d) Putrescine

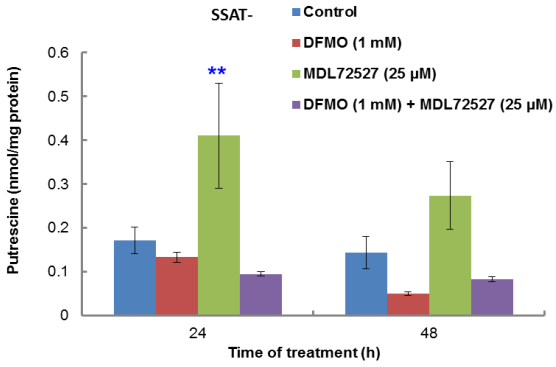

e) Spermidine

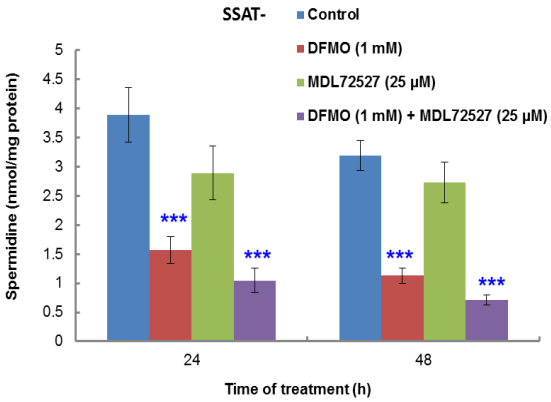

f) Spermine

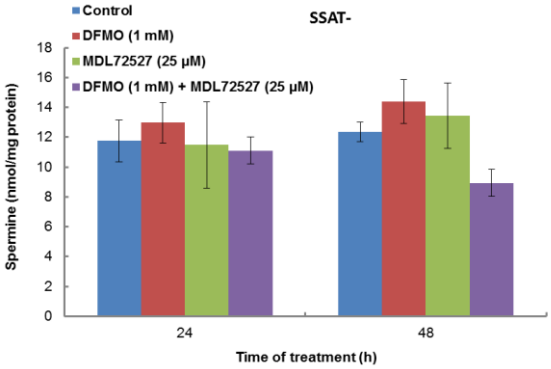

Fig. 3.45 Cells were seeded at a density of 2.4 x 10^4 cells / cm^2 on a 60 x 15 mm cell culture dish in duplicate. The cells were treated with the drugs after 48 h incubation and harvested at 24 and 48 h treatment; polyamine fraction was extracted by perchloric acid and finally quantified by LC-MS (Section 2.3.7; values are mean ± SEM with n = 3, with 2 duplicates per experiment). Statistical analysis was performed using Two-way ANOVA with Bonferroni post-tests comparing with Control. $p^* < 0.05$; $p^{**} < 0.01$; $p^{***} < 0.001$.

3.3.4 Inhibition of ODC, APAO and SMO on intracellular polyamine content in SSAT+ cells

Total intracellular polyamine pools of SSAT+ cells were decreased (4 fold) by DFMO. Although the total polyamines appeared to be decreased by MDL72527 and the combination of these two inhibitors, it was not statistically significant (Fig. 3.46a).

Fig. 3.46 Effect of DFMO and MDL72527 on intracellular polyamines in SSAT+ cells

a) Total

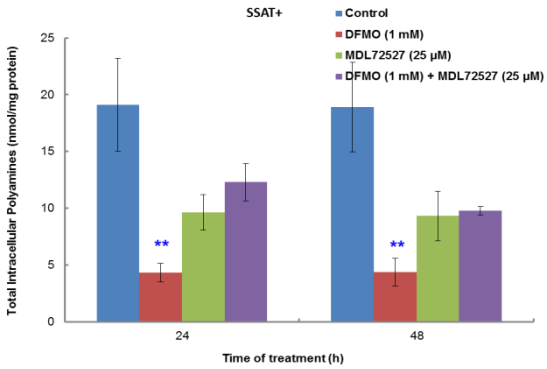

N^1-acetylspermidine was decreased by DFMO (14-18 fold), MDL72527 (2 fold) and their combined treatments (7-15 fold) (Fig. 3.46b). This is consistent with the results of decreased spermidine (Fig. 3.46e), since spermidine is the substrate for SSAT to form N^1-acetylspermidine. N^1-acetylspermine was also decreased by DFMO (4-5 fold) but increased by the combination of the inhibitors (2-3 fold), with no effect of MDL72527 alone (Fig. 3.46c). Spermine showed the similar manner (Fig. 3.46f), since SSAT used spermine as the substrate to form N^1-acetylspermine.

b) N^1-acetylspermidine

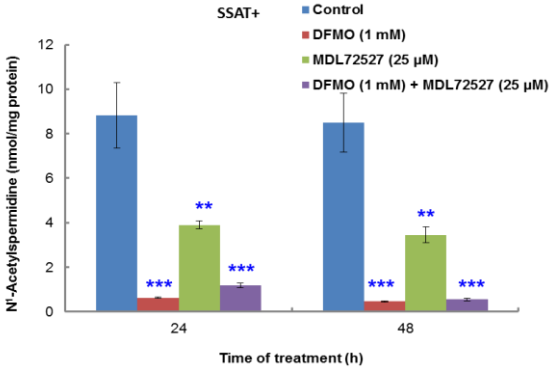

c) N^1-acetylspermine

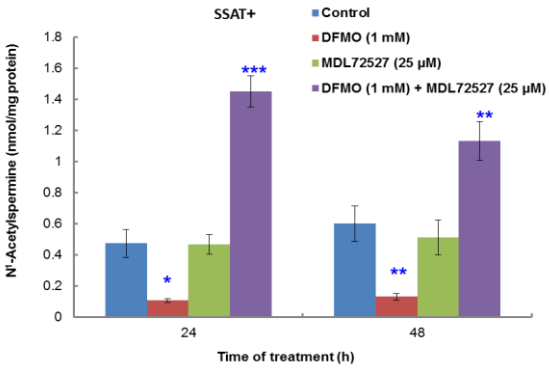

Putrescine was markedly decreased by DFMO (10-18 fold) and the combined treatment with MDL72527 (11-14 fold), but with only a slight decrease with MDL72527 (1.5 fold) (Fig. 3.46d). Likewise, spermidine was decreased by DFMO (4 fold), MDL72527 (2 fold), and the combination of the two inhibitors (2-3 fold) (Fig. 3.46e). However, spermine was increased by the combined treatments (2 fold), either alone did not have much effect (Fig. 3.46f).

d) Putrescine

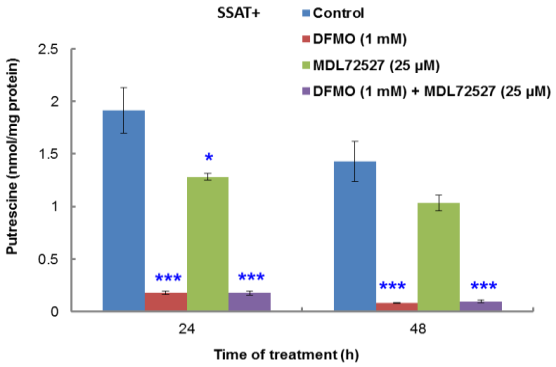

e) Spermidine

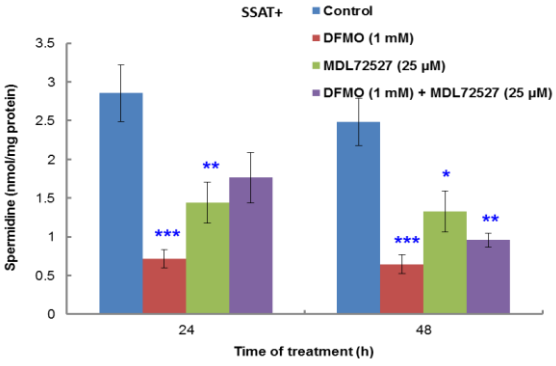

f) Spermine

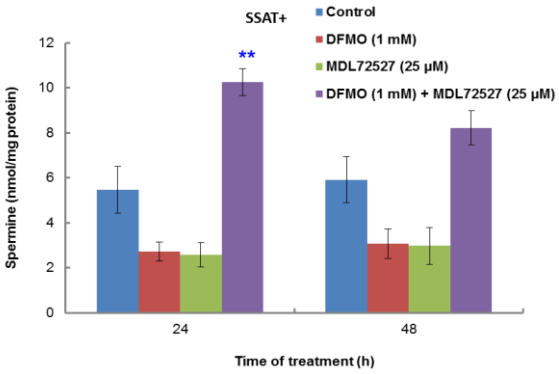

Fig. 3.46 Cells were seeded at a density of 2.4 x 10^4 cells / cm^2 on a 60 x 15 mm cell culture dish in duplicate. The cells were treated with the drugs after 48 h incubation and harvested at 24 and 48 h treatment; polyamine fraction was extracted by perchloric acid and finally quantified by LC-MS (Section 2.3.7; values are mean ± SEM with n = 3, with 2 duplicates per experiment). Statistical analysis was performed using Two-way ANOVA with Bonferroni post-tests comparing with Control. p* < 0.05; p** < 0.01; p*** < 0.001.

3.4 Preliminary investigation for future study

3.4.1 Effect of exogenous addition of N^1-acetylspermidine and putrescine on the growth of $SSAT^-$ and WT cells

The accumulation of N^1-acetylspermdine and putrescine in $SSAT^+$ is the major difference when comparing all the cells used in the study. The low proliferation of $SSAT^+$ cells might be associated with the accumulation of these polyamines perhaps to a toxic level. In order to investigate whether the accumulation was toxic, a range of concentrations (0.1, 1 and 10 μM) of N^1-acetylspermidine and putrescine was added to the culture medium for 48 h and viable cell numbers were determined.

The preliminary results showed no toxic effect of N^1-acetylspermidine in both $SSAT^-$ and WT cells (Fig. 3.47a & b). This indicates that the accumulation of N^1-acetylspermidine did not seem to be growth inhibitory or toxic.

Likewise, the addition of putrescine to the culture medium did not have much effect on the growth of both $SSAT^-$ and WT cells either (Fig. 3.48a & b).

A higher concentration of the exogenous N^1-acetylspermidine and putrescine may be needed.

Fig. 3.47 Effect of exogenous N^1-acetylspermidine on cell growth

a) SSAT$^-$

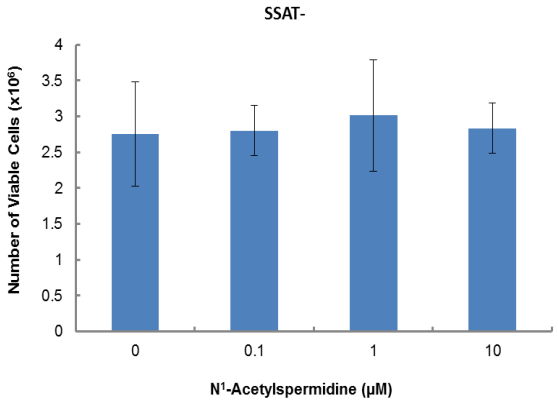

b) WT

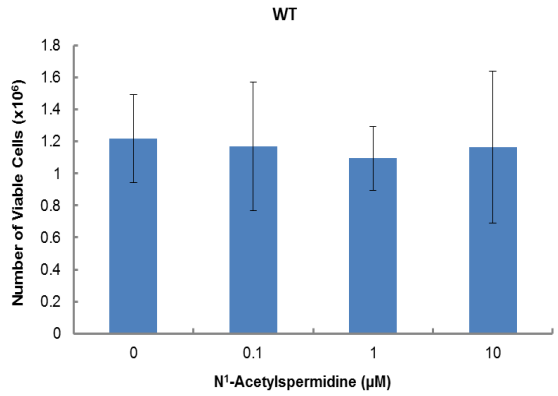

Fig. 3.47 Cells were seeded at a density of 2.4 x 10^4 / cm^2 in 60 mm diam. cell culture dish in duplicate. The cells were incubated for 48 h and the medium was replaced with fresh medium containing N^1-acetylspermidine or putrescine. Viable cell numbers were counted using Trypan blue exclusion assay (Section 2.2.5). Results shown are mean ± rang (n = 1, with 2 duplicates per experiment).

Fig. 3.48 Effect of exogenous putrescine on cell growth

a) SSAT$^-$

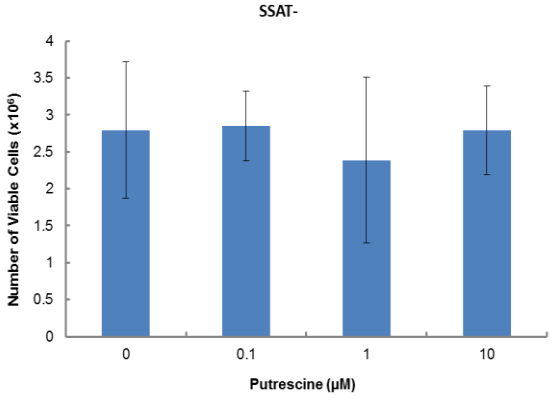

b) WT

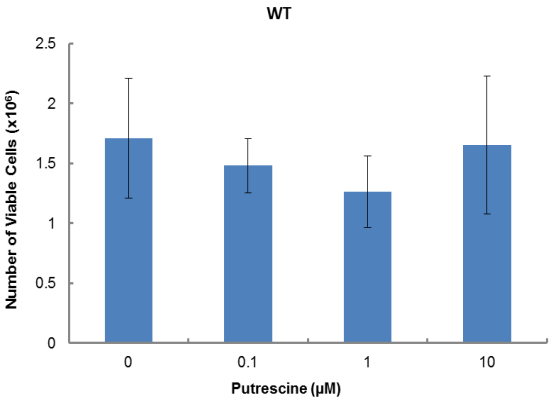

Fig. 3.48 Cells were seeded at a density of 2.4 x 10^4 / cm^2 in 60 mm diam. cell culture dish in duplicate. The cells were incubated for 48 h and the medium was replaced with fresh medium containing N^1-acetylspermidine or putrescine. Viable cell numbers were counted using Trypan blue exclusion assay (Section 2.2.5). Results shown are mean ± rang (n = 1, with 2 duplicates per experiment).

3.4.2 Effect of aspirin and 5-FU on apoptosis in WT, SSAT$^-$, and SSAT$^+$

Since SSAT$^+$ cells proliferated at a low rate, an alternative explanation for this was that these cells may be more prone to undergoing apoptosis. With 24 h treatment of aspirin (2 mM) and 5-FU (50 µM), preliminary results of DAPI fluorescent nuclei staining (chromatin condensation and/or nucleus fragmentation) showed that SSAT$^+$ cells appeared to develop more apoptosis than SSAT$^-$ and WT cells.

Without treatment, 15% SSAT$^+$ cells underwent apoptosis, which was about 2-fold higher than WT (7%) and 3-fold higher than SSAT$^-$ (5%). In response to aspirin, SSAT$^-$ and WT cells seemed to be more sensitive than SSAT$^+$ cells as there was only 2% rise of apoptotic cells in SSAT$^+$, but 5% in WT and 11% in SSAT$^-$. Similar trend was found in response to 5-FU. The apoptotic cells rose 11% in WT, 10% in SSAT$^-$, and 9% in SSAT$^+$ cells (Fig. 3.49a-c & Fig. 3.50). These results were consistent with the results of growth inhibition (Table 3.2). Overall, the results indicate that although cells with increased SSAT tend to develop apoptosis, these cells are less sensitive to the anticancer drugs.

Fig. 3.49 Effect of aspirin and 5-FU on apoptosis

a) WT

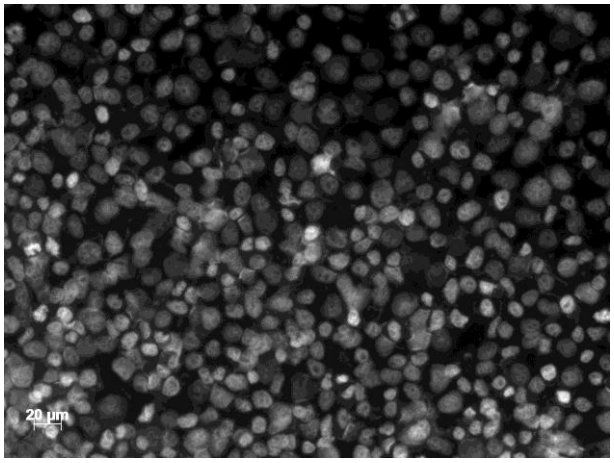

WT Control (X20)

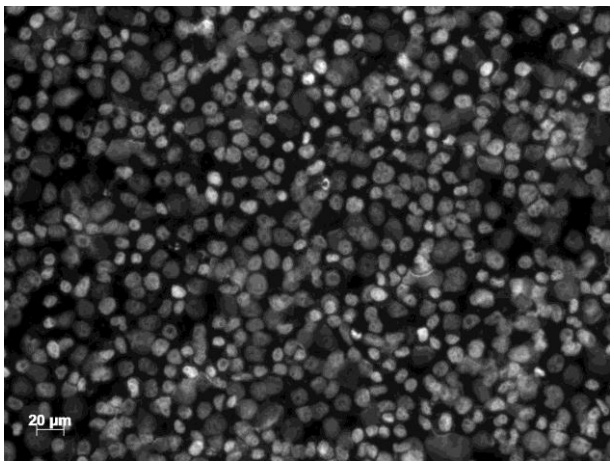

Aspirin (2 mM) (X20)

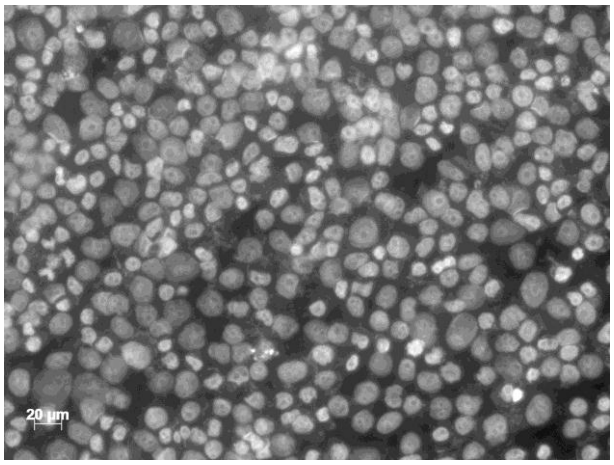

5-FU (50 µM) (X20)

b) SSAT$^-$

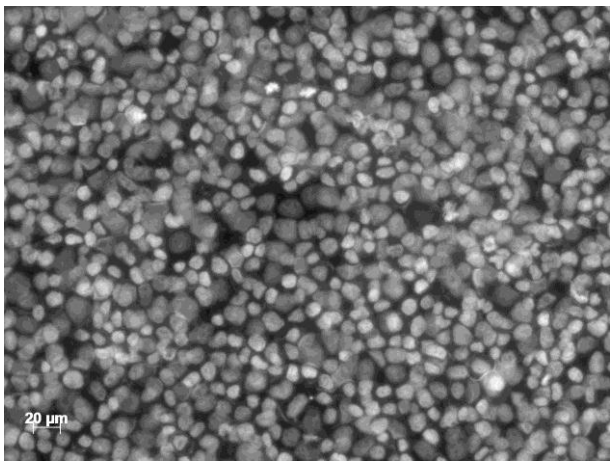

SSAT$^-$ Control (X20)

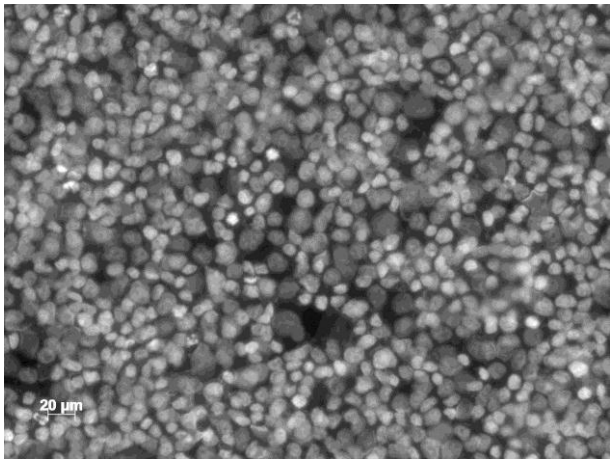

Aspirin (2 mM) (X20)

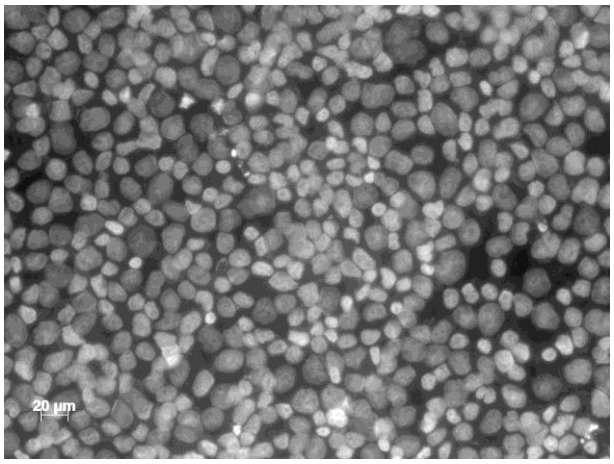

5-FU (50 µM) (X20)

c) SSAT$^+$

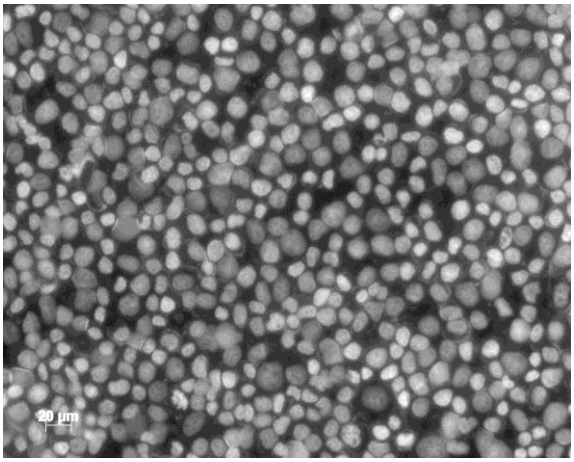

SSAT$^+$ Control (X20)

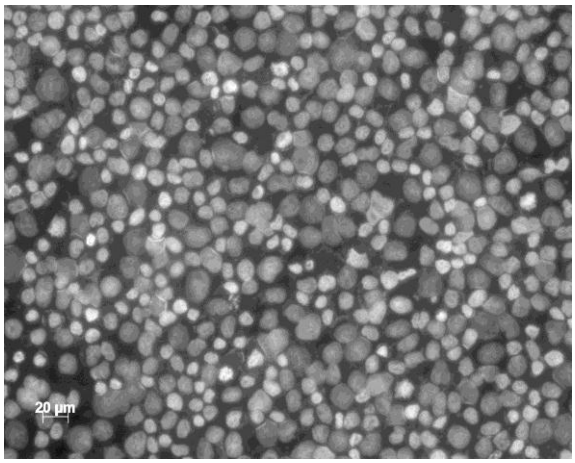

Aspirin (2 mM) (X20)

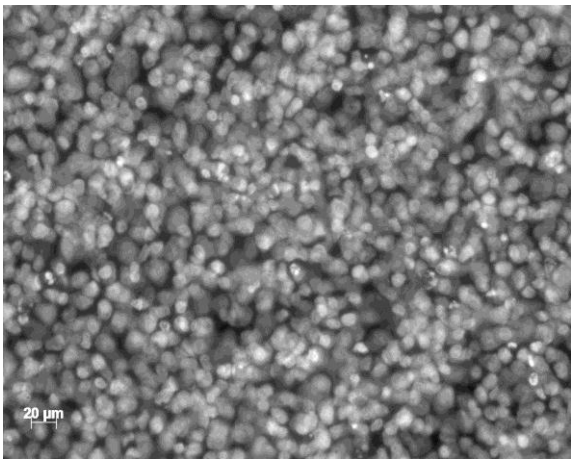

5-FU (50 µM) (X20)

Fig. 3.49 Cells were plated at a density of 2.4 x 10^6/cm^2 in a 90 mm cell culture dish in duplicate. The cells were treated with the drug(s) after 48 h incubation and harvested at 24 h drug exposure. The cells were spun down onto a microcopy slide and stained with the VECTASHIELD Hard Set Mounting Medium with DAPI. The photographs were taken using a Zeiss fluorescent microscopy according to the protocol (Section 2.2.24).

Fig. 3.50 Effect of aspirin and 5-FU on apoptosis in WT, SSAT$^-$, and SSAT$^+$ cells at 24 h

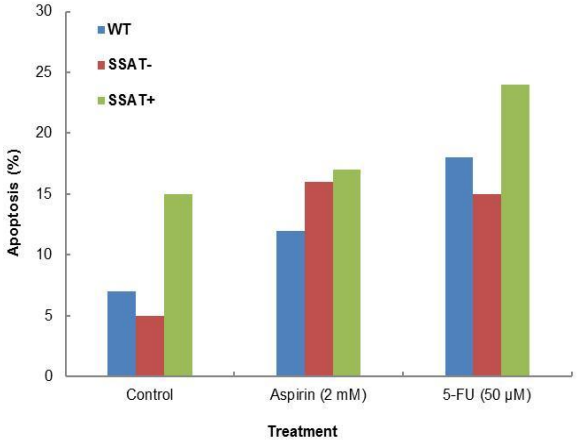

Fig. 3.50 According to the results in Fig. 3.49a-c, the number of nuclei was counted using ImageJ. Results were shown as a percentage of nuclei of apoptosis out of the total number of nuclei. (n=1 with 2 duplicates per experiment).

3.4.3 Effect of aspirin and 5-fu on the production of H_2O_2 in WT, SSAT$^-$, SSAT$^+$ cells

An enhanced SSAT/APAO retroconversion pathway will tend to generate a higher amount of H_2O_2 as the by-product of polyamine oxidation. The oxidative stress caused by the generation of H_2O_2 could lead to DNA damage to the cells with increased SSAT activity. In order to investigate the difference of H_2O_2 production between each cell type, cells were stained with DCFDA to detect H_2O_2 and 10,000 cells were quantified by the flow cytometry.

More H_2O_2 was generated by WT cells and SSAT$^+$ cells generated the least (Fig. 3.51), suggesting that oxidative stress might not play a role in the slower growth in SSAT$^+$ cells.

Fig. 3.51 Generation of H_2O_2 in WT, SSAT$^-$, and SSAT$^+$ cells

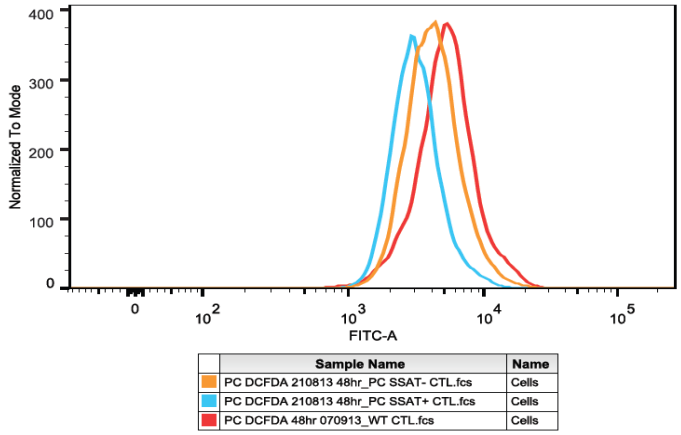

Fig. 3.51 Cells were seeded at a density of 2.4 x 10^4 / cm^2 in a 90 mm cell culture dish in duplicates. The cells were grown for 96 h, harvested and stained with DCFDA for 45 min. The fluorescence of 10,000 cells per assay was detected by flow cytometry (Section 2.2.22). (n=1, with 2 duplicates per experiment).

The results showed that the size and granularity of WT cells were higher than the SSAT transfected cells. The cell size and granularity of WT cells were both increased in the treatment of 5-FU. However, the WT cells seemed to shrink in the presence of aspirin. 5-FU appeared to be more potent than aspirin in the inhibition of H_2O_2 production.

Fig. 3.52a Effect of aspirin and 5-FU on the size and granularity of WT cells

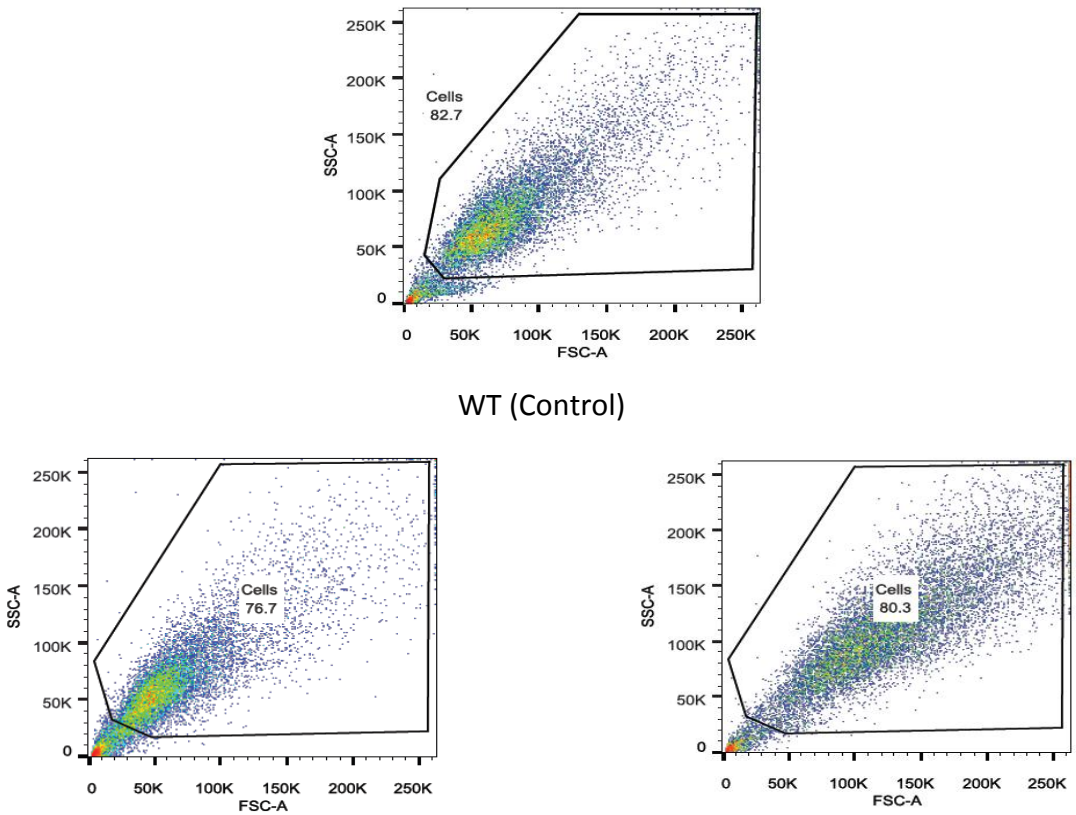

Fig. 3.52b Effect of aspirin and 5-FU on the production of H_2O_2 in WT cells

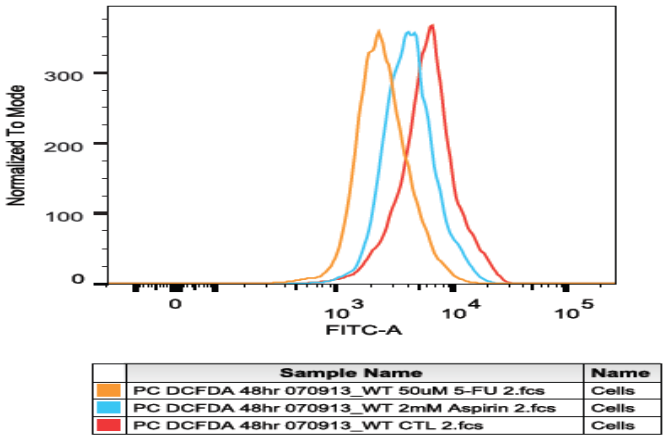

Fig. 3.52 Cells were seeded at a density of 2.4 x 10^4 / cm^2 in a 90 mm cell culture dish in duplicates. The cells were treated with aspirin (2 mM) and 5-FU (50 µM) for 48 h after 48 h growth, and then harvested and stained with DCFDA for 45 min. The fluorescence of 10,000 cells per assay was detected by flow cytometry (Section 2.2.22). (n=1, with 2 duplicates per experiment). X-axis is the FSC (forward scatter) parameter measuring a relative size for the cell. Y-axis is the SSC (side scatter) parameter measuring granularity for the cell.

Similar results were seen in SSAT$^-$ cells in the treatment of aspirin and 5-FU in terms of cell size and granularity (Fig. 3.53a). Aspirin was more effective than 5-FU in the reduction of H_2O_2 generation in SSAT$^-$ cells (Fig. 3.53b).

Fig. 3.53a Effect of aspirin and 5-FU on the size and granularity of SSAT$^-$ cells

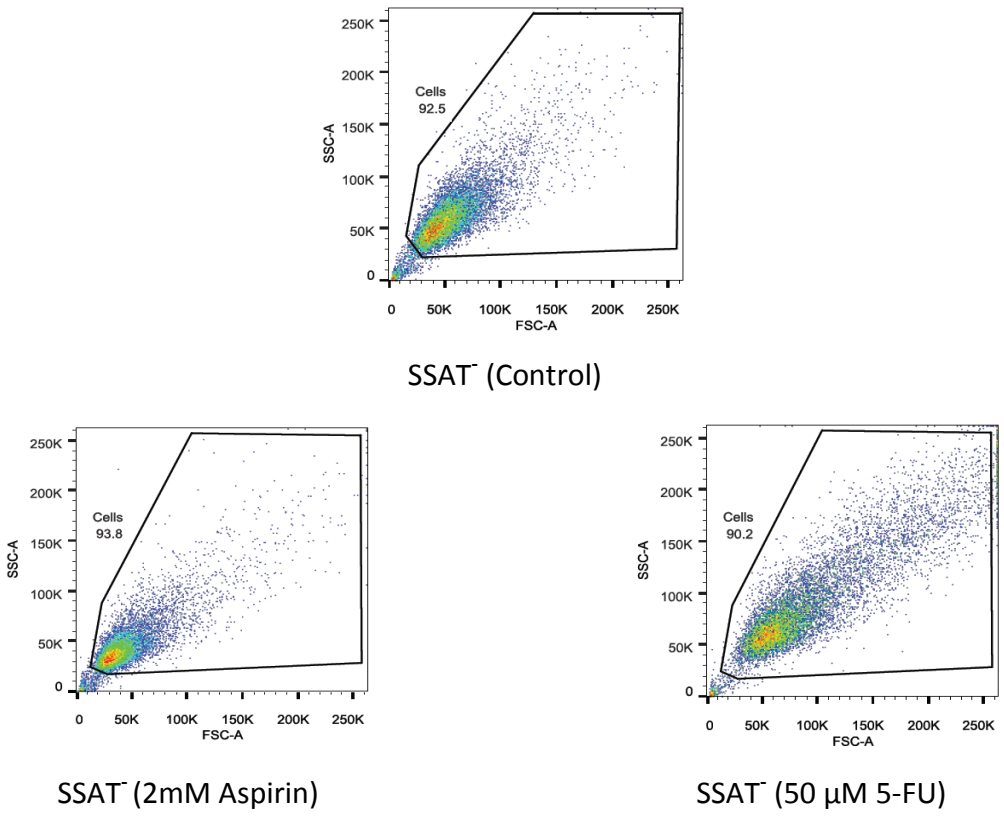

Fig. 3.53b Effect of aspirin and 5-FU on H_2O_2 production in SSAT$^-$ cells

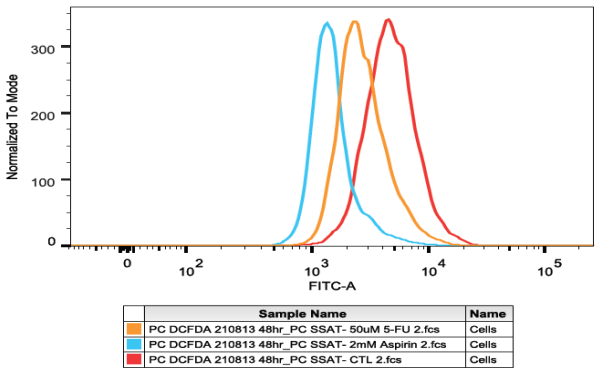

Fig. 3.53 Cells were seeded at a density of 2.4 x 10^4 / cm^2 in a 90 mm cell culture dish in duplicates. The cells were treated with aspirin (2 mM) and 5-FU (50 µM) for 48 h after 48 h growth, and then harvested and stained with DCFDA for 45 min. The fluorescence of 10,000 cells per assay was detected by flow cytometry (Section 2.2.22). (n=1, with 2 duplicates per experiment).

The size and granularity of SSAT$^+$ cells was reduced by aspirin (Fig. 3.54a). Unlike the other cells, 5-FU did not increase the size and granularity of SSAT$^+$ cells. Comparing to 5-FU, aspirin tended to be more efficient in lowing H_2O_2 production (Fig. 3.54b).

Fig. 3.54a Effect of aspirin and 5-FU on the size and granularity of SSAT$^+$ cells

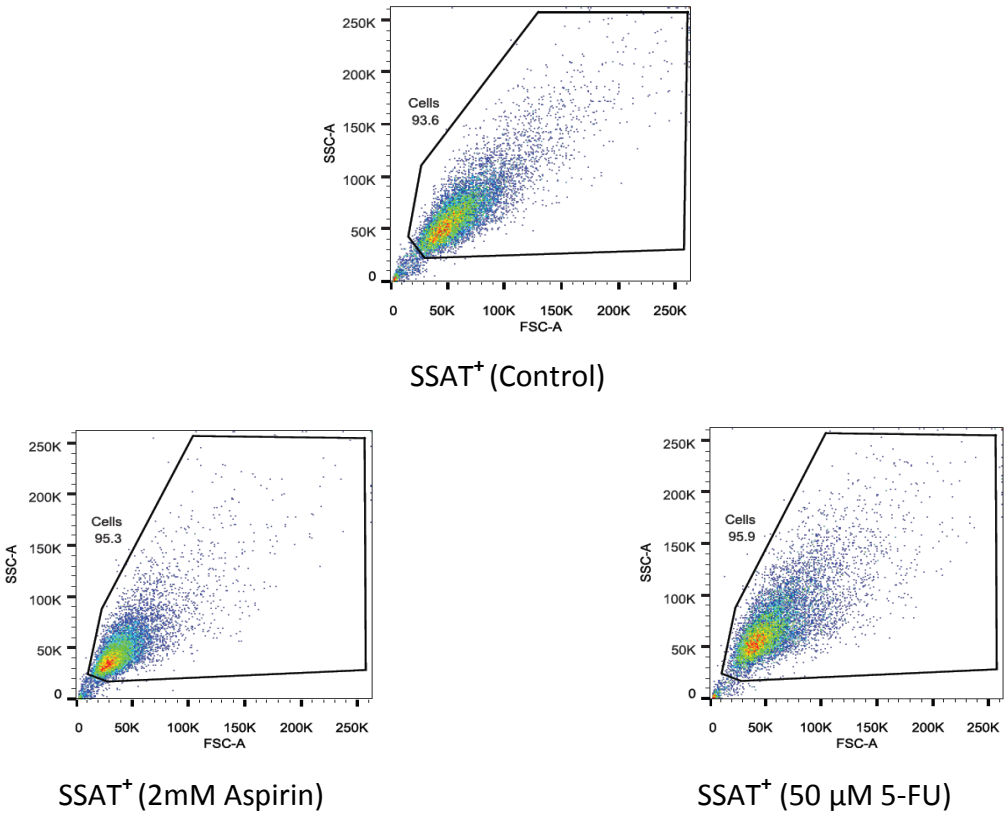

Fig. 3.54b Effect of aspirin and 5-FU on H_2O_2 production in SSAT$^+$ cells

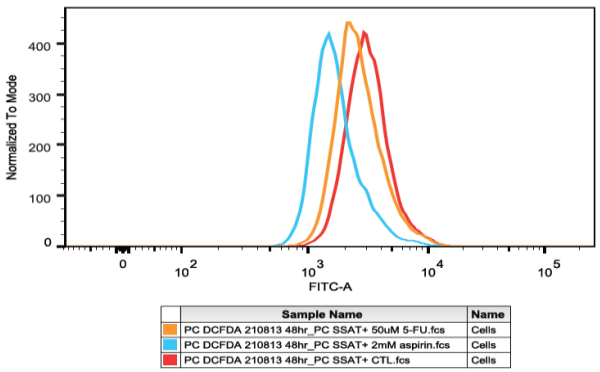

Fig. 3.54 Cells were seeded at a density of 2.4 x 10^4 / cm^2 in a 90 mm cell culture dish in duplicates. The cells were treated with aspirin (2 mM) and 5-FU (50 µM) for 48 h after 48 h growth, and then harvested and stained with DCFDA for 45 min. The fluorescence of 10,000 cells per assay was detected by flow cytometry (Section 2.2.22). (n=1, with 2 duplicates per experiment).

4 Discussion

The aim of the present study was to characterise the role of the key degradative enzyme, SSAT, in the growth of LNCaP prostate carcinoma cells and in the cellular response to anticancer drugs. Our hypothesis was that increased SSAT activity will inhibit cell growth and that this is associated with a compensatory alteration of intracellular polyamine pools. Furthermore, altered SSAT activity may affect sensitivity of the cells in response to anticancer drugs. Many studies have shown that the cytotoxicity of anticancer drugs is associated with SSAT induction and the subsequent changes in intracellular polyamine concentrations and polyamine efflux may contribute to the inhibition of cell growth.

Polyamines are indispensable growth factors in high demand in prostate cancer cells. Either excess or insufficient production of intracellular polyamines can lead to a disturbance of cell growth. Polyamine metabolism is therefore critical to the cancer cell survival or death and polyamine concentration is maintained in a narrow range by the cell. Understanding the role of SSAT is an important key to the study of polyamine metabolism as polyamine degradation relies on SSAT activity. The outcomes would further benefit understanding of the mechanisms of prostate carcinogenesis and of drug resistance in chemotherapy, and finally may provide novel insights for cancer treatment.

In this study, the model system used was a stably transfected cell line under Tetracycline-controlled transcriptional activation (Tet-off advanced inducible gene expression system). The Tet-off system is reversible and controlled at the level of *Sat1* gene expression. Therefore, changes following the "Tet switch" in the polyamine pathway are a result of SSAT alteration. Additionally, WT LNCaP cells were included as a "reference control." Thus, all the experimental results can be compared on the background of low ($SSAT^-$), basal (WT), and high ($SSAT^+$) SSAT activity. The model system was established successfully at the level of *Sat1* mRNA expression, SSAT protein and SSAT activity (Fig. 3.3, 3.4, & 3.6). This model system is simple to control and allows for the analyses of the effects of these changes in the polyamine system.

A correlation between a decreased cell growth and an increased SSAT activity has been established by Libby, *et al.* (1991). In this study, a lower SSAT activity is correlated with a shorter cell generation time (48-96 h), and vice versa (Fig. 4.1). This is consistent with the study by Kee *et al.* (2004b) in which this SSAT transfected LNCaP cell model system was firstly published. The WT cells were not part of their study. Involvement of the WT cells demonstrates clearly the difference in cell growth between these cells. Similar correlations are found in MCF-7 human breast cancer (Vujcic *et al.*, 2000), CHO Chinese ovarian cancer (McCloskey *et al.*, 1999), and NCI-H82 small-cell lung carcinoma (Murray-Stewart *et al.*, 2003) SSAT transfected cell lines. In addition, a large number of studies using polyamine analogues, BENSpm (or DENSpm) in particular, also show a growth inhibition associated with a superinduction of SSAT in some cell lines (Libby *et al.*, 1991; Vujcic *et al.*, 2000; Murray-Stewart *et al.*, 2003; Pegg, 2008). However, in our study the polyamine analogue CPENSpm does not affect cell growth but is a superinducer of SSAT. Accordingly, it is likely that an increase of SSAT activity appears to be a common feature involved in growth inhibition in a variety of tumour cell lines. Since SSAT is responsible for polyamine degradation, the growth inhibition is connected somehow to an alteration of intracellular polyamine pools.

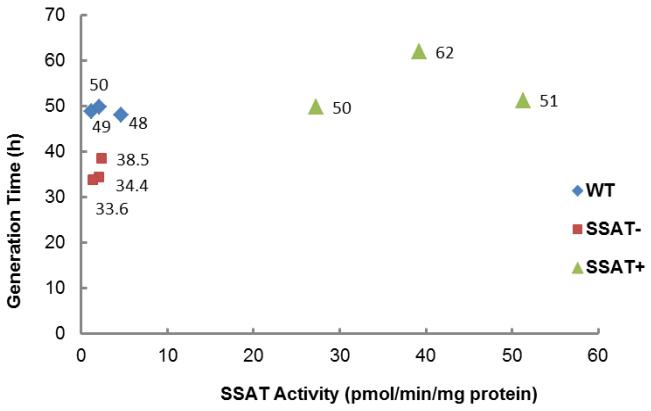

Fig. 4.1 The correlation between SSAT activity and generation time of the cells.

Alteration of SSAT activity exerts a dramatic impact on the individual polyamine concentrations. Polyamine metabolism is a pathway that is tightly regulated by biosynthesis, degradation, uptake and export. When one parameter is altered in the pathway this gives rise to compensatory changes in other parameters. All of the changes

observed in the polyamine system in this study, such as increased ODC, APAO and SMO, are aiming to maintain the intracellular polyamine concentrations in the appropriate range for cell survival and growth. As a result, the total polyamine content in $SSAT^+$ cells does not decrease, which is consistent with the study of Kee *et al.* (2004b). Instead, both total intracellular and extracellular polyamine pools in $SSAT^+$ cells tend to increase (Fig. 3.13 & Fig. 3.40a-f). This is mainly attributable to the accumulation of N^1-acetylspermidine inside and outside of the cells (Fig. 3.35e & f). Acetylation of spermidine by SSAT to form N^1-acetylspermidine and its subsequent efflux are the main mechanisms lowering intracellular polyamines pools. Additionally, N^1,N^{12}-diacetylspermine (Fig. 3.33d) acetylated from N^1-acetylspermine, and putrescine (Fig. 3.37f) synthesised from ODC and the retroconversion pathway, are the second most abundant polyamines exported as a result of increased SSAT activity. Thus, polyamine acetylation is the first essential step to reduce polyamine content instead of direct export of spermidine and spermine out of the cell, despite that a small amount of spermidine can be exported without acetylation.

A depletion of spermidine and spermine leads to an arrest of cell growth or cell death. Spermidine and spermine are degraded although total polyamine content is maintained or even tends to increase, while SSAT is induced. SSAT overexpression leads to a fall of spermidine and spermine that can result in DNA damage and subsequent decreased cell proliferation (Zahedi *et al.*, 2007). The loss of spermine (significant) and spermidine (not significant) in $SSAT^+$ and the accumulation of spermidine and spermine in $SSAT^-$ cells are likely to cause the discrepancy in cell growth in the current study, for spermidine and spermine are critical in the modulation of functions of RNA, DNA and of protein synthesis (Igarashi & Kashiwagi, 2000). For example, spermidine is required in hypusine modification that is essential for eIF5A activity, which is critical for eukaryotic cell growth and survival (Lee *et al.*, 2011). Sufficient amounts of intracellular spermidine and spermine are essential for cell survival or growth. The accumulation of spermidine and spermine due to insufficient degradation by low SSAT activity can stimulate cell proliferation. This may explain why $SSAT^-$ cells have the highest proliferation rate. Spermine is absent from the culture medium of all the cell types also indicates its essential nature as a growth factor required by the cells. Given that spermine is the major polyamine in the prostate gland and LNCaP cells (Schipper *et al.*, 2003; McCloskey *et al.*, 2000), the loss of spermine could attenuate cell growth. A dynamic equilibrium state of

polyamine metabolism is supposed to be reached under physiological conditions. When the equilibrium is disturbed such as by SSAT alteration, the priority for the cells is to survive rather than proliferate. Thus, proliferation rate would decrease. SSAT induced decrease of intracellular spermine can be growth inhibitory to the prostate cancer cells.

In terms of spermidine and spermine content, there was almost no difference between $SSAT^+$ and WT (Fig. 3.14d & e), but WT cells grew faster than $SSAT^+$ cells. This suggests that the accumulation of N^1-acetylspermidine, N^1-acetylspermine, and/or putrescine is likely to be growth inhibitory. Co-treatments of DFMO and MDL72527 partially restored $SSAT^+$ cell growth (Fig. 3.43c). This is associated with the decreased putrescine but increased spermine, suggesting that putrescine accumulation is growth inhibitory and spermine restoration is growth stimulating. In addition, growth inhibition of lymphocytes by MGBG is thought to be caused by the decrease of spermidine and spermine but not by the accumulation of putrescine, because the growth inhibition can be reversed by exogenously added spermidine and spermine (Fillingame *et al.*, 1975). With regard to N^1-acetylspermidine in the co-treatments in $SSAT^+$ cells, the lack of N^1-acetylspermidine accumulation but accumulation of N^1-acetylspermine are due to the decreased spermidine and increased spermine. On the other hand, the accumulation of the N^1-acetylpolyamines is not growth inhibitory as the growth of $SSAT^-$ and WT cells were not inhibited by the accumulation of the N^1-acetylpolyamines in the presence of MDL 72527.

In vivo studies of SSAT transgenic mice presented a typical hairless phenotype that is thought to be due to the toxic accumulation of putrescine in hair follicles, which is phenotypically similar to ODC overexpressing transgenic mice (Pietilä *et al.*, 1997). However, the exogenous addition of N^1-acetylspermidine or putrescine (≤ 10 μM) to the cell culture medium did not seem to inhibit the growth of both $SSAT^-$ and WT cells. This lack of growth inhibition might be also due to a failure of uptake of these polyamines into the $SSAT^-$ and WT cells. Similarly, an addition of putrescine (5 mM) to the culture medium of the tolerant CHO cells did not result in a toxic intracellular because of the upregulated export and decreased uptake of putrescine (Pastorian & Byus, 1997). On the contrary, ODC overexpressing CHO cells have been found to undergo cell death by apoptosis due to an over-accumulation of intracellular putrescine (Takao *et al.*, 2006), indicating the toxicity of putrescine accumulation.

N^1,N^{12}-diacetylspermine is known as a tumour marker found in the urine of a range of cancer patients. Although its concentration is very low, it is more reliable and specific than monoacetylpolyamines such as N^1-acetylspermidine and N^8-acetylspermidine (Kawakita & Hiramatsu, 2006). However, the SSAT activity is not measured in their study. Wallace *et al.* (2000) reported that an increase in SSAT activity in the tumour tissue of breast cancer comparing with normal tissue. This implies an increase of acetylpolyamines by SSAT in tumour tissue. What is consistent with our findings is that N^1,N^{12}-diacetylspermine is present only in the culture medium. It is supposed to be exported out of the cell as a result of increased SSAT activity since it is only found intracellularly in $SSAT^+$ cells, at least *in vitro*. It is believed that N^1,N^{12}-diacetylspermine can serve as a prognostic indicator and marker for recurrence of prostate and colon cancers, because it rises rapidly concomitant with the recurrence (Kawakita *et al.*, 2004). If this is the case, an increase of SSAT would be a sign of increased carcinogenesis or relapse, which is consistent with the findings in the SSAT transgenic $Apc^{min/+}$ mice (Tucker *et al.*, 2005). However, N^1,N^{12}-diacetylspermine content was not determined in that study.

Polyamine acetylation by SSAT is closely connected to polyamine export. Polyamine export is known as a selective and regulated process dependent on the growth status of the cell (Wallace *et al.*, 2003). Efflux is the major mechanism to decrease excess intracellular polyamines and prevent their accumulation. With the increase of SSAT, polyamine efflux is greatly increased. N^1-acetylspermidine and putrescine consist of the major part of the increased polyamines in the culture medium of $SSAT^+$ cells, which is consistent with the findings by Wallace & Mackarel (1998). It confirms that N^1-acetylspermidine and putrescine are the predominant forms of polyamines for export and polyamines are required to be metabolised (i.e. acetylated) before efflux (Wallace *et al.*, 2003). This might suggest that polyamine transport is a selective process determined by the requirements of the cell.

The compensatory increase in ODC is also found in SSAT transgenic livers (Pietilä *et al.*, 1997), transgenic fibroblasts (Alhonen *et al.*, 1998) and SSAT-transfected CHO cells (McCloskey *et al.*, 1999). On the other hand, these findings are not consistent with the findings using human melanoma MALME-3 (Porter *et al.*, 1991) and MCF-7 cells (Vujcic *et al.*, 2000), in which the growth inhibition is associated with a depletion of intracellular

polyamine pools as a result of increased polyamine catabolism by SSAT and the absence of increased ODC activity. The mechanism of this discrepancy is not fully understood. It might be cell-type dependent response, and further experimentation is thus required.

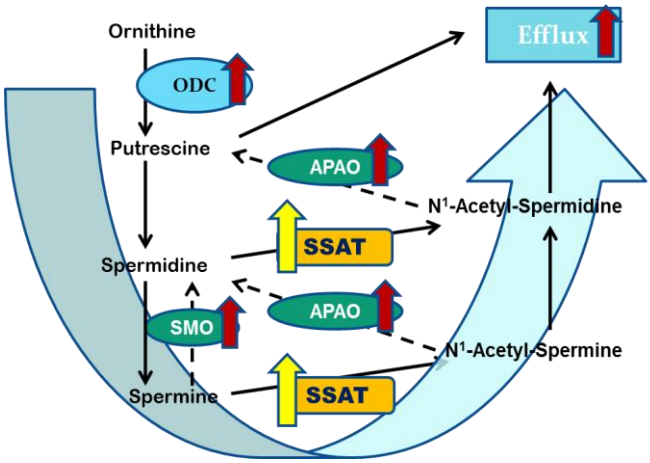

Fig. 4.2 Illustration of SSAT induced enhancement of polyamine metabolic flux (adapted from Kramer *et al.*, 2008).

One of the most intriguing features as a result of increased SSAT is probably the enhanced polyamine metabolic flux (Fig. 4.2). The heightened flux was firstly tested by Kramer *et al.* (2008) using 4-fluoro-L-ornithine in the SSAT transfected cells. The polyamine acetylation by SSAT induction leads to a reduction of spermidine and spermine. In order to compensate the loss of the higher polyamines, the precursor putrescine synthesis by ODC is therefore increased. Putrescine comes not only from ornithine by ODC but also from the oxidation of N^1-acetylspermidine. On the other side, accumulation of N^1-acetylpolyamines gives rise to an increase in APAO for their oxidation (Chopra & Wallace, 1998). Efflux is also enhanced due to the over-accumulation of N^1-acetylpolyamines and putrescine. Thus, the polyamine flux consisting of biosynthetic, degrading and efflux pathways is dramatically increased by increased SSAT. The consequences of increased polyamine flux are consumption of substrates and co-factors of the enzymatic reactions and accumulation of products and toxic by-products, which may influence the cell growth.

H_2O_2, one of the by-products of polyamine oxidation and a ROS, is generated by APAO and SMO. ROS can cause oxidative stress and subsequent DNA damage and cell death (Wang & Casero, 2006; Basu *et al.*, 2009; Babbar *et al.*, 2007). It is likely that the growth

inhibition of $SSAT^+$ cells could be due to the oxidative stress by H_2O_2 production from increased APAO and SMO activity. Inhibition of APAO and SMO by MDL72527 not only causes the accumulation of N^1-acetylpolyamines but also prevents the generation of H_2O_2 by polyamine oxidation. Niiranen *et al.* (2002) suggested the growth inhibition was rather a result of toxic by-products of the SSAT/APAO pathway. However, this does not appear to be the case in this study, since higher content of H_2O_2 tends to present in WT cells. In addition, a lack of signs of oxidative stress is also confirmed by an unchanged content of reduced GSH, which acts as one of the main antioxidant systems. Thereby, SSAT induced growth inhibition might not be associated with an oxidative stress by H_2O_2 from the APAO and SMO pathways.

On the other hand, ROS induced inflammation has been implicated in the prostate carcinogenesis. In addition, ROS production is associated not only with enhanced SSAT/APAO polyamine catabolic pathway but also with androgen receptor signalling (Thapa & Ghosh, 2012; Khandrika *et al.*, 2009; Babbar *et al.*, 2007). LNCaP is an androgen dependent prostate carcinoma cell line. The higher level of H_2O_2 in WT LNCaP cells detected by the flow cytometry might be associated with its androgen stimulated ROS production, which needs further investigation. In addition, it is likely that the androgen dependent ROS induced inflammation in the WT cells is inhibited by aspirin.

Acetyl-CoA, the co-factor required for polyamine acetylation by SSAT, is believed to be decreased with SSAT induction (Pegg, 2008). Kee *et al.* (2004b) firstly demonstrated the link between polyamine metabolism and depletion of acetyl-CoA stores in these cells. Prostate cancer cells present increased production of *de novo* fatty acids (Medes *et al.*, 1953; Suburu & Chen, 2012). A fall of acetyl-CoA and related malonyl-CoA can lead to a low fatty acid synthesis and a stimulation of fatty acid oxidation, which can eventually result in the growth arrest of LNCaP cells (Beckers *et al.*, 2007). The depletion of acetyl-CoA is also confirmed by a lean phenotype of SSAT transgenic mice (Kee *et al.*, 2004a; Jell *et al.*, 2007). Thus, acetyl-CoA depletion dependent interruption of fatty acid synthesis could be one of the explanations why SSAT induction results in the cell growth inhibition.

SSAT is one of the most inducible genes responsive not only to polyamine analogues but a range of anticancer drugs such as aspirin and 5-FU. Aspirin and 5-FU did not show a

dramatic ability of inducing SSAT activity in our model system. However, SSAT inducibility of the cells is considerably high due to their responses to the polyamine analogue CPENSpm. It has been suggested that SSAT induction is a universal response of cancer cells to anticancer agents and cytotoxicity of the drugs is associated with a disturbance of polyamine homeostasis via SSAT alteration.

Aspirin is not only known as a NSAID but also a chemopreventative agent. COX-2 dependent inflammation is associated with prostate carcinogenesis and aspirin can prevent the inflammation by inhibiting COX-2, reducing the incidence of prostate cancer (Lin & Nelson, 2003; Hussain *et al.*, 2003; Bardia *et al.*, 2009). Moreover, an induction of SSAT is associated with chemoprevention of aspirin in Caco-2 and HT-29 colon cancer cells (Babbar *et al.*, 2006). Thus, a connection between SSAT induction and chemoprevention of aspirin has been established. Aspirin was therefore chosen for this study.

A moderate level of oxidative stress caused by ROS can stimulate cell proliferation and induce carcinogenesis (Acharya *et al.*, 2010). Both aspirin and 5-FU have the ability to reduce the H_2O_2 production in all the cells. COX-2 levels were shown not only to be increased in prostate cancer cell lines but also COX-2 catalysed reactions involve the formation of ROS that gives rise to DNA oxidation and activation of carcinogenesis (Lin & Nelson, 2003). In this study, the inhibition of cell growth by aspirin is therefore associated with COX-2 inhibition, which is consistent with a decreased level of H_2O_2 production detected by flow cytometry.

Sensitivity of the cell to aspirin may be associated with an alteration of pre-induced SSAT. SSAT activity does not seem to be critical for the cytotoxicity of aspirin in regard to MTT assay as little difference in IC_{50} values was observed. MTT assay was conducted at one-time point; therefore, it is unable to demonstrate the tendency of a time course. In the growth experiments, however, with a decrease of SSAT activity by aspirin there was an increase of growth inhibition. Since SSAT activity started to decrease at 48 h treatment of aspirin, the growth inhibition increased simultaneously. Thereby, a decrease of a pre-induced SSAT activity can increase the cell's sensitivity to aspirin. To our knowledge this is

the first time demonstrating SSAT induction is linked to the sensitivity of LNCaP cells to the treatment of aspirin.

In this study, aspirin at a higher concentration (2 mM) appear to induce SSAT activity while it is low and inducible, whereas aspirin can also suppress SSAT activity when it is high and pre-induced. This induction seems to occur at an early stage of the treatment. With regard to the concentration of aspirin in SSAT induction, Babbar *et al.* (2006) has found that aspirin at 20 μM is more potent than at 100 μM in increasing SSAT enzyme activity in Caco-2 cells. 1 mM aspirin was not able to increase SSAT protein further when compared to 100 μM. However, our preliminary results of western blot showed a slight increase (1 fold) of SSAT protein by 2 mM aspirin. It is likely that higher concentration of aspirin might be less potent in SSAT induction but more potent in the inhibition of SSAT activity.

5-FU has been shown as an inducer of SSAT gene expression in RKO and HT-29 cells. 5-FU induced apoptosis is associated with a dramatic decrease of polyamines (Zhang *et al.*, 2003). In our study, cells with a high SSAT activity are more sensitive to 5-FU by MTT assay. This seems to contradict the observation in the growth experiment that the cells with a low SSAT activity were more sensitive to the treatment of 5-FU. At 48 h treatment with 5-FU, however, SSAT activity was decreased in $SSAT^+$ cells while this was consistent with the time when MTT was done i.e. an increased sensitivity to 5-FU was observed. Thus, a decrease in pre-induced SSAT activity may be a prerequisite to increase the sensitivity of the cells to 5-FU. In other words, cells with sustained high SSAT activity are more resistant to anticancer drugs, but the process of SSAT activity reduction from high to relatively low provides the cells with sensitivity to the drugs. Furthermore, this increase in sensitivity is associated with a decrease of intracellular polyamine pools. Thereby, a correlation between a depletion of total intracellular polyamine pools by an anticancer drug and an increase in the sensitivity of the cells that have pre-induced SSAT activity to the drug has been established.

The growth inhibition of all the cells by aspirin is likely to be related to a loss of total intracellular polyamine pools, and aspirin shows a dose-dependent manner. Likewise, a loss of total intracellular polyamine pools by 5-FU is associated with its cytotoxic effect on

the cell growth inhibition. These findings further consolidate the concept that a depletion of intracellular polyamines by anticancer drugs is a major mechanism in association with their cytotoxic effect.

The WT and SSAT transfected LNCaP cell lines in this study demonstrated insensitivity to the treatment of etoposide. LNCaP is an androgen dependent prostate carcinoma cell line. Androgen plays an important role in the multiple drug resistance in prostate cancers. It has been found that androgen is closely associated with the regulation of resistance to etoposide in LNCaP cells (Coffey *et al.*, 2002; Salido *et al.*, 2004; Serafin *et al.*, 2002). More resistance shown in the SSAT transfected cells to etoposide than WT cells might be due to the discrepancy of cell origin.

Synthesis of ODC is subject to the feedback regulation by polyamines (Holm *et al.*, 1989). Inhibition of ODC activity by aspirin and 5-FU took place only at an early stage (< 24 h) in this study. This might be due to an increased uptake of putrescine from the extracellular environment to compensate the consequence of inhibited ODC activity by 5-FU. A study by Babbar *et al.* (2006) shows aspirin at 20 µM has no effect on ODC expression and a slight increase in ODC mRNA expression at 100 µM. The ODC activity was unfortunately not measured in that study. In comparison, a higher aspirin concentration in mM might be more efficient in inhibiting ODC activity than in µM ranges. However, if the biosynthesis pathway is blocked, the cell would increase polyamine uptake to maintaining intracellular polyamine pools.

An increase of polyamine efflux in the treatment of aspirin and 5-FU measured by using [^{3}H]-labelled polyamines was observed in WT cells (Fig. 3.32a). This is not consistent with the total extracellular polyamine content that did not increase in response to the treatments (Fig. 3.40b). The reason could be due to the proportions of radiolabelled polyamines only reflected a low fraction of the total polyamine pools in LNCaP cells. HCT115 cells can accumulate 75% of the [^{3}H]-putrescine added (Wallace & Mackarel, 1998), however, the percentage of cellular [^{3}H]-labelled polyamine distribution out of the total polyamines in LNCaP cells has not been measured.

The accumulation of N^1-aceytlpolyamines in WT and $SSAT^-$ cells was consistent with the inhibition of APAO and SMO activity by MDL 72527 (enzyme activity was not obtained,

thereby results are not shown). However, there was a lack of the N^1-acetylspermidine accumulation in $SSAT^+$ cells in the treatment of MDL72527 and combination of DFMO and MDL72527. This is because spermidine was inhibited by the treatments and therefore it was not enough to be acetylated by SSAT to form N^1-acetylspermidine although APAO was inhibited simultaneously.

Two cell lines but three types of cells (WT, $SSAT^-$ and $SSAT^+$) were used as the model systems in this study. Experimental approaches were fulfilled mostly on a time course basis with varied cell growth rate.

In the future, a range of novel investigations should be carried out. The consumption of acetyl-CoA and the effect of decreased acetyl-CoA on fatty acid synthesis could be explored with regard to the effect on cell growth inhibition. The association of SSAT induction with apoptosis needs further experimentation on measurement of caspase activities, cytochrome c, and membrane potential. It would also be worth measuring the polyamine flux by using a fluorescent or radio-labelled substrate to determine the speed of flux accelerated by SSAT overexpression. In terms of glucose metabolism in cancer cells, an increase in SSAT has been reported to be able to increase insulin sensitivity. This may be related to energy metabolism in cancer, which is an interesting novel field.

In summary, the model system provides a simple but useful tool for studying the effect of SSAT on polyamine metabolism in cancer cells. SSAT plays an important role in the maintenance of intracellular polyamine concentrations that is critical for cell survival and growth. SSAT overexpression disturbs the equilibrium of intracellular polyamine concentrations and thus exerts an inhibitory impact on the cell growth. The attenuated cell proliferation by increased SSAT is associated with a loss of spermine, an accumulation of intracellular putrescine, an increase in polyamine efflux, and an increase in apoptosis. The cytotoxic effects of aspirin and 5-FU were related to a depletion of total intracellular polyamine pools and an inhibition of ROS by H_2O_2 production. An increase of cell sensitivity to antiproliferative drugs was associated with a decrease of pre-induced SSAT activity. Thus, SSAT is a key regulator in the maintenance of polyamine homeostasis. This study provides novel insights into the mechanisms of SSAT regulated polyamine metabolism in prostate cancer cells, and further understands the role of polyamine in

prostate carcinogenesis. The association of SSAT induction with the alteration in sensitivity of anticancer drugs sheds a new light onto the discovery of novel chemotherapeutic or chemopreventative drugs with SSAT as a target.

5 References

Acharya, A., Das, I., Chandhok, D. & Saha, T. 2010. Redox regulation in cancer: A double-edged sword with therapeutic potential. *Oxidative Medicine and Cellular Longevity.* **3,** 23-34.

Alhonen, L., Halmekytö, M., Kosma, V., Wahlfors, J., Kauppinen, R. & Jänne, J. 1995. Life-long over-expression of ornithine decarboxylase (ODC) gene in transgenic mice does not lead to generally enhanced tumorigenesis or neuronal degeneration. *International Journal of Cancer.* **63,** 402-404.

Alhonen, L., Karppinen, A., Uusi-Oukari, M., Vujcic, S., Korhonen, V., Halmekytö, M., Kramer, D.L., Hines, R., Jänne, J. & Porter, C.W. 1998. Correlation of polyamine and growth responses to N 1, N 11-diethylnorspermine in primary fetal fibroblasts derived from transgenic mice overexpressing Spermidine/SpermineN 1-acetyltransferase. *Journal of Biological Chemistry.* **273,** 1964-1969.

Alhonen, L., Rasanen, T., Sinervirta, R., Korhonen, V., Pietila, M. & Janne, J. 2002. Polyamines are required for the initiation of rat liver regeneration. *Biochem.J.* **362,** 149-153.

Ali, M.A., Poortvliet, E., Strömberg, R. & Yngve, A. 2011. Polyamines in foods: Development of a food database. *Food & Nutrition Research.* **55,** 5572.

Allen, W.L., McLean, E.G., Boyer, J., McCulla, A., Wilson, P.M., Coyle, V., Longley, D.B., Casero, R.A. & Johnston, P.G. 2007. The role of spermidine/spermine N1-acetyltransferase in determining response to chemotherapeutic agents in colorectal cancer cells. *Molecular Cancer Therapeutics.* **6,** 128.

Ames, B.N. & Wakimoto, P. 2002. Are vitamin and mineral deficiencies a major cancer risk? *Nature Reviews Cancer.* **2,** 694-704.

Andreoiu, M. & Cheng, L. 2010. Multifocal prostate cancer: Biologic, prognostic, and therapeutic implications. *Human Pathology.* **41,** 781-793.

Armstrong, J., Steinauer, K., Hornung, B., Irish, J., Lecane, P., Birrell, G., Peehl, D. & Knox, S. 2002. Role of glutathione depletion and reactive oxygen species generation in apoptotic signaling in a human B lymphoma cell line. *Cell Death and Differentiation.* **9,** 252-263.

Auvinen, M., Laine, A., Paasinen-Sohns, A., Kangas, A., Kangas, L., Saksela, O., Anderson, L.C. & Hölttä, E. 1997. Human ornithine decarboxylase-overproducing NIH3T3 cells induce rapidly growing, highly vascularized tumors in nude mice. *Cancer Res*. **57**, 3016-3025.

Babbar, N., Gerner, E.W. & Casero Jr, R.A. 2006. Induction of spermidine/spermine N1-acetyltransferase (SSAT) by aspirin in caco-2 colon cancer cells. *Biochemical Journal.* **394,** 317.

Babbar, N. & Gerner, E.W. 2011. Targeting polyamines and inflammation for cancer prevention. *Clinical Cancer Prevention.* 49-64.

Babbar, N., Hacker, A., Huang, Y. & Casero, R.A. 2006. Tumor necrosis factor α induces Spermidine/Spermine N1-acetyltransferase through nuclear factor κBin non-small cell lung cancer cells. *Journal of Biological Chemistry.* **281,** 24182-24192.

Babbar, N., Ignatenko, N.A., Casero, R.A. & Gerner, E.W. 2003. Cyclooxygenase-independent induction of apoptosis by sulindac sulfone is mediated by polyamines in colon cancer. *Journal of Biological Chemistry.* **278,** 47762-47775.

Babbar, N., Murray-Stewart, T. & Casero, R.A.,Jr. 2007. Inflammation and polyamine catabolism: The good, the bad and the ugly. *Biochemical Society Transactions.* **35,** 300-304.

Bardia, A., Platz, E.A., Yegnasubramanian, S., De Marzo, A.M. & Nelson, W.G. 2009. Anti-inflammatory drugs, antioxidants, and prostate cancer prevention. *Current Opinion in Pharmacology.* **9,** 419-426.

Bardia, A., Platz, E.A., Yegnasubramanian, S., De Marzo, A.M. & Nelson, W.G. 2009. Anti-inflammatory drugs, antioxidants, and prostate cancer prevention. *Current Opinion in Pharmacology.* **9,** 419.

Basu, H.S., Thompson, T.A., Church, D.R., Clower, C.C., Mehraein-Ghomi, F., Amlong, C.A., Martin, C.T., Woster, P.M., Lindstrom, M.J. & Wilding, G. 2009. A small molecule polyamine oxidase inhibitor blocks androgen-induced oxidative stress and delays prostate cancer progression in the transgenic adenocarcinoma of the mouse prostate model. *Cancer Research.* **69,** 7689-7695.

Battaglia, V., Shields, C.D., Murray-Stewart, T. & Casero Jr, R.A. 2013. Polyamine catabolism in carcinogenesis: Potential targets for chemotherapy and chemoprevention. *Amino Acids.* 1-9.

Bauer, D.E., Hatzivassiliou, G., Zhao, F., Andreadis, C. & Thompson, C.B. 2005. ATP citrate lyase is an important component of cell growth and transformation. *Oncogene.* **24,** 6314-6322.

Beckers, A., Organe, S., Timmermans, L., Scheys, K., Peeters, A., Brusselmans, K., Verhoeven, G. & Swinnen, J.V. 2007. Chemical inhibition of acetyl-CoA carboxylase induces growth arrest and cytotoxicity selectively in cancer cells. *Cancer Research.* **67,** 8180-8187.

Bellelli, A., Cavallo, S., Nicolini, L., Cervelli, M., Bianchi, M., Mariottini, P., Zelli, M. & Federico, R. 2004. Mouse spermine oxidase: A model of the catalytic cycle and its

inhibition by N,N^1-bis(2,3-butadienyl)-1,4-butanediamine. *Biochemical and Biophysical Research Communications.* **322,** 1-8.

Belting, M., Mani, K., Jönsson, M., Cheng, F., Sandgren, S., Jonsson, S., Ding, K., Delcros, J. & Fransson, L. 2003. Glypican-1 is a vehicle for polyamine uptake in mammalian cells. *Journal of Biological Chemistry.* **278,** 47181-47189.

Benedettini, E., Nguyen, P. & Loda, M. 2008. The pathogenesis of prostate cancer: From molecular to metabolic alterations. *Diagnostic Histopathology.* **14,** 195-201.

Borowsky, A.D., Dingley, K.H., Ubick, E., Turteltaub, K.W., Cardiff, R.D. & DeVere-White, R. 2006. Inflammation and atrophy precede prostatic neoplasia in a PhIP-induced rat model. *Neoplasia.* **8,** 708-715.

Bray, F., Jemal, A., Grey, N., Ferlay, J. & Forman, D. 2012. Global cancer transitions according to the human development index (2008–2030): A population-based study. *The Lancet Oncology.* **13,** 790-801.

Cai, Y., Wang, J., Li, R., Ayala, G., Ittmann, M. & Liu, M. 2009. GGAP2/PIKE-a directly activates both the akt and nuclear factor-κB pathways and promotes prostate cancer progression. *Cancer Research.* **69,** 819-827.

Cairns, R.A., Harris, I.S. & Mak, T.W. 2011. Regulation of cancer cell metabolism. *Nature Reviews Cancer.* **11,** 85-95.

Cancer fact sheet N°297. 2013. World Health Organization. Available from: http://www.who.int/mediacentre/factsheets/fs297/en [Accessed 7 Nov 2013].

Casero Jr, R.A. & Pegg, A.E. 1993. Spermidine/spermine N^1-acetyltransferase--the turning point in polyamine metabolism. *The FASEB Journal.* **7,** 653.

Casero, R.A. & Marton, L.J. 2007. Targeting polyamine metabolism and function in cancer and other hyperproliferative diseases. *Nature Reviews Drug Discovery.* **6,** 373-390.

Casero, R.A. & Pegg, A.E. 2009. Polyamine catabolism and disease. *The Biochemical Journal.* **421,** 323-338.

Cavalli, F. 2013. An appeal to world leaders: Stop cancer now. *The Lancet.* **381,** 425-426.

Cervelli, M., Amendola, R., Polticelli, F. & Mariottini, P. 2012. Spermine oxidase: Ten years after. *Amino Acids.* **42,** 441-450.

Chen, J., Giridhar, K.V., Zhang, L., Xu, S. & Wang, Q.J. 2011. A protein kinase C/protein kinase D pathway protects LNCaP prostate cancer cells from phorbol ester-induced apoptosis by promoting ERK1/2 and NF-κB activities. *Carcinogenesis.* **32,** 1198-1206.

Chen, Y., Vujcic, S., Liang, P., Diegelman, P., Kramer, D. & Porter, C. 2003. Genomic identification and biochemical characterization of a second spermidine/spermine N1-acetyltransferase. *Biochem. J.* **373,** 661-667.

Cheng, L.L., Wu, C., Smith, M.R. & Gonzalez, R.G. 2001. Non-destructive quantitation of spermine in human prostate tissue samples using HRMAS 1H NMR spectroscopy at 9.4 T. *FEBS Letters.* **494,** 112-116.

Choi, W., Proctor, L., Xia, Q., Feng, Y., Gerner, E.W., Chiao, P.J., Hamilton, S.R. & Zhang, W. 2006. Inactivation of IκB contributes to transcriptional activation of spermidine/spermine N (1)-acetyltransferase. *Molecular Carcinogenesis.* **45,** 685-693.

Chopra, S. & Wallace, H.M. 1998. Induction of spermidine/spermine N1-acetyltransferase in human cancer cells in response to increased production of reactive oxygen species. *Biochemical Pharmacology.* **55,** 1119-1123.

Coffey, R.N., Watson, R.W.G., O'Neill, A.J., Mc Eleny, K. & Fitzpatrick, J.M. 2002. Androgen-mediated resistance to apoptosis. *The Prostate.* **53,** 300-309.

Coffino, P. & Poznanski, A. 1991. Killer polyamines? *Journal of Cellular Biochemistry.* **45,** 54-58.

Cohn, V.H. & Lyle, J. 1966. A fluorometric assay for glutathione. *Analytical Biochemistry.* **14,** 434-440.

Coleman, C.S. & Pegg, A.E. 1997. Proteasomal degradation of spermidine/spermine N 1-acetyltransferase requires the carboxyl-terminal glutamic acid residues. *Journal of Biological Chemistry.* **272,** 12164-12169.

Coleman, C.S., Pegg, A.E., Megosh, L.C., Guo, Y., Sawicki, J.A. & O'Brien, T.G. 2002. Targeted expression of spermidine/spermine N1-acetyltransferase increases susceptibility to chemically induced skin carcinogenesis. *Carcinogenesis.* **23,** 359-364.

Criss, W.E. 2003. A review of polyamines and cancer. *Turkish Journal of Medical Sciences.* **33,** 195-206.

Cullis, P.M., Green, R.E., Merson-Davies, L. & Travis, N. 1999. Probing the mechanism of transport and compartmentalisation of polyamines in mammalian cells. *Chemistry & Biology.* **6,** 717-729.

De Marzo, A.M., Marchi, V.L., Epstein, J.I. & Nelson, W.G. 1999. Proliferative inflammatory atrophy of the prostate: Implications for prostatic carcinogenesis. *The American Journal of Pathology.* **155,** 1985-1992.

De Marzo, A.M., Platz, E.A., Sutcliffe, S., Xu, J., Grönberg, H., Drake, C.G., Nakai, Y., Isaacs, W.B. & Nelson, W.G. 2007. Inflammation in prostate carcinogenesis. *Nature Reviews Cancer.* **7,** 256-269.

Della Ragione, F.& Pegg, A.E. 1983. Studies of the specificity and kinetics of rat liver spermidine/spermine N1-acetyltransferase. *Biochem. J.* **213,** 701-706.

Denizot, F. & Lang, R. 1986. Rapid colorimetric assay for cell growth and survival: modifications to the tetrazolium dye procedure giving improved sensitivity and reliability. *J. Immunol. Methods*. **89**, 271-277.

Dudkowska, M., Stachurska, A., Grzelakowska-Sztabert, B. & Manteuffel-Cymborowska, M. 2002. Up-regulation of spermidine/spermine N^1-acetyltransferase (SSAT) expression is a part of proliferative but not anabolic response of mouse kidney. *Acta Biochimica Polonica-English Edition-*. **49,** 969-978.

Eruslanov, E. and Kusmartsev, S., 2010. Identification of ROS using oxidized DCFDA and flow-cytometry. *Advanced Protocols in Oxidative Stress II.* Springer, pp. 57-72.

Ettinger, S.L., Sobel, R., Whitmore, T.G., Akbari, M., Bradley, D.R., Gleave, M.E. & Nelson, C.C. 2004. Dysregulation of sterol response element-binding proteins and downstream effectors in prostate cancer during progression to androgen independence. *Cancer Research.* **64,** 2212-2221.

Feith, D.J., Shantz, L.M., Shoop, P.L., Keefer, K.A., Prakashagowda, C. & Pegg, A.E. 2007. Mouse skin chemical carcinogenesis is inhibited by antizyme in promotion-sensitive and promotion-resistant genetic backgrounds. *Molecular Carcinogenesis.* **46,** 453-465.

Felschow, D., Mi, Z., Stanek, J., Frei, J. & Porter, C. 1997. Selective labelling of cell-surface polyamine-binding proteins on leukaemic and solid-tumour cell types using a new polyamine photoprobe. *Biochem. J.* **328,** 889-895.

Fillingame, R.H., Jorstad, C.M. & Morris, D.R. 1975. Increased cellular levels of spermidine or spermine are required for optimal DNA synthesis in lymphocytes activated by concanavalin A. *Proceedings of the National Academy of Sciences.* **72,** 4042-4045.

Flavin, R., Zadra, G. & Loda, M. 2011. Metabolic alterations and targeted therapies in prostate cancer. *The Journal of Pathology.* **223,** 284-295.

Fogel-Petrovic, M., Kramer, D., Ganis, B., Casero, R. & Porter, C. 1993. Cloning and sequence analysis of the gene and cDNA encoding mouse spermidine/spermine< i> N^1-acetyltransferase—a gene uniquely regulated by polyamines and their analogs. *Biochimica Et Biophysica Acta (BBA)-Gene Structure and Expression.* **1216,** 255-264.

Fogel-Petrovic, M., Kramer, D.L., Vujcic, S., Miller, J., Mcmanis, J.S., Bergeron, R.J. & Porter, C.W. 1997. Structural basis for differential induction of spermidine/spermine N 1-acetyltransferase activity by novel spermine analogs. *Molecular Pharmacology.* **52,** 69-74.

Fogel-Petrovic, M., Vujcic, S., Brown, P.J., Haddox, M.K. & Porter, C.W. 1996. Effects of polyamines, polyamine analogs, and inhibitors of protein synthesis on spermidine-spermine N1-acetyltransferase gene expression. *Biochemistry.* **35,** 14436-14444.

Fong, L.Y., Feith, D.J. & Pegg, A.E. 2003. Antizyme overexpression in transgenic mice reduces cell proliferation, increases apoptosis, and reduces N-nitrosomethylbenzylamine-induced forestomach carcinogenesis. *Cancer Research.* **63,** 3945-3954.

Freshney, I. 2005. Culture of animal cells: A manual of basic technique 5th ed. 441-442.

Gerner, E.W. & Meyskens, F.L. 2004. Polyamines and cancer: Old molecules, new understanding. *Nature Reviews Cancer.* **4,** 781-792.

Gimelli, G., Giglio, S., Zuffardi, O., Alhonen, L., Suppola, S., Cusano, R., Nigro, C.L., Gatti, R., Ravazzolo, R. & Seri, M. 2002. Gene dosage of the spermidine/spermine N1-acetyltransferase (SSAT) gene with putrescine accumulation in a patient with a Xp21. 1p22. 12 duplication and keratosis follicularis spinulosa decalvans (KFSD). *Human Genetics.* **111,** 235-241.

Giskeødegård, G.F., Bertilsson, H., Selnæs, K.M., Wright, A.J., Bathen, T.F., Viset, T., Halgunset, J., Angelsen, A., Gribbestad, I.S. & Tessem, M. 2013. Spermine and citrate as metabolic biomarkers for assessing prostate cancer aggressiveness. *PloS One.* **8,** e62375.

Globocan 2008: Cancer incidence and mortality worldwide. International Agency for Research on Cancer, WHO. Available from: http://www.iarc.fr/en/media-centre/iarcnews/2010/globocan2008.php [Accessed 12 Nov 2013].

Goodwin, A.C., Jadallah, S., Toubaji, A., Lecksell, K., Hicks, J.L., Kowalski, J., Bova, G.S., De Marzo, A.M., Netto, G.J. & Casero, R.A. 2008. Increased spermine oxidase expression in human prostate cancer and prostatic intraepithelial neoplasia tissues. *The Prostate.* **68,** 766-772.

Graham, J., Baker, M., Macbeth, F. & Titshall, V. 2008. Guidelines: Diagnosis and treatment of prostate cancer: Summary of NICE guidance. *BMJ: British Medical Journal.* **336,** 610.

Gugliucci, A. & Menini, T. 2003. The polyamines spermine and spermidine protect proteins from structural and functional damage by AGE precursors: A new role for old molecules? *Life Sciences.* **72,** 2603-2616.

Gupta, S., Ahmad, N., Marengo, S.R., MacLennan, G.T., Greenberg, N.M. & Mukhtar, H. 2000. Chemoprevention of prostate carcinogenesis by α-Difluoromethylornithine in TRAMP mice. *Cancer Res*. **60**, 5125-5133.

Hanahan, D. & Weinberg, R.A. 2011. Hallmarks of cancer: The next generation. *Cell.* **144,** 646-674.

Heby, O., Marton, L.J., Zardi, L., Russell, O.H. & Baserga, R. 1975. Changes in polyamine metabolism in WI38 cells stimulated to proliferate. *Experimental Cell Research*. **90**, 8-14.

Hector, S., Porter, C.W., Kramer, D.L., Clark, K., Prey, J., Kisiel, N., Diegelman, P., Chen, Y. & Pendyala, L. 2004. Polyamine catabolism in platinum drug action: Interactions between oxaliplatin and the polyamine analogue N1, N11-diethylnorspermine at the level of spermidine/spermine N1-acetyltransferase. *Molecular Cancer Therapeutics.* **3,** 813-822.

Heidenreich, A., Aus, G., Bolla, M., Joniau, S., Matveev, V.B., Schmid, H.P. & Zattoni, F. 2008. EAU guidelines on prostate cancer. *European Urology.* **53,** 68-80.

Heljasvaara, R., Veress, I., Halmekyto, M., Alhonen, L., Janne, J., Laajala, P. & Pajunen, A. 1997. Transgenic mice overexpressing ornithine and S-adenosylmethionine decarboxylases maintain a physiological polyamine homoeostasis in their tissues. *Biochem. J.* **323,** 457-462.

Hissin, P.J.& Hilf, R. 1976. A fluorometric method for determination of oxidized and reduced glutathione in tissues. *Analytical Biochemistry.* **74,** 214-226.

Holm, I., Persson, L., Stjernborg, L., Thorsson, L. & Heby, O. 1989. Feedback control of ornithine decarboxylase expression by polyamines. analysis of ornithine decarboxylase mRNA distribution in polysome profiles and of translation of this mRNA in vitro. *Biochem. J.* **258,** 343-350.

Holst, C.M., Nevsten, P., Johansson, F., Carlemalm, E. & Oredsson, S.M. 2008. Subcellular distribution of spermidine/spermine N^1-acetyltransferase. *Cell Biology International.* **32,** 39-47.

Horoszewicz, J.S., Leong, S.S., Kawinski, E., Karr, J.P., Rosenthal, H., Chu, T.M., Mirand, E.A. & Murphy, G.P. 1983. LNCaP model of human prostatic carcinoma. *Cancer Research.* **43,** 1809.

Horoszewicz, J.S., Leong, S.S., Chu, T.M., Wajsman, Z.L., Friedman, M., Papsidero, L., Kim, U., Chai, L.S., Kakati, S., Arya, S.K. & Sandberg, A.A. 1980. The LNCaP cell line--a new model for studies on human prostatic carcinoma. *Progress in Clinical and Biological Research.* **37,** 115-132.

Hughes, A., Smith, N. & Wallace, H. 2003. Polyamines reverse non-steroidal anti-inflammatory drug-induced toxicity in human colorectal cancer cells. *Biochem.J.* **374,** 481-488.

Hussain, T., Gupta, S. & Mukhtar, H. 2003. Cyclooxygenase-2 and prostate carcinogenesis. *Cancer Letters.* **191,** 125-135.

Hyvönen, M.T., Keinänen, T.A., Cerrada-Gimenez, M., Sinervirta, R., Grigorenko, N., Khomutov, A.R., Vepsäläinen, J., Alhonen, L. & Jänne, J. 2007. Role of hypusinated eukaryotic translation initiation factor 5A in polyamine depletion-induced cytostasis. *Journal of Biological Chemistry.* **282,** 34700-34706.

Igarashi, K. & Kashiwagi, K. 2010. Modulation of cellular function by polyamines. *The International Journal of Biochemistry & Cell Biology.* **42,** 39-51.

Isaacs, W., De Marzo, A. & Nelson, W.G. 2002. Focus on prostate cancer. *Cancer Cell.* **2,** 113.

Jell, J., Merali, S., Hensen, M.L., Mazurchuk, R., Spernyak, J.A., Diegelman, P., Kisiel, N.D., Barrero, C., Deeb, K.K., Alhonen, L., Patel, M.S. & Porter, C.W. 2007. Genetically altered expression of spermidine/spermine N1-acetyltransferase affects fat metabolism in mice via acetyl-CoA. *The Journal of Biological Chemistry.* **282,** 8404-8413.

Kawakita, M. & Hiramatsu, K. 2006. Diacetylated derivatives of spermine and spermidine as novel promising tumor markers. *Journal of Biochemistry.* **139,** 315-322.

Kawakita, M., Hiramatsu, K., Sugimoto, M., Takahashi, K. & Toi, M. 2004. Clinical usefulness of urinary diacetylpolyamines as novel tumor markers. *Rinsho Byori.the Japanese Journal of Clinical Pathology.* **52,** 321-327.

Kee, K., Foster, B.A., Merali, S., Kramer, D.L., Hensen, M.L., Diegelman, P., Kisiel, N., Vujcic, S., Mazurchuk, R.V. & Porter, C.W. 2004a. Activated polyamine catabolism depletes acetyl-CoA pools and suppresses prostate tumor growth in TRAMP mice. *Journal of Biological Chemistry.* **279,** 40076.

Kee, K., Vujcic, S., Merali, S., Diegelman, P., Kisiel, N., Powell, C.T., Kramer, D.L. & Porter, C.W. 2004b. Metabolic and antiproliferative consequences of activated polyamine catabolism in LNCaP prostate carcinoma cells. *Journal of Biological Chemistry.* **279,** 27050.

Keren-Paz, A., Bercovich, Z., Porat, Z., Erez, O., Brener, O. & Kahana, C. 2006. Overexpression of antizyme-inhibitor in NIH3T3 fibroblasts provides growth advantage through neutralization of antizyme functions. *Oncogene.* **25,** 5163-5172.

Khandrika, L., Kumar, B., Koul, S., Maroni, P. & Koul, H.K. 2009. Oxidative stress in prostate cancer. *Cancer Letters.* **282,** 125-136.

Khuhawar, M. & Qureshi, G. 2001. Polyamines as cancer markers: Applicable separation methods. *Journal of Chromatography B: Biomedical Sciences and Applications.* **764,** 385-407.

Kim, S.W., Mangold, U., Waghorne, C., Mobascher, A., Shantz, L., Banyard, J. & Zetter, B.R. 2006. Regulation of cell proliferation by the antizyme inhibitor: Evidence for an antizyme-independent mechanism. *Journal of Cell Science.* **119,** 2583-2591.

Knize, M.G.& Felton, J.S. 2005. Formation and human risk of carcinogenic heterocyclic amines formed from natural precursors in meat. *Nutrition Reviews.* **63,** 158-165.

Kramer, D.L., Diegelman, P., Jell, J., Vujcic, S., Merali, S. & Porter, C.W. 2008. Polyamine acetylation modulates polyamine metabolic flux, a prelude to broader metabolic consequences. *Journal of Biological Chemistry.* **283,** 4241.

Kuhajda, F. 2008. AMP-activated protein kinase and human cancer: Cancer metabolism revisited. *International Journal of Obesity.* **32,** S36-S41.

Kuhajda, F.P. 2000. Fatty-acid synthase and human cancer: New perspectives on its role in tumor biology. *Nutrition.* **16,** 202-208.

Kumar, B., Koul, S., Khandrika, L., Meacham, R.B. & Koul, H.K. 2008. Oxidative stress is inherent in prostate cancer cells and is required for aggressive phenotype. *Cancer Research.* **68,** 1777-1785.

Lalani, E., Laniado, M.E. & Abel, P.D. 1997. Molecular and cellular biology of prostate cancer. *Cancer and Metastasis Reviews.* **16,** 29-66.

Larqué, E., Sabater-Molina, M. & Zamora, S. 2007. Biological significance of dietary polyamines. *Nutrition.* **23,** 87-95.

Lee, S., Park, J., Folk, J., Deck, J., Pegg, A., Sokabe, M., Fraser, C. & Park, M. 2011. Inactivation of eukaryotic initiation factor 5A (eIF5A) by specific acetylation of its hypusine residue by spermidine/spermine acetyltransferase 1 (SSAT1). *Biochem. J.* **433,** 205-213.

Leissner, K. & Tisell, L. 1979. The weight of the human prostate. *Scandinavian Journal of Urology and Nephrology.* **13,** 137-142.

Libby, P.R., Ganis, B., Bergeron, R.J. & Porter, C.W. 1991. Characterization of human spermidine/spermine N^1-acetyltransferase purified from cultured melanoma cells. *Archives of Biochemistry and Biophysics.* **284,** 238-244.

Lilja, H., Oldbring, J., Rannevik, G. & Laurell, C. 1987. Seminal vesicle-secreted proteins and their reactions during gelation and liquefaction of human semen. *Journal of Clinical Investigation.* **80,** 281.

Lim, S.D., Sun, C., Lambeth, J.D., Marshall, F., Amin, M., Chung, L., Petros, J.A. & Arnold, R.S. 2005. Increased Nox1 and hydrogen peroxide in prostate cancer. *The Prostate.* **62,** 200-207.

Lin, D.W.& Nelson, P.S. 2003. The role of cyclooxygenase-2 inhibition for the prevention and treatment of prostate carcinoma. *Clinical Prostate Cancer.* **2,** 119-126.

Liu, C., Perez-Leal, O., Barrero, C., Zahedi, K., Soleimani, M., Porter, C. & Merali, S. 2014. Modulation of polyamine metabolic flux in adipose tissue alters the accumulation of body fat by affecting glucose homeostasis. *Amino Acids.* **46**, 701-715.

Liu, X., Wang, L., Lin, Y., Teng, Q., Zhao, C., Hu, H. & Chi, W. 2000. Ornithine decarboxylase activity and its gene expression are increased in benign hyperplastic prostate. *The Prostate.* **43,** 83-87.

Lowry, O.H., Rosebrough, N.J., Farr, A.L. & Randall, R.J. 1951. Protein measurement with the Folin phenol reagent. *J. Biol. Chem*. **193**, 265-275.

Lozano, R., Naghavi, M., Foreman, K., Lim, S., Shibuya, K., Aboyans, V., Abraham, J., Adair, T., Aggarwal, R. & Ahn, S.Y. 2013. Global and regional mortality from 235 causes of death for 20 age groups in 1990 and 2010: A systematic analysis for the global burden of disease study 2010. *The Lancet.* **380,** 2095-2128.

Mahmud, S.M., Tanguay, S., Bégin, L.R., Franco, E.L. & Aprikian, A.G. 2006. Non-steroidal anti-inflammatory drug use and prostate cancer in a high-risk population. *European Journal of Cancer Prevention.* **15,** 158-164.

Mamont, P.S., Duchesne, M., Grove, J. & Bey, P. 1978. Anti-proliferative properties of DL-α-difluoromethyl ornithine in cultured cells. A consequence of the irreversible inhibition of ornithine decarboxylase. *Biochemical and Biophysical Research Communications.* **81,** 58-66.

Mandal, S., Mandal, A., Johansson, H.E., Orjalo, A.V. & Park, M.H. 2013. Depletion of cellular polyamines, spermidine and spermine, causes a total arrest in translation and growth in mammalian cells. *Proceedings of the National Academy of Sciences.* **110,** 2169-2174.

Martinon, F., Pétrilli, V., Mayor, A., Tardivel, A. & Tschopp, J. 2006. Gout-associated uric acid crystals activate the NALP3 inflammasome. *Nature.* **440,** 237-241.

Marton, L.J. & Pegg, A.E. 1995. Polyamines as targets for therapeutic intervention. *Annual Review of Pharmacology and Toxicology.* **35,** 55-91.

Matsui-Yuasa, I., Otani, S., Yano, Y., Takada, N., Shibata, M. & Fukushima, S. 1992. Spermidine/Spermine N-Acetyltransferase, a new biochemical marker for epithelial proliferation in rat bladder. *Cancer Science.* **83,** 1037-1040.

Maxwell, P.J., Longley, D.B., Latif, T., Boyer, J., Allen, W., Lynch, M., McDermott, U., Harkin, D.P., Allegra, C.J. & Johnston, P.G. 2003. Identification of 5-fluorouracil-inducible target genes using cDNA microarray profiling. *Cancer Research.* **63,** 4602-4606.

McCloskey, D.E., Coleman, C.S. & Pegg, A.E. 1999. Properties and regulation of human spermidine/spermine N1-acetyltransferase stably expressed in chinese hamster ovary cells. *The Journal of Biological Chemistry.* **274,** 6175-6182.

McCloskey, D.E., Woster, P.M., Robert A. Casero, Jr. R.A. & Davidson, N.E. 2000. Effects of the polyamine analogues N^1-Ethyl-N11-((cyclopropyl)methyl)-4,8-diazaundecane and N^1-Ethyl-N^{11}-((cycloheptyl)methyl)-4,8-diazaundecane in human prostate cancer cells. *Clinical Cancer Research*. **6**, 17-23.

Medes, G., Thomas, A. & Weinhouse, S. 1953. Metabolism of neoplastic tissue. IV. A study of lipid synthesis in neoplastic tissue slices in vitro. *Cancer Research.* **13,** 27-29.

Merentie, M., Uimari, A., Pietilä, M., Sinervirta, R., Keinänen, T., Vepsäläinen, J., Khomutov, A., Grigorenko, N., Herzig, K. & Jänne, J. 2007. Oxidative stress and inflammation in the pathogenesis of activated polyamine catabolism-induced acute pancreatitis. *Amino Acids.* **33,** 323-330.

Meyskens, F.L., McLaren, C.E., Pelot, D., Fujikawa-Brooks, S., Carpenter, P.M., Hawk, E., Kelloff, G., Lawson, M.J., Kidao, J. & McCracken, J. 2008. Difluoromethylornithine plus sulindac for the prevention of sporadic colorectal adenomas: A randomized placebo-controlled, double-blind trial. *Cancer Prevention Research.* **1,** 32-38.

Miller, D.C., Hafez, K.S., Stewart, A., Montie, J.E. & Wei, J.T. 2003. Prostate carcinoma presentation, diagnosis, and staging. *Cancer.* **98,** 1169-1178.

Mohan, R.R., Challa, A., Gupta, S., Bostwick, D.G., Ahmad, N., Agarwal, R., Marengo, S.R., Amini, S.B., Paras, F. & MacLennan, G.T. 1999. Overexpression of ornithine decarboxylase in prostate cancer and prostatic fluid in humans. *Clinical Cancer Research.* **5,** 143-147.

Montironi, R., Mazzucchelli, R. & Scarpelli, M. 2002. Precancerous lesions and conditions of the prostate. *Annals of the New York Academy of Sciences.* **963,** 169-184.

Moshier, J.A, Dosescu, J., Skunca, M & Luk, G.D. 1993. Transformation of NIH/3T3 Cells by Ornithine Decarboxylase Overexpression. *Cancer Research*. **53**, 2618-2622.

Mosmann, T. 1983. Rapid colorimetric assay for cellular growth and survival: application to proliferation and cytotoxicity assays. *J. Immunol. Methods*. **65**, 55-63.

Murakami, Y., Matsufuji, S., Miyazaki, Y. & Hayashi, S. 1994. Forced expression of antizyme abolishes ornithine decarboxylase activity, suppresses cellular levels of polyamines and inhibits cell growth. *Biochem. J.* **304,** 183-187.

Murray-Stewart, T., Applegren, N.B., Devereux, W., Hacker, A., Smith, R., Wang, Y. & Casero Jr, R.A. 2003. Spermidine/spermine N1-acetyltransferase (SSAT) activity in human small-cell lung carcinoma cells following transfection with a genomic SSAT construct. *Biochemical Journal.* **373,** 629.

Myers, R.P. 2000. Structure of the adult prostate from a clinician's standpoint. *Clinical Anatomy.* **13,** 214-215.

Nathan, C.& Ding, A. 2010. SnapShot: Reactive oxygen intermediates (ROI). *Cell.* **140,** 951-951. e2.

Niiranen, K., Pietilä, M., Pirttilä, T.J., Järvinen, A., Halmekytö, M., Korhonen, V., Keinänen, T.A., Alhonen, L. & Jänne, J. 2002. Targeted disruption of Spermidine/SpermineN 1-acetyltransferase gene in mouse embryonic stem cells. Effects on polyamine homeostasis and sensitivity to polyamine analogues. *Journal of Biological Chemistry.* **277,** 25323-25328.

Nilsson, J.A., Keller, U.B., Baudino, T.A., Yang, C., Norton, S., Old, J.A., Nilsson, L.M., Neale, G., Kramer, D.L. & Porter, C.W. 2005. Targeting ornithine decarboxylase in myc-induced lymphomagenesis prevents tumor formation. *Cancer Cell.* **7,** 433-444.

Nishimura, K., Nakatsu, F., Kashiwagi, K., Ohno, H., Saito, T. & Igarashi, K. 2002. Essential role of S-adenosylmethionine decarboxylase in mouse embryonic development. *Genes to Cells.* **7,** 41-47.

Nowotarski, S.L., Woster, P.M. & Casero, R.A. 2013. Polyamines and cancer: Implications for chemotherapy and chemoprevention. *Expert Reviews in Molecular Medicine.* **15,** e3.

O'Brien, T.G., Megosh, L.C., Gilliard, G. & Soler, A.P. 1997. Ornithine decarboxylase overexpression is a sufficient condition for tumor promotion in mouse skin. *Cancer Research*. **57**, 2630-2637.

Omabe, M. & Ezeani, M. 2011. Infection, inflammation and prostate carcinogenesis. *Infection, Genetics and Evolution: Journal of Molecular Epidemiology and Evolutionary Genetics in Infectious Diseases.* **11,** 1195-1198.

Palavan-Unsal, N., Aloglu-Senturk, S. & Arsan, D. 2006. The function of poliamine metabolism in prostate cancer. *Exp Oncol.* **28,** 178-186.

Palmer, A., Ghani, R., Kaur, N., Phanstiel, O. & Wallace, H. 2009. A putrescine-anthracene conjugate: A paradigm for selective drug delivery. *Biochem. J.* **424,** 431-438.

Palmer, A.J. & Wallace, H.M. 2010. The polyamine transport system as a target for anticancer drug development. *Amino Acids.* **38,** 415-422.

Park, M.H. 2006. The post-translational synthesis of a polyamine-derived amino acid, hypusine, in the eukaryotic translation initiation factor 5A (eIF5A). *Journal of Biochemistry.* **139,** 161-169.

Pastorian, K.E. & Byus, C.V. 1997. Tolerance to putrescine toxicity in chinese hamster ovary cells is associated with altered uptake and export. *Experimental Cell Research.* **231,** 284-295.

Pegg, A.E. 2008. Spermidine/spermine-N1-acetyltransferase: A key metabolic regulator. *American Journal of Physiology- Endocrinology and Metabolism.* **294,** E995.

Pegg, A., Feith, D., Fong, L., Coleman, C., O'Brien, T. & Shantz, L. 2003. Transgenic mouse models for studies of the role of polyamines in normal, hypertrophic and neoplastic growth. *Biochemical Society Transactions.* **31,** 356-360.

Pegg, A.E. 2009. Mammalian polyamine metabolism and function. *IUBMB Life.* **61,** 880-894.

Pegg, A.E. and Casero Jr, R.A., 2011. Current status of the polyamine research field. *Polyamines: Methods and Protocols, Methods in Molecular Biology*. Springer. **720**, 3-35.

Pegg, A.E. & Feith, D.J. 2007. Polyamines and neoplastic growth. *Biochemical Society Transactions.* **35,** 295-299.

Pendeville, H., Carpino, N., Marine, J., Takahashi, Y., Muller, M., Martial, J.A. & Cleveland, J.L. 2001. The ornithine decarboxylase gene is essential for cell survival during early murine development. *Molecular and Cellular Biology.* **21,** 6549-6558.

Perez-Leal, O.& Merali, S. 2012. Regulation of polyamine metabolism by translational control. *Amino Acids.* **42,** 611-617.

Perez-Stable, C., 2011. Prostate Cancer Chemotherapy. In: Manfred Schwab, ed, *Encyclopedia of Cancer.* 3rd edn. Springer-Verlag Berlin Heidelberg: Springer.

Pietilä, M., Alhonen, L., Halmekytö, M., Kanter, P., Jänne, J. & Porter, C.W. 1997. Activation of polyamine catabolism profoundly alters tissue polyamine pools and affects

hair growth and female fertility in transgenic mice overexpressing Spermidine/SpermineN 1-acetyltransferase. *Journal of Biological Chemistry.* **272,** 18746-18751.

Pietilä, M., Parkkinen, J.J., Alhonen, L. & Jänne, J. 2001. Relation of skin polyamines to the hairless phenotype in transgenic mice overexpressing spermidine/spermine N1-acetyltransferase. *Journal of Investigative Dermatology.* **116,** 801-805.

Pirinen, E., Kuulasmaa, T., Pietilä, M., Heikkinen, S., Tusa, M., Itkonen, P., Boman, S., Skommer, J., Virkamäki, A. & Hohtola, E. 2007. Enhanced polyamine catabolism alters homeostatic control of white adipose tissue mass, energy expenditure, and glucose metabolism. *Molecular and Cellular Biology.* **27,** 4953-4967.

Pizer, E.S., Jackisch, C., Wood, F.D., Pasternack, G.R., Davidson, N.E. & Kuhajda, F.P. 1996. Inhibition of fatty acid synthesis induces programmed cell death in human breast cancer cells. *Cancer Research.* **56,** 2745-2747.

Pledgie, A., Huang, Y., Hacker, A., Zhang, Z., Woster, P.M., Davidson, N.E. & Casero, R.A. 2005. Spermine oxidase SMO (PAOh1), not N1-acetylpolyamine oxidase PAO, is the primary source of cytotoxic H2O2 in polyamine analogue-treated human breast cancer cell lines. *Journal of Biological Chemistry.* **280,** 39843-39851.

Poletti, F., Medici, M.C., Alinovi, A., Menozzi, M.G., Sacchini, P., Stagni, G., Toni, M. & Benoldi, D. 1985. Isolation of chlamydia trachomatis from the prostatic cells in patients affected by nonacute abacterial prostatitis. *The Journal of Urology.* **134,** 691-693.

Porter, C.W., Ganis, B., Libby, P.R. & Bergeron, R.J. 1991. Correlations between polyamine analogue-induced Increases in spermidine/spermine N^1-acetyltransferase activity, polyamine pool depletion, and growth inhibition in human melanoma cell lines. *Cancer Res*. **51**, 3715-3720.

Putzi, M.J. & De Marzo, A.M. 2000. Morphologic transitions between proliferative inflammatory atrophy and high-grade prostatic intraepithelial neoplasia. *Urology.* **56,** 828-832.

Rendina, A.X. & Cheng, D. 2005. Characterization of the inactivation of rat fatty acid synthase by C75: Inhibition of partial reactions and protection by substrates. *Biochem. J.* **388,** 895-903.

Ripple, M.O., Wilding, G., Henry, W.F. & Rago, R.P. 1997. Prooxidant-antioxidant shift induced by androgen treatment of human prostate carcinoma cells. *Journal of the National Cancer Institute.* **89,** 40-48.

Rossi, S., Graner, E., Febbo, P., Weinstein, L., Bhattacharya, N., Onody, T., Bubley, G., Balk, S. & Loda, M. 2003. Fatty acid synthase expression defines distinct molecular signatures in prostate Cancer1 1 NCI (director's challenge CA84995-04, SPORE in prostate cancer CA90381-01A1, and PO1 CA89021-02), novartis investigator, and CaPCURE awards. *Molecular Cancer Research.* **1,** 707-715.

Roy, U.K.B., Rial, N.S., Kachel, K.L. & Gerner, E.W. 2008. Activated K-RAS increases polyamine uptake in human colon cancer cells through modulation of caveolar endocytosis. Molecular Carcinogenesis. **47**, 538–553.

Rubinstein, S. & Breitbart, H. 1994. Cellular localization of polyamines: Cytochemical and ultrastructural methods providing new clues to polyamine function in ram spermatozoa. *Biology of the Cell.* **81,** 177-183.

Ryu, J., Cho, Y., Chun, Y. & Park, J. 2008. Myocardial SSAT induction via AMPK signaling and its implication for ischemic injury. *Biochemical and Biophysical Research Communications.* **366,** 438-444.

Sakata, K., Kashiwagi, K. & Igarashi, K. 2000. Properties of a polyamine transporter regulated by antizyme. *Biochem. J.* **347,** 297-303.

Salido, M., Vilches, J. & Roomans, G. 2004. Changes in elemental concentrations in LNCaP cells are associated with a protective effect of neuropeptides on etoposide-induced apoptosis. *Cell Biology International.* **28,** 397-402.

Sandhu, J.S. and Schlegel, P.N., 2004. Prostate Cancer. In: EDITOR-IN-CHIEF: LUCIANO MARTINI, ed, *Encyclopedia of Endocrine Diseases.* New York: Elsevier, pp. 125-130.

Saverio, B., Pierpaola, D., Serenella, A., Cesare, C., Bruno, M., Auro, T. & Arnaldo, C. 2000. Tumor progression is accompanied by significant changes in the levels of expression of polyamine metabolism regulatory genes and clusterin (sulfated glycoprotein 2) in human prostate cancer specimens. *Cancer Research.* **60,** 28-34.

Schipper, R., Romijn, J., Cuijpers, V. & Verhofstad, A. 2003. Polyamines and prostatic cancer. *Biochemical Society Transactions.* **31,** 375-380.

Schipper, R.G., Penning, L.C. & Verhofstad, A.A.J., 2000. Involvement of polyamines in apoptosis. Facts and controversies: effectors or protectors? *Seminars in cancer biology,* 2000, Elsevier pp55-68.

Seiler, N. 2003. Thirty years of polyamine-related approaches to cancer therapy. retrospect and prospect. part 1. selective enzyme inhibitors. *Current Drug Targets.* **4,** 537-564.

Seiler, N., Delcros, J. & Moulinoux, J.P. 1996. Polyamine transport in mammalian cells. an update. *The International Journal of Biochemistry & Cell Biology.* **28,** 843-861.

Seiler, N. & Dezeure, F. 1990. Polyamine transport in mammalian cells. *International Journal of Biochemistry.* **22,** 211-218.

Seiler, N. 2003. Thirty years of polyamine-related approaches to cancer therapy. retrospect and prospect. part 2. Structural analogues and derivatives. *Current Drug Targets.* **4,** 565-585.

Seiler, N. 1983. [2] liquid chromatographic methods for assaying polyamines using prechromatographic derivatization. *Methods in Enzymology.* **94,** 10-25.

Serafin, A.M., Akudugu, J.M. & Bohm, L. 2002. Drug resistance in prostate cancer cell lines is influenced by androgen dependence and p53 status. *Urological Research.* **30,** 289-294.

Smith, R.C., Litwin, M.S., Lu, Y. & Zetter, B.R. 1995. Identification of an endogenous inhibitor of prostatic carcinoma cell growth. *Nature Medicine.* **1,** 1040-1045.

Soerjomataram, I., Lortet-Tieulent, J., Parkin, D.M., Ferlay, J., Mathers, C., Forman, D. & Bray, F. 2012. Global burden of cancer in 2008: A systematic analysis of disability-adjusted life-years in 12 world regions. *The Lancet.* **380**, 1840-1850.

Soler, A.P., Gilliard, G., Megosh, L.C. & O'Brien, T.G. 1996. Modulation of murine hair follicle function by alterations in ornithine decarboxylase activity. *Journal of Investigative Dermatology.* **106,** 1108-1113.

Soulet, D., Gagnon, B., Rivest, S., Audette, M. & Poulin, R. 2004. A fluorescent probe of polyamine transport accumulates into intracellular acidic vesicles via a two-step mechanism. *Journal of Biological Chemistry.* **279,** 49355-49366.

Strickler, H.D.& Goedert, J.J. 2001. Sexual behavior and evidence for an infectious cause of prostate cancer. *Epidemiologic Reviews.* **23,** 144-151.

Suburu, J.& Chen, Y.Q. 2012. Lipids and prostate cancer. *Prostaglandins & Other Lipid Mediators.* **98,** 1-10.

Sugimura, T., Wakabayashi, K., Nakagama, H. & Nagao, M. 2004. Heterocyclic amines: Mutagens/carcinogens produced during cooking of meat and fish. *Cancer Science.* **95,** 290-299.

Suzuki, O., Matsumoto, T. & Katsumata, Y. 1984. Determination of polyamine oxidase activities in human tissues. *Cellular and Molecular Life Sciences.* **40,** 838-839.

Swinnen, J.V., Vanderhoydonc, F., Elgamal, A.A., Eelen, M., Vercaeren, I., Joniau, S., Van Poppel, H., Baert, L., Goossens, K. & Heyns, W. 2000. Selective activation of the fatty acid synthesis pathway in human prostate cancer. *International Journal of Cancer.* **88,** 176-179.

Szatrowski, T.P. & Nathan, C.F. 1991. Production of large amounts of hydrogen peroxide by human tumor cells. *Cancer Research.* **51,** 794-798.

Räsänen T.-L., Alhonen L., Sinervirta R., Uimari A., Kaasinen K., Keinänen T., Herzig K.-H. & Jänne J. 2003. Gossypol activates pancreatic polyamine catabolism in normal rats and induces acute pancreatitis in transgenic rats over-expressing spermidine/spermine N^1-acetyltransferase. *Scandinavian Journal of Gastroenterology.* **38,** 787-793.

Tabib, A. 1998. Determination of ornithine decarboxylase activity using [^{3}H]ornithine. Methods in Molecular Biology, Vol**79**: Polyamine Protocols. Edited by Morgan, D.M. Totowa, New Jersey: Humana Press. pp. 33-39.

Takao, K., Rickhag, M., Hegardt, C., Oredsson, S. & Persson, L. 2006. Induction of apoptotic cell death by putrescine. *The International Journal of Biochemistry & Cell Biology.* **38,** 621-628.

Teti, D., Visalli, M. & McNair, H. 2002. Analysis of polyamines as markers of (patho) physiological conditions. *Journal of Chromatography B.* **781,** 107-149.

Thapa, D. & Ghosh, R. 2012. Antioxidants for prostate cancer chemoprevention: Challenges and opportunities. *Biochemical Pharmacology.* **83,** 1319-1330.

Thomas, T. & Thomas, T.J. 2001. Polyamines in cell growth and cell death: molecular mechanisms and therapeutic applications. CMLS, Cell. Mol. Life Sci. **58**, 244-258.

Tolbert, W.D., Ekstrom, J.L., Mathews, I.I., Secrist, J.A., Kapoor, P., Pegg, A.E. & Ealick, S.E. 2001. The structural basis for substrate specificity and inhibition of human S-adenosylmethionine decarboxylase. *Biochemistry.* **40,** 9484-9494.

Tome, M., Fiser, S., Payne, C. & Gerner, E. 1997. Excess putrescine accumulation inhibits the formation of modified eukaryotic initiation factor 5A (eIF-5A) and induces apoptosis. *Biochem.J.* **328,** 847-854.

Tucker, J.M., Murphy, J.T., Kisiel, N., Diegelman, P., Barbour, K.W., Davis, C., Medda, M., Alhonen, L., Jänne, J. & Kramer, D.L. 2005. Potent modulation of intestinal tumorigenesis in apcmin/ mice by the polyamine catabolic enzyme spermidine/spermine N1-acetyltransferase. *Cancer Research.* **65,** 5390-5398.

Turchanowa, L., Dauletbaev, N., Milovic, V. & Stein, J. 2001. Nonsteroidal anti-inflammatory drugs stimulate spermidine/spermine acetyltransferase and deplete polyamine content in colon cancer cells. *European Journal of Clinical Investigation.* **31,** 887-893.

Uemura, T., Yerushalmi, H.F., Tsaprailis, G., Stringer, D.E., Pastorian, K.E., Hawel III, L., Byus, C.V. & Gerner, E.W. 2008. Identification and characterization of a diamine exporter in colon epithelial cells. *Journal of Biological Chemistry.* **283,** 26428-26435.

van der Cruijsen-Koeter I.W., Vis, A.N., Roobol, M.J., Wildhagen, M.F., de Koning, H.J., van der Kwast, T. & Schröder, F.H. 2005. Comparison of screen detected and clinically diagnosed prostate cancer in the european randomized study of screening for prostate cancer, section rotterdam. *The Journal of Urology.* **174,** 121-125.

van der Graaf, M., Schipper, R.G., Oosterhof, G.O., Schalken, J.A., Verhofstad, A.A. & Heerschap, A. 2000. Proton MR spectroscopy of prostatic tissue focused on the etection of spermine, a possible biomarker of malignant behavior in prostate cancer. *Magnetic Resonance Materials in Physics, Biology and Medicine.* **10,** 153-159.

Voeller, D., Rahman, L. & Zajac-Kaye, M. 2004. Elevated levels of thymidylate synthase linked to neoplastic transformation of mammalian cells. *Cell Cycle.* **3,** 1003-1005.

Vujcic, S., Diegelman, P., Bacchi, C., Kramer, D. & Porter, C. 2002. Identification and characterization of a novel flavin-containing spermine oxidase of mammalian cell origin. *Biochem.J.* **367,** 665-675.

Vujcic, S., Halmekyto, M., Diegelman, P., Gan, G., Kramer, D.L., Janne, J. & Porter, C.W. 2000. Effects of conditional overexpression of spermidine/spermine N1-acetyltransferase on polyamine pool dynamics, cell growth, and sensitivity to polyamine analogs. *The Journal of Biological Chemistry.* **275,** 38319-38328.

Wallace, H.M. 2000. The physiological role of the polyamines. *European Journal of Clinical Investigation.* **30,** 1-3.

Wallace, H.M., Duthie, J., Evans, D.M., Lamond, S., Nicoll, K.M. & Heys, S.D. 2000. Alterations in polyamine catabolic enzymes in human breast cancer tissue. *Clinical Cancer Research.* **6,** 3657-3661.

Wallace, H.M. & Evans, D.M. Measurement of spermidine/spermine N^1-acetyltransferase activity. 1998. Methods in Molecular Biology, Vol**79**: Polyamine Protocols. Edited by Morgan, D.M. Totowa, New Jersey: Humana Press. pp. 59-68.

Wallace, H.M., Fraser, A.V. & Hughes, A. 2003. A perspective of polyamine metabolism. *Biochemical Journal.* **376,** 1-14.

Wallace, H. & Mackarel, J. 1998. Regulation of polyamine acetylation and efflux in human cancer cells. *Biochem.J.* **291,** 131-137.

Wang, X., Feith, D.J., Welsh, P., Coleman, C.S., Lopez, C., Woster, P.M., O'Brien, T.G. & Pegg, A.E. 2007. Studies of the mechanism by which increased spermidine/spermine N1-acetyltransferase activity increases susceptibility to skin carcinogenesis. *Carcinogenesis.* **28,** 2404-2411.

Wang, Y. & Casero Jr, R.A. 2006. Mammalian polyamine catabolism: A therapeutic target, a pathological problem, or both? *Journal of Biochemistry.* **139,** 17-25.

Wang, Y., Devereux, W., Stewart, T.M. & Casero, R.A. 1999. Cloning and characterization of human polyamine-modulated factor-1, a transcriptional cofactor that regulates the transcription of the spermidine/spermine N 1-acetyltransferase gene. *Journal of Biological Chemistry.* **274,** 22095-22101.

Wang, Y., Devereux, W., Woster, P.M., Stewart, T.M., Hacker, A. & Casero, R.A. 2001. Cloning and characterization of a human polyamine oxidase that is inducible by polyamine analogue exposure. *Cancer Research.* **61,** 5370-5373.

Wang, Y., Hacker, A., Murray-Stewart, T., Frydman, B., Valasinas, A., Fraser, A.V., Woster, P.M. & Casero Jr, R.A. 2005. Properties of recombinant human N1-acetylpolyamine oxidase (hPAO): Potential role in determining drug sensitivity. *Cancer Chemotherapy and Pharmacology.* **56,** 83-90.

Wang, Y., Murray-Stewart, T., Devereux, W., Hacker, A., Frydman, B., Woster, P.M. & Casero, R.A. 2003. Properties of purified recombinant human polyamine oxidase, PAOh1/SMO. *Biochemical and Biophysical Research Communications.* **304,** 605-611.

Warburg, O. 1956. On respiratory impairment in cancer cells. *Science (New York, N.Y.).* **124,** 269-270.

Wong, K., Engelman, J.A. & Cantley, L.C. 2010. Targeting the PI3K signaling pathway in cancer. *Current Opinion in Genetics & Development.* **20,** 87-90.

Wu, T., Ling, K., Sayre, L.M. & McIntire, W.S. 2005. Inhibition of murine N^1-acetylated polyamine oxidase by an acetylenic amine and the allenic amine, MDL 72527. *Biochemical and Biophysical Research Communications.* **326,** 483-490.

Wu, T., Yankovskaya, V. & McIntire, W.S. 2003. Cloning, sequencing, and heterologous expression of the murine peroxisomal flavoprotein, N1-acetylated polyamine oxidase. *Journal of Biological Chemistry.* **278,** 20514-20525.

Xiao, L. & Casero, R. 1996. Differential transcription of the human spermidine/spermine N1-acetyltransferase (SSAT) gene in human lung carcinoma cells. *Biochem.J.* **313,** 691-696.

Xiao, L., Paul, C., Mank, A.R., Griffin, C., Jabs, E.W., Hawkins, A.L. & Casero Jr, R.A. 1992. Structure of the human spermidine/spermine N< sup> 1</sup>-acetyltransferase gene: Kxon/intron gene organization and localization to Xp22. 1. *Biochemical and Biophysical Research Communications.* **187,** 1493-1502.

Yanagawa, K., Yamashita, T., Yada, K., Ohira, M., Ishikawa, T., Yano, Y., Otani, S. & Sowa, M. 1998. The antiproliferative effect of HGF on hepatoma cells involves induction of apoptosis with increase in intracellular polyamine concentration levels. *Oncology Reports.* **5,** 185-275.

Yousef, G.M.& Diamandis, E.P. 2001. The new human tissue kallikrein gene family: Structure, function, and association to disease. *Endocrine Reviews.* **22,** 184-204.

Zahedi, K., Bissler, J.J., Wang, Z., Josyula, A., Lu, L., Diegelman, P., Kisiel, N., Porter, C.W. & Soleimani, M. 2007. Spermidine/spermine N1-acetyltransferase overexpression in kidney epithelial cells disrupts polyamine homeostasis, leads to DNA damage, and causes G2 arrest. *American Journal of Physiology-Cell Physiology.* **292,** C1204-C1215.

Zhang, W., Ramdas, L., Shen, W., Song, S.W., Hu, L. & Hamilton, S.R. 2003. Apoptotic response to 5-fluorouracil treatment is mediated by reduced polyamines, non-autocrine fas ligand and induced tumor necrosis factor receptor 2. *Cancer Biology & Therapy.* **2,** 572-578.

6 Appendix

6.1 Cytotoxicity of CPENSpm upon SSAT$^-$ and SSAT$^+$ cells

Fig. 6.1 Cytotoxicity of CPENSpm at 48 h exposure

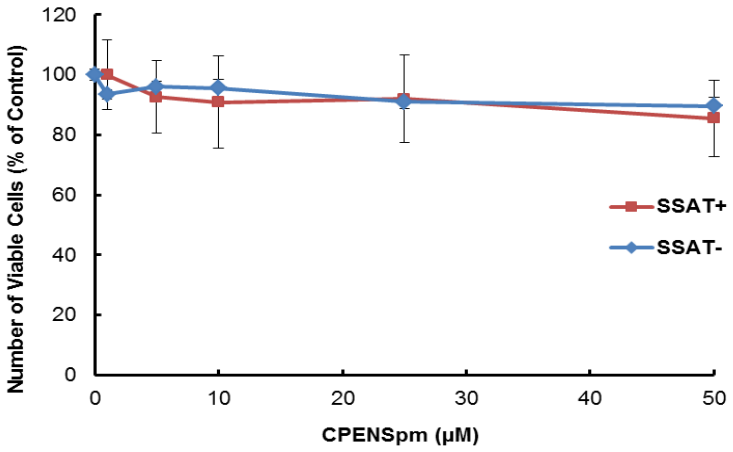

Fig. 6.1 Cells were seeded at a density of 2.4 x 10^4 cells / cm^2 on a 96 well microtitre plate and allowed for 48 h attachment and growth. After 48 h, medium was replaced with vehicle control and medium containing CPENSpm in a concentration range of 0 to 50 µM. The plate was incubated for further 48 h and assayed by MTT (Section 2.3.3). Results were shown as mean ± SD or SEM (n=2 of SSAT$^+$; n=3 of SSAT$^-$, with 6 replicates per experiment).

6.2 Effect of aspirin and 5-FU on SSAT, APAO, SMO, AZ1, and AZIn protein expression

Fig. 6.2 Effect of aspirin and 5-FU on SSAT protein (28 kDa) expression at 24 h

a) WT

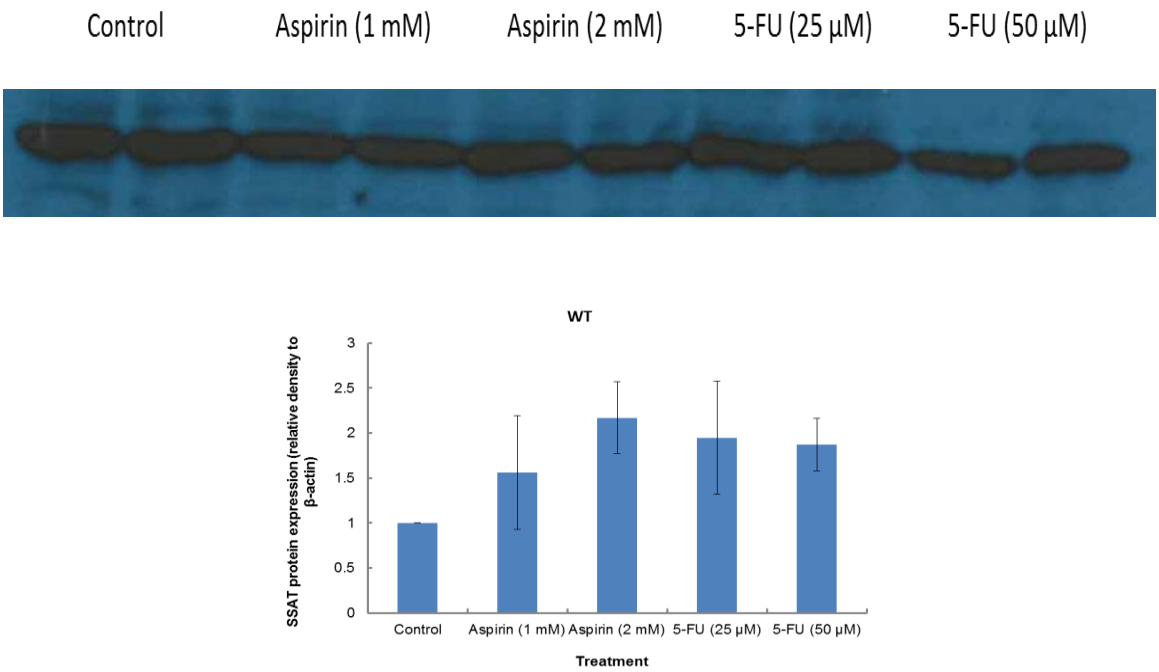

b) SSAT^{-}

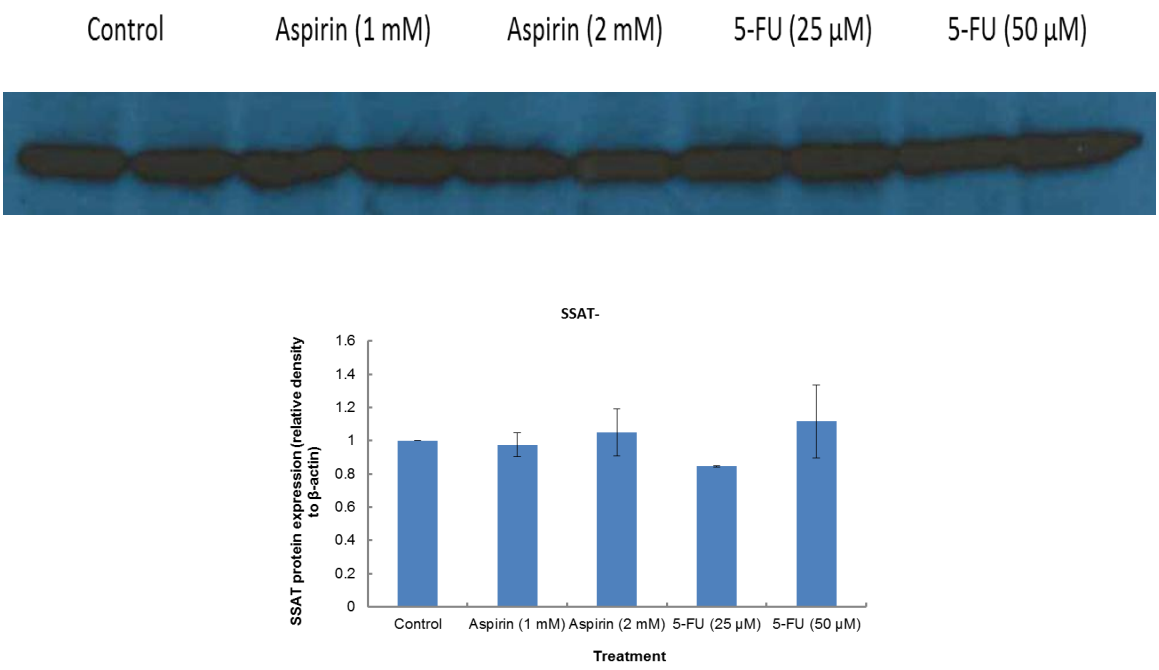

c) SSAT^{+}

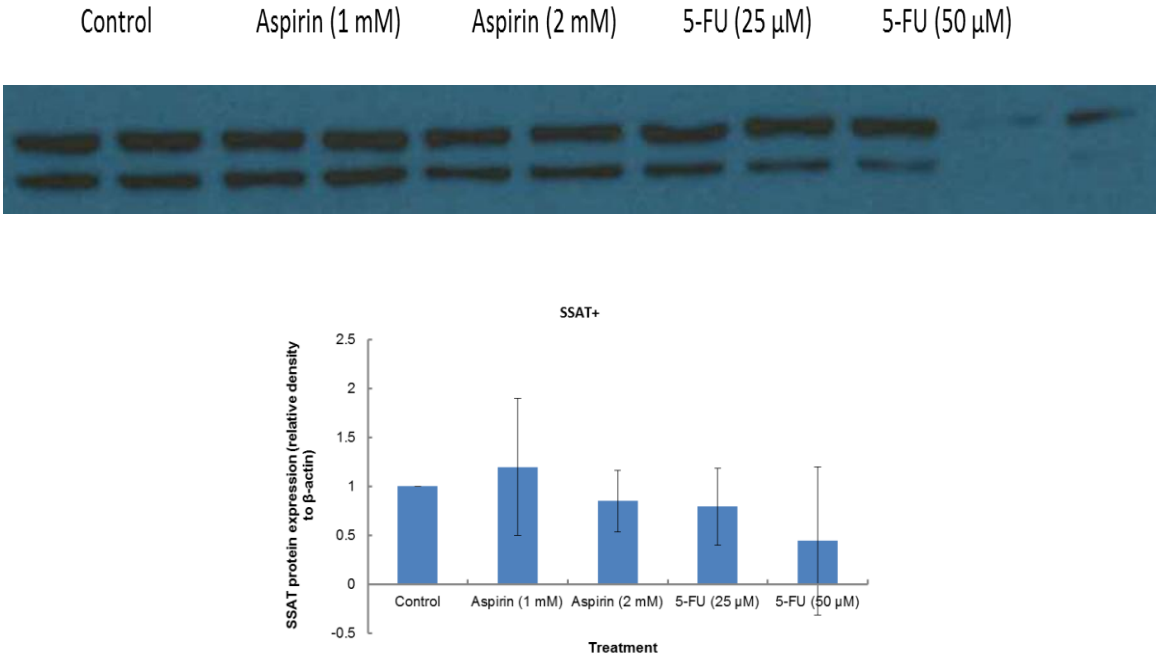

Fig. 6.3 Effect of aspirin and 5-FU on APAO protein (56 kDa) expression at 24 h

a) WT

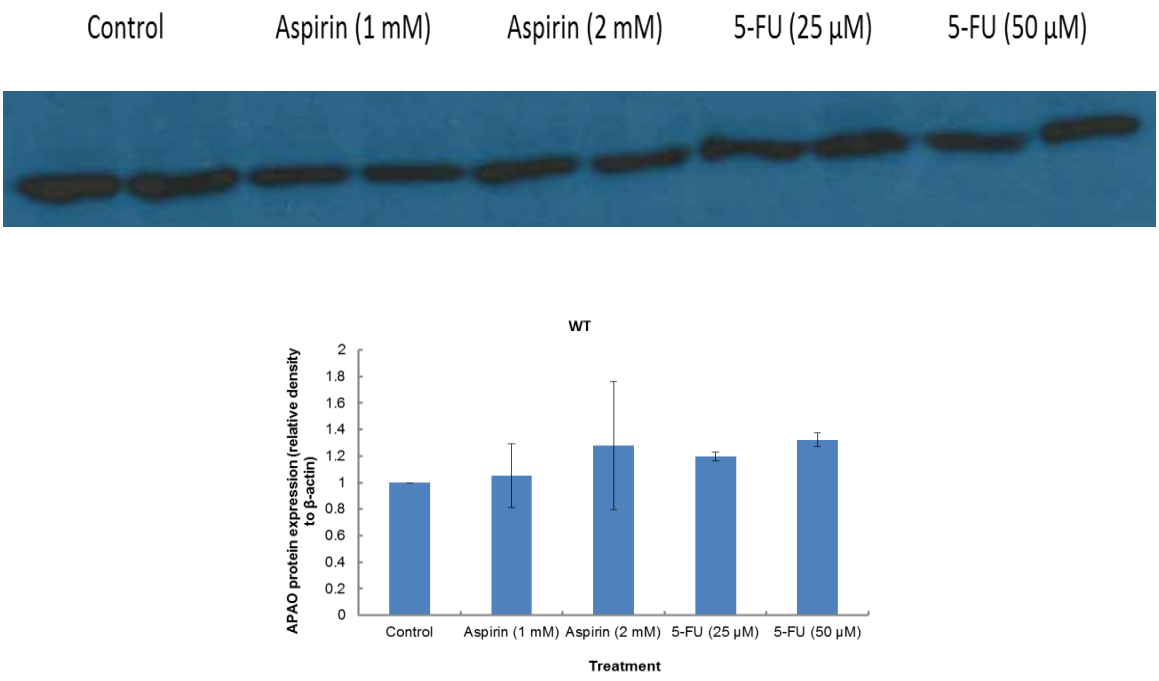

b) SSAT^{-}

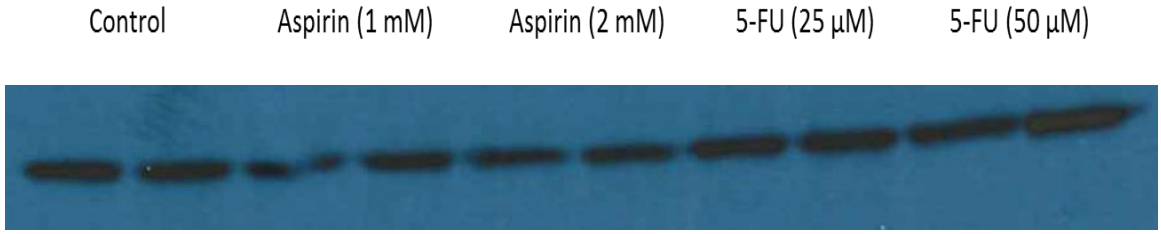
Control
Aspirin (1 mM)
Aspirin (2 mM)
5-FU (25 µM)
5-FU (50 µM)

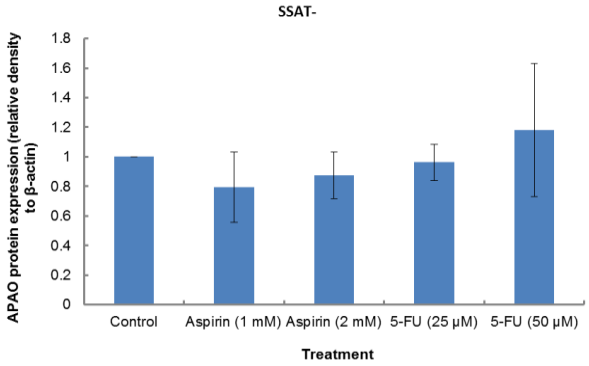
SSAT-
APAO protein expression (relative density to β-actin)
1.8
1.6
1.4
1.2
1
0.8
0.6
0.4
0.2
0
Control
Aspirin (1 mM)
Aspirin (2 mM)
5-FU (25 µM)
5-FU (50 µM)
Treatment

c) SSAT^{+}

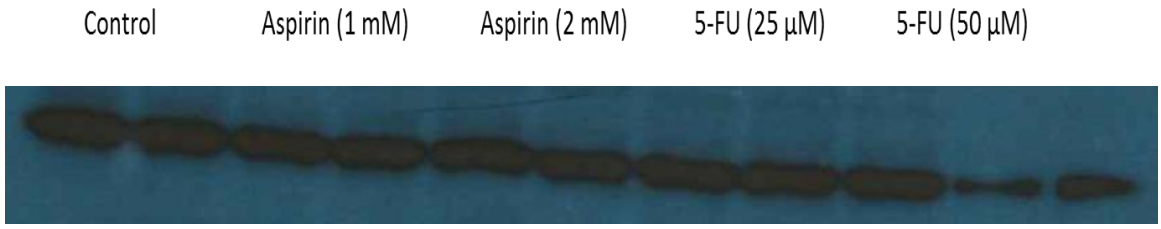
Control
Aspirin (1 mM)
Aspirin (2 mM)
5-FU (25 µM)
5-FU (50 µM)

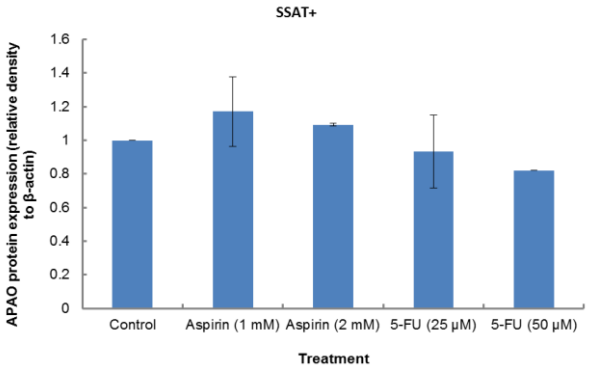
SSAT+
APAO protein expression (relative density to β-actin)
1.6
1.4
1.2
1
0.8
0.6
0.4
0.2
0
Control
Aspirin (1 mM)
Aspirin (2 mM)
5-FU (25 µM)
5-FU (50 µM)
Treatment

Fig. 6.4 Effect of aspirin and 5-FU on SMO protein (80 kDa) expression at 24 h

a) WT

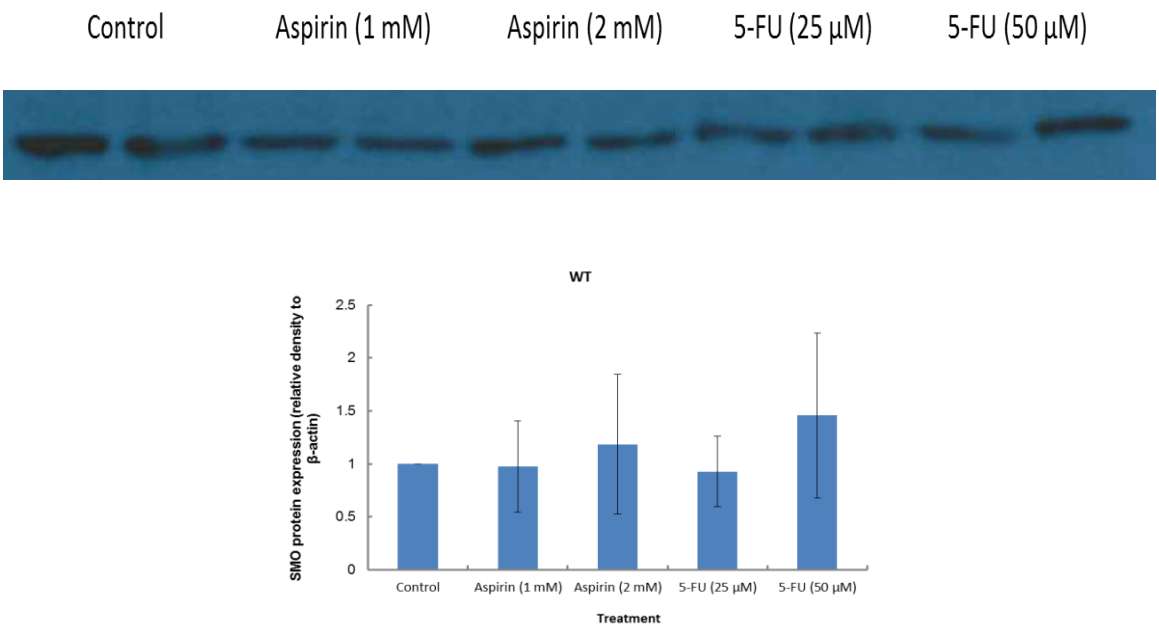

b) SSAT$^-$

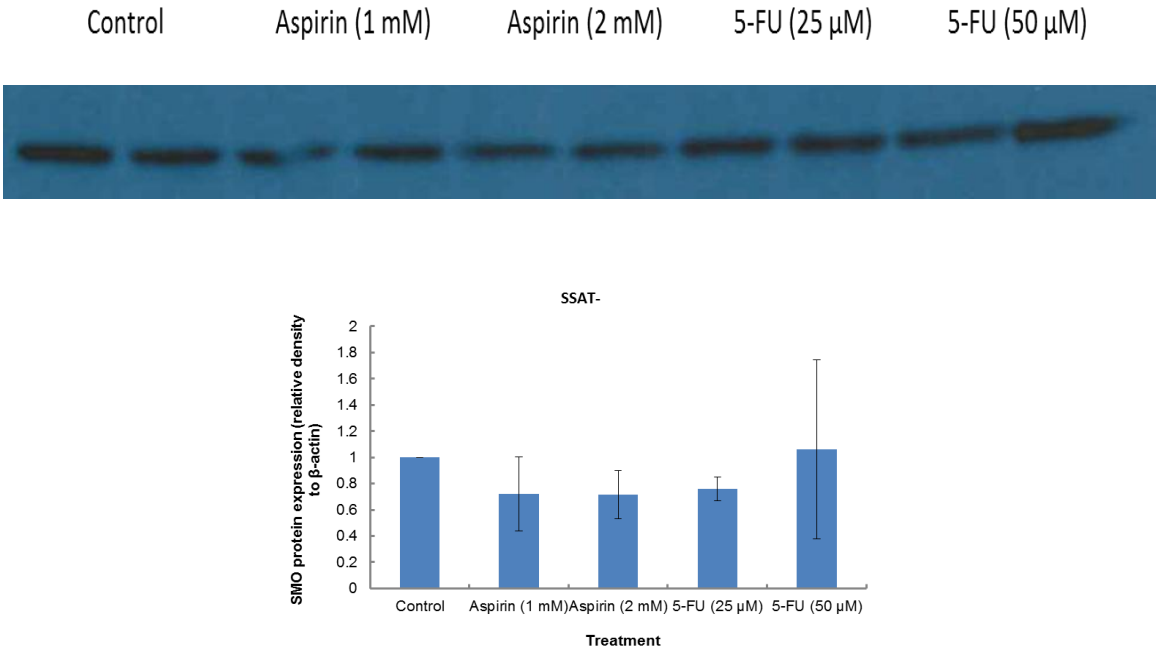

c) SSAT^{+}

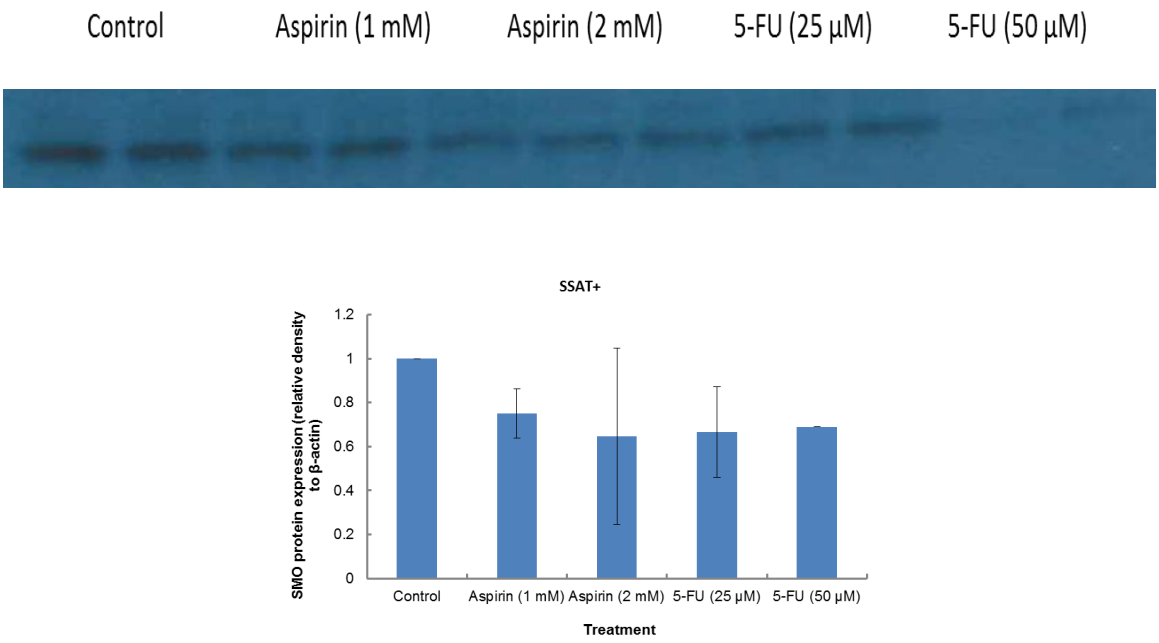

Fig. 6.5 Effect of aspirin and 5-FU on antizyme1 protein (28 kDa) expression at 24 h

a) WT

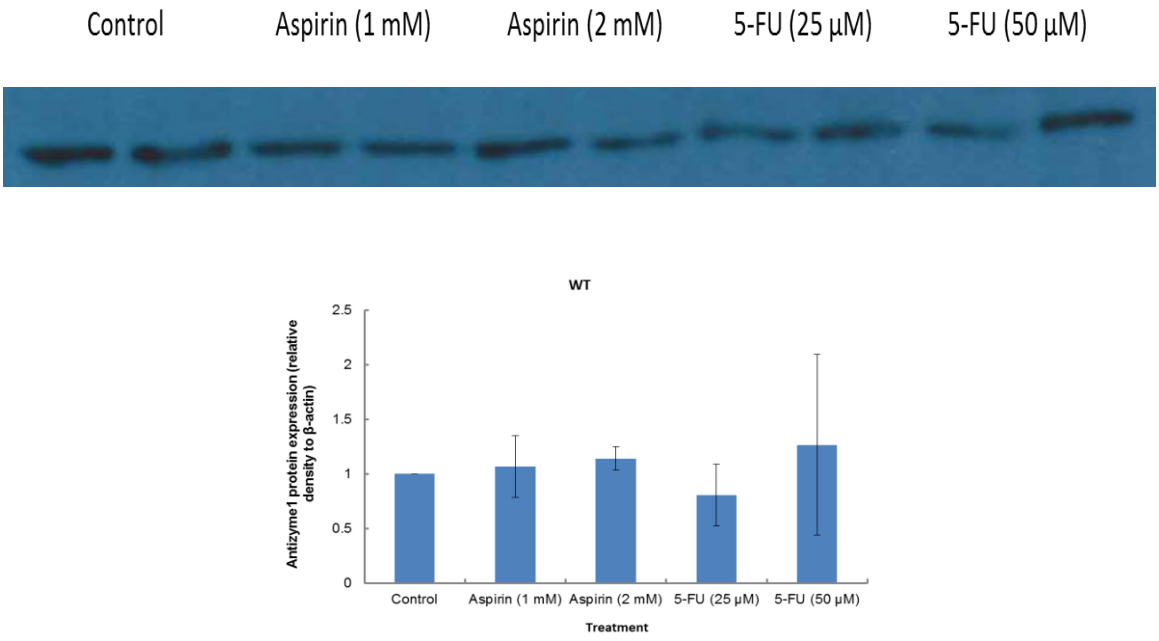

b) SSAT^{-}

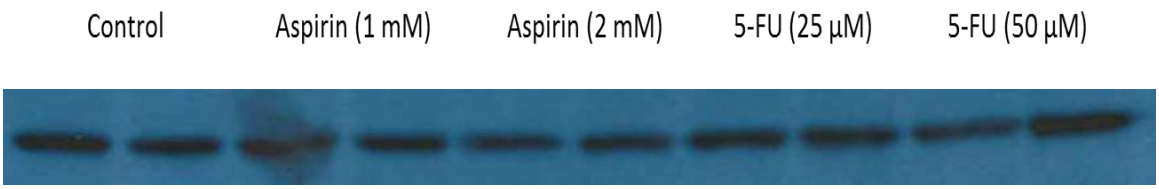
Control
Aspirin (1 mM)
Aspirin (2 mM)
5-FU (25 µM)
5-FU (50 µM)

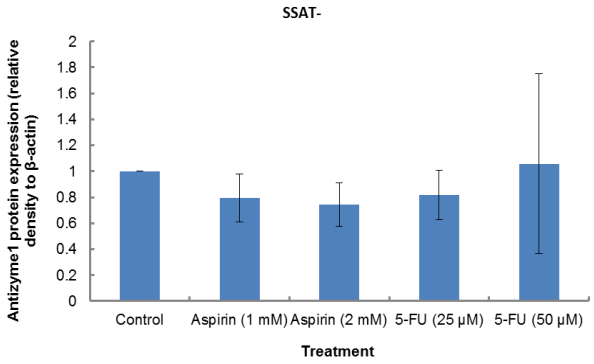
SSAT-
Antizyme1 protein expression (relative density to β-actin)
2
1.8
1.6
1.4
1.2
1
0.8
0.6
0.4
0.2
0
Control
Aspirin (1 mM)
Aspirin (2 mM)
5-FU (25 µM)
5-FU (50 µM)
Treatment

c) SSAT^{+}

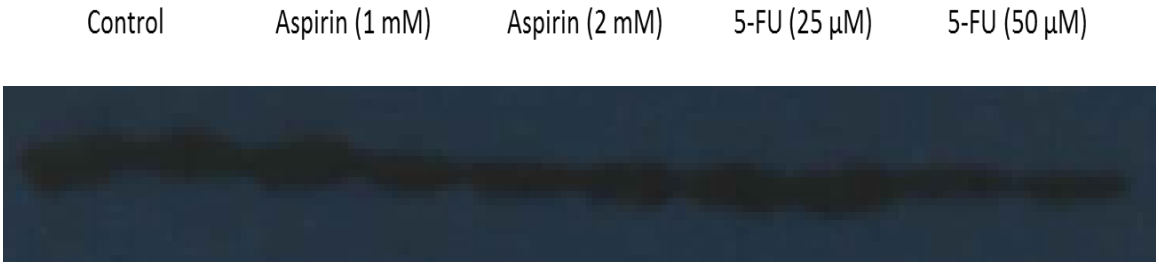
Control
Aspirin (1 mM)
Aspirin (2 mM)
5-FU (25 µM)
5-FU (50 µM)

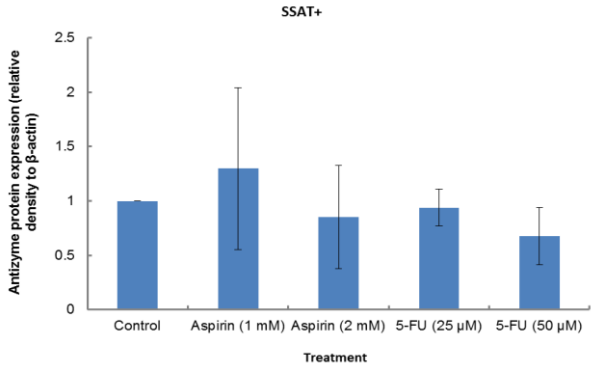
SSAT+
Antizyme protein expression (relative density to β-actin)
2.5
2
1.5
1
0.5
0
Control
Aspirin (1 mM)
Aspirin (2 mM)
5-FU (25 µM)
5-FU (50 µM)
Treatment

Fig. 6.6 Effect of aspirin and 5-FU on antizyme inhibitor1 protein (50 kDa) expression at 24 h

a) WT

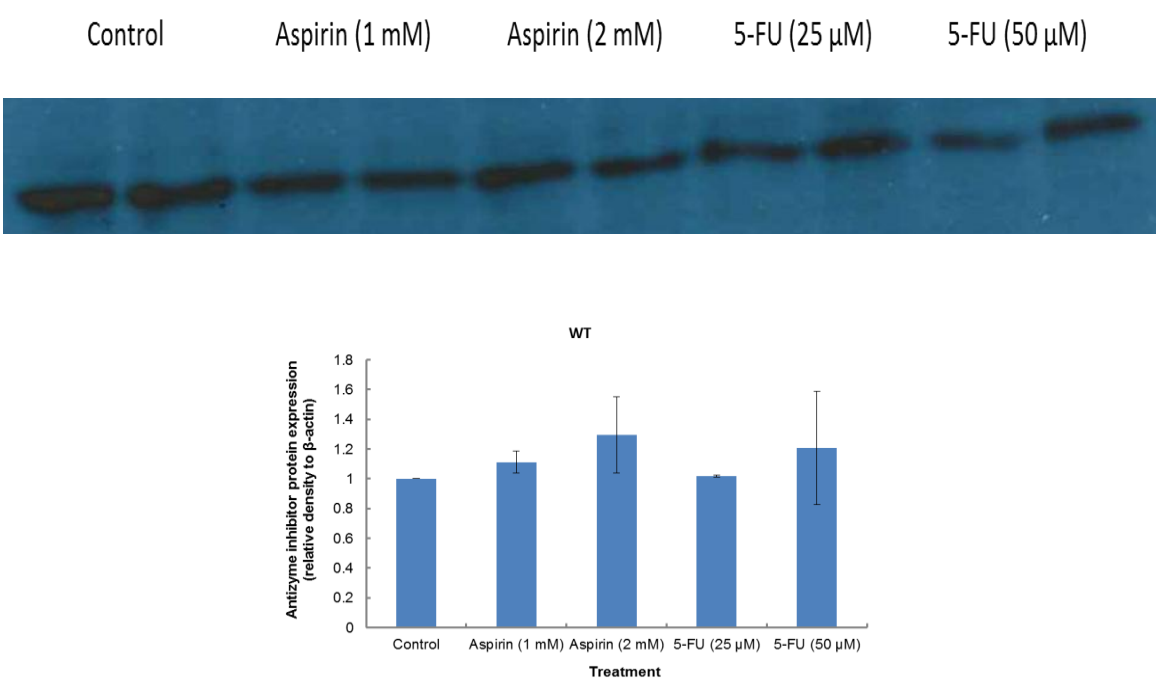

b) SSAT⁻

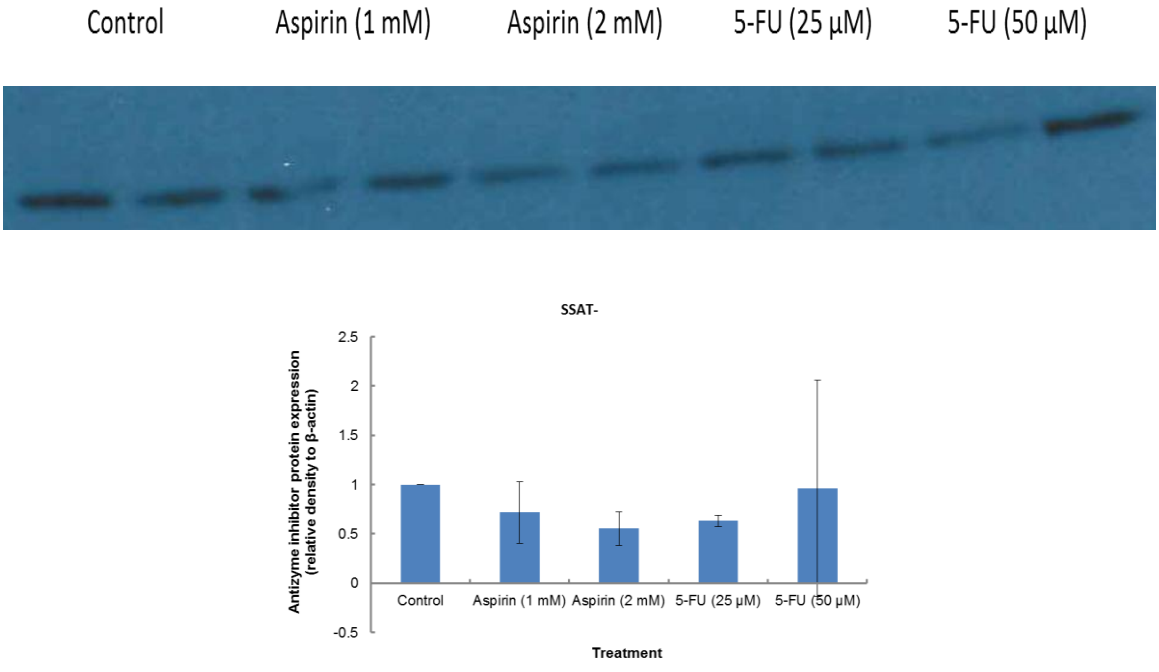

c) SSAT$^+$

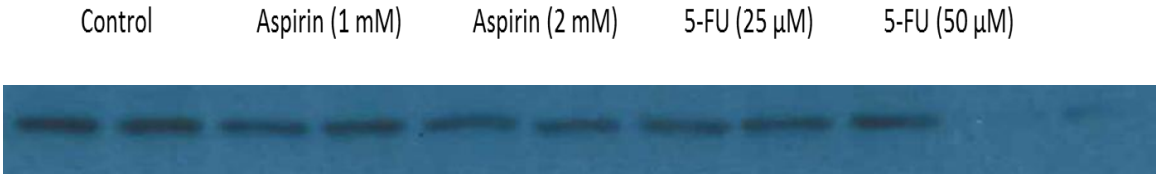

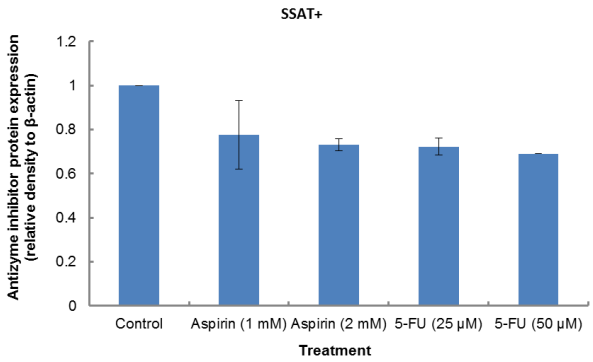

Fig. 6.7 Effect of aspirin and 5-FU on β-actin (43 KDa) protein expression at 24 h

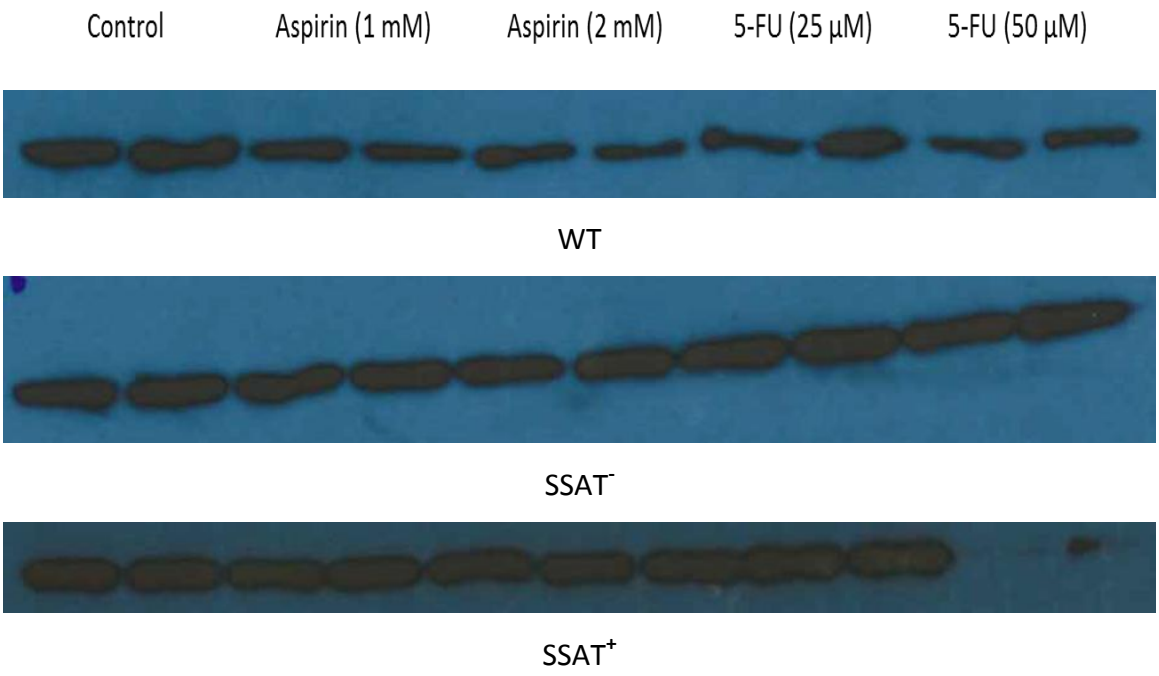

Cells were seeded at a density of 2.4 x 10^6/cm^2 in a 90 mm cell culture dish in triplicate. The cells were treated with the drug after 48 h growth, harvested 24 h afterwards and lysed (section 2.2.15). Protein content was determined by Lowry assay (section 2.2.8). 30 µg of protein lysates were loaded onto a Novex Bis-Tris SDS 4 – 12 % gel for electrophoresis. The gel was electroblotted onto a PVDF membrane. Polyclonal antibodies were used in conjunction with an IgG peroxidase conjugate secondary antibody. β-Actin was used as internal control. Band images were analysed by ImageJ. Results were shown as a relative density by calculating a percentage against its corresponding internal control (n=1, with 2 replicates per experiment).

Fig. 6.8 Total cellular protein content in WT, SSAT-, SSAT+

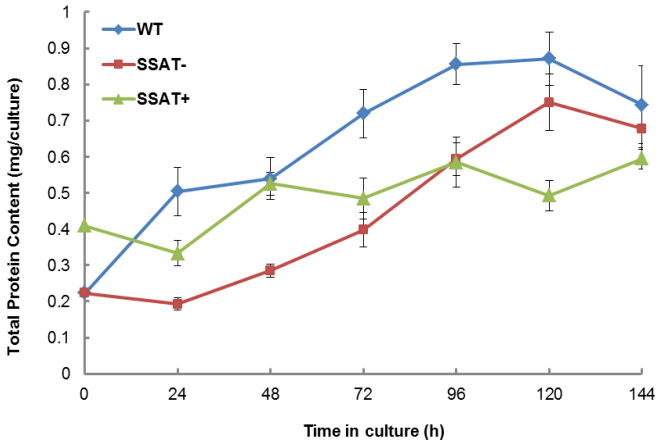

Fig. 6.8 Cells were plated at a density of $2.4x10^6/cm^2$ in a 60 mm cell culture dish in duplicate and harvested at a 24 h interval. Cellular protein fraction was extracted by 0.3 M NaOH, and measured by Lowry assay (Section2.2.8). Results shown are mean ± SEM (n=3-9, with 2 duplicate per experiment).

Fig. 6.9 Protein standard graph by Lowry assay

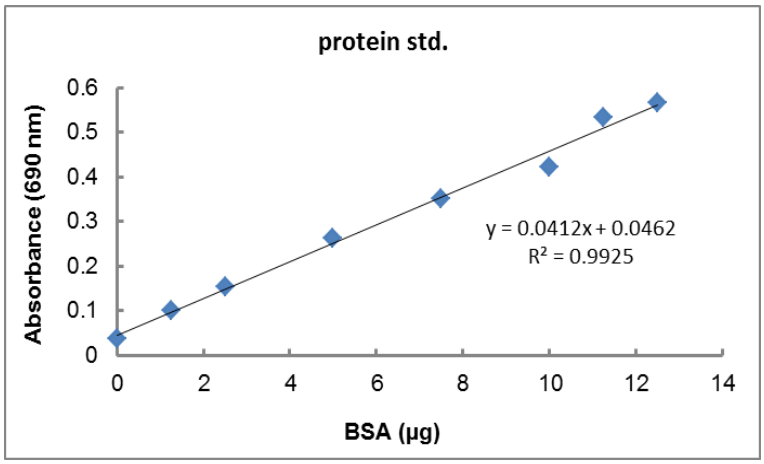

Fig. 6.9 A BSA protein standard curve was generated by Lowry assay (Section 2.2.8) and used for calculation of total cellular protein content.

Fig. 6.10 H_2O_2 standard graph for APAO and SMO assay

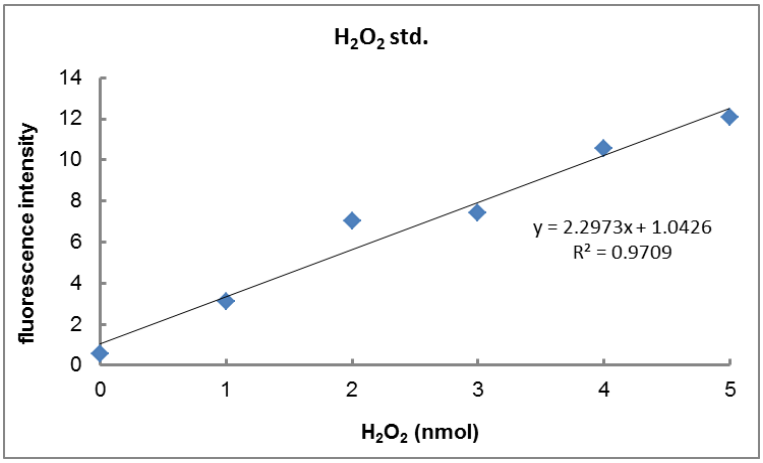

Fig. 6.10 H_2O_2 standard was generated by APAO and SMO assay (Section 2.2.12) Results are mean (n=10, with 2 replicate per assay).

6.3 Dansylated Polyamines: Product ion spectra by LC-MS

Fig. 6.11 a) Dansylated putrescine ion spectra

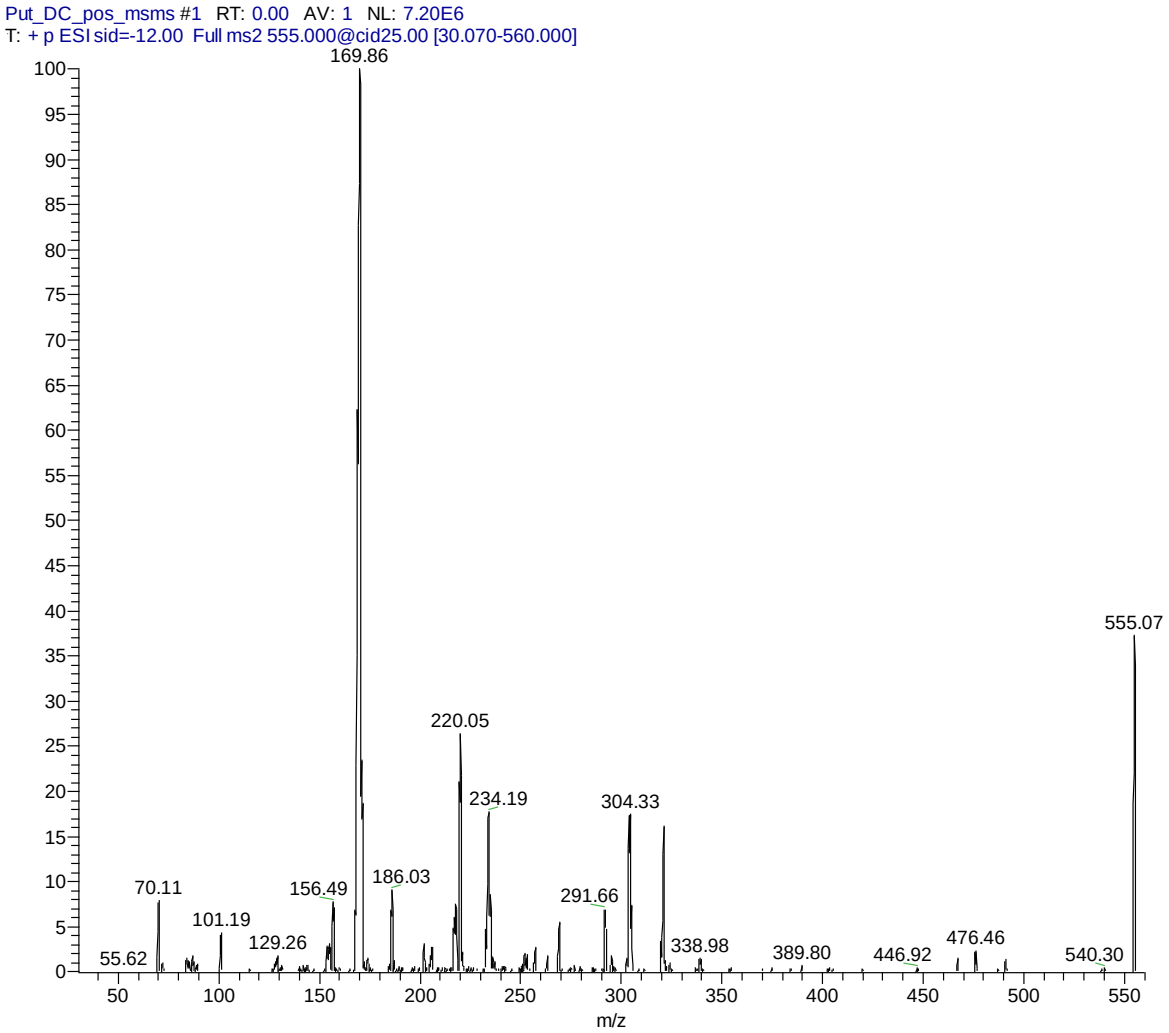

b) Dansylated N^1-acetylspermidine ion spectra

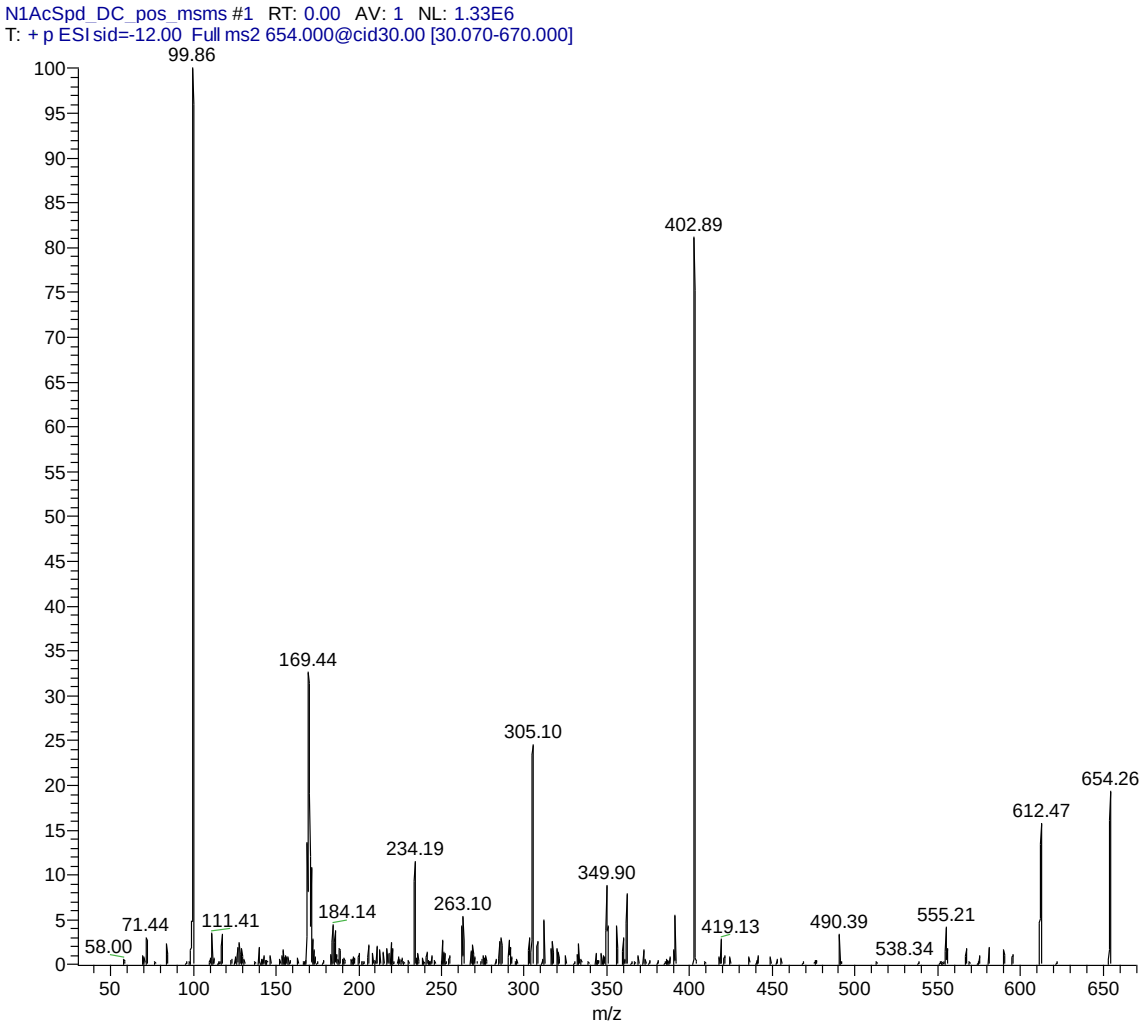

c) Dansylated N^1-acetylspermine ion spectra

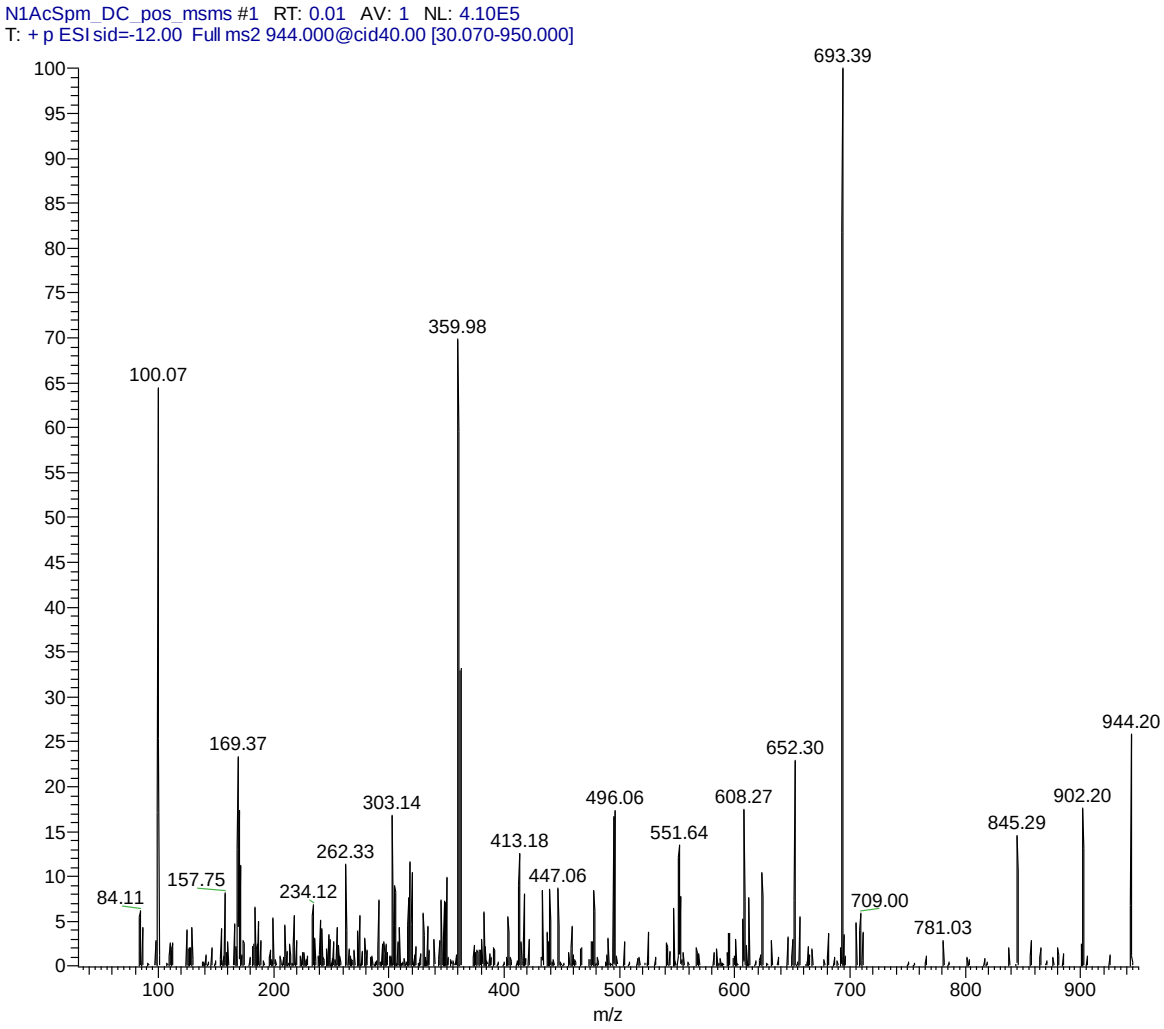

d) Dansylated N^8-acetylspermidine ion spectra

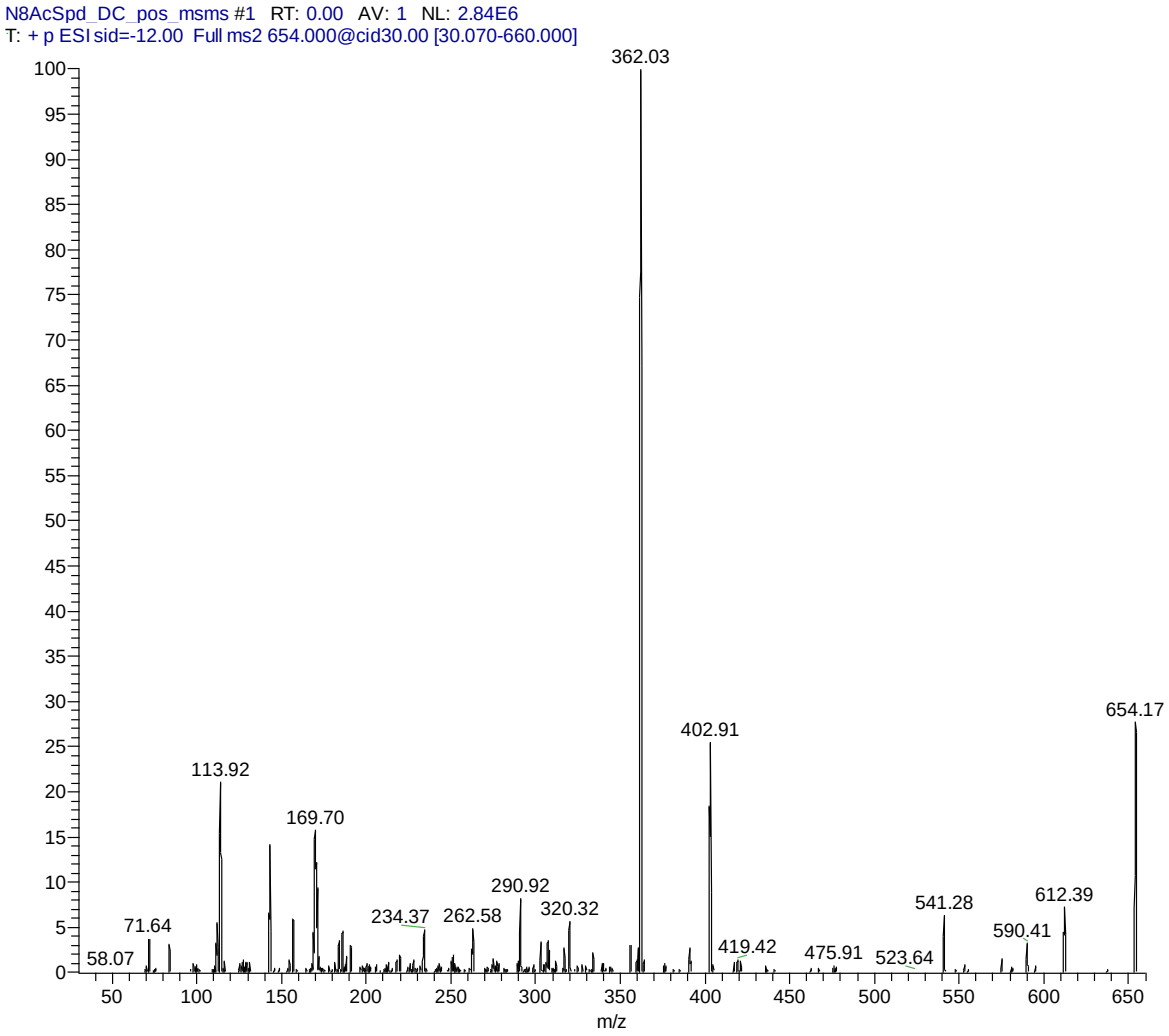

e) Dansylated N^1,N^{12}-diacetylspermine ion spectra

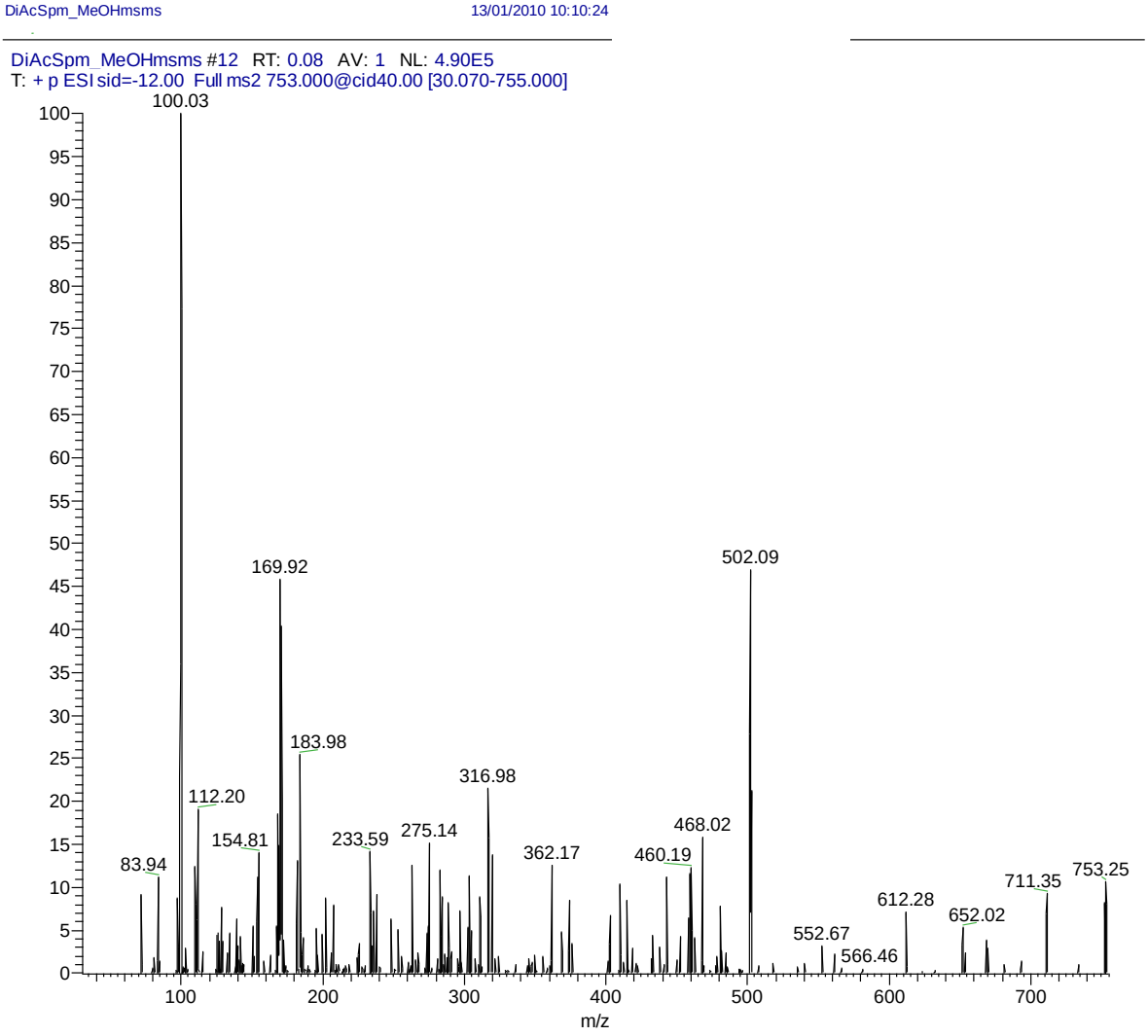

f) Dansylated spermidine ion spectra

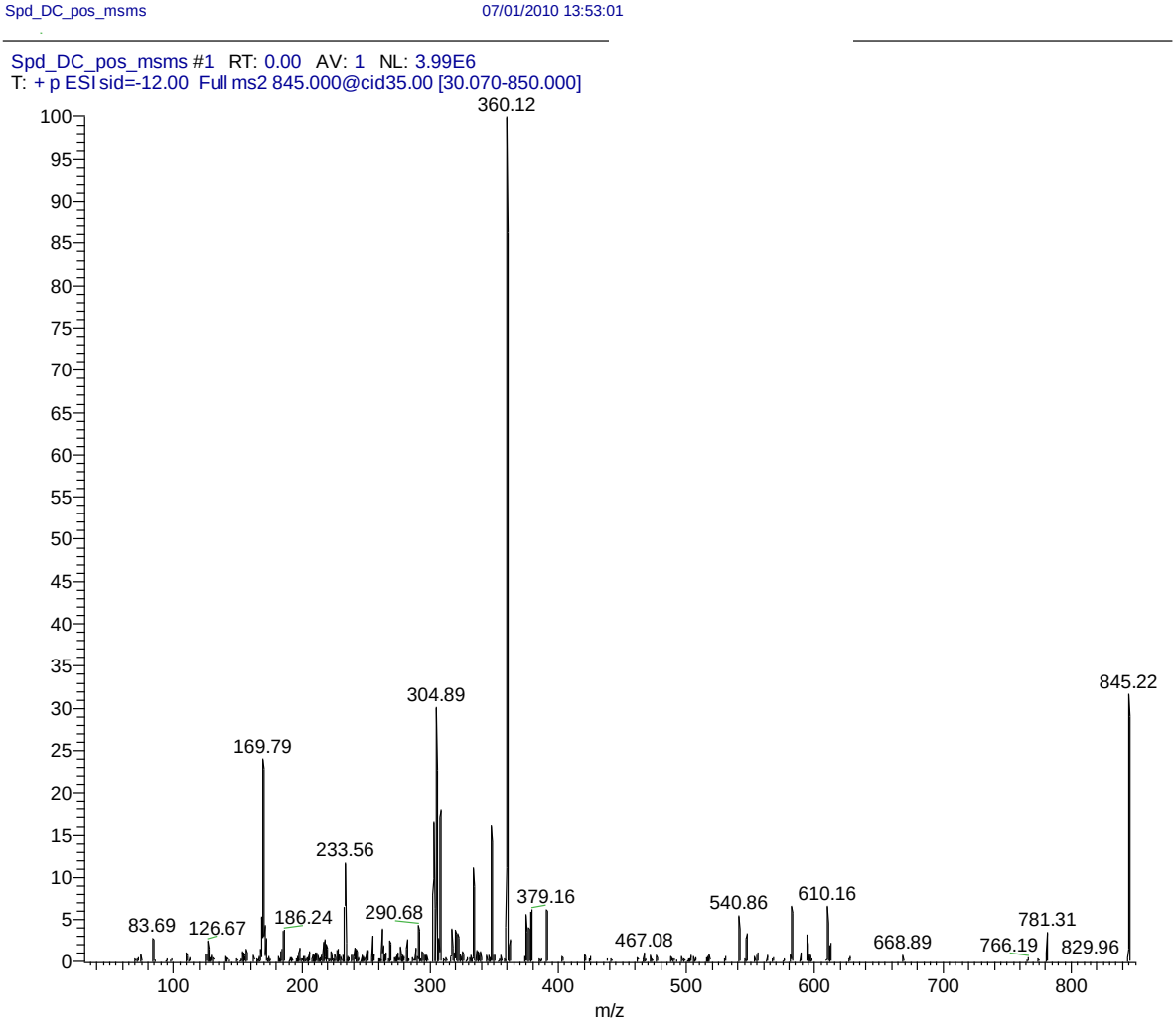

g) Dansylated spermine ion spectra

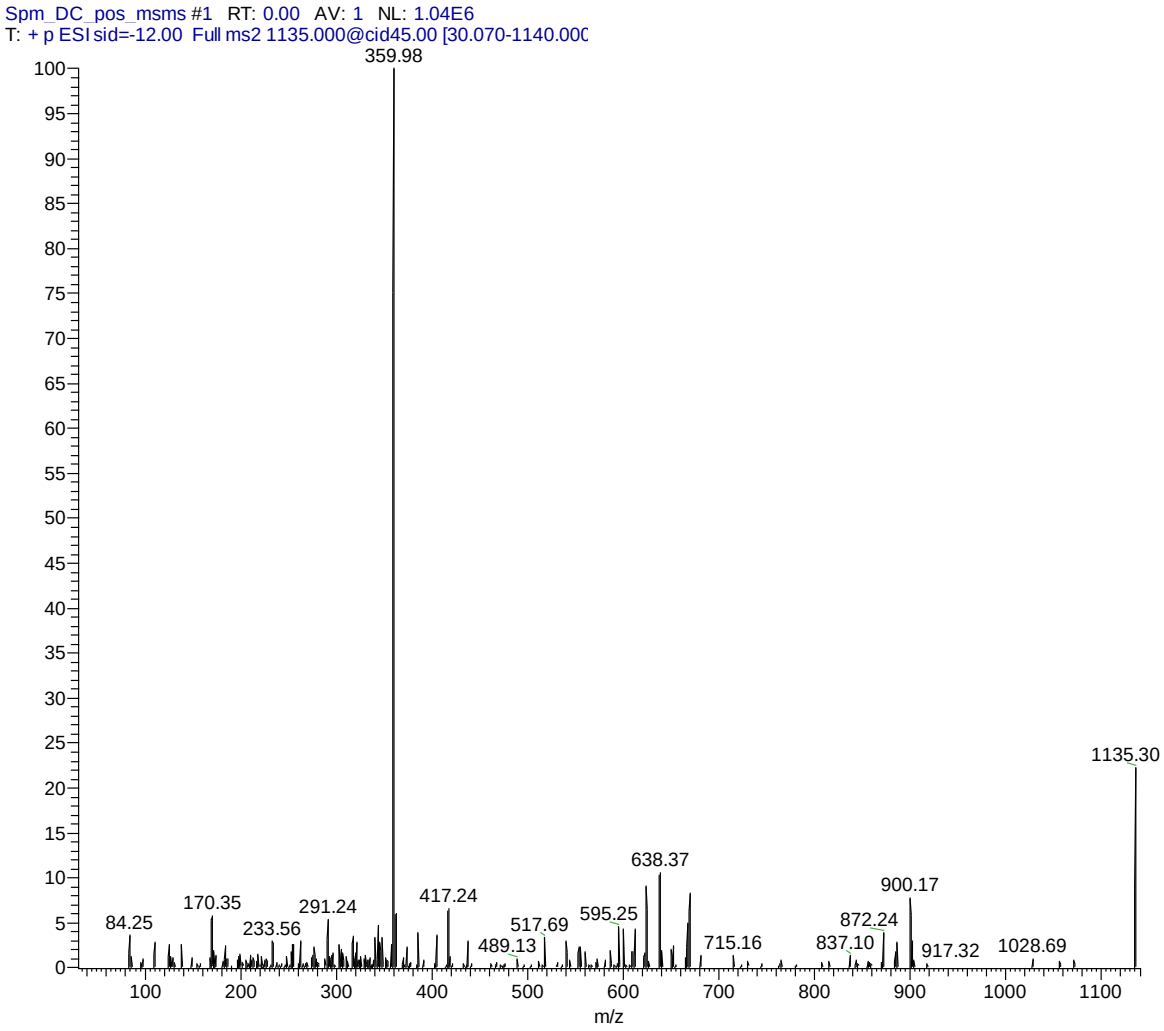

h) Dansylated internal standard (1,7-diaminoheptane) ion spectra

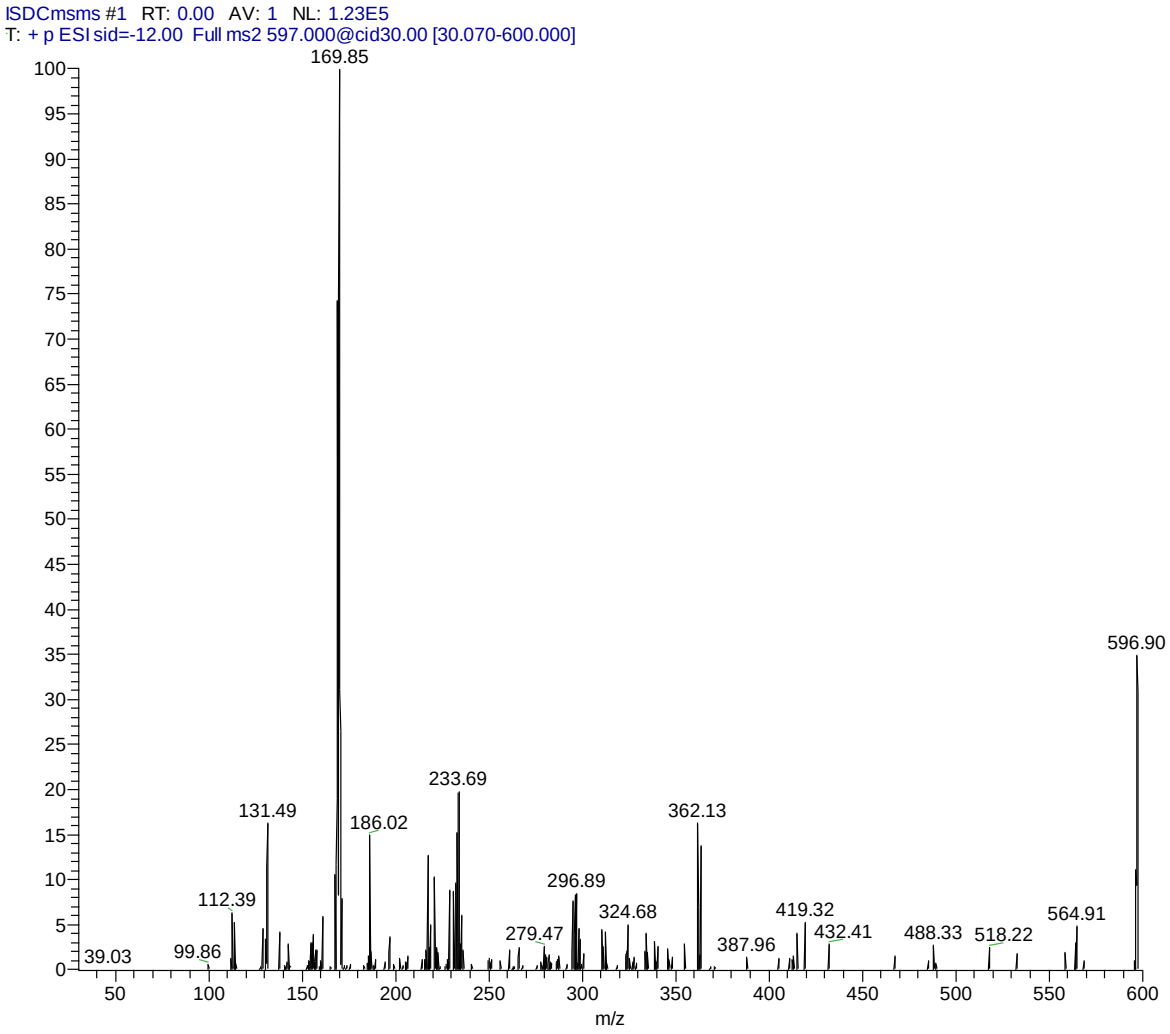

6.4 Calibration of polyamines by LC-MS

Fig. 6.12 Standard calibration graphs of polyamines by LC-MS

a) Putrescine

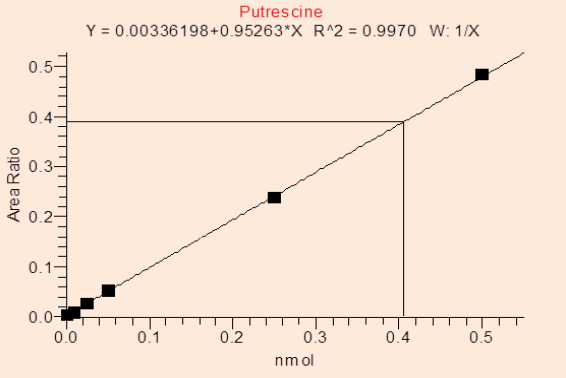

c) Spermine

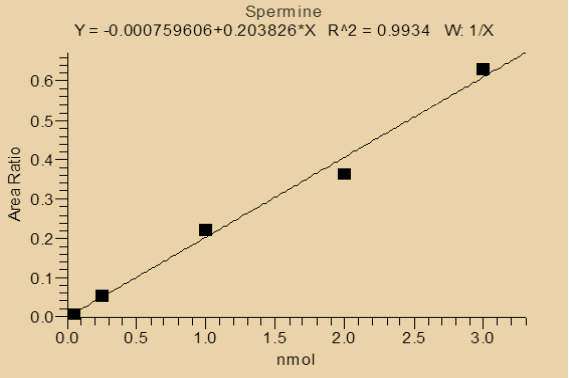

b) Spermidine

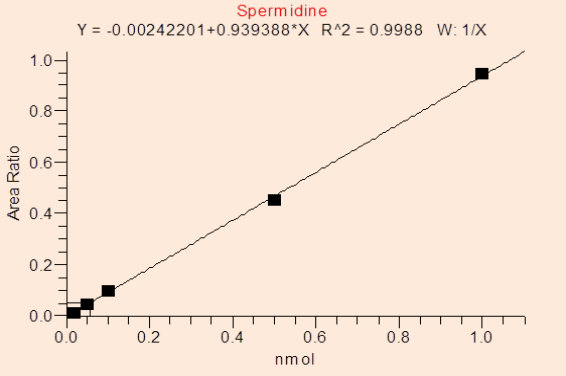

d) N^1-acetylspermidine

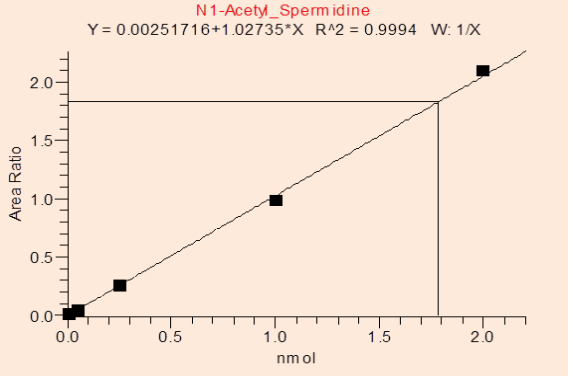

e) N^8-acetylspermidine

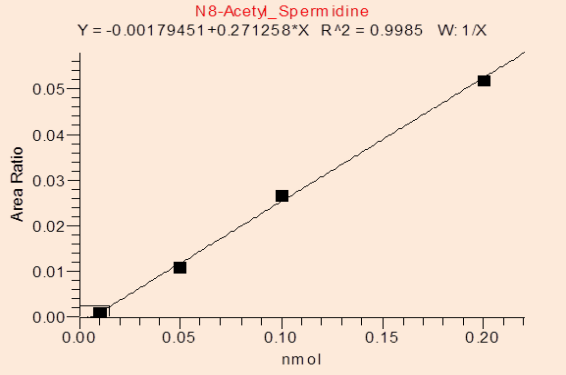

f) N^1-acetylspermine

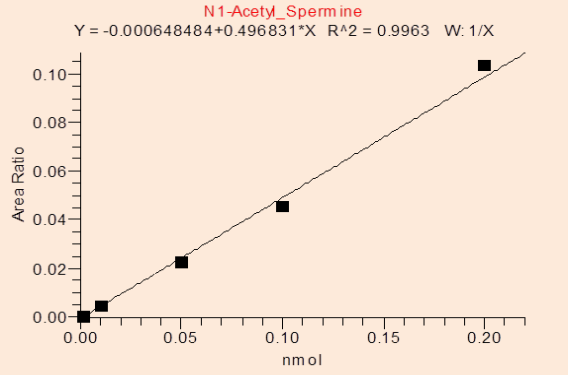

g) N^1,N^{12}-diacetylspermine

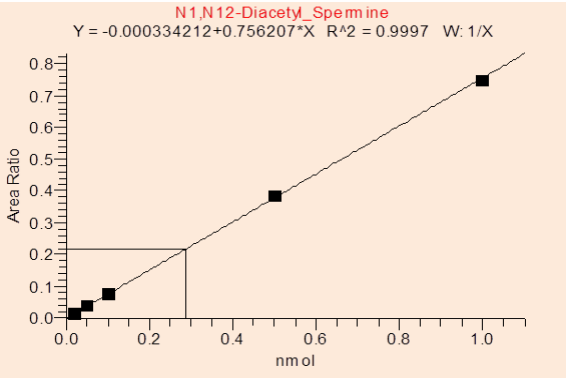

6.5 Experimental Solutions

1 M Acetylsalicylic acid (Aspirin)
1.8 g was dissolved in 10 ml 100% ethanol.

Bovine serum albumin (BSA)
25 mg BSA was dissolved in 0.3 M sodium hydroxide to make 0.5 mg/ml BSA stock solution 50 ml. Aliquot 1 ml in eppendorf, stored at -20 °C.

1% (w/v) Copper sulfate solution ($CuSO_4$)
1 g was dissolved and made up to 100 ml with dH_2O.

Dansyl chloride
0.15 g dansyl chloride powder was dissolved in acetone to give a final concentration of 15 mg/ml in 10 ml. Fresh solution of dansyl chloride was needed every time. Acetone was used as solvent to dissolve dansyl chloride, and then the solution was incubated in a shaking water bath for 1 h at 37 °C to help it dissolving. The undissolved dansyl chloride was discarded by brief centrifuge.

0.1 M DTT
0.15 g DTT was dissolved to 10 ml with distilled water, stored at 4 °C.

0.1 M EDTA
0.37 g EDTA was dissolved to 10 ml with distilled water, stored at 4 °C.

1 M Tris HCl (PH 7.2 at 4 °C)
121.1 g of tris base was dissolved in distilled water, temperature was lowered to 4 °C and then PH was adjusted to 7.2. Final volume of the solution was made up to 1 L with distilled water.

1 M Tris HCl (PH 7.8 at 37 °C)
12.1 g of tris base was dissolved in 80 ml of distilled water and heated to 37 °C in a water bath for 1 h, and then the PH was adjusted to 7.8. The solution volume was made up to 100 ml with distilled water.

10 mM Etoposide
0.0589 g etoposide was dissolved in 10 ml of 100% DMSO. Aliquot and Stored at -20 °C.

2% (w/v) potassium sodium tartrate ($KNaC_4H_4O_6 \cdot 4H_2O$; MW 282.1)
2 g was dissolved in 100 dH_2O.

MTT solution
0.1 g of MTT powder was dissolved in complete PBS making up to 20 ml, giving a 5 mg/ml MTT solution. The solution was sterile filtered and stored as 700 µl aliquots in eppendorfs at -20 °C. Be aware that MTT is light sensitive.

Phosphate buffered saline (PBS)
PBS A: 17.5 g of disodium hydrogen orthophosphate ($Na_2HPO_4 \cdot 2H_2O$), 3 g of potassium chloride (KCl), 100 g of sodium chloride (NaCl) and 3 g of potassium dihydrogen orthophosphate (KH_2PO_4) were dissolved in 800 ml distilled water, and then PH was adjusted to 7.2, and final volume was made up to 1 L.

PBS B: 1 g of calcium chloride ($CaCl_2 \cdot 2H_2O$) was dissolved in 1 L distilled water.
PBS C: 1 g of magnesium chloride ($MgCl_2 \cdot 6H_2O$) was dissolved in 1 L distilled water.
Complete PBS: 100 ml of PBS C and 100 ml of PBS B were added to 920 ml distilled water, afterwards 80 ml of PBS A was added to make up to 1 L. Stored at 4 °C.

Perchloric acid ($HClO_4$; MW = 100.46, concentration 70%, density = 1.67 g/cm^3)
85.94 ml of 70% (equals to 60.16 ml of 100%) $HClO_4$ and 914.06 ml of dH_2O were needed to make 1 L of 1 M $HClO_4$ solution.
To make 0.2 M of 1 L HClO4, 17.19 ml of 70% (equals to 12 ml of 100%) $HClO_4$ + 982.81 ml of dH2O were needed.

Sodium carbonate 2% (w/v)
20 g sodium carbonate was dissolved in 1 L dH2O. Stored at room temperature.

0.3 M Sodium hydroxide
6 g of sodium hydroxide was dissolved in 500 dH_2O. Stored at room temperature.

0.1 M sodium hydroxide
2 g was dissolved in 500 ml dH_2O, stored at room temperature.

30 mM spermidine
76.38 mg spermidine was dissolved to 10 ml with distilled water. Stored at -20 °C.

Trypan blue 0.4% (w/v)
0.4 g was dissolved in 100 ml of 0.81% sodium chloride and 0.06% potassium phosphate (dibasic)

250 µM Acetyl-CoA (MW = 878)
2.195 mg was dissolved in 10 ml dH2O, stored at -20°C.

100 mM Aminoguanidine
615.5 mg was dissolved in 50 ml dH2O, sterile filtered and stored at -20°C.

50 mg/ml G418 (Geneticin)
2.5 g was dissolved in 50 ml of dH2O, stored at -20°C.

50 mg/ml Hygromycin B
1 g was dissolved in 20 ml dH2O, stored at 4°C.

10 mg/ml Tetracycline
10 mg was dissolved in 1 ml of 50% (v/v) Ethanol. Stored at -20°C. Protected from light.

1 M Hydroxylamine
0.694 g was dissolved in 10 ml H2O, stored at 4°C.
10 mM MDL72527
13.3 mg was dissolved in 5 ml of 100% DMSO. Stored at -20°C.

ODC assay
Homogenising Buffer (10 mM Tris-HCl, 2.5 mM dithiothreitol and 0.1 mM EDTA): 0.1 ml of 1 M Tris-HCl (pH 7.2 at 4°C), 0.1 ml of 250 mM Dithiothreitol (DTT) and 10 µl of 0.1 M EDTA, make up to 10 ml with deionised water.

SSAT assay
The hypotonic lysis buffer: 100 µl of 1 M Tris (PH 7.2 at 4°C) + 100 µl of 100 mM EDTA + 250 µl of 100 mM dithiothreitiol (DTT), make up to 10 ml with distilled H_2O and stored at 4°C.

Mild stripping buffer for western blot
15 g glycine, 1 g SDS, 10 ml Tween20, pH 2.2, volume was brought up to 1 L by dH2O.

1 g/ml sodium carbonate decahydrate ($Na_2CO_3 \cdot 10H_2O$)
This solution is very saturated. The powder was dissolved in a glass bottle with a stir and soaked in a beaker with hot water (80-90°C) on a heating pad. Very small amount of dH_2O can be added to help dissolve the powder. Be aware that one molecule of sodium carbonate produces 10 molecules of H2O itself. Alternatively, the solution can be made by adding the powder into hot water with a stir until it dissolves to give 1g/ml.

Sodium phosphate anhydrous 0.2 M
2.4 g was dissolved in 100 ml of dH_2O.

di-sodium hydrogen orthophosphate (Na2HPO4·2H2O) 0.25 M
4.45 g was dissolved in 100 ml of dH_2O.

EDTA 0.5 mM: 18.6 mg in 100 ml H_2O
EDTA 5 mM: 0.186 g in 100 ml H_2O

Use 0.2 M $NaH_2PO_4 \cdot 2H_2O$ + 0.5 mM EDTA to adjust 0.25 mM Na_2HPO_4 + 5 mM EDTA pH to 8.0.

DCFDA 10 mM: 4.9 mg was dissolved in 1 ml of 100% DMSO.